Carnegie Mellon University
MELLON COLLEGE OF SCIENCE

THESIS

SUBMITTED IN PARTIAL FULFILLMENT OF THE REQUIREMENTS
FOR THE DEGREE OF

DOCTOR OF PHILOSOPHY IN THE FIELD OF PHYSICS

TITLE: "Curvature-Tilt Theories of Lipid Membranes."

PRESENTED BY: Mustafa Mert Terzi

ACCEPTED BY THE DEPARTMENT OF PHYSICS

Markus Deserno	9/24/18
MARKUS DESERNO, CHAIR PROFESSOR	DATE

Scott Dodelson	9/25/18
SCOTT DODELSON, DEPT HEAD	DATE

APPROVED BY THE COLLEGE COUNCIL

Rebecca Doerge	9/27/18
REBECCA DOERGE, DEAN	DATE

Curvature-Tilt Theories of Lipid Membranes

M. Mert Terzi

2018

Department of Physics
Carnegie Mellon University
Pittsburgh, PA

Submitted in partial fulfillment of the requirements
for the degree of Doctor of Philosophy

advised by Prof. Markus Deserno

Abstract

On mesoscopic scales lipid membranes are well described by continuum theories whose main ingredients are the curvature of a membrane's reference surface and the tilt of its lipid constituents. In particular, Hamm and Kozlov [Eur. Phys. J. E **3**, 323 (2000)] showed how to systematically derive such a tilt-curvature Hamiltonian, based on the elementary assumption of a thin fluid elastic sheet experiencing internal lateral pre-stress. Performing a dimensional reduction, they not only derived the basic form of the effective surface Hamiltonian, but also made connections between the trans-membrane moments of lower-level material parameters and the emergent elastic couplings of surface energy. In the present thesis we argue, though, that their derivation unfortunately missed a coupling term between curvature and tilt. The origin of this term is the change of transverse distances due to the variation in the curvature along the membranes. This change gives rise to a contribution to the energy which was believed to be small, but nevertheless ends up contributing at the same (quadratic) order as other terms in their Hamiltonian. We show the immediate consequences of this novel coupling term by by deriving the monolayer and bilayer Euler-Lagrange equations for the tilt, as well as the power spectra of shape, tilt, and director fluctuations.

We also obtain a novel set of terms, quadratic in both curvature and tilt, of which only two were part of the quadratic theory. These biquadratics manifest as geometry-dependent corrections to the tilt modulus, converting it into a position-dependent tilt modulus tensor. For typical material parameters, the resulting effective tilt modulus softens compared to the bare one, except within a small off-center domain of curvatures near the flat state. For sufficiently large curvatures, set by the characteristic length of tilt decay, the effective modulus even becomes negative. We show that biquadratics matter for strongly curved geometries, such as open edges, triple line junctions, fusion stalks, and even bicontinuous phases, and as an illustration we calculate the line tension of edges and junctions.

Acknowledgements

First and foremost, I would like to thank my advisor, Markus Deserno, for everything that he taught me. Without his help and guidance none of this work was possible. His support and understanding for the past five years helped me get through hard times more than once.

I would like to thank my thesis defense committee, John Nagle, Michael Widom, and Dmitry Kopelevich for advice on this thesis. In particular, I would like to thank John Nagle for his interest in my work and all his valuable advice over the years.

Thank you to all past and present members of the Deserno group, especially Patrick, Xin, Nicholas, Zach, and Martina for everything that I learned from them.

I would like to thank Muhittin Mungan, for teaching me physics, being my mentor, being my friend, for his support and guidance, and everything else. I would like to thank KITP for hosting me during the Memory Formation in Matter Program, and to Muhittin Mungan for making my visit to KITP possible.

Thanks to my parents and my brother for their loving support. Without them it would not be possible to complete this thesis.

I would like to thank my family in North America; Ate, Begüm, Berrak, and Can, for the times they made me forget I was away from home.

Thanks to my Pittsburgh friends Onur, Sercan, Günay, Meriç, Volkan, Ekin, Berkin, and Tanmay for making this strange city wonderful. Thanks to Christian for teaching me how to pass clubs and all the other juggling friends for catching clubs together.

Thanks to Ilgım for showing me how to have a conscience.

Thanks to İdil for being my friend despite the distances.

Finally, I would like to thank Lâle for sharing everything.

Contents

Chapter 1

Introduction

Biological systems are highly complex both in composition and behavior. The common approach in biology is to try to explain a given system in its entire complexity. The approach of physics on the other hand is to simplify a complex system to an extent that can be explained by mathematics, the most precise language that we have to describe nature. However, the caveat of simplifying too much is that we may miss interesting behavior along with the complexity. In other words, the physicist's aim should be to simplify the system enough to be accessible mathematically but complex enough to capture the interesting phenomena. Finding this sweet spot boils down to choosing relevant degrees of freedom of the system. To give an example, we can look at the physicists' favorite toy model, the simple harmonic oscillator, which models the one-dimensional movement of a mass attached to a spring. In this model, for *small* displacements, the degree of freedom is the displacement of the system. Even though we know that both the spring and the mass are composed of atoms, those atoms' degrees of freedom are ignored because they are irrelevant to the behavior of the simple harmonic oscillator.

In this thesis work, the systems at hand are lipid membranes and the behavior of interest is their elasticity, *i. e.* how the energetics of membranes depends on geometry and topology changes. Lipid membranes are quasi-two dimensional structures which typically span length scales a couple orders of magnitude larger than their thickness. Therefore, describing them as a two-dimensional surface is a good approximation. Since *geometry* is sufficient to describe a surface, it is also the relevant degree of freedom for the elastic behavior of lipid membranes. Indeed, the curvature elastic description, *i. e.* the Helfrich theory [Hel73], has been used successfully for more than forty years to explain the energetics of lipid membranes. However, for highly curved membranes, a description based on geometry alone breaks down. For those structures, we need to consider what is going on inside the membrane, *i. e.* what the lipids are doing. Probably the most prominent internal degree of freedom is *lipid tilt*, which measures the deviation of the average lipid orientation from the average membrane normal. Here, we will focus on curvature-tilt theory for lipid membranes.

Once we choose the relevant degree of freedom for our system, the next matter to decide on should be the way to proceed. Here, we have two options. The first one is to take a top-down

approach which uses relevant degrees of freedom to postulate a macroscopic theory. This theory is written as an expansion in terms of the relevant degrees of freedom (and their derivative) and includes only the terms allowed by the symmetries of the system. One of the limitations of this approach is that, because it ignores the underlying theory, we are not able to predict the parameters themselves. Therefore, the parameters at the macroscopic level need to be measured. Alternatively we can take a bottom-up approach which starts from an underlying theory to get to a macroscopic description of the system. This way we link the large scale theories with the small scale descriptions and thus elucidate the dependence of the larger scale parameters on the microscopic foundation.

In this thesis, we will take a bottom-up approach to curvature-tilt theories of lipid membranes. We will begin by a review of essential differential geometry which will be followed by a discussion of lipid membranes in Chapter 2. As an illustration, we will derive the curvature theory by both top-down and bottom-up approaches. Then in Chapter 3, we will again use both approaches to derive the quadratic curvature-tilt theory, and demonstrate the power of the bottom-up approach. Subsequently, we will look at the immediate consequences of the quadratic theory in Chapter 4. Finally, we will derive the higher order curvature-tilt couplings using the bottom-up approach and look at the applications of this theory in Chapters 5 and 6, respectively.

Chapter 2

Differential geometry of surfaces and elasticity: Derivation of Helfrich theory

In this Chapter, the curvature elastic theory for lipid membranes, widely referred as to the Helfrich Hamiltonian, will be reviewed. The Helfrich Hamiltonian represents the elastic energy of lipid membranes in terms of the curvature of the membrane surface. Before presenting the derivation, we will introduce the essential differential geometry and some physical properties of lipid membranes. Because the tools that we use for ordinary calculus in Euclidean space are not enough to tackle curved surfaces, we need to use a generalization of these tools—differential geometry.

After having the necessary mathematics at our disposal, we will derive the Helfrich Hamiltonian using top-down and bottom-up approaches. Both paths will lead to the same energy functional, as we expect, but there are interesting conceptual differences. The top-down approach is straightforward and doesn't require much calculation. In contrast, the bottom-up approach permits us to derive the curvature elastic energy starting from an underlying theory which offers more knowledge at the expense of significantly more work. To do this, we will first need to derive the three-dimensional elastic energy density of a thin film starting from a general elastic theory. Then, we will find the relationship between strain terms in the energy density and curvatures of the membranes surface. After dimensional reduction, we will arrive at the curvature elastic theory for monolayers. Finally, the bilayer energy density will be derived by adding the energies of individual leaflets.

2.1 Differential Geometry of Surfaces

In this section, we review some fundamental results in differential geometry of surfaces. The intent of this section is not to cover the whole topic but to introduce the necessary tools for us to develop the elasticity of fluid membranes. More complete discussions can be found in a review paper by Deserno [Des15] or in differential geometry textbooks by Kreyszig [Kre59], do Carmo [dC76], Schutz [Sch80], Spivak [Spi79], and Frankel [Fra11].

The geometry of two-dimensional surfaces embedded into three-dimensional space can be represented by their metric and curvature tensors. Before defining them, we start with a general parametrization of a surface. While this helps keeping things concrete, the ultimate goal is nevertheless to derive general relations that are parametrization free.

First, we introduce a local coordinate system on the surface: $\{u^1, u^2\}$. Each point on a two-dimensional coordinate domain then maps to a point on the surface, embedded in three-dimensional space

$$\boldsymbol{X}(u^1, u^2) = \begin{pmatrix} X(u^1, u^2) \\ Y(u^1, u^2) \\ Z(u^1, u^2) \end{pmatrix} , \tag{2.1}$$

where the bold-face font $\boldsymbol{X}(u^1, u^2)$ means that it is a vector in three-dimensional space. A pair of tangent vectors in the direction of the two surface coordinates u^α is defined as

$$\boldsymbol{e}_\alpha := \frac{\partial \boldsymbol{X}}{\partial u^\alpha} = \partial_\alpha \boldsymbol{X} , \tag{2.2}$$

where $\alpha \in \{1, 2\}$. The set of tangent vectors $\{\boldsymbol{e}_1, \boldsymbol{e}_2\}$ spans the local tangent plane to the surface. We can extend these two vectors into a local basis for three-dimensional space by defining the local surface normal

$$\boldsymbol{N} := \frac{\boldsymbol{e}_1 \times \boldsymbol{e}_2}{|\boldsymbol{e}_1 \times \boldsymbol{e}_2|} , \tag{2.3}$$

By construction, the normal vector has length one: $\boldsymbol{N} \cdot \boldsymbol{N} = 1$. However, the tangent vectors are not necessarily unit vectors, nor are they necessarily orthogonal to each other. Let us hence define the *metric tensor* as the dot product of the tangent vectors,

$$g_{\alpha\beta} := \boldsymbol{e}_\alpha \cdot \boldsymbol{e}_\beta . \tag{2.4}$$

In the case of orthonormal tangent vectors, the metric tensor is equal to the identity. The difference between the identity and the metric tensor is a measure of the "lack of orthonormality" of the tangent vectors. The metric tensor, $g_{\alpha\beta}$, is the first fundamental form of the surface. It is symmetric in the exchange of two indices, $g_{12} = g_{21}$ and its inverse $g^{\alpha\beta}$ is defined via the condition

$$g^{\alpha\beta} g_{\gamma\beta} := \delta^\alpha_\gamma , \tag{2.5}$$

where we also employed Einstein's summation convention over double indices—one up and one down. The components of the inverse metric tensor easily found to be

$$g^{\alpha\beta} = \frac{1}{g} \begin{pmatrix} g_{22} & -g_{12} \\ -g_{21} & g_{11} \end{pmatrix} , \tag{2.6}$$

where g is the determinant of the metric

$$g = \det g_{\alpha\beta} = g_{11} g_{22} - g_{12} g_{21} . \tag{2.7}$$

The determinant of the metric tensor can also be written as the square of the cross product of tangent vectors

$$g = |\boldsymbol{e}_1 \times \boldsymbol{e}_2|^2 \ . \tag{2.8}$$

This relation helps us to write the area element on the surface in terms of the determinant of its metric

$$\mathrm{d}A = \left|\boldsymbol{e}_1 \mathrm{d}u^1 \times \boldsymbol{e}_2 \mathrm{d}u^2\right| = \sqrt{g}\, \mathrm{d}u^1 \mathrm{d}u^2 \ . \tag{2.9}$$

Using the metric tensor and its inverse, we can create covariant and contravariant versions of vectors

$$V^\gamma = g^{\alpha\gamma} V_\alpha \ , \quad \text{and} \quad Y_\gamma = Y^\alpha g_{\alpha\gamma} \ . \tag{2.10}$$

Let us define the second fundamental form

$$K_{\alpha\beta} = \boldsymbol{e}_\alpha \cdot \partial_\beta \boldsymbol{N} \ . \tag{2.11}$$

which is also called the *curvature tensor*. We know that the normal vector is perpendicular to the tangent vectors, $\boldsymbol{e}_\alpha \cdot \boldsymbol{N} = 0$. The derivative of this relation leads to $\boldsymbol{e}_\alpha \cdot \partial_\beta \boldsymbol{N} = -\boldsymbol{N} \cdot \partial_\beta \boldsymbol{e}_\alpha$, and hence Eq (2.11) is also written as

$$K_{\alpha\beta} = -\boldsymbol{N} \cdot \partial_\beta \boldsymbol{e}_\alpha \ , \tag{2.12}$$

Because the tangent vector can be written as a derivative of a vector $\boldsymbol{X}$, the curvature tensor becomes $K_{\alpha\beta} = -\boldsymbol{N} \cdot \partial_\alpha \partial_\beta \boldsymbol{X}$. Since partial derivatives commute, $K_{\alpha\beta}$ is symmetric under exchange of indices. Total and Gaussian curvatures are defined as the trace and determinant of the "mixed" curvature tensor K_α^β,

$$K = \ \mathrm{Tr}(K_\alpha^\beta) \ = g^{\alpha\beta} K_{\alpha\beta} \ , \tag{2.13a}$$

$$K_\mathrm{G} = \det(K_\alpha^\beta) = \tfrac{1}{2} \varepsilon^{\alpha\gamma} \varepsilon_{\beta\delta} K_\alpha^\beta K_\gamma^\delta \ , \tag{2.13b}$$

where ε^{ij} is the (contravariant) *Levi-Civita tensor density*.[1] The total and Gaussian curvatures can be written in terms of principle curvatures, which are the eigenvalues of K_α^β: c_1 and c_2, $K = c_1 + c_2$ and $K_\mathrm{G} = c_1 c_2$.

One of the important aspects in differential geometry is the need to introduce covariant derivatives. The regular derivative of a vector does not transform as a tensor. This for instance means that the partial derivative of a tangent vector, $\partial_\alpha \boldsymbol{e}_\beta$, is not a tensor. We want a derivative operator that gives us a tensor upon applying it to a vector, or indeed to any higher order tensor.

[1] The Levi-Civita *symbol* ϵ_{ij} is defined such that $\epsilon_{11} = \epsilon_{22} = 0$ and $\epsilon_{12} = -\epsilon_{21} = 1$. The placement of the indices is irrelevant, since this is merely a set of numbers, and so we can also write the symbol as ϵ^{ij}. In contrast, the Levi-Civita *tensor density* is defined as $\varepsilon_{ij} = \sqrt{g}\, \epsilon_{ij}$. This also implies $\varepsilon^{ij} = \epsilon^{ij}/\sqrt{g}$, showing that the placement of indices is now important. Three useful identities are $\varepsilon^{ij}\varepsilon_{ij} = 2$, $\varepsilon^{ij}\varepsilon_{ik} = g_k^j \equiv \delta_k^j$ (*i. e.*, the Kronecker-delta), and $\varepsilon_{ij}\varepsilon_{kl} = g_{ik}g_{jl} - g_{il}g_{jk}$.

The solution to this problem is introducing the *covariant derivatives*

$$\nabla_\beta V^\alpha = \partial_\beta V^\alpha + V^\gamma \Gamma^\alpha_{\beta\gamma} \,, \tag{2.14a}$$

$$\nabla_\beta V_\alpha = \partial_\beta V_\alpha - V_\gamma \Gamma^\gamma_{\beta\alpha} \,, \tag{2.14b}$$

where $\Gamma^\alpha_{\beta\gamma}$ is the Cristoffel symbol of the second kind. It is called a symbol because it is not a tensor. We already mentioned that the partial derivative $\partial_\alpha V^\beta$ also is not a tensor. However, the sum on the right hand sides of Eqs 2.14 are proper tensors.

The normal vector is a unit vector and is perpendicular to the tangent vectors, $\boldsymbol{N} \cdot \boldsymbol{N} = 1$ and $\boldsymbol{N} \cdot \boldsymbol{e}_\alpha = 0$. Taking covariant derivatives of these two equations and comparing with the definition of the curvature tensor, we arrive at two very useful equations. The equation of Weingarten

$$\nabla_\alpha \boldsymbol{N} = K^\beta_\alpha \boldsymbol{e}_\beta \,, \tag{2.15}$$

and the equation of Gauss

$$\nabla_\alpha \boldsymbol{e}_\beta = -K_{\alpha\beta} \boldsymbol{N} \,. \tag{2.16}$$

As opposed to the regular derivatives, the covariant ones do not necessarily commute and the commutation relation gives us the Riemann curvature tensor $R_{\alpha\beta\gamma\delta}$,

$$[\nabla_\alpha, \nabla_\beta] V_\gamma = \nabla_\alpha \nabla_\beta V_\gamma - \nabla_\beta \nabla_\alpha V_\gamma = R_{\alpha\beta\gamma\delta} V^\delta \,, \tag{2.17}$$

where in two-dimensions, the Riemann curvature tensor is written in terms of the Gaussian curvature and the metric tensor,

$$R_{\alpha\beta\gamma\delta} = K_\mathrm{G} [g_{\alpha\gamma} g_{\beta\delta} - g_{\alpha\delta} g_{\beta\gamma}] \,. \tag{2.18}$$

Then, in two-dimensions Eq (2.17) become,

$$[\nabla_\alpha, \nabla_\beta] V_\gamma = K_\mathrm{G} [g_{\alpha\gamma} g_{\beta\delta} - g_{\alpha\delta} g_{\beta\gamma}] V^\delta \,. \tag{2.19}$$

The commutation of a covariant derivative is proportional to the Gaussian curvature.

In order for a metric and a curvature tensor to describe a surface, integrability conditions must be satisfied. These are very useful equations.[2] The first one is called the Codazzi-Mainardi equation

$$\nabla_\alpha K_{\beta\gamma} - \nabla_\beta K_{\alpha\gamma} = 0 \,, \tag{2.20}$$

and the second one is known as the equation of Gauss[3]

$$K_{\alpha\beta} K_{\gamma\delta} - K_{\alpha\delta} K_{\beta\gamma} = R_{\alpha\beta\gamma\delta} \,, \tag{2.21}$$

[2] Derivation of these equations are lengthy and beyond the scope of this section. However, they are derived from normal and tangential components of the equality $\partial_\alpha \partial_\beta \boldsymbol{e}_\gamma = \partial_\beta \partial_\alpha \boldsymbol{e}_\gamma$.

[3] Both Eq (2.16) and Eq (2.21) are named after the pioneer of this field, Carl Friedrich Gauss.

where $R_{\alpha\beta\gamma\delta}$ is the Riemann tensor. The single and double contractions of this equation of Gauss lead to the identities

$$K_{\mathrm{G}} g_{\alpha\beta} = R_{\alpha\beta} = K K_{\alpha\beta} - K_{\gamma\alpha} K^{\gamma}_{\beta} \,, \tag{2.22a}$$

$$2K_{\mathrm{G}} = K^2 - K_{\gamma\alpha} K^{\gamma}_{\alpha} \,, \tag{2.22b}$$

where we use again the fact that in two-dimensions, the Riemann curvature tensor is written in terms of the Gaussian curvature and the metric tensor as given in Eq (2.18).

2.2 Fluid Lipid Membranes

In the previous section, we compiled some mathematical tools to use while modeling lipid membranes. However, before starting the physical modeling, we should first briefly look at membranes and their properties. A detailed discussion of the structure and dynamics of membranes can be found in [LS95].

Biological membranes are entities that separate the cell from its environment. In eukaryotes, membranes also divide the cells into compartments with distinct biochemical properties, these are called organelles. The exchange of molecules between these different compartments is highly regulated by the cell. The separation of the intracellular environment from its surroundings by a membrane is a crucial ingredient for the origin of life, as the survival and self-replication of the hereditary materials depends on it.

The biological functions of membranes are not limited to compartmentalization or molecular exchange. Signal transduction and mechanical support for polymer networks are other examples of the diverse functions of biological membranes. In order to provide these diverse functions, the compositions of the membranes have to be adjusted to the task at hand. However, the basic structure always rests on the same basic motif: lipids bilayers.

Lipids are amphiphilic molecules that consist of two parts. A hydrophilic part—called the *head group*, and a hydrophobic *tail* that (usually) consists of two hydrocarbon chains. Due to its amphiphilic nature, in aqueous solutions lipids self-assemble into bilayers. Bilayers can span dimensions a couple of orders of magnitude larger than their thickness. Therefore, they are quasi two-dimensional structures. In addition, above a certain temperature, lipid bilayers are two-dimensional fluids, in other words, the lipids move freely inside the bilayer but cannot escape from it. Moreover, each lipid within the bilayer can change its direction with respect to the membrane surface. This behavior is related with the *lipid tilt* which we will formally define later.

2.3 Curvature Theory: Top-down Approach—Helfrich Theory

In the previous section, we talked about the physical properties of lipids and membranes. With the insight from these physical properties, we start reviewing the elasticity of lipid membranes by

deriving the curvature elastic energy by using a top-down approach. On the macroscopic scales, lipid membranes are quasi-two-dimensional structures which are just a few nanometers thick, but easily span the size of a cell—thousands of times bigger. Therefore, at large scales lipid membrane elasticity is an essentially *geometric* problem. The membrane can be conceptualized as a two-dimensional surface.

As we have seen, the geometry of any smooth two-dimensional surface can be represented by its metric tensor and its curvature tensor. The membrane elastic energy is a scalar and it must be a functional of scalars. The only scalars constructed by using the metric and curvature tensors up to quadratic order in curvature are

$$1, \quad K\,, \quad K^2\,, \quad \text{and} \quad K_{\mathrm{G}}\,. \tag{2.23}$$

All the other symmetrically allowable scalars can be constructed from these. In principle, the energy density also includes the derivatives of the relevant fields. However, in our case, the derivative of curvature, $\nabla_\alpha K$, has a free index which must be contracted with another object. The lowest order allowable term is $\nabla_\alpha K \nabla^\alpha K$ which is of the fourth order in inverse length, and so we will neglect it.

Finally, the integration of the energy density over the area of the reference surface of the membrane gives the elastic energy

$$\mathcal{H} = \int \mathrm{d}A \big\{ \frac{1}{2}\kappa (K - K_0)^2 + \overline{\kappa} K_{\mathrm{G}} \big\}\,, \tag{2.24}$$

where κ is the total curvature modulus, $\overline{\kappa}$ is the Gaussian curvature modulus, and K_0 is the spontaneous curvature. Eq (2.24) is widely referred as the "Helfrich Hamiltonian", and has indeed been a cornerstone of lipid membrane theory [Can70, Hel73]. For symmetric bilayers, spontaneous curvature must be zero.

This top-down derivation of membrane elasticity is quick and straightforward. Notice, though, that this approach does not give us any information about the elastic parameters κ, $\overline{\kappa}$ and K_0. If we wish to derive them, then we need a more detailed theory underlying Eq (2.24), and we must then understand how that more detailed theory gives rise to the Helfrich Hamiltonian. In the next section, we demonstrate the bottom-up approach for curvature elastic theory for membranes, which is a way for achieving this goal.

2.4 Bottom-up Approach to Curvature Elastic Theory: Elasticity and Membranes As Thin Plates

To illustrate the power of the bottom-up approach and how it differs from the top-down approach, we will derive the curvature elastic energy, Eq (2.24), from the underlying elastic theory. First, we start with the most general three dimensional energy density which is quadratic in strains.

Then, we will apply the symmetries of the membrane and use the fluidity and thin plate assumptions to find the three-dimensional energy density for lipid membranes. After that point, our task is to represent all the terms in that energy density in terms of geometry of a reference surface so that the integral of the three-dimensional energy density in the transverse direction gives us the surface energy. The following analysis rests on work by Hamm and Kozlov [HK00] and some parts of the following section are adopted from Terzi and Deserno [TD18].

2.4.1 Three-dimensional elastic energy density

The most general expression for the elastic energy density quadratic in strain, u_{ij} in three-dimensions can be written down as

$$e_{\text{3d}} = \frac{1}{2}\lambda_{ijkl}\, u_{ij} u_{kl} \,, \tag{2.25}$$

where λ_{ijkl} is the elastic modulus tensor [LL86]. Without loss of generality, the exchange symmetries $i \leftrightarrow j$, $k \leftrightarrow l$, and $ij \leftrightarrow kl$ can be assumed, leaving at most 21 independent components. But we want to use this expression for the energy of a fluid lipid monolayer, and in that case additional symmetries reduce the number of components much further [HK00, CAMK14].

Assume the leaflet lies in the xy-plane. First of all note that the two reflection symmetries $(x, y, z) \to (-x, y, z)$ and $(x, y, z) \to (x, -y, z)$ imply that neither an x- nor a y- index can occur in λ_{ijkl} an odd number of times. Curiously, this implies that the same must hold for the z-index, even though a monolayer does *not* have an up-down reflection symmetry that would enforce this all by itself. Furthermore, one consequence of in-plane isotropy is that the x- and the y-directions are indistinguishable, and so their λ-coefficients must be equal. This already massively reduces the permissible terms to the following six:

$$\begin{aligned} e_{\text{3d}} = {} & \frac{1}{2}\lambda_{xxxx}\big(u_{xx}^2 + u_{yy}^2\big) + \lambda_{xxyy} u_{xx} u_{yy} + 2\lambda_{xyxy} u_{xy}^2 \\ & + \lambda_{xxzz}\big(u_{xx} + u_{yy}\big) u_{zz} + 2\lambda_{xzxz}\big(u_{xz}^2 + u_{yz}^2\big) + \frac{1}{2}\lambda_{zzzz} u_{zz}^2 \,, \end{aligned} \tag{2.26}$$

where the prefactors account for obvious permutation multiplicities—such as $\lambda_{xyxy} = \lambda_{yxyx} = \lambda_{xyyx} = \lambda_{yxxy}$. It is now useful to rework the quadratic strain expressions in the following way:

$$\begin{aligned} e_{\text{3d}} = {} & \frac{1}{2}\lambda_{xxxx}\big(u_{xx} + u_{yy}\big)^2 + \big(\lambda_{xxyy} - \lambda_{xxxx}\big)\big(u_{xx} u_{yy} - u_{xy}^2\big) \\ & + \big(2\lambda_{xyxy} + \lambda_{xxyy} - \lambda_{xxxx}\big)\, u_{xy}^2 \\ & + \lambda_{xxzz}\big(u_{xx} + u_{yy}\big) u_{zz} + 2\lambda_{xzxz}\big(u_{xz}^2 + u_{yz}^2\big) + \frac{1}{2}\lambda_{zzzz} u_{zz}^2 \,. \end{aligned} \tag{2.27}$$

At this point we can exploit full in-plane rotational symmetry. The first two strain terms in Eq (2.27) are quadratic invariants under in-plane rotation: they are (i) the square of the trace and (ii) the determinant of the strain tensor's xy-subspace, respectively. But the term in the second line is not an invariant, and there is no term left to combine it with to remedy this flaw; hence,

this term must vanish

$$\lambda_{xxyy} - \lambda_{xxxx} = 2\lambda_{xyxy} \,. \tag{2.28}$$

The resulting energy density is given as [LL86, HK00]

$$\begin{aligned} e_{\text{3d}} = \frac{1}{2}\lambda_{xxxx}\big(u_{xx}+u_{yy}\big)^2 + \big(\lambda_{xxyy}-\lambda_{xxxx}\big)\big(u_{xx}u_{yy}-u_{xy}^2\big) \\ + \lambda_{xxzz}\big(u_{xx}+u_{yy}\big)u_{zz} + 2\lambda_{xzxz}\big(u_{xz}^2+u_{yz}^2\big) + \frac{1}{2}\lambda_{zzzz}u_{zz}^2 \,, \end{aligned} \tag{2.29}$$

which agrees with the energy density for crystals that have hexagonal symmetry (C^6), as shown in Chapter 10 of Landau and Lifshitz [LL86]. It turns out that the in-plane (xy-plane) elasticity can be determined by only two elastic moduli like an isotropic body. Therefore, the elastic properties of a hexagonal crystal and an in-plane isotropic body (C^6 and C^∞ symmetries) agree in the xy-plane.

Next, recall that we intend to describe a *thin* leaflet, which has the following consequence: the normal stress σ_{zz} at the leaflet's upper and lower surface vanishes if the surface is free, but since the leaflet is thin, σ_{zz} does not have much opportunity to considerably grow anywhere within the material. We will hence assume that it vanishes *throughout* the material, and this implies

$$0 \stackrel{!}{=} \sigma_{zz} = \frac{\partial e_{\text{3d}}}{\partial u_{zz}} = \lambda_{xxzz}\big(u_{xx}+u_{yy}\big) + \lambda_{zzzz}u_{zz} \,, \tag{2.30}$$

and this means that the in-plane and transverse strains are related by

$$u_{zz} = -\frac{\lambda_{xxzz}}{\lambda_{zzzz}}\big(u_{xx}+u_{yy}\big) \,. \tag{2.31}$$

Finally, we look at the fluid behavior of lipid membranes. Fluid materials do not have a resistance to shear stress and this is incorporated into the theory by insisting that the shear modulus, which is the ratio of shear stress and shear strain, vanishes. The quadratic shear strain is given as the contraction of the deviatory part of the in-plane strain tensor with itself. The in-plane strain tensor can be written as the sum of pure contraction and pure shear parts

$$u_\alpha^\beta = \frac{1}{2}u_\gamma^\gamma\delta_\alpha^\beta + \big(u_\alpha^\beta - \frac{1}{2}u_\gamma^\gamma\delta_\alpha^\beta\big) \,, \tag{2.32}$$

where the second term on the right hand side is the traceless deviatory part of the in-plane strain tensor. The contraction with itself is [LL86, HK00]

$$\big(u_\alpha^\beta - \frac{1}{2}u_\gamma^\gamma\delta_\alpha^\beta\big)\big(u_\beta^\alpha - \frac{1}{2}u_\nu^\nu\delta_\beta^\alpha\big) = \frac{1}{2}\big[(u_\alpha^\alpha)^2 - 4\det u_\alpha^\beta\big] \,. \tag{2.33}$$

Then, we can rearrange the energy density as

$$e_{\text{3d}} = \frac{1}{2}\tilde{E}(z)\big(u_\alpha^\alpha\big)^2 + \frac{1}{4}\lambda_{\text{s}}(z)\big((u_\alpha^\alpha)^2 - 4\det u_\alpha^\beta\big) + 2\lambda_{\text{t}}(z)\big(u_{xz}^2+u_{yz}^2\big) \,, \tag{2.34}$$

where we define or rename the three-dimensional elastic parameters,

$$\tilde{E}(z) = \frac{1}{2}\lambda_{xxxx} + \frac{1}{2}\lambda_{xxyy} - \frac{\lambda_{xxzz}^2}{\lambda_{zzzz}}\,, \tag{2.35}$$

$$\lambda_{\mathrm{s}}(z) = \lambda_{xxxx} - \lambda_{xxyy}\,, \tag{2.36}$$

$$\lambda_{\mathrm{t}}(z) = \lambda_{xzxz}\,. \tag{2.37}$$

The elastic moduli $\tilde{E}$, λ_{s} and λ_{t} are not assumed to be constant in the transverse direction z because lipid membranes are not uniform in the transverse direction, *i. e.*, lipid tails and head groups do not necessarily have the same elastic properties.

Lateral prestress distribution

Curvature and tilt create area strains, which in turn will result in local stresses. However, there is a second source of *intrinsic* stress in a lipid monolayer which exists even in the absence of curvature and tilt, *i. e.*, even for the flat untilted state. Its origin is the concentration of a large interfacial free energy over a very narrow but chemically inhomogeneous region, which leads to a spatially varying profile with local lateral pressures corresponding to many hundreds of atmospheres [SBSG90, Saf94, BS95, Mar96, Can97, Can99]. Let us denote this stress as a function of depth z in the flat monolayer by the function $\sigma_0(z)$, whose most notable feature is a large positive stress located at the hydrophilic-hydrophobic interface within the lipid (*i. e.*, roughly at a lipid's glycerol backbone), and a weaker negative stress (*i. e.*, positive pressure) in the tail region, where lipids are compressed.

Crucially, this stress contributes a new term to the elastic energy which is *linear* in the area strain, $\epsilon(\zeta)$:

$$e_{\text{3d,pre-stress}} = \sigma_0(z(\zeta))\epsilon(\zeta)\,. \tag{2.38}$$

Since we defined the stress profile in the flat untilted state, we also need to convert between the coordinates z and ζ which are the transverse coordinates on the flat and deformed monolayer, respectively. We will explain differences between these two coordinates in more detail later in this section. However, due to the illustrative purpose of this section, we assume $\zeta(z) \approx z$ and derive the relation later in Chapter 3. Let us look closer to the lateral stress profile and how $\sigma_0(z)$ looks for a membrane.

First, consider that there is the equivalent of a hydrophilic-hydrophobic interface at the backbone of a lipid, and so roughly at that height in the monolayer we have a relatively large lateral tension. This is where the bilayer is being pulled together, where the effect is localized that gives rise to a membrane in the first place. As a consequence, both the tails and the heads of the lipids are now being compressed, leaving us with a positive pressure (or negative tension) in the tail and upper head region that strives to expand the leaflet. For a membrane that is not subject to a net lateral tension, these stresses must balance, such that the net total stress (the integral over $\sigma_0(z)$) vanishes, thereby setting the equilibrium area per lipid. Hence, we expect $\sigma_0(z)$ to be a function that features (positive) peaks near the two hydrophilic/hydrophobic transition regions

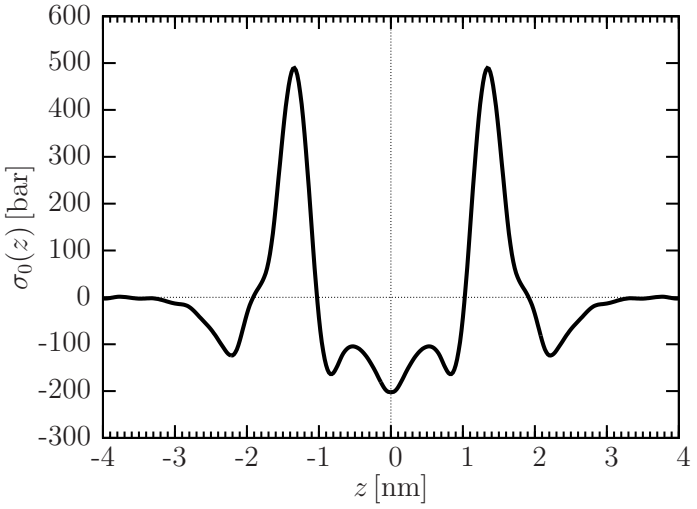

Figure 2.1: Lateral stress profile $\sigma_0(z)$ of a lipid bilayer, using a coarse-grained model of the lipid DMPC (MARTINI force field) at 300 K. This profile is based on simulation results presented in [WD15].

in a lipid bilayer, while being negative both in the center and further out beyond the transition regions, such that the overall positive and negative areas balance.

Figure 2.1 shows the function $\sigma_0(z)$ as measured for a particular lipid membrane model (the MARTINI version of DMPC, at a temperature of 300 K). Our overall expectations are met, even though we could not have anticipated all the extra wiggles. What might look extremely surprising, though, is how very large the effective stresses are: hundreds of bars! However, upon second thought, this makes sense: a typical value for the oil-water surface tension is about $50\,\mathrm{mN/m}$ [GL97]. Chemistry and Figure 2.1 suggest that the transition between the hydrophilic and hydrophobic environment occurs over a region of approximately 1 nm width, and hence the pressure we would expect at the peak is about

$$\sigma_0(z_{\text{peak}}) \sim \frac{50\,\mathrm{mN/m}}{1\,\mathrm{nm}} = 500\,\mathrm{bar}\,. \tag{2.39}$$

Which is very close to what the simulation finds (fortuitously so, of course, but it is only the order of magnitude that counts).

Armed with the new insight that an in-plane lateral stress $\sigma_0(z)$ exists in a lipid membrane, we should amend the monolayer elastic energy from Eq (2.34) with a term that penalizes stretching or compression against that pre-existing stress, which leads to a term that is *linear* in the area strain:

$$e_{\text{3d}} = \sigma_0(z(\zeta))\epsilon(\zeta) + \frac{1}{2}\tilde{E}(z)\big(u_\alpha^\alpha\big)^2 + \frac{1}{4}\lambda_{\text{s}}(z)\big((u_\alpha^\alpha)^2 - 4\det u_\alpha^\beta\big) + 2\lambda_{\text{t}}(z)u_{\alpha z}u^{\alpha z}\,, \tag{2.40}$$

where ζ is also used as transverse coordinate. Here we also defined two more concepts:

1. $z(\zeta)$ is the transverse coordinate z of a piece of material in the flat monolayer as a function of its transverse position ζ in the curved monolayer. Since curving leads to local lateral

stretching or compression, this impacts the transverse coordinates, because the Poisson ratio[4] generally does not vanish—see Eq (2.30). We will soon exploit this to connect z with ζ.

2. $\epsilon(\zeta)$ is the lateral area strain as a function of the curved transverse coordinate ζ. To first order in ζ, it is equal to u^α_α, but at next order it differs. But since this difference takes the form of a lateral shear, which meets no resistance in fluid leaflets, we can ignore it—that's how [HK00] argue. One could also state, though, that the true area strain should linearly couple to the true area stress, and that is why ε should naturally multiply the stress profile σ_0. Of course, the outcome is the same. Also, notice that the difference only matters in the linear (pre-stress) term, because it becomes higher than quadratic order in the already quadratic elastic term.

Note that the three dimensional energy density given in Eq (2.40) is a general result. It does not depend on parameters of the two-dimensional theory. In other words, we will use Eq (2.40) for both curvature only theory as well as curvature-tilt theory. The details of choice of parameters for the two-dimensional theory will come to play when we are determining the individual strain terms in Eq (2.40).

2.4.2 Dimensional Reduction—Monolayer Energy

In the previous section, we derived the three-dimensional energy density for lipid membranes as a function of the strain terms. Here, we will derive an expression for the individual strains in Eq (2.40) in terms of membrane curvatures. But before that, we need to apply the fluidity assumption. For the purpose of this chapter, we will assume that the three dimensional lateral shear modulus $\lambda_{\rm s}(z)$ vanishes throughout the membrane due to the fluidity assumption. Therefore, the second term in Eq (2.34) vanishes. However, application of the two-dimensional fluidity assumption is more subtle than just setting $\lambda_{\rm s}$ to zero. In Section 3.2.4.1 we will revisit the fluidity assumption and investigate what happens if we use a more relaxed version of it.

In the curvature elastic theory, lipid membranes are described solely by their geometry, without any in-plane degree of freedom, such as the lipid tilt. Therefore, the transverse shear must be zero, $u_{\alpha z} = 0$, and hence the last term in Eq (2.40) vanishes. Two terms are left to be determined in the energy density, $\epsilon(\zeta)$, and $(u^\alpha_\alpha)^2$. Up to first order in ζ, we have $\epsilon(\zeta) = u^\alpha_\alpha(\zeta)$, but at higher orders they differ [HK00]. We choose the pivotal plane as a reference surface with respect to which the transverse coordinates, z and ζ, are measured. The pivotal plane is the surface whose area does not change upon curvature deformations. Therefore, we know that the area strain vanishes on the reference surface, $\epsilon(\zeta = 0) = 0$ so we have $(u^\alpha_\alpha(\zeta))^2 = \epsilon^2(\zeta) + \mathcal{O}(\zeta^3)$. Therefore,

[4]The Poisson ratio is the measure of the expansion (contraction) perpendicular to the direction of compression (stretching). For isotropic elastic materials, it can be expressed in terms of bulk modulus and shear modulus. Allowable range for Poisson ratio is between -1 and $1/2$. In the incompressibility limit, the Poisson ratio becomes $1/2$. Monolayers are not isotropic, and in principle we can define more than one Poisson ratio. However, only the one that relates change in the transverse direction with the strain in the in-plane directions is important. Furthermore, we assume that lipid membranes are locally incompressible, so we take the Poisson ratio constant and equal to $1/2$ throughout the monolayer.

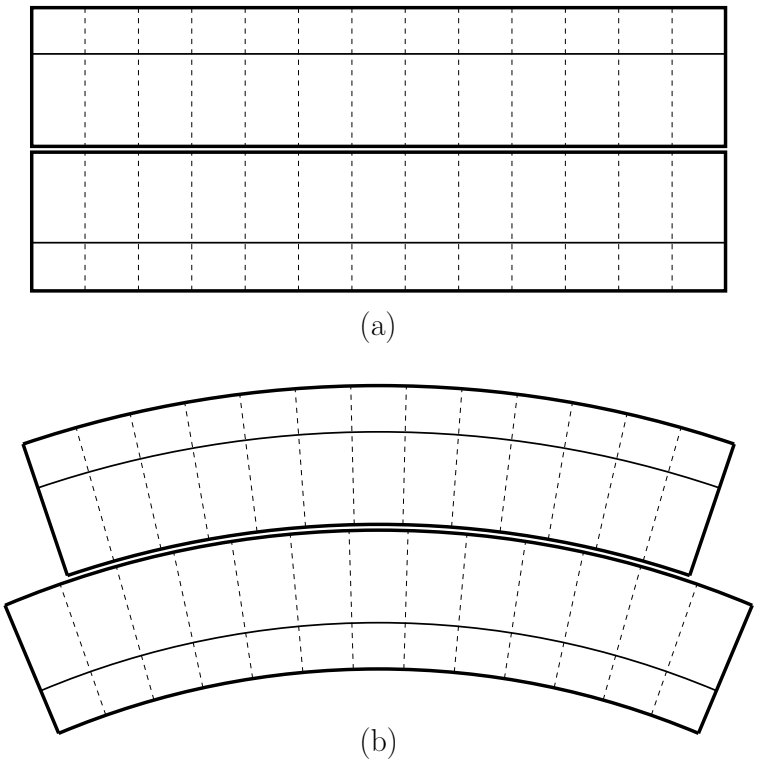

Figure 2.2: Illustration of one-dimensional bending of a bilayer. The panel (a) shows the cross section of a flat bilayer, and panel (b) shows the same cross section after bending. This figure illustrates the stretching towards the bending (upper parts of the monolayers in panel (b)) and the compression inside the curvature (lower parts of monolayers in panel (b)). The solid lines inside both monolayers, which represent the pivotal planes of corresponding monolayer, have the same length in both pictures.

we replace $(u_\alpha^\alpha)^2$ by ϵ^2, and the three-dimensional energy density Eq (2.40) becomes

$$e_{3\mathrm{d}} = \sigma_0(z)\epsilon(\zeta) + \frac{1}{2}\tilde{E}(z)\epsilon^2(\zeta)\ , \tag{2.41}$$

The energy density is now a functional of area strain only. Therefore, we need to determine the area strain in terms of curvatures of the pivotal plane. In order to do that, we need to write down the kinematics and the parametrization for the monolayer.

Parallel surfaces

We choose the flat membrane as the reference configuration where the strain terms vanish. When we curve the membrane, some parts are laterally stretched and some other parts are laterally compressed. These stretchings and compressions cost energy, and the sum of these energy costs gives us the bending energy of the membrane. As illustrated one-dimensionally in Figure 2.2, upon bending, grid size increases towards the curvature, and decreases inside the curved surface. However, there is a surface within a leaflet in which the grid sizes stay constant upon bending. We call this surface the *pivotal plane*, on which strains vanish. We will use the pivotal plane as our reference surface.

For illustrative purposes of this chapter, we assume that the surfaces that are parallel to each other in the flat configuration stay *parallel*. We parametrize the rest of the monolayer using the pivotal plane and the surfaces parallel to it. We say two surfaces are *parallel* if their normal vectors coincide everywhere. Also, we can show that anywhere on the surfaces, the distance between two parallel surface is constant in the direction of the normal vectors. Therefore, the coordinate of any point on the membrane can be written in terms of the coordinate of the pivotal plane:

$$\boldsymbol{X}' = \boldsymbol{X} + z\boldsymbol{N} \,, \tag{2.42}$$

where $\boldsymbol{X}$ is the coordinate of the pivotal plane and $\boldsymbol{X}'$ is the coordinate of a surface parallel to pivotal plane. Therefore, each value of z gives a different surface that is parallel to pivotal plane. The relationship between the pivotal plane and a parallel surface is illustrated in Figure 2.3. Actually, in the present discussion we can assume that the transverse distances does not change upon bending: $\zeta = z$.

The position dependent area strain on a parallel surface can now be written as

$$\epsilon(z) = \frac{\mathrm{d}A' - \mathrm{d}A}{\mathrm{d}A} = \frac{\sqrt{g'}}{\sqrt{g}} - 1 \,, \tag{2.43}$$

where we used the relation $\mathrm{d}A = \sqrt{g}\,\mathrm{d}u^1\,\mathrm{d}u^2$ between the area element $\mathrm{d}A$, the coordinate element $\mathrm{d}u^1\,\mathrm{d}u^2$, and the metric determinant $g = \det(g_{\alpha\beta})$, where $g_{\alpha\beta} = \boldsymbol{e}_\alpha \cdot \boldsymbol{e}_\beta$ is the metric implied by the coordinate basis. Since the metric determinants are related to the cross product of the coordinate basis, we can further calculate

$$\frac{\sqrt{g'}}{\sqrt{g}} = \frac{1}{\sqrt{g}}\left|\boldsymbol{e}_1' \times \boldsymbol{e}_2'\right| \overset{*}{=} \frac{1}{2}\left|\varepsilon^{\alpha\beta}\nabla_\alpha \boldsymbol{X}' \times \nabla_\beta \boldsymbol{X}'\right| \,, \tag{2.44}$$

where $\varepsilon^{\alpha\beta}$ is the (contravariant) Levi-Civita tensor [LR89], and where at "$*$" we used the definition of the coordinate basis, $\boldsymbol{e}_\alpha = \partial\boldsymbol{X}/\partial u^\alpha = \nabla_\alpha \boldsymbol{X}$ (∇_α is the metric-compatible covariant derivative). To work this out, we insert the expression for $\boldsymbol{X}'$ from Eq (2.42), and find the tangent vector on a parallel surface

$$\boldsymbol{e}_i' = \nabla_i(\boldsymbol{X} + \zeta\boldsymbol{N}) = \boldsymbol{e}_i + zK_i^j\boldsymbol{e}_j \,, \tag{2.45}$$

where $K_{ij} = -\boldsymbol{N}\cdot\nabla_i\boldsymbol{e}_j$ is the (extrinsic) curvature tensor, and we find for the metric determinant on the parallel surface

$$\sqrt{g'} = |\boldsymbol{e}_1' \times \boldsymbol{e}_2'| = \sqrt{g}\,(1 + Kz + K_{\mathrm{G}}z^2) \,. \tag{2.46}$$

The definitions of the total curvature K and the Gaussian curvature K_{G} are given in Eqs 2.13. Since $\mathrm{d}A = \sqrt{g}\,\mathrm{d}u^1\mathrm{d}u^2$ and $\mathrm{d}A' = \sqrt{g'}\,\mathrm{d}u^1\mathrm{d}u^2$, Eq (2.44) and (2.46) give the area strain

$$\epsilon(z) = Kz + K_{\mathrm{G}}z^2 \,. \tag{2.47}$$

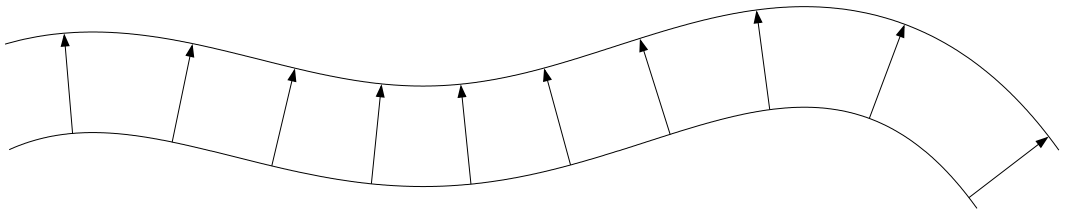

Figure 2.3: Illustration how to create a parallel surface from a reference surface (bottom curve). We obtain the parallel surface by displacing a fixed distance along the local surface normal $\boldsymbol{N}$.

This is remarkable because it is exact.

The total elastic energy of a lipid monolayer is written as the volume integral of the three-dimensional energy density

$$\mathcal{H}_{\mathrm{m}} = \int \mathrm{d}V \, e_{\mathrm{3d}} = \int \mathrm{d}A' \mathrm{d}z \, e_{\mathrm{3d}} \, , \tag{2.48}$$

where $\mathrm{d}A'$ is the area element on the parallel surface. We determine the connection between $\mathrm{d}A'$ and the area element on the pivotal plane, by combining Eq (2.44) and Eq (2.47)

$$\mathrm{d}A' = \mathrm{d}A\big[1 + Kz + K_{\mathrm{G}} z^2\big] \, . \tag{2.49}$$

Then, the elastic energy is written as a surface integral of the two-dimensional energy density

$$\begin{aligned} \mathcal{H}_{\mathrm{m}} &= \int \mathrm{d}A \, e_{\mathrm{2d}} \\ &= \int \mathrm{d}A \, \mathrm{d}z \Big\{ \sigma_0(z) z K + \frac{1}{2} \tilde{E}(z) z^2 K^2 + \sigma_0(z) z^2 K_{\mathrm{G}} \Big\} \, , \end{aligned} \tag{2.50}$$

where the surface energy up to a constant is usually written as

$$e_{\mathrm{2d}} = \frac{1}{2} \kappa_{\mathrm{m}} (K - K_{0,\mathrm{m}})^2 + \overline{\kappa}_{\mathrm{m}} K_{\mathrm{G}} \, , \tag{2.51}$$

from which one identifies the monolayer bending modulus κ_{m}, the monolayer Gaussian curvature modulus $\overline{\kappa}_{\mathrm{m}}$, and the monolayer spontaneous curvature $K_{0,\mathrm{m}}$ as

$$\kappa_{\mathrm{m}} = \int \mathrm{d}z \, \tilde{E}(z) z \, , \tag{2.52}$$

$$\overline{\kappa}_{\mathrm{m}} = \int \mathrm{d}z \, \sigma_0(z) z^2 \, , \tag{2.53}$$

$$-\kappa_{\mathrm{m}} K_{0,\mathrm{m}} = \int \mathrm{d}z \, \sigma_0(z) z \, . \tag{2.54}$$

In Eq (2.51), we derive the monolayer version of the Helfrich Hamiltonian. The derivation of Eq (2.51) is longer and more involved. However, at the end, the bottom-up approach reveals the elastic constants in terms of an underlying theory. For example, Eq (2.53) gives a well known result: the Gaussian curvature modulus is the second moment of the lateral stress profile

[Hel81, HK00].[5]

2.4.3 Bilayer energy

In the previous section we derive the monolayer energy density, and in the present section we will determine the bilayer Hamiltonian by adding the energies of two leaflets. However, we use the pivotal plane as a reference surface for curvatures. The natural reference surface for the bilayer is the mid-plane where two monolayers touch. Therefore, we need to find the relationships between curvatures of the pivotal plane and mid-plane.

While deriving the bilayer Hamiltonian, we change the notation and use the prime for representing the pivotal plane and unprimed objects to represent the mid-plane. Therefore, the coordinate of the pivotal plane is written as

$$\boldsymbol{X}' = \boldsymbol{X} + z_0 \boldsymbol{N} \,, \tag{2.55}$$

where z_0 is the distance between the pivotal plane and the mid-plane.

In order to calculate the relationship between curvatures of two parallel surfaces (with a distance ζ between them), we use the fact that their normal vectors coincide, $\boldsymbol{N} = \boldsymbol{N}'$. We can also write an equality between derivatives of the normal vectors, $\nabla_\beta \boldsymbol{N} = \nabla'_\beta \boldsymbol{N}'$. The latter follows because (i) $\nabla_\beta = \partial_\beta$ when acting on an index-less object; and (ii) $\partial_\beta = \partial'_\beta$, because the coordinates u^i are the same on the primed and unprimed surfaces. Using the Weingarten equation, this now leads to

$$K^\gamma_\beta \boldsymbol{e}_\gamma = K'^\gamma_\beta \boldsymbol{e}'_\gamma \overset{(2.45)}{=} K'^\gamma_\beta (\delta^\delta_\gamma + \zeta K^\delta_\gamma) \boldsymbol{e}_\delta \,. \tag{2.56}$$

Multiplying this with $\boldsymbol{e}^\mu$ yields a relation between the primed and unprimed curvature tensors:

$$K^\mu_\beta = \left(\delta^\mu_\gamma + \zeta K^\mu_\gamma\right) K'^\gamma_\beta =: A^\delta_\gamma K'^\gamma_\beta \,, \tag{2.57}$$

or, as a matrix equation, $\mathbf{K} = \mathbf{A}\mathbf{K}'$. By matrix inversion this gives the new curvature tensor as $\mathbf{K}' = \mathbf{A}^{-1}\mathbf{K}$. Since by definition $\zeta\mathbf{K} = \mathbf{A} - \mathbb{1}$, we readily find $\zeta\mathbf{K}' = \mathbb{1} - \mathbf{A}^{-1}$. To get K', we take the trace, which is coordinate invariant:

$$\zeta K' = \mathrm{Tr}(\zeta\mathbf{K}') = \mathrm{Tr}(\mathbb{1} - \mathbf{A}^{-1}) = 2 - \mathrm{Tr}(\mathbf{A}^{-1}) \,, \tag{2.58}$$

and because our matrices are 2×2 matrices, the trace of the inverse matrix can be written as $\mathrm{Tr}(\mathbf{A}^{-1}) = \mathrm{Tr}(\mathbf{A})/\det(\mathbf{A})$. It is now a simple matter to check that

$$\det(\mathbf{A}) = 1 + \zeta K + \zeta^2 K_\mathrm{G} \,, \tag{2.59}$$

[5] In Chapter 3, we will derive a correction to the second moment condition.

and so we finally arrive at the new curvature

$$K' = \frac{K + 2\zeta K_{\mathrm{G}}}{1 + \zeta K + \zeta^2 K_{\mathrm{G}}} \,. \tag{2.60a}$$

To calculate the new Gaussian curvature is even simpler, because $K'_{\mathrm{G}} = \det(\mathbf{K}') = \det(\mathbf{A}^{-1}\mathbf{K}) = \det(\mathbf{K})/\det(\mathbf{A})$, and so we immediately get

$$K'_{\mathrm{G}} = \frac{K_{\mathrm{G}}}{1 + \zeta K + \zeta^2 K_{\mathrm{G}}} \,. \tag{2.60b}$$

Equations (2.60a) and (2.60b) are the well known transformations of total and Gaussian curvature for parallel surfaces [Wil12, dC76].

We now know the relationship between curvatures and the area element between the pivotal plane and the mid-plane. We need to write the energies of two leaflets in terms of the curvature and the area element of the mid-plane and sum them up. Note that, for the upper leaflet $\zeta = z_0$ and for the lower leaflet $\zeta = -z_0$. Therefore, the bilayer energy density is written up to quadratic order in curvature

$$e_{\mathrm{2d}} = \frac{1}{2}\kappa K^2 + \overline{\kappa} K_{\mathrm{G}} \,, \tag{2.61}$$

where the bilayer bending modulus and Gaussian curvature modulus is found in terms of their monolayer counterparts

$$\kappa = 2\kappa_{\mathrm{m}} \,, \tag{2.62}$$

$$\overline{\kappa} = 2\overline{\kappa}_{\mathrm{m}} - 4\kappa_{\mathrm{m}} K_{0,\mathrm{m}} z_0 \,. \tag{2.63}$$

2.5 Conclusion

We reviewed the basic tools of differential geometry that are necessary for our derivations. Then, we derived the curvature elastic theory for lipid membranes using bottom-up and top-down approaches. The final Hamiltonian for both approaches are in agreement. However, the bottom-up approach additionally reveals the expressions for the elastic constants in terms of the parameters of the underlying theory.

Chapter 3

Quadratic Curvature-Tilt Theory

In Chapter 2, we demonstrate the difference between top-down and bottom-up approaches by deriving the curvature elastic theory for lipid membranes with both approaches. Curvature only theory successfully describes the energetics of lipid membranes at scales mildly exceeding the molecular scale. However, on more local scales geometry must be amended by internal degrees of freedom, of which *lipid tilt* is probably the most prominent one. Tilt essentially describes the extent to which the average lipid orientation deviates from the average membrane normal. As such, it evidently must play a role for highly curved structures such as edges [May00a, AMV$^+$14], pores [AMV$^+$14], and fusion stalks [KZCC01, May02, KK02, KCK02, KESK04], or in the vicinity of transmembrane proteins [MBS99, May00b, AFK$^+$08], or the contact line between two different lipid phases [AKZ$^+$04, KAC$^+$05, AKZC07]. However, it has also been argued that tilt affects shape fluctuations of membranes for wavelengths below about $10\,\mathrm{nm}$ [MNK07b, MNK07a, WPWB11, WBWB12], even though the corresponding curvatures are quite small.

Following a classical top-down physics approach, a shape-centric membrane theory can be upgraded to include tilt essentially by decree: postulate a tilt field, construct all symmetry-permitted scalar terms involving this field and its derivatives (up to some desired order), and decorate each one with its own empirical prefactor. This path has been walked numerous times, and a great deal of fascinating physics phenomenology has been discovered along the way [ML91, NP92, NP93, LM93, PN95, SSN96, SS93, SMS96, MDG05, JHPP07]. However, it is afflicted with the latent danger of missing potential connections between those empirical prefactors—connections that originate from a more microscopic physical underpinning about which larger scale phenomenology is agnostic.

In this chapter we are rather interested in the opposite question: what can a microscopic foundation teach us about coupling constants and their connections on the phenomenological level? The obvious trouble here is that there are many conceivable lower-scale theories to start with, such as molecular-level mean-field [SBSG90, FBS93, MBS99, May00b, May00a, MKBSK04, KGDM16] or free energy [WPWB11, WBWB12, WMAWB13, BCF12] functionals, or approaches based on continuum mechanics [Jen77a, Jen77b, Ste99, BRBM04, DPZ08,

Ste13, MSF13, DZ13, RBA$^+$14, DPZD16, Ste18, Des18]. To keep the framework as universal as possible, we will look at a foundation that *itself* rests on general symmetry principles, while only adding a small but crucial amount of structure. Specifically, we will revisit the influential paper by Hamm and Kozlov ("HK" in the following), who conceptualize a lipid membrane as a thin sheet subject to the most general linear elastic constitutive equation compatible with in-plane fluidity, and amended by a pre-existing trans-membrane stress profile [HK00]. These authors argue that, after dimensional reduction, this ansatz results in a membrane Hamiltonian that amends the curvature-elastic Helfrich functional in two places: first, a tilt field emerges whose excitation is quadratically penalized by a tilt modulus (which turns out to be the only new parameter in this theory); and second, the divergence of the tilt adds to the mean membrane curvature and thus couples tilt to curvature.

HK theory has offered an impressive amount of insight into the microscopic foundations of membrane elasticity, and it has been applied to numerous fascinating situations of practical interest [KZCC01, May02, KK02, KCK02, KESK04, MNK07b, MNK07a, WPWB11, WBWB12, WD16]. But, unfortunately, we will argue that in its existing form the theory is *incomplete*, because of two important reasons: (i) a mesoscopic term that follows from its microscopic underpinning has been missed in the original derivation, and (ii) historically, the way in which the *fluid* nature of lipids is incorporated into the theory requires more general approach than what classical HK theory does.

Making these amendments does not invalidate many of the key insights gained from HK theory, nor does it fundamentally change its structure (even though it breaks an accidental symmetry which the original theory seems to have but which turns out to be spurious). However, our additions have numerous important quantitative and qualitative consequences, both for the resulting shape- and tilt-equations, as well as for the thermal fluctuations which such membranes exhibit, which will be addressed in the next chapter.

In order to illustrate the effectiveness of the bottom-up approach to membrane elasticity, we also derive the elastic energy by the top-down approach and compare the result of the two approaches. This chapter is partially based on work published by Terzi and Deserno [TD17].

3.1 Top-down approach to curvature tilt elastic theory

In the top down approach, the energy functional is basically the collection of all symmetry-permissible scalar terms that are constructed from the relevant fields and their derivatives, up to a certain order. However, first we need to know the ingredients of our theory. For the purpose of this theses, we have already decided that the lipid tilt is the additional degree of freedom to membrane geometry. However, for the top-down approach we neither need to to know the molecular and the physical origin of lipid tilt, nor define it formally in terms of microscopic entities. Therefore, lipid tilt will be postulated on the macroscopic level, and we leave its formal definition in terms of underlying membrane structures to the next section, before going into the bottom-up approach. The two properties of the tilt field that need to be defined are (i) it

is a vector field and (ii) it is confined in the two dimensional membrane surface. The second property allows us to write the tilt field as $\boldsymbol{T}= T^{\alpha}\boldsymbol{e}_{\alpha}$ where $\boldsymbol{e}_{\alpha}$ are the tangent vectors on the membrane surface.

Our gaol in this section is to determine the quadratic curvature-tilt energy density. Therefore, all symmetry-permitted scalar terms up to the quadratic order, either in curvature or tilt field, should go into the energy density with their own prefactor (elastic constant). From Chapter 2, we already know that there are three possible curvature terms up to the quadratic order,

$$1, \quad K, \quad K^2 \quad \text{and} \quad K_{\mathrm{G}}. \tag{3.1}$$

In addition to these curvature terms, we write all the possible tilt terms up to the quadratic order: T^2, $\boldsymbol{\nabla}\cdot\boldsymbol{T}$, $(\boldsymbol{\nabla}\cdot\boldsymbol{T})^2$, $(\boldsymbol{\nabla}\times\boldsymbol{T})^2$ and $T^{\alpha}\nabla_{\beta}\nabla_{\alpha}T^{\beta}$, where ∇_{α} is the covariant derivative and T is the magnitude of the tilt field, $T=|\boldsymbol{T}|=(g_{\alpha\beta}T^{\alpha}T^{\beta})^{1/2}$. However, the term $T^{\alpha}\nabla_{\beta}\nabla_{\alpha}T^{\beta}$ is equal to $(\boldsymbol{\nabla}\cdot\boldsymbol{T})^2$ plus a boundary term and a higher order term. This is due to the commutation relation of the covariant derivatives which is given in Eq (2.19), where in two-dimensions the commutation of covariant derivatives gives us the Gaussian curvature,

$$\begin{aligned} T^{\alpha}[\nabla_{\beta},\nabla_{\alpha}]T^{\beta} &= g^{\beta\gamma}T^{\alpha}[\nabla_{\beta},\nabla_{\alpha}]T_{\gamma} \\ &\overset{(2.19)}{=} g^{\beta\gamma}T^{\alpha}K_{\mathrm{G}}[g_{\alpha\gamma}g_{\beta\delta}-g_{\alpha\delta}g_{\beta\gamma}]T^{\delta} \\ &= -K_{\mathrm{G}}g_{\alpha\delta}T^{\alpha}T^{\delta}=-K_{\mathrm{G}}T^2\,. \end{aligned} \tag{3.2}$$

Therefore, the term $T^{\alpha}\nabla_{\beta}\nabla_{\alpha}T^{\beta}$ is written as,

$$\begin{aligned} T^{\alpha}\nabla_{\beta}\nabla_{\alpha}T^{\beta} &= T^{\alpha}[\nabla_{\beta},\nabla_{\alpha}]T^{\beta}+T^{\alpha}\nabla_{\alpha}\nabla_{\beta}T^{\beta} \\ &\overset{(3.2)}{=} -K_{\mathrm{G}}T^2+\nabla_{\alpha}\big(T^{\alpha}\nabla_{\beta}T^{\beta}\big)-\nabla_{\alpha}T^{\alpha}\nabla_{\beta}T^{\beta}\,. \end{aligned} \tag{3.3}$$

Here, the first term on the right hand side is higher order and the second term can be pushed to boundary upon integration. The last term in Eq (3.3) is indeed equal to $(\boldsymbol{\nabla}\cdot\boldsymbol{T})^2$ so $T^{\alpha}\nabla_{\beta}\nabla_{\alpha}T^{\beta}$ is not an independent scalar. Then, the total list of independent scalar tilt terms is,

$$T^2 \quad , \quad \boldsymbol{\nabla}\cdot\boldsymbol{T} \quad , \quad (\boldsymbol{\nabla}\cdot\boldsymbol{T})^2 \quad \text{and} \quad (\boldsymbol{\nabla}\times\boldsymbol{T})^2\,. \tag{3.4}$$

Moreover, there are curvature-tilt coupling terms. The curvature tensor has two indices and the tilt field has only one index, so in order to have a scalar we need one more index to contract. However, we cannot use one more tilt field because it would make the coupling term higher order in fields. The only way to make the coupling term scalar is contracting it with a derivative, ∇_{α}. Up to a boundary term, there are two ways to contract these four indices, $K\boldsymbol{\nabla}\cdot\boldsymbol{T}$ and $T^{\alpha}\nabla_{\beta}K^{\beta}_{\alpha}$. However, the second one is actually equal to the first one,

$$T^{\alpha}\nabla_{\beta}K^{\beta}_{\alpha}=T^{\alpha}g^{\beta\gamma}\nabla_{\beta}K_{\alpha\gamma}\overset{(2.20)}{=}T^{\alpha}g^{\beta\gamma}\nabla_{\alpha}K_{\beta\gamma}=\boldsymbol{T}\cdot\boldsymbol{\nabla}K\,, \tag{3.5}$$

where we use the Codazzi-Mainardi equation Eq (2.20).

The number of all possible terms up to the quadratic order in both curvature and tilt is eight. Thus, the energy functional for curvature-tilt theory can be written as,

$$\mathcal{H} = \int \mathrm{d}A \Big\{ \frac{1}{2}\kappa(K - K_0)^2 + \overline{\kappa} K_\mathrm{G} + \kappa_\mathrm{ct} K \boldsymbol{\nabla} \cdot \boldsymbol{T} + \frac{1}{2}\kappa_\mathrm{dt}(\boldsymbol{\nabla} \cdot \boldsymbol{T} - K_\mathrm{t})^2 + \frac{1}{2}\kappa_\mathrm{t} T^2 + \frac{1}{2}\kappa_\mathrm{tw}(\boldsymbol{\nabla} \times \boldsymbol{T})^2 \Big\}, \tag{3.6}$$

with the eight elastic parameters: κ, K_0, $\overline{\kappa}$, κ_ct, κ_dt, K_t, κ_t and κ_tw.

The top-down approach gives us the curvature-tilt elastic theory given in Eq (3.6) with little effort. However, this approach does not provide us with any insight about these elastic parameters. Note that, for symmetric bilayers, linear curvature and linear tilt terms disappear, in other words the spontaneous curvature K_0 and the spontaneous tilt divergence K_t must vanish.

3.2 Bottom-up approach to curvature tilt elastic theory: Hamm-Kozlov theory

Bending a thin plate will laterally stretch its outer surface and compress its inner one. Assuming a simple isotropic elastic material, this leads to classical curvature elasticity for thin-plate-bending, including formulas that link the two bending moduli to the material's Young modulus and Poisson ratio [LL86]. HK have extended this calculation [HK00] to a material (namely: a monolayer lipid leaflet) not merely characterized by these two material parameters but instead by an elastic tensor λ_{ijkl}, subject however to all obvious symmetries and the condition of lateral fluidity. Moreover, they added a depth-dependent lateral pre-stress, which originates from the forces that drive self-assembly in the first place [Mar96, Can97, Can99].

Using differential geometric techniques to calculate the strain of a volume element in the leaflet as a function of the leaflet's larger-scale curvature state, followed by a dimensional reduction to the zero-strain reference surface inside the leaflet (also known as the "pivotal plane"), HK arrived at an effective surface functional that accounts for both curvature and tilt. We will first summarize HK's results and point out the benefits of the bottom-up approaches. Then, we revisit the derivation of HK theory and give a detailed explanation of the parts that we disagree with, including their choice for incorporating fluidity, and we argue why this should be generalized—in fact, by employing a formalism also adopted by HK, subsequently discarded by them. Finally, we derive the bilayer Hamiltonian. However, first of all we need to give a definition of the tilt field in terms of microscopic parameters.

3.2.1 Lipid Tilt and Effective Curvatures

Before going into the details of the derivation of the curvature tilt theory, we want to define the lipid tilt more formally. The tilt of a lipid is the projection of the difference between the normal vector of a reference surface and the lipid director onto the reference surface. Therefore,

lipid tilt is a two-dimensional vector field defined on a reference surface of the membrane as the difference between a lipid direction and a surface normal [ML91, HK00],

$$\boldsymbol{T}_{\mathrm{p}} = T_{\mathrm{p}}^{\alpha}\boldsymbol{e}_{\alpha} = \frac{\boldsymbol{n}}{\boldsymbol{N}\cdot\boldsymbol{n}} - \boldsymbol{N}\ , \tag{3.7}$$

where $\boldsymbol{e}_\alpha$ are the tangent vectors, $\boldsymbol{N}$ is the normal of the surface and $\boldsymbol{n}$ is the lipid director. Both the surface normal $\boldsymbol{N}$ and the lipid director have unit length. The subscript 'p' on the tilt field reminds us that it refers to the *pivotal plane*[1] which we use as a reference surface to measure the curvature and the tilt field. For convenience we drop the subscript 'p' and later we will revisit the definition of the tilt field in Section 3.2.5 and calculate the curvature corrections to the tilt field due to a change of reference surface.

The definition in Eq (3.7) makes the transversality of $\boldsymbol{T}$ manifest, since $\boldsymbol{T}\cdot\boldsymbol{N} = 0$ by construction (*i. e.*, independent of any other conditions that would have to hold, such as $\boldsymbol{T}$ being the solution of some Euler-Lagrange equation). Therefore, $\boldsymbol{T}$ has components only in the direction of the surface tangents with the (contravariant) components given as $T^\alpha = \boldsymbol{T}\cdot\boldsymbol{e}^\alpha = g^{\alpha\beta}\boldsymbol{T}\cdot\boldsymbol{e}_\beta$. Also, $\boldsymbol{T}$ is not normalized; instead, its magnitude is $|\boldsymbol{T}| = \tan\theta$, where θ is the tilt angle (*i. e.*, the angle between $\boldsymbol{n}$ and $\boldsymbol{N}$). Alternatively, we can write

$$\frac{1}{\cos\theta} = \frac{1}{\cos\arctan|\boldsymbol{T}|} = \sqrt{1+\boldsymbol{T}^2} = 1 + \frac{1}{2}\boldsymbol{T}^2 + \mathcal{O}\big((\boldsymbol{T}^2)^2\big)\ . \tag{3.8}$$

The relationship between the lipid tilt and transverse shear u_{xz} and u_{yz} is illustrated in Figure 3.1, in which an undeformed (flat) thin plate is illustrated on the left and a deformed thin plate is illustrated on the right hand side. The deformation which is illustrated in Figure 3.1 is related to the fact that the material director of a sheet does not need to coincide with the surface normal, $\boldsymbol{n} \neq \boldsymbol{N}$. In shear deformation plate theories, such a deformation is related to the transverse shear strain. For a lipid monolayer, the tilt-field $\boldsymbol{T}$ that measures the deviation between material director and surface normal so transverse shear components of strain tensor, u_{xz} and u_{yz}, are proportional to the lipid tilt, $u_{\alpha z} \sim T_\alpha$. Hamm and Kozlov uses this proportionality, exact up to the quadratic order, $2u_{\alpha z} = \boldsymbol{T}\cdot\boldsymbol{e}_\alpha$, and this is the origin of a quadratic tilt term in the Hamiltonian. However, we will show later that there is a curvature correction to this relation.

Having defined the tilt field, we can now introduce a useful object that we call the *tilt derivative tensor* $\nabla_\alpha T^\beta$. Finally, the *effective curvature tensor* is defined as the sum of the curvature and the tilt derivative tensor,

$$\tilde{K}_\alpha^{\ \beta} := K_\alpha^\beta + \nabla_\alpha T^\beta\ . \tag{3.9}$$

Note that $\tilde{K}_{\alpha\beta}$ is generally not a symmetric tensor (unlike $K_{\alpha\beta}$), because $\nabla_\alpha T_\beta \neq \nabla_\beta T_\alpha$. This means we must be careful when contracting indices, or when raising one of them: $\tilde{K}_\alpha^{\ \beta}$ is not the same as $\tilde{K}^\alpha_{\ \beta}$. Similar to the total and the Gaussian curvature, the *effective total curvature* and

[1] The detailed definition of the pivotal plane and the reason why we are allowed to define such a surface will be given in Section 3.2.4.

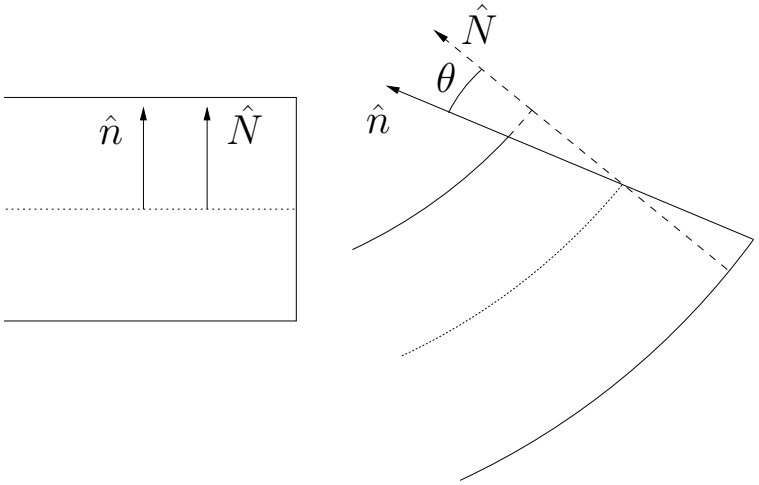

Figure 3.1: The material director $\boldsymbol{n}$ in a flat thin plate is by construction aligned with the local surface normal $\boldsymbol{N}$. But upon bending, $\boldsymbol{n}$ may deviate from $\boldsymbol{N}$ by an angle θ due to transverse shear. (Figure adapted from [Red06].)

the *effective Gaussian curvature* are defined as the trace and determinant of $\tilde{K}_\alpha^{\ \beta}$,

$$\tilde{K} := \mathrm{Tr}\big(\tilde{K}_\alpha^{\ \beta}\big) = g^{\alpha\beta}\tilde{K}_{\alpha\beta} = K + \boldsymbol{\nabla}\cdot\boldsymbol{T}\,, \tag{3.10a}$$

$$\tilde{K}_{\mathrm{G}} := \det\big(\tilde{K}_\alpha^{\ \beta}\big) = \frac{1}{2}\varepsilon^{\alpha\gamma}\varepsilon_{\beta\delta}\tilde{K}_\alpha^{\ \beta}\tilde{K}_\gamma^{\ \delta}\,, \tag{3.10b}$$

where ε^{ij} is the (contravariant) Levi-Civita tensor [LR89].[2] In Section 3.2.2, we will show that, the effective total and Gaussian curvature will replace the total and Gaussian curvature in the HK theory.

3.2.2 Hamm-Kozlov Theory and Its Accidental Symmetry

In their seminal work Hamm and Kozlov (HK) start from the most general three dimensional elastic energy functional which is quadratic in the strain tensor and satisfies three main conditions, as we explained in detail in Section 2.4.1 of Chapter 2. The first condition is in-plane rotational symmetry, which enforces in-plane coordinate isotropy. The second one is local lateral fluidity, which implies that the lateral shear modulus vanishes throughout the membrane.[3] And the third one is the thin plate assumption, which renders the normal stresses zero and, assuming incompressibility,[4] permits the normal strains to be written in terms of the lateral ones.

[2]There is a subtle point worth clarifying: the Levi-Civita *symbol* ϵ^{ij}—defined as $\epsilon^{12} = -\epsilon^{21} = 1$ and $\epsilon^{11} = \epsilon^{22} = 0$—looks like a tensor, but it isn't. It is a tensor *density*. This means that under a coordinate transformation it picks up the Jacobi determinant of the transformation as an additional prefactor [LR89]. But if we divide the Levi-Civita symbol by the square root of the metric determinant, itself a tensor density, we arrive at a proper tensor—the Levi-Civita tensor $\varepsilon^{ij} = \epsilon^{ij}/\sqrt{g}$.

[3]HK call this the assumption of *global lateral fluidity* [HK00]. However, we feel that the word *local* would be more appropriate, because under this assumption the shear modulus vanishes *pointwise* (*i. e.*, locally) throughout the membrane's cross-section, not merely globally as an integral over the shear modulus profile.

[4]Incompressibility amounts to assuming a Poisson ratio of $\nu = \frac{1}{2}$.

The three dimensional energy of a fluid membrane leaflet can now be written as a volume integral over the three dimensional elastic energy density

$$e_{3\mathrm{d}} = \sigma_0(z)\epsilon(\zeta) + \frac{1}{2}\tilde{E}(z)\epsilon(\zeta)^2 + \frac{1}{2}\lambda_{\mathrm{t}}(z)T^2 \,, \tag{3.11}$$

where z is the transverse coordinate in the flat monolayer, ζ is its corresponding counterpart in the curved one, ϵ is the area strain, and $\boldsymbol{T}$ is the tilt field. The elastic moduli $\tilde{E}(z)$ and $\lambda_{\mathrm{t}}(z)$, as well as the lateral stress profile $\sigma_0(z)$, are material parameters that we assume to be given. The lateral stress profile $\sigma_0(z)$ in particular constitutes positionally varying but *pre-existing* stresses in the membrane, against which one does stress-strain work upon membrane deformation. This is why they result in a term that is linear in the area strain ϵ, even in the absence of curvature and tilt. When we compare Eq (3.11) with Eq (2.40), we recognize three differences: (i) HK set the in-plane shear modulus $\lambda_{\mathrm{s}}(z)$ to be zero everywhere, (ii) HK used the fact that $u_\alpha^\alpha = \epsilon(\zeta) + \mathcal{O}(\zeta^2)$ and (iii) HK derived that the transverse shear term is equal to the square of tilt field, $4(u_{xz}^2 + u_{yz}^2) = T^2$. Later in this Chapter, we will revisit point (i), which gets us to the meaning of in-plane fluidity and point (iii), which will clarify the notion of transverse shear strain. In this way we calculate the missing parts of HK theory and consistently determine the complete quadratic curvature-tilt theory.

The only object in Eq (3.11) left to be determined is the area strain $\epsilon(\zeta)$ which is defined as the relative area element change with respect to the reference surface. Hamm and Kozlov parametrized the monolayer and determined the change in the area element everywhere in the monolayer with respect to a reference surface,[5] and they found,

$$\epsilon(z) = z\tilde{K} + z^2\big(\tilde{K}_{\mathrm{G}} - \frac{1}{2}\tilde{K}^2\big) \,, \tag{3.12}$$

where $\tilde{K}$ and $\tilde{K}_{\mathrm{G}}$ are the effective total curvature and the effective Gaussian curvature respectively. In this section, we do not give the derivation of Eq (3.12) but a detailed derivation of the area strain including the missing part by HK will be given in Section 3.2.4. Note that ϵ in Eq (3.12), is given as a function of z not ζ, because HK use the relation between z and ζ which they find using the incompressibility of fluid membranes. Next, the two dimensional energy density is written by integrating the three dimensional energy density along the transverse direction, leading to the surface Hamiltonian

$$\mathcal{H}_{\mathrm{m}} = \int \mathrm{d}A \left\{ \frac{1}{2}\kappa_{\mathrm{m}}\big(\tilde{K} - K_{0,\mathrm{m}}\big)^2 + \overline{\kappa}_{\mathrm{m}}\tilde{K}_{\mathrm{G}} + \frac{1}{2}\kappa_{\mathrm{t,m}}T^2 \right\} , \tag{3.13}$$

[5] As reference surface, HK choose the neutral surface, where the curvature deformations are decoupled from stretching deformations, while we use the pivotal plane, where the area element does not change under curvature deformations [HK00].

where HK define the elastic constants, the bending modulus κ, the spontaneous curvature $K_{0,\mathrm{m}}$, the Gaussian curvature modulus $\overline{\kappa}_{\mathrm{m}}$ and the tilt modulus $\kappa_{\mathrm{t,m}}$ as

$$\kappa_{\mathrm{m}} = [\![\tilde{E}]\!]_2 - [\![\sigma_0]\!]_2 \,, \tag{3.14a}$$

$$-\kappa_{\mathrm{m}} K_{0,\mathrm{m}} = [\![\sigma_0]\!]_1 \,, \tag{3.14b}$$

$$\overline{\kappa}_{\mathrm{m}} = [\![\sigma_0]\!]_2 \,, \tag{3.14c}$$

$$\kappa_{\mathrm{t,m}} = [\![\lambda_{\mathrm{t}}]\!]_0 \,. \tag{3.14d}$$

The useful double bracket notation defines moments of its argument in transverse direction as

$$[\![F]\!]_n = \int \mathrm{d}z \, F(z) z^n \,, \tag{3.15}$$

where the transverse coordinate z measures the distance away from the reference surface. The integral in Eq (3.15) is over the *thickness* of the monolayer, without however having to address the precise notion of "thickness". Technically, the limits of the z integral are $(-\infty, \infty)$, but practically, all observables we care about have non-zero values only in a finite region. The membrane thickness may for instance be defined as the region where the elastic moduli have non-zero values.

The HK Hamiltonian (3.13) has a couple of interesting properties. The most peculiar one is that Eq (3.13) is exclusively a functional of the effective curvature tensor $\tilde{K}_\alpha^{\ \beta}$. In other words, the curvature tensor always appears in the Hamiltonian additively with the tilt derivative tensor, and vice versa. We will call this an *accidental symmetry*, because later we will show that, due to the missing coupling term in the HK theory, this symmetry turns out to be spurious. The existence of this accidental symmetry nevertheless raises the question *what physical symmetry is behind it*. One possible answer to this question comes from an analogy to the curvature-only theory. The curvature tensor of a surface can be written as the derivative of the normal vector on the surface Eq (2.15). A similar expression is written in Eq (C.5) for the lipid director and the effective curvature tensor, $\boldsymbol{e}^\beta \cdot \nabla_\alpha \boldsymbol{n} = \tilde{K}_\alpha^{\ \beta}$. However, later we will show that curvature-tilt coupling, which results from the thickness variation due to deformations, breaks this accidental symmetry.

HK theory is a great example of the power of the bottom-up approach. In HK theory there is only *one* extra elastic constant added to the already existing curvature elastic theory. As we showed in Section 3.1 there are *eight* possible elastic constants in the energy density calculated by the top-down approach, and HK showed that we only need four independent constants, the rest of the elastic parameters are either zero or can be written in terms of others.

3.2.3 Bottom-up approach to curvature tilt elastic theory: Revisiting the quadratic theory

In the previous section, we summarized the results of Hamm and Kozlov, Let us now revisit their derivation and point out where terms went missing in HK's original approach. Firstly, we start

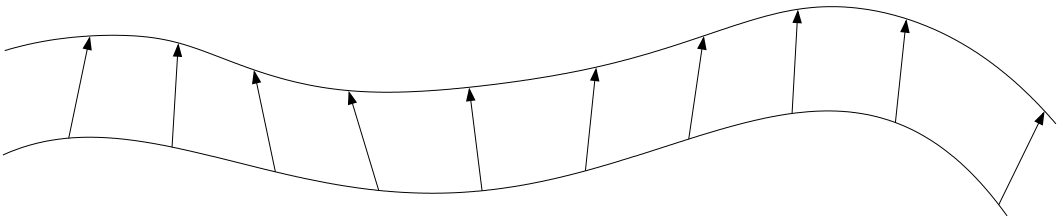

Figure 3.2: Illustration how to create a lipid shifted surface from a reference surface (bottom curve).We obtain a lipid shifted surface by displacing a constant distance along a local director field $\boldsymbol{n}$ which is not necessarily aligned with the surface normal $\boldsymbol{N}$.

with Eq (2.40), the three-dimensional energy density for a monolayer ,

$$e_{3\mathrm{d}} = \sigma_0(z)\epsilon(\zeta) + \frac{1}{2}\tilde{E}(z)\big(\epsilon(\zeta)\big)^2 + \frac{1}{4}\lambda_{\mathrm{s}}(z)\big((u_\alpha^\alpha)^2 - 4\det u_\alpha^\beta\big) + 2\lambda_{\mathrm{t}}(z)[T(z)]^2\,, \quad (3.16)$$

where we use the fact that $u_\alpha^\alpha = \epsilon(\zeta) + \mathcal{O}(\zeta^2)$ for the second term. Eq (3.16) differs from Hamm and Kozlov's three-dimensional energy density Eq (3.11) in both lateral and transverse shear terms. The lateral shear term, the third term in Eq (3.16), is related to the in-plane fluidity assumption, which we will revisit in Section 3.2.4.1. The transverse shear, which is the last term in Eq (3.16), is related to the quadratic tilt field, and we will calculate a correction to HK theory for it in Section 3.2.5. Before calculating both transverse and lateral shear terms in Eq (3.16), we will first drive the area strain $\epsilon(\zeta)$ in Section 3.2.4 and show that it contains a missing curvature tilt coupling term which was neglected in HK theory.

3.2.4 Area strain

The *area strain* $\epsilon(\zeta)$ is the relative change of a local area element between a deformed configuration and an undeformed reference state (which we assume to be the flat unstressed leaflet). This strain arises because curving a leaflet will laterally stretch material elements lying towards the side from which one bends away, and laterally compress material elements on the side one bends towards. This also means that there will be a surface inside the bilayer at which the strain vanishes. This is called the "*pivotal plane*",[6] and we will use it as the reference surface for describing the membrane position. The transverse coordinate ζ then measures the distance of any material element from the pivotal plane along the local lipid direction *in the deformed configuration*. In the *undeformed* reference state, the corresponding distance will be called z.

To derive an *elastic surface energy density*, we must integrate the three dimensional energy density (3.16) across the transverse direction. But before we can do that, we need to (i) find the area strain as a function of membrane curvature and lipid tilt and (ii) determine a relation between the two transverse coordinates ζ and z. To find the area strain, let us define a family of

[6] Strictly speaking, the situation is slightly more subtle: for a flat leaflet we must still distinguish whether or not the lipids are tilted (say, as an intermediate state from flat/untilted to curved/tilted). If they are, this contributes a term $\frac{1}{2}T^2$ to the zeroth order area strain in Eq (2.43). However, up to the quadratic order of HK theory this difference is inconsequential, because it gives rise to terms that are either of higher order or happen to cancel. We will therefore not elaborate on this distinction in the rest of this section. But we will revisit the issue in Chapter 5.

surfaces which we call *lipid shifted surfaces*. These are surfaces with the special property that their pre-image (under the mapping leading to the deformed configuration) is flat and parallel to the pre-image of the pivotal plane in the undeformed configuration. Or, these are the surfaces to which undeformed material planes parallel to the leaflet get mapped under the action of bending and tilting. Hence, any material element in the undeformed leaflet, and its image in the deformed one, can then be parametrized as follows:

$$\boldsymbol{X}_0' = \boldsymbol{X}_0 + z\boldsymbol{N}_0 \,, \tag{3.17a}$$

$$\boldsymbol{X}' = \boldsymbol{X} + \zeta\boldsymbol{n} \,, \tag{3.17b}$$

where the subscript "0" refers to the undeformed configuration. $\boldsymbol{X}$ is the coordinate of the pivotal plane, $\boldsymbol{X}'$ is the coordinate of the lipid shifted surface, and $\boldsymbol{N}_0$ is the normal vector on the pivotal plane in the flat configuration. In Figure 3.2, we illustrate the relation between pivotal plane and a lipid shifted surface. The comparison between parallel surfaces and its generalization, lipid shifted surfaces, is seen by comparing Figure 2.3 and Figure 3.2.

The position dependent area strain on a lipid shifted surface is found in terms of the covariant derivative of $\boldsymbol{X}'$. From combination of Eq (2.43) and Eq (2.44)

$$\epsilon(\zeta) = \frac{1}{2}\varepsilon^{\alpha\beta}\left|\nabla_\alpha \boldsymbol{X}' \times \nabla_\beta \boldsymbol{X}'\right| - 1 \,. \tag{3.18}$$

To work this out, we insert the expression for $\boldsymbol{X}'$ from Eq (3.17b). The only piece that is not straightforward is $\nabla_\alpha\zeta$, which addresses the question how the distance of a given lipid shifted surface from the pivotal plane changes laterally as a consequence of bending and tilting. Consider as an illustration the curved lipid leaflet shown in Fig. 3.3, which results from solving the elastic equations at a given pivotal-plane deformation: the distance between the leaflet's top and bottom surface (which are special cases of lipid shifted surfaces) from the pivotal plane (marked as a red curve) changes along the contour of the membrane, documenting that $\nabla_\alpha\zeta \neq 0$.

Of course, Hamm and Kozlov knew that $\nabla_\alpha\zeta$ does not vanish, but they knew it to be proportional to $\nabla_\alpha\tilde{K}$ (see Eq (3.26) below). Since curvature gradients do not feature in the original Helfrich Hamiltonian, HK took $\nabla_\alpha\zeta$ to be a higher order correction that is irrelevant at the accuracy they aimed for [HK00]. Notice, though, that the variation of ζ with lateral position is easily visible in Fig. 3.3, suggesting that this term might not be negligible. Indeed, the major point of the present section is to show that $\nabla_\alpha\zeta$ is not a higher order correction, and that it leads to terms that matter at the quadratic level of the classical HK energy density—with several interesting consequences.

We can derive a relation between the transverse coordinates z and ζ in the flat and curved leaflet by exploiting local incompressibility, a good assumption for soft systems. It implies that local lateral strains must go along with compensating transverse strains:

$$\mathrm{d}z = \mathrm{d}\zeta\left[1 + \epsilon(\zeta)\right] . \tag{3.19}$$

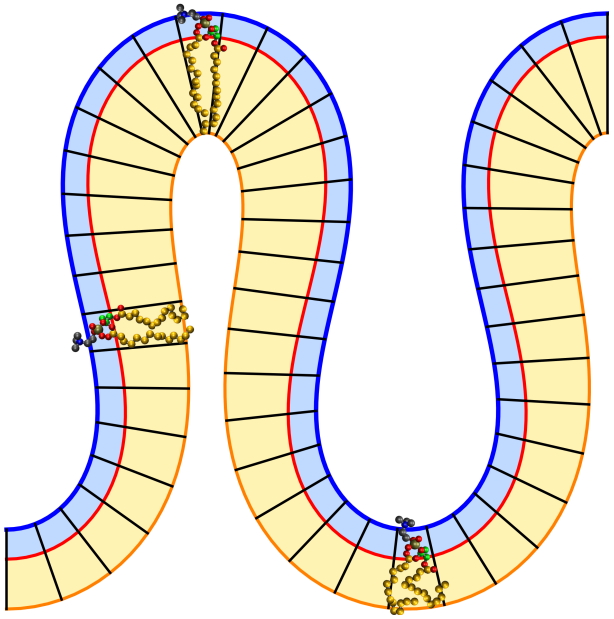

Figure 3.3: Illustration of a strongly curved lipid leaflet and the underlying local deformations. The red curve is the pivotal plane, the blue and orange curves are the "top" and "bottom" of the leaflet. The straight black lines indicate the local lipid tilt, and the three lipid molecules illustrate the type of lipid deformations that underly the macroscopic elastic strains. Observe in particular that the distance between the top and bottom surface from the pivotal plane changes noticeably as one moves along the leaflet.

This can be integrated to yield $\zeta(z)$, provided we know the strain $\epsilon(\zeta)$. To make progress, we can start with an ansatz: since on the pivotal plane (*i. e.*, at $\zeta = 0$) the area strain vanishes, we can expand the strain as follows:

$$\epsilon(\zeta) = \zeta\epsilon_1 + \zeta^2\epsilon_2 + \mathcal{O}(\zeta^3)\,. \tag{3.20}$$

Inserting this into Eq (3.19) and integrating leads to

$$\zeta(z) = z - \frac{1}{2}z^2\epsilon_1 + \mathcal{O}(z^3)\,. \tag{3.21}$$

Notice that z^2 and ζ^2 are equal up to a quadratic order. Hence, the covariant derivative of ζ must have the form

$$\nabla_\alpha\zeta = -\frac{1}{2}\zeta^2\nabla_\alpha\epsilon_1\,. \tag{3.22}$$

This result has a very convenient implication: finding $\nabla_\alpha\zeta$ up to *quadratic* order in ζ only requires knowing the area strain (3.20) up to *linear* order in ζ.

The remaining calculation of the area strain is straightforward and differs from HK [HK00] only by the additional term $\nabla_i\zeta$. It is, however, also somewhat tedious. Let us hence give a few pointers to some crucial steps along the way to guide the reader and leave the detailed derivation to Appendix A. To begin with, we obtain an expression for the tangent vectors on the lipid shifted

surface by taking the derivative of Eq (3.17b):

$$\boldsymbol{e}'_\alpha = \nabla_\alpha \boldsymbol{X}' \overset{(3.17b)}{=} \nabla_\alpha \boldsymbol{X} + \zeta \nabla_\alpha \boldsymbol{n} + (\nabla_\alpha \zeta)\boldsymbol{n} \,. \tag{3.23}$$

Here, the first term is merely the tangent vector on the reference surface; the derivative $\nabla_\alpha \boldsymbol{n}$ of the lipid director in the second term is calculated in Appendix C and given by Eq (C.4c); the derivative $\nabla_\alpha \zeta$ has just been calculated in Eq (3.22); and the director $\boldsymbol{n}$ itself can be exchanged for the normal vector $\boldsymbol{N}$ by using Eq (C.1). This way, we arrive at an expansion of the new tangent vectors in the coordinate frame of the reference surface:

$$\boldsymbol{e}'_\alpha = \Big[\delta_\alpha^\gamma + \zeta \tilde{K}_\alpha{}^\gamma - \frac{1}{2}\zeta^2 T^\gamma \nabla_\alpha \epsilon_1\Big]\boldsymbol{e}_\gamma - \Big[\zeta T^\gamma \tilde{K}_{\alpha\gamma} + \frac{1}{2}\zeta^2 \nabla_\alpha \epsilon_1 \Big(1 - \frac{1}{2}T^2\Big)\Big]\boldsymbol{N} \,. \tag{3.24}$$

We now insert the new tangent vectors from Eq (3.24) into Eq (2.44); to work out the cross product and ε-contractions, the identities $\boldsymbol{N} \times \boldsymbol{e}_\alpha = \varepsilon_{\alpha\beta}\boldsymbol{e}^\beta$, $\boldsymbol{e}_\alpha \times \boldsymbol{e}_\beta = \varepsilon_{\alpha\beta}\boldsymbol{N}$, $\varepsilon^{\alpha\beta}\varepsilon_{\gamma\beta} = \delta^\alpha_\gamma$ and $\varepsilon^{\alpha\beta}\varepsilon_{\alpha\beta} = 2$ come in handy. Using Eq (2.43), this then yields the area strain

$$\epsilon(\zeta) = \zeta \tilde{K} + \zeta^2 \tilde{K}_\mathrm{G} - \frac{1}{2}\zeta^2 T^\alpha \nabla_\alpha \epsilon_1 \,. \tag{3.25}$$

The last term is the addition beyond HK, which originates from the nonvanishing derivative $\nabla_\alpha \zeta$. Since it only contributes at second order in ζ, we can consistently use the first order area strain to "close" Eq (3.25). Comparing Eqn. (3.20) and (3.25), we find $\epsilon_1 = \tilde{K}$, and hence, from Eq (3.22),

$$\nabla_\alpha \zeta = -\frac{1}{2}\zeta^2 \nabla_\alpha \tilde{K} \,. \tag{3.26}$$

In the tilt-free case ($\tilde{K} \to K$), this result had in fact been previously derived by Kolzov [Koz92]. Likewise, inserting $\epsilon_1 = \tilde{K}$ in Eq (3.25) yields the area strain

$$\epsilon(\zeta) = \zeta \tilde{K} + \zeta^2 \tilde{K}_\mathrm{G} - \frac{1}{2}\zeta^2 T^\alpha \nabla_\alpha \tilde{K} \,. \tag{3.27}$$

Thus, the expansion terms of area strain are $\epsilon_1 = \tilde{K}$ and $\epsilon_2 = \tilde{K}_\mathrm{G} - \frac{1}{2}\boldsymbol{T} \cdot \boldsymbol{\nabla}\tilde{K}$. Therefore, we can now write the tangent vector on a lipid shifted surface up to quadratic order in fields,

$$\boldsymbol{e}'_\alpha = \Big[\delta_\alpha^\gamma + \zeta \tilde{K}_\alpha{}^\gamma - \frac{1}{2}\zeta^2 T^\gamma \nabla_\alpha \tilde{K}\Big]\boldsymbol{e}_\gamma - \Big[\zeta T^\gamma \tilde{K}_{\alpha\gamma} + \frac{1}{2}\zeta^2 \nabla_\alpha \tilde{K}\Big]\boldsymbol{N} \,. \tag{3.28}$$

Finally, using the relation between z and ζ by combining Eq (3.21) and $\epsilon_1 = \tilde{K}$ from Eq (3.27),

$$\zeta(z) = z - \frac{1}{2}z^2 \tilde{K} \,, \tag{3.29}$$

we arrive at

$$\epsilon(\zeta) = z\tilde{K} + z^2\big(\tilde{K}_\mathrm{G} - \frac{1}{2}\tilde{K}^2 - \frac{1}{2}\boldsymbol{T} \cdot \boldsymbol{\nabla}\tilde{K}\big) \,. \tag{3.30}$$

Note that the only difference between Eq (3.30) and Eq (3.12) is the last coupling term, $\boldsymbol{T} \cdot \boldsymbol{\nabla}\tilde{K}$.

3.2.4.1 Revisiting the in-plane fluidity assumption

Fluid materials do not have a resistance to shear stress, and this is incorporated into elastic theory by vanishing shear moduli, which are ratios of shear stresses and their associated shear strains: when a shear modulus is zero, a shear strain deformations does not generate any shear stress. In our case, membranes are modeled as *two-dimensional* fluid surfaces, where the lipids are free to move in the in-plane directions but restricted in the out-of plane direction. Therefore, curvature and lipid tilt deformations do not generate any in-plane shear stress because *the lateral shear modulus* is zero. However, there is a subtlety in the present situation related to the dimensional reduction procedure. The two-dimensional energy density is determined after dimensional reduction, *i. e.*, after integrating transverse coordinate, z, over the three dimensional energy density, Eq (3.16). Applying the fluidity assumption before or after the dimensional reduction can lead to different results, because there is more than one way to make the z-integral vanish. In fact, HK suggest two ways to apply the in-plane fluidity assumption, which can be summarized as follows,

$$\lambda_{\rm s}(z) := 0\,, \quad \text{fluidity assumption 1,} \tag{3.31a}$$

$$\int \mathrm{d}z\, \lambda_{\rm s}(z) := 0\,, \quad \text{fluidity assumption 2,} \tag{3.31b}$$

where in the first fluidity assumption the lateral shear modulus vanishes *locally* everywhere in the membrane and the lateral shear term drops from the energy functional as—it happened as in HK theory Eq (3.11). This is more restrictive than the second way of applying in-plane fluidity, in which only the *integral* of $\lambda_{\rm s}(z)$ vanishes. Therefore, the higher moments of the lateral shear modulus survive and they matter, as we will see.

In-plane shear strain

If we use the second fluidity assumption, Eq (3.31b), the penultimate term of Eq (3.16) survives and it is determined by HK in terms of curvature and tilt field [HK00],

$$(u^{\alpha}_{\alpha})^2 - 4\det u_{\alpha\beta} = z^2(\tilde{K}^2 - 4\tilde{K}_{\rm G} + (\boldsymbol{\nabla}\times\boldsymbol{T})^2)\,, \tag{3.32}$$

where the last term is the quadratic lipid twist. The expressions in Eq (3.32) are multiplied by $\lambda_{\rm s}(z)$ in Eq (3.16). There are three terms in the right hand side of Eq (3.32): the quadratic effective curvature, the effective Gaussian curvature, and the lipid twist. We already have occurrences $\tilde{K}^2$ and $\tilde{K}_{\rm G}$ in the energy functional, so addition of these two terms to the energy density only makes quantitative changes to some elastic constants. But the quadratic lipid twist term is new, and it makes a qualitative change to the energy functional of HK theory [HK00].

In the two-dimensional energy density, which is determined by integrating z coordinate, the term $(\boldsymbol{\nabla}\times\boldsymbol{T})^2$ is multiplied by the second moment of the three-dimensional lateral shear modulus, $\int \mathrm{d}z\lambda_{\rm s}(z)z^2$. Therefore, the lipid twist modulus is the second moment of the three-dimensional lateral shear modulus $\lambda_{\rm s}(z)$. In recent studies, the lipid twist modulus has been measured from molecular dynamics simulations and its value is found to be significant [WPWB11,

LVW$^+$14, VBP15]. Therefore, the second moment of the lateral shear profile does indeed not vanish, and the more realistic fluidity assumption sets only the integral of the lateral shear modulus to zero, as stated by the second fluidity assumption Eq (3.31b); it does not set the higher moments to zero.

Surprisingly, the lateral shear term, Eq (3.32), contributes to both the quadratic total curvature and the Gaussian curvature energy. As pointed out by HK [HK00], this means that the definition of both bending modulus and Gaussian curvature modulus [HK00, TD17] is modified by the lipid twist modulus. We will come back to this point and discuss the implications of this modification to some simulation results in Chapter 4.

3.2.5 Transverse shear strain

The quadratic tilt term in Eq (3.16) comes from the transverse shear component of the strain tensor and has been treated as a constant in the transverse direction. In shear deformation plate theories, the transverse shear strain is given as the deformations away from the normal of the plate [Red06]. In membrane theory language, transverse shear strain is the lipid tilt which is defined as the difference between lipid director (deformed state of lipids) and membrane normal as we defined it in Eq (3.7).

In earlier studies [HK00, TD17], the transverse shear, in other words the lipid tilt, is treated as constant in z direction. However, if we look closer at the definition of the tilt field in Eq (3.7), we see that there is a surface normal on the left hand side which depends on z. Therefore, the surface normal changes when we move away from the pivotal plane, and the director $\boldsymbol{n}$ is, by definition, constant. The difference between the normal vector of a lipid shifted surface and the pivotal plane, *i. e.* the tilt field, is not constant when we move away from the pivotal plane.

In order to incorporate the change in the surface normal in the transverse direction to the tilt field, we more precisely define the tilt field as

$$\boldsymbol{T}(z) = \frac{\boldsymbol{n}}{\boldsymbol{n} \cdot \boldsymbol{N}(z)} - \boldsymbol{N}(z)\,, \tag{3.33}$$

where each value of z represents a different lipid shifted surface. In the dimensional reduction procedure, the three-dimensional energy density (3.16) is integrated along the z direction. Therefore, we need to determine the exact form of the z dependence of the tilt field. The component of the tilt field on a lipid shifted surface is given by its projection on to the lipid shifted surface,

$$T'_\alpha(\zeta) = \boldsymbol{e}'_\alpha \cdot \boldsymbol{T}'(\zeta) = \frac{\boldsymbol{e}'_\alpha \cdot \boldsymbol{n}}{\boldsymbol{n} \cdot \boldsymbol{N}'(\zeta)} - \boldsymbol{e}'_\alpha \cdot \boldsymbol{N}'(\zeta)\,, \tag{3.34}$$

where $\boldsymbol{e}'_\alpha$ is the tangent vector on the lipid shifted surface and ζ is lipid distance measure along the lipid. The last term in Eq (3.34) is zero because the normal and the tangent vectors of any surface are perpendicular. If we insert the tangent vector of a lipid shifted surface, Eq (3.28), into Eq (3.34), we can calculate the tilt field up to quadratic order on a lipid shifted surface in

terms of tilt field and curvature on the pivotal plane,

$$T^\alpha = T_{\rm p}^\alpha - \frac{1}{2}\zeta^2 \nabla^\alpha \tilde{K}\,, \tag{3.35}$$

and the quadratic tilt term in Eq (3.16) up to quadratic order becomes,

$$[T(z)]^2 = T_{\rm p}^2 - z^2 \boldsymbol{T}_{\rm p}\cdot\boldsymbol{\nabla}\tilde{K}\,, \tag{3.36}$$

where we use the relation $\zeta^2 = z^2 + \mathcal{O}(z^3)$. Note that the last term in Eq (3.36) has the same form as the novel term in the area strain (3.27). This is no coincidence: the origin of both terms is the z dependence of the normal vector of the lipid shifted surfaces.

The modification to the tilt field given in Eq (3.36) will matter only in the quadratic tilt term in Eq (3.16) because in the rest of the Hamiltonian the tilt field appears with an additional derivative, which renders the correction higher order: $\nabla_\alpha[\zeta^2\nabla_\beta\tilde{K}] = \zeta^2\nabla_\alpha\nabla_\beta\tilde{K} + \mathcal{O}(\zeta^3)$, where the second derivative of curvature is of third order in inverse length, which we always neglect. As we have already determined the exact z dependence of the tilt field, we can now write the three-dimensional energy density in terms of the parameters of the pivotal plane, and further integrate over the z coordinate to get a two-dimensional energy density. For convenience, we drop the subscript "p", $T_p \to T$.

3.2.6 Monolayer Hamiltonian—Dimensional Reduction

Now that we have explicit expressions for $\epsilon(\zeta)$, $\zeta(z)$, and both shear terms, we can return to our goal of deriving an effective surface Hamiltonian by integrating the volume energy density (3.16) across the width of the thin elastic sheet. Inserting Eq (3.21), Eq (3.27), Eq (3.32) and Eq (3.36) into Eq (3.16), we get

$$\begin{aligned}\mathcal{H}_{\rm m} = \int {\rm d}A\,{\rm d}z \Big\{ &\sigma_0(z)\big[z\tilde{K} - \frac{1}{2}z^2\tilde{K}^2 + z^2\tilde{K}_{\rm G} + \frac{1}{2}z^2\tilde{K}\boldsymbol{\nabla}\cdot\boldsymbol{T}\big] \\ &+ \frac{1}{2}\tilde{E}(z)z^2\tilde{K}^2 + \frac{1}{2}\lambda_{\rm s}(z)z^2\big[\tilde{K}^2 - 4\tilde{K}_{\rm G} + (\boldsymbol{\nabla}\times\boldsymbol{T})^2\big] \\ &+ \frac{1}{2}\lambda_{\rm t}(z)\big[\boldsymbol{T}^2 + z^2\tilde{K}\boldsymbol{\nabla}\cdot\boldsymbol{T}\big]\Big\}\,.\end{aligned} \tag{3.37}$$

The last term in the first line is a novel coupling terms, arising from the last term in Eq (3.27), and the last term in the third line is also a novel coupling term from Eq (3.36). Notice that we have integrated both of them by parts, using $\boldsymbol{T}\cdot\boldsymbol{\nabla}\tilde{K} = \boldsymbol{\nabla}\cdot(\tilde{K}\boldsymbol{T}) - \tilde{K}\boldsymbol{\nabla}\cdot\boldsymbol{T}$ and pushing the total divergence term to the boundary. The reason is that integrals over total divergences can always be pushed to the boundary, but monolayers often have no boundary. Even if the *bilayer* membrane has an edge, the *monolayer* curves continuously around the edge and is hence itself edgeless. An important exception is if the monolayer (or bilayer) integrity is interrupted, for instance by transmembrane proteins. Then we will get a contribution from this edge, involving B^β, but in this thesis work we will not dwell on this case.

Let us rearrange the terms in Eq (3.37) such that the same field terms appear together,

$$\mathcal{H}_\mathrm{m} = \int \mathrm{d}A\,\mathrm{d}z \Big\{ \sigma_0(z) z \tilde{K} + \frac{1}{2}\big[\tilde{E}(z) - \sigma_0(z) + \lambda_\mathrm{s}(z)\big] z^2 \tilde{K}^2 + \big[\sigma_0(z) - 2\lambda_\mathrm{s}(z)\big] z^2 \tilde{K}_\mathrm{G} \\ \frac{1}{2}\big[\sigma_0(z) + \lambda_\mathrm{t}(z)\big] z^2 \tilde{K} \boldsymbol{\nabla}\cdot\boldsymbol{T} + \frac{1}{2}\lambda_\mathrm{t}(z)\boldsymbol{T}^2 + \frac{1}{2}\lambda_\mathrm{s}(z) z^2 (\boldsymbol{\nabla}\times\boldsymbol{T})^2 \Big\} . \quad (3.38)$$

After taking the transverse z-integral, we finally arrive at the elastic surface energy density of a monolayer

$$e_\mathrm{2d}^\mathrm{mono} = \frac{1}{2}\kappa_\mathrm{m}\big(K + \boldsymbol{\nabla}\cdot\boldsymbol{T} - K_{0,\mathrm{m}}\big)^2 - \frac{1}{2}\kappa_\mathrm{m} K_{0,\mathrm{m}}^2 + \overline{\kappa}_\mathrm{m}\tilde{K}_\mathrm{G} \\ + \frac{1}{2}\kappa_\mathrm{d,m}\big(K + \boldsymbol{\nabla}\cdot\boldsymbol{T}\big)\boldsymbol{\nabla}\cdot\boldsymbol{T} + \frac{1}{2}\kappa_\mathrm{t,m}\boldsymbol{T}^2 + \frac{1}{2}\kappa_\mathrm{tw,m}(\boldsymbol{\nabla}\times\boldsymbol{T})^2 , \quad (3.39)$$

with new elastic parameters that arise as moments over moduli or stress profiles:

$$\kappa_\mathrm{m} = [\![\tilde{E}]\!]_2 - [\![\sigma_0]\!]_2 + [\![\lambda_\mathrm{s}]\!]_2 , \quad (3.40a)$$

$$\overline{\kappa}_\mathrm{m} = [\![\sigma_0]\!]_2 - 2[\![\lambda_\mathrm{s}]\!]_2 , \quad (3.40b)$$

$$-\kappa_\mathrm{m} K_{0,\mathrm{m}} = [\![\sigma_0]\!]_1 , \quad (3.40c)$$

$$\kappa_\mathrm{t,m} = [\![\lambda_\mathrm{t}]\!]_0 , \quad (3.40d)$$

$$\kappa_\mathrm{d,m} = [\![\sigma_0]\!]_2 + [\![\lambda_\mathrm{t}]\!]_2 , \quad (3.40e)$$

$$\kappa_\mathrm{tw,m} = [\![\lambda_\mathrm{s}]\!]_2 . \quad (3.40f)$$

Recall the double bracket notation, defined in Eq (3.15). Here, κ_m is the monolayer bending modulus, $\overline{\kappa}_\mathrm{m}$ is the monolayer Gaussian curvature modulus, $K_{0,\mathrm{m}}$ is the monolayer spontaneous curvature, $\kappa_\mathrm{t,m}$ is the monolayer tilt modulus, $\kappa_\mathrm{d,m}$ is the monolayer coupling modulus, and $\kappa_\mathrm{tw,m}$ is the monolayer lipid twist modulus. Note that the twist modulus, which is equal to $[\![\lambda_\mathrm{s}]\!]_2$, appears in the definition of κ_m and $\overline{\kappa}_\mathrm{m}$ as well. This is a result of the three functionally distinct term occurring on the right hand side of Eq (3.32).

When we compare Eqs (3.40) with the elastic constant definitions of HK theory, which are given in Eqs (3.14), we detect differences in four relations. Three of these involve the twist modulus ($\kappa_\mathrm{tw,m} = [\![\lambda_\mathrm{s}]\!]_2$), which appeared when using the relaxed fluidity assumption (3.31b). Hamm and Kozlov have indeed derived these terms in their original paper [HK00], but they subsequently neglected them, because back then they had no compelling reason to prefer the more "complicated" fluidity assumption. We will discuss the effects of the twist modulus corrections to the microscopic definition of κ_m (3.40a) and $\overline{\kappa}_\mathrm{m}$ (3.40b) in Chapter 4.

In Ref. [TD17], the modulus of new curvature-tilt coupling term, $\kappa_\mathrm{d,m}$, and the monolayer Gaussian curvature modulus, $\overline{\kappa}_\mathrm{m}$, are both equal to the second moment of stress profile. However, we now have different modifications to both of them: the addition to $\kappa_\mathrm{d,m}$ comes from the redefinition of transverse shear as a local tilt field, and the modification of $\overline{\kappa}_\mathrm{m}$ comes from the lateral shear. Therefore, the coefficient of the novel coupling term is no longer the monolayer Gaussian curvature modulus $\kappa_\mathrm{d,m} \neq \kappa_\mathrm{m}$.

The differences between our theory and HK theory is not limited to the definitions of the elastic constants. Our surface energy density (3.39) has two new terms: the first and the last terms in the second line of Eq (3.39). Observe that the first term in the second line of Eq (3.39) contributes to the coupling between curvature and tilt divergence, but instead of κ_{m} it is multiplied by the monolayer coupling modulus, $\kappa_{\mathrm{d,m}}$. Also, the form of this term unfortunately breaks the nice accidental symmetry which the original theory had: curvature and tilt divergence only entered in the combination $\tilde{K} = K + \boldsymbol{\nabla} \cdot \boldsymbol{T}$. This is no longer true. We will see that this has a number of important consequences for the predictions of our new theory. The last term in the second line of the surface energy density is the lipid twist term which couples to the curvature only minimally through the covariant derivative $\boldsymbol{\nabla}$.

We must not forget that the total energy also includes a term which we delegated to the boundary. If we consider a membrane patch $\mathcal{P}$, this term is readily seen to be

$$\mathcal{H}^{\partial}_{\mathrm{m}} = -\frac{1}{2}\overline{\kappa}_{\mathrm{m}} \int_{\partial\mathcal{P}} \mathrm{d}s \; T_{\perp}\tilde{K} \; , \tag{3.41}$$

where $T_{\perp} = \boldsymbol{l} \cdot \boldsymbol{T}$ is the projection of the tilt field onto the outward pointing normal vector $\boldsymbol{l} = l^a \boldsymbol{e}_a$ on the boundary curve. This term vanishes if the patch $\mathcal{P}$ has no boundary (consider *e. g.* an open membrane disc who's monolayer is contiguous), or when the effective curvature or the (projection of the) tilt field vanishes on the boundary. If neither of these happens, then $\mathcal{H}^{\partial}_{\mathrm{m}}$ contributes nontrivially to the full energy.

Notice that our novel term started as a curvature *gradient*, $\nabla_i \tilde{K}$, and as such was deemed higher order in the original HK paper. Indeed, such a term does not occur in the original Helfrich theory, because the lowest order scalar that could be constructed from it is the contraction with itself, $(\nabla_i K)(\nabla^i K)$. Even though this is still quadratic (two occurrences of the field, K), it has dimension $1/\mathrm{length}^4$ and is thus higher order. However, HK theory contains a second field, the tilt, which is dimensionless and itself a vector. This permits the curvature gradient to appear in a novel contraction $T^i \nabla_i \tilde{K}$ that is both quadratic (two occurrences of fields) and of dimension $1/\mathrm{length}^2$, just like the competing curvature terms. Its relevance becomes obvious after integration by parts (which does of course not change the order), when it takes the form of an *already existing* term in the HK functional. But even before this step, power counting shows that it may not be neglected.

One might wonder, though, what happens in constant-curvature situations, where $\nabla_i \tilde{K} \equiv 0$. The last term in Eq (3.27) now vanishes, and yet the second line in Eq (3.39) still appears to provide a nontrivial correction. The answer is that surfaces with constant curvature do not excite tilt (see the Euler-Lagrange equation (4.12) in Chapter 4), and then the *solution* to the tilt field effectively removes our new correction term.

3.2.7 Bilayer Energy Density

Eq (3.39) is an expression for a single lipid leaflet—a *monolayer*. To obtain an expression for a full *bilayer*, we need to add the contributions of its two individual leaflets. However, a bilayer's

most natural geometric reference surface is its midplane, where the two individual leaflets touch. We hence need to translate curvature and tilt fields from their individual pivotal planes to this midplane.

Generally, curvature and tilt change upon mapping to a different reference surface. However, the lowest order correction due to this shift is of the order of the distance between the pivotal plane and the midplane, and so the corrections of any field contain at least one more inverse length order than the field itself. Using primed observables when referring to the pivotal plane and unprimed ones when referring to the midplane, this for instance means $\tilde{K}' = \tilde{K} + \mathcal{O}(\tilde{K}^2)$. Consequently, shift corrections are irrelevant for all quadratic or bilinear terms—except for the quadratic tilt term, which is zeroth order in inverse length.

As an addition to the quadratic tilt term $\boldsymbol{T}^2$, there is, however, one *linear* term in Eq (3.39), namely $\kappa_{\mathrm{m}}\tilde{K}K_{0,\mathrm{m}}$, and these two terms are indeed the only ones that acquire non-negligible corrections. The value of the tilt field on a surface away from the pivotal plane has already been determined in Eq (3.35), and the value of the quadratic tilt term is found by the values of Eq (3.36) at $z = z_0$, where z_0 is the distance between the pivotal plane and the mid-plane,

$$T^2 = T'^2 - z_0 \boldsymbol{T}' \cdot \boldsymbol{\nabla}\tilde{K} \,. \tag{3.42}$$

The calculations of the corrections to the linear term are straightforward but slightly technical, and we defer them to Appendix B.1. The final answer is given in Eq (B.9).

Another aspect of the monolayer-to-bilayer conversion is that the two tilt fields $\boldsymbol{T}_\uparrow$ and $\boldsymbol{T}_\downarrow$ of the upper and lower leaflet are independent degrees of freedom. It turns out to be useful to define symmetrized tilt sum and difference fields,

$$\boldsymbol{T}_\pm = \frac{1}{2}(\boldsymbol{T}_\uparrow \pm \boldsymbol{T}_\downarrow) \,, \tag{3.43}$$

because the way in which they enter the full bilayer Hamiltonian is distinctly different.

Combining Eq (3.43) and Eq (B.9) with the sum of two monolayer Hamiltonians, the resulting elastic bilayer surface energy density turns out to be

$$\begin{aligned} e_{2\mathrm{d}}^{\mathrm{bi}} = \;& \frac{1}{2}\kappa\big(K + \boldsymbol{\nabla}\cdot\boldsymbol{T}_-\big)^2 + \overline{\kappa}\tilde{K}_{\mathrm{G}}^- + \frac{1}{2}\kappa_{\mathrm{t}}T_-^2 \\ & + \frac{1}{2}\kappa_{\mathrm{d}}\big(K + \boldsymbol{\nabla}\cdot\boldsymbol{T}_-\big)\boldsymbol{\nabla}\cdot\boldsymbol{T}_- + \frac{1}{2}\kappa_{\mathrm{tw}}(\boldsymbol{\nabla}\times\boldsymbol{T}_-)^2 \\ & + \frac{1}{2}\kappa\big(\boldsymbol{\nabla}\cdot\boldsymbol{T}_+ - K_{0,\mathrm{m}}\big)^2 - \frac{1}{2}\kappa K_{0,\mathrm{m}}^2 + \frac{1}{2}\kappa_{\mathrm{t}}T_+^2 \\ & + \frac{1}{2}\kappa_{\mathrm{d}}(\boldsymbol{\nabla}\cdot\boldsymbol{T}_+)^2 + \frac{1}{2}\kappa_{\mathrm{tw}}(\boldsymbol{\nabla}\times\boldsymbol{T}_+)^2 \,, \end{aligned} \tag{3.44}$$

where, in analogy to the monolayer case in Eqns. (3.9,3.10), we can define an effective tilt-renormalized bilayer curvature tensor and its associated curvatures:

$$\tilde{K}^-_{ij} := K_{ij} + \nabla_i T_{-j} \to \begin{cases} \tilde{K}^- := \mathrm{Tr}(\tilde{K}^-_{ij}) = K + \boldsymbol{\nabla}\cdot\boldsymbol{T}_- \\ \\ \tilde{K}^-_{\mathrm{G}} := \det(\tilde{K}^-_{ij}) \quad . \end{cases} \tag{3.45}$$

The bilayer Hamiltonian (3.44) features new moduli, which can be expressed in terms of their monolayer counterparts:

$$\kappa = 2[\![\tilde{E}]\!]_2 - 2[\![\sigma_0]\!]_2 + 2[\![\lambda_{\mathrm{s}}]\!]_2 \tag{3.46a}$$

$$\overline{\kappa} = 2[\![\sigma_0]\!]_2 + 4z_0[\![\sigma_0]\!]_1 - 4[\![\lambda_{\mathrm{s}}]\!]_2 \ , \tag{3.46b}$$

$$\kappa_{\mathrm{t}} = 2[\![\lambda_{\mathrm{T}}]\!]_0 \ , \tag{3.46c}$$

$$\kappa_{\mathrm{d}} = [\![\sigma_0]\!]_2 + [\![\lambda_{\mathrm{T}}]\!]_2 + z_0^2[\![\lambda_{\mathrm{T}}]\!]_0 \ , \tag{3.46d}$$

$$\kappa_{\mathrm{tw}} = 2[\![\lambda_{\mathrm{s}}]\!]_2 \ . \tag{3.46e}$$

Some of these relations have also been derived before, see for instance [Hel81] for Eq (3.46a), [PB84] for Eq (3.46b), and [WPWB11] for Eq (3.46c).

Again, we should not forget about the boundary term, which in the bilayer case reads

$$\mathcal{H}^{\partial}_{\mathrm{bi}} = -\overline{\kappa}_{\mathrm{m}} \int_{\partial P} \mathrm{d}s \left\{ T_{-\perp}\tilde{K}^- + T_{+\perp}\boldsymbol{\nabla}\cdot\boldsymbol{T}_+ \right\} , \tag{3.47}$$

with $T_{\pm\perp} = \boldsymbol{l}\cdot\boldsymbol{T}_\pm$ being the projection of the tilt fields onto the outward pointing unit normal $\boldsymbol{l} = l^a\boldsymbol{e}_a$ of the boundary curve ∂P.

Several aspects of this bilayer Hamiltonian are noteworthy: The first line in Eq (3.44) mirrors the monolayer Hamiltonian (3.39), but with the spontaneous curvature removed (due to up-down symmetry of the bilayer) and the tilt field replaced by the tilt-difference field. The second line is the new term that arises from the non-vanishing of $\nabla_i\zeta$; it again matches the first term in the second line of the monolayer Hamiltonian (3.39), with the tilt-difference field taking over the role of a single leaflet tilt. These first two lines are the only ones that involve $\boldsymbol{T}_-$. Line 3 and 4 contain the $\boldsymbol{T}_+$ contribution to the Hamiltonian. Line 4 is again new, and it mimics line 2, except that the curvature K has dropped out. The latter is more generally true: observe that, unlike $\boldsymbol{T}_-$, the tilt-sum field does *not* explicitly couple to the extrinsic curvature K and hence cannot be excited by it.[7]

[7] To be slightly more precise: both $\boldsymbol{T}_-$ and $\boldsymbol{T}_+$ couple *implicitly* to the geometry via the Christoffel symbols in the covariant derivatives. This is sometimes called "minimal coupling". However, since the Christoffel symbols are constructed from the metric, they only know about *intrinsic* curvature, which in the case of surfaces embedded in three dimensions is merely the *Gaussian* curvature K_{G}. But the Gaussian curvature is *quadratic* in the curvature eigenvalues, not linear (like K). Hence, any term involving both $\boldsymbol{T}_\pm$ and K_{G} is necessarily higher order, and so minimal curvature coupling has no effect at the level we presently work on.

3.3 Conclusion

Revisiting the original calculation of Hamm and Kozlov [HK00], who systematically derived an elastic surface functional for lipid membranes based on a dimensional reduction of a laterally fluid pre-stressed sheet, we have uncovered a previously overlooked term that couples tilt with curvature. Its progenitor in the derivation describes how transverse distances in a leaflet change as one moves along a curved membrane. This position dependence had been previously acknowledged [HK00], but only believed to yield a higher order correction, while in fact it produces a quadratic term at the same order as all other terms in HK theory. The curvature tensor always appears in HK theory additive with the tilt derivative tensor. This accidental symmetry is broken as a consequence of the novel coupling term.

Our final energy density includes the lipid twist term which originates from the fluidity of lipid molecules. There are two ways to incorporate the fluidity of lipids into the bottom-up approach. Hamm and Kozlov actually derived the lipid twist term, but they subsequently neglected it [HK00], because they did not have any particular reason to choose the more "complicated" fluidity assumption. However, now we have insight from recent studies [WPWB11] that suggests the opposite, and therefore we keep the lipid twist term.

We also derive the bilayer Hamiltonian by shifting the reference surface from the pivotal plane to the mid-plane and adding the energies of two individual monolayers. We showed that the sum of individual tilt fields of two leaflets decouples from the curvature, while the difference of these tilt fields couples with it in the same way as tilt couples with curvature in the monolayer energy density.

Chapter 4

Application of the Quadratic Theory and Consequences of the Novel Coupling Term

In the previous chapter, we have shown that the elastic surface energy functional due to Hamm and Kozlov [HK00] should be amended by an extra tilt-curvature coupling and lipid twist. The extra terms change the connection between the two-dimensional elastic parameters and the underlying microscopic descriptors of elasticity, and the extra coupling term breaks an accidental symmetry between the curvature tensor and the tilt derivative tensor. In this Chapter, we will explore how we can make use of the modified definitions of moduli and what consequences arise from the existence of the novel coupling and lipid tilt terms.

To do so, we will specifically look at three questions: (i) How well do the definitions of elastic moduli work? (ii) How do the extra terms change the *Euler-Lagrange equation* for tilt, and hence the magnitude of the tilt fields induced via bending? (iii) How do they modify the *power spectra* of shape, tilt, and director fluctuations? We show that in each case the modifications can be very significant, which, for instance, has implications for a variety of methods previously proposed to extract elastic moduli in experiments [JAN14, Nag17a] or in simulations [WBWB12, LVW$^+$14, WD16].

First, we start in Section 4.1 by deriving estimates for bending, coupling, and Gaussian curvature moduli. Then, we determine the Euler-Lagrange equations for tilt from both monolayer and bilayer Hamiltonians in Section 4.2. We explore the immediate consequences of what we discuss in the previous chapter, with regard to various fluctuation spectra in Section 4.3. In Sec. 4.4 we then discuss a few situations where these changes matter, focusing in particular on the issue of determining elastic parameters from fits to simulated power spectra. The present chapter is partially based on work by Terzi and Deserno [TD17]. Material not contained in [TD17] is in preparation for a second publications.

4.1 On Elastic Moduli

In Chapter 3, the elastic constants of the curvature-tilt theory were defined in terms of the underlying material properties by using the bottom-up approach. The monolayer elastic constants are given in Eqs (3.40), and the bilayer counterparts are given in Eqs (3.46). In the present section, we will discuss the definition of elastic constants and their relationship to each other.

4.1.1 Bending Modulus

The bending modulus κ, if not the most important elastic parameter for lipid membranes, is probably the one studied most extensively. The most widely-used way to measure κ in both simulations [GGL99, LE00, MM01, AV02, HLE03, Far03, MdVM04, BTB04, WF05, ISL05, CKD05, CD05, BPB05, WD10b, WD10a, WB10, SN11] and experiments [BL75, BdGP76, SJW84a, SJW84b, FMM$^+$89, HRI04, LN04] is measuring the power spectrum of the thermal undulations. However, it is not always possible to access the bending modulus, κ, and in such cases the underlying theories come to our rescue and provide us with approximations of κ in terms of other parameters. Besides estimating the values of the bending modulus, one can also use these approximations to check the validity of the theory by comparing them and the direct measurements.

In our derivation of the membrane energy, the bending modulus is expressed in terms of the underlying mechanical parameters and is given by combining Eq (3.40a) and Eq (3.46a),

$$\kappa = 2\big([\![\tilde{E}]\!]_2 - [\![\sigma_0]\!]_2 + [\![\lambda_\mathrm{s}]\!]_2\big)\,, \tag{4.1}$$

where the three terms on the right are the second moments of the bilayer's young modulus, lateral stress, and lateral shear modulus profile, respectively. Both of them can be measured via computer simulations. However, there is no way to directly measure $[\![\tilde{E}]\!]_2$, either experimentally or in simulations. Therefore, we use an approximation for $[\![\tilde{E}]\!]_2$: In the case of constant $\tilde{E}(z) = \tilde{E}$, its second moment becomes,

$$[\![\tilde{E}]\!]_2 = \tilde{E} d_\mathrm{m}^3 \Big[\frac{1}{3} - \frac{z_0}{d_\mathrm{m}} + \Big(\frac{z_0}{d_\mathrm{m}}\Big)^2\Big]\,, \tag{4.2}$$

where d_m and z_0 are the thickness of the monolayer and the position of pivotal plane away from the midplane, respectively. Obviously, the assumption of constant $\tilde{E}(z)$ does not give us an exact relation for the second moment. Still, even more crude estimations work remarkably well for estimations of κ [LL86, GGL99, ROM$^+$00].

Thickness of a monolayer leaflet in Eq (4.2) comes from the integral over the transverse coordinate z. However, from an atomistic perspective the thickness of a monolayer is not well defined [NTN00], as we discussed in Section 3.2.2. Technically, the limits of the z integral are $(-\infty, \infty)$, but practically, all the observables we are integrating over only have non-zero values in a finite region. We can choose different definitions for the membrane thickness. For example,

one can define it as the region where elastic moduli have a non-zero values or the region between Luzatti planes [LH62] where the water/lipids average volume ratio is equal to one. Due to the ambiguity, we will treat d_{m} as an effective thickness.

In a bottom-up approach that includes the membrane stretching as an addition to bending, the area extension modulus K_{A} is derived as the zeroth moment of $\tilde{E}(z)$ [CAMK14],

$$K_{\mathrm{A}} = 2[\![\tilde{E}]\!]_0 = 2\tilde{E}d_{\mathrm{m}}\,, \tag{4.3}$$

where in the second equality, we again use the assumption of constant $\tilde{E}$. An expression for the bending modulus is found by inserting Eq (4.3) and Eq (4.2) into Eq (4.1),

$$\kappa^{\mathrm{est}} = 2K_{\mathrm{A}}(d_{\mathrm{m}})\Big[\frac{1}{3} - \frac{z_0}{d_{\mathrm{m}}} + \Big(\frac{z_0}{d_{\mathrm{m}}}\Big)^2\Big] - 2[\![\sigma_0]\!]_2 + \kappa_{\mathrm{tw}}\,. \tag{4.4}$$

This time, all the terms on the right hand side can be measured by computer simulations independent of the measurement of κ.

4.1.2 Coupling Modulus κ_{d}

The definition of this coupling modulus is given in Eq (3.40e) and Eq (3.46d),

$$\kappa_{\mathrm{d}} = 2[\![\sigma_0]\!]_2 - 2[\![\lambda_{\mathrm{t}}]\!]_2 + \kappa_{\mathrm{t}} z_0^2\,, \tag{4.5}$$

where z_0 is the distance between the mid-plane and the pivotal plane. In order to find an estimation for κ_{d}, we follow the idea from the previous section and make the assumption of a constant $\lambda_{\mathrm{t}}(z) = \lambda_{\mathrm{t}}$:

$$[\![\lambda_{\mathrm{t}}]\!]_2 = \lambda_{\mathrm{t}} d_{\mathrm{m}}^3\Big[\frac{1}{3} - \frac{z_0}{d_{\mathrm{m}}} + \Big(\frac{z_0}{d_{\mathrm{m}}}\Big)^2\Big]\,, \tag{4.6}$$

where d_{m} is the monolayer thickness. In this case, the tilt modulus becomes

$$\kappa_{\mathrm{t}} = [\![\lambda_{\mathrm{t}}]\!]_0 = \lambda_{\mathrm{t}} d_{\mathrm{m}}\,. \tag{4.7}$$

Now the estimation for the coupling modulus can be written in terms of the second moment of the stress profile, the tilt modulus, the monolayer thickness, and the position of the pivotal plane in the monolayer,

$$\kappa_{\mathrm{d}}^{\mathrm{est}} = 2[\![\sigma_0]\!]_2 + \kappa_{\mathrm{t}} d_{\mathrm{m}}^2\Big[\frac{1}{3} - \frac{z_0}{d_{\mathrm{m}}} + 2\Big(\frac{z_0}{d_{\mathrm{m}}}\Big)^2\Big]\,. \tag{4.8}$$

4.1.3 Gaussian Curvature Modulus

In Chapter 3, we showed that the choice of the fluidity assumption changes the definition of the monolayer Gaussian curvature modulus. In standard HK theory, this definition is given as the second moment of the lateral stress profile. However, we derived $\overline{\kappa}_{\mathrm{m}}$ and it is given in Eq (3.40b),

$$\overline{\kappa}_{\mathrm{m}} = [\![\sigma_0]\!]_2 - 2[\![\lambda_{\mathrm{s}}]\!]_2 \,, \tag{4.9a}$$

$$= [\![\sigma_0]\!]_2 - \kappa_{\mathrm{tw}} \,. \tag{4.9b}$$

Actually, HK derived this equation but later ignored the twist modulus contribution [HK00]. We know that the integral over Gaussian curvature K_{G} in the energy functional can be written as a topological constant and a boundary term, because of the Gauss-Bonnet theorem [Kre59, dC76]. Therefore, in order for $\overline{\kappa}_{\mathrm{m}}$ to have any effect on the energetics, membranes typically need to go through topological changes. This makes the measurement of the Gaussian curvature modulus a very hard task. We will show in Section 4.3 that the twist modulus can be measured from director fluctuations. We know that the second moment of stress profile also can be measured from computer simulations. Therefore, using computer simulations and Eq (4.9b), we can estimate the value of the Gaussian curvature modulus.

4.2 Euler-Lagrange Equation

As we have claimed earlier, tilt is a relatively local phenomenon: it only matters on a sufficiently small scale. To find that scale, observe that the two key moduli in a lipid leaflet—those for bending and tilting—permit us to define a characteristic length ℓ according to

$$\ell^2 = \kappa_{\mathrm{m}}/\kappa_{\mathrm{t,m}} \overset{(3.46)}{=} \kappa/\kappa_{\mathrm{t}} \,, \tag{4.10}$$

which for typical material parameters lies indeed in the nanometer range. Since that is about the size of a lipid, tilt varies on a scale that coincides with the local molecular basis for its own existence. This calls for a cautious handling of the associated continuum theory, as we had anticipated in Chapter 3.

It is straightforward to see that in the original HK theory—Eq (3.39) without the extra coupling and the lipid twist term—the Euler-Lagrange (EL) equation for the tilt field is

$$\boldsymbol{\nabla\nabla}\cdot\boldsymbol{T} - \ell^{-2}\boldsymbol{T} = -\boldsymbol{\nabla}K \,. \tag{4.11}$$

This shows that (i) the tilt field satisfies a second order differential equation, in which ℓ plays the role of a decay length, and (ii) this field is sourced by gradients in the curvature.

In our modified theory, Eq (3.39), this EL equation changes to

$$(1 + r_{\mathrm{d,m}})\boldsymbol{\nabla\nabla}\cdot\boldsymbol{T} + r_{\mathrm{tw}}(\nabla^2\boldsymbol{T} - \boldsymbol{\nabla\nabla}\cdot\boldsymbol{T}) - \ell^{-2}\boldsymbol{T} = -\big(1 + \tfrac{1}{2}r_{\mathrm{d,m}}\big)\boldsymbol{\nabla}K \,, \tag{4.12}$$

where we defined two new dimensionless parameters, the *elastic ratios*

$$r_{\mathrm{d,m}} := \kappa_{\mathrm{d,m}}/\kappa_{\mathrm{m}} \,, \tag{4.13a}$$

$$r_{\mathrm{tw}} := \kappa_{\mathrm{tw,m}}/\kappa_{\mathrm{m}} = \kappa_{\mathrm{tw}}/\kappa \,. \tag{4.13b}$$

Let us look at the range of values $r_{\mathrm{d,m}}$ and r_{tw} can take. The lipid twist term is quadratic and hence positive definite, so the twist modulus cannot be negative,

$$r_{\mathrm{tw}} \geq 0 \,. \tag{4.14}$$

where we use the stability condition which states that the bending modulus must be positive. For the elastic monolayer ratio $r_{\mathrm{d,m}}$ we use the definition of the monolayer coupling modulus Eq (3.40e),

$$r_{\mathrm{d,m}} = \frac{[\![\sigma_0]\!]_2}{\kappa_{\mathrm{m}}} + \frac{d_{\mathrm{m}}^2}{2\ell^2} \underbrace{\left[\frac{1}{3} - \frac{z_0}{d_{\mathrm{m}}} + \left(\frac{z_0}{d_{\mathrm{m}}}\right)^2\right]}_{>0} \,, \tag{4.15}$$

where, you will recall, we relied on the assumption of constant λ_{t}. The term inside the square brackets in Eq (4.15) is positive definite for all values of z_0/d_{m} so the second term in the right hand side on Eq (4.15) cannot be negative. From experimental studies, we know that z_0 is closer to head groups, and $z_0/d_{\mathrm{m}} \approx 2/3$ is a good approximation [RFGP90, LKFR96, CR98]. We also know the typical values for the tilt characteristic length, ℓ, are around one nanometer [Nag17a] and the thickness of a monolayer is also of the order of a nanometer. Therefore, the second term in Eq (4.15) is generally close to 0.1. The range of possible values for the ratio $[\![\sigma_0]\!]_2/\kappa_{\mathrm{m}}$ is found by looking at the definition of the monolayer Gaussian curvature modulus. First we define the following useful dimensionless parameter,

$$r_{\mathrm{m}} := \frac{\overline{\kappa}_{\mathrm{m}}}{\kappa_{\mathrm{m}}} = \frac{[\![\sigma_0]\!]_2}{\kappa_{\mathrm{m}}} - 2r_{\mathrm{tw}} \,, \tag{4.16}$$

which due to general stability requirements must lie within the range $-1 \leq r_{\mathrm{m}} \leq 0$ [TKS98]. Therefore, the ratio of the second moment of stress profile and the monolayer bending modulus is bounded below, $[\![\sigma_0]\!]_2/\kappa_{\mathrm{m}} \geq -1$ with the use of the condition (4.14). Finally, we find the lower bound for $r_{\mathrm{d,m}}$,

$$r_{\mathrm{d,m}} \geq -1 \,. \tag{4.17}$$

However, the conditions Eq (4.14) and Eq (4.17) are not totally independent. For example, the difference $r_{\mathrm{d,m}} - 2r_{\mathrm{tw}}$ is also bounded below by -1. In order to see this condition we combine Eq (4.15) and Eq (4.16),

$$r_{\mathrm{d,m}} - 2r_{\mathrm{tw}} = r_{\mathrm{m}} + \frac{d_{\mathrm{m}}^2}{2\ell^2}\left[\frac{1}{3} - \frac{z_0}{d_{\mathrm{m}}} + \left(\frac{z_0}{d_{\mathrm{m}}}\right)^2\right] \,, \tag{4.18}$$

where the second term must be non-negative and the first term is in the range $-1 \leq r_{\mathrm{m}} \leq 0$. Therefore,

$$r_{\mathrm{d,m}} - 2r_{\mathrm{tw}} \geq -1 \,. \tag{4.19}$$

After dividing out the prefactor $1 + r_{\mathrm{d,m}} - r_{\mathrm{tw}}$ of the $\boldsymbol{\nabla\nabla} \cdot \boldsymbol{T}$ term in Eq (4.12), which we now know to be non-negative, it becomes easier to see that this revised differential equation leads to a shortened effective tilt decay length and a stronger coupling to the curvature gradient:

$$\boldsymbol{\nabla\nabla} \cdot \boldsymbol{T} + \big(\tilde{\nabla}^2 - \ell_{\mathrm{eff}}^{-2}\big)\boldsymbol{T} = -\Big[1 - \frac{r_{\mathrm{d,m}}/2 - r_{\mathrm{tw}}}{1 + r_{\mathrm{d,m}} - r_{\mathrm{tw}}}\Big]\boldsymbol{\nabla} K \,, \tag{4.20}$$

where the effective tilt decay length is

$$\ell_{\mathrm{eff}} := \sqrt{1 + r_{\mathrm{d,m}} - r_{\mathrm{tw}}}\,\ell \,, \tag{4.21}$$

and the renormalized Laplacian is

$$\tilde{\nabla}^2 := \frac{r_{\mathrm{tw}}}{1 + r_{\mathrm{d,m}} - r_{\mathrm{tw}}}\nabla^2 \,. \tag{4.22}$$

Formally, we can recover the old theory by setting $r_{\mathrm{d,m}} \to 0$ and $r_{\mathrm{tw}} \to 0$, which implies $\ell_{\mathrm{eff}} \to \ell$ and sets the prefactor on the right hand side in front of the curvature gradient back to -1. But as $r_{\mathrm{d,m}} - r_{\mathrm{tw}}$ becomes negative (recall that $r_{\mathrm{d,m}} - r_{\mathrm{tw}} \geq -1$), the effective tilt decay length may decrease, while simultaneously the strength with which curvature gradients source tilt increases. In the limit $r_{\mathrm{d,m}} - r_{\mathrm{tw}} \to -1$, the effective tilt decay length becomes zero. If the twist term also vanishes simultaneously $r_{\mathrm{tw}} \to 0$, the coupling becomes infinite. In this limit it is easier to go back to Eq (4.12), which shows that tilt is now directly proportional to the curvature gradient:

$$\boldsymbol{T} = \tfrac{1}{2}\ell^2\boldsymbol{\nabla} K \qquad (\text{for } r_{\mathrm{d,m}} = -1 \text{ and } r_{\mathrm{tw}} = 0) \,. \tag{4.23}$$

For the bilayer case, the Euler-Lagrange equations for the two tilt fields are

$$\boldsymbol{\nabla\nabla} \cdot \boldsymbol{T}_- + \big(\overline{\nabla}^2 - \ell_{\mathrm{eff}}^{-2}\big)\boldsymbol{T}_- = -\Big[1 - \frac{r_{\mathrm{d}}/2 - r_{\mathrm{tw}}}{1 + r_{\mathrm{d}} - r_{\mathrm{tw}}}\Big]\boldsymbol{\nabla} K \,, \tag{4.24a}$$

$$\boldsymbol{\nabla\nabla} \cdot \boldsymbol{T}_+ + \big(\overline{\nabla}^2 - \ell_{\mathrm{eff}}^{-2}\big)\boldsymbol{T}_+ = 0 \,, \tag{4.24b}$$

where we define the dimensionless elastic bilayer ratio,

$$r_{\mathrm{d}} := \frac{\kappa_{\mathrm{d}}}{\kappa} \,, \tag{4.25}$$

and the renormalized Laplacian,

$$\overline{\nabla}^2 := \frac{r_{\mathrm{tw}}}{1 + r_{\mathrm{d}} - r_{\mathrm{tw}}}\nabla^2 \,. \tag{4.26}$$

By using the lower bound on $r_{\mathrm{d,m}}$ (4.17) and the definition of κ_{d} given in Eq (3.46d), we find a lower bound also for r_{d}

$$r_{\mathrm{d}} \geq \left(\frac{z_0}{\ell}\right)^2 - 1 \,. \tag{4.27}$$

Eqs (4.24) show that the differential operator for both tilt fields is the same, but that only $\boldsymbol{T}_-$ is sourced by curvature gradients (in a manner identical to the monolayer case). The fact that $\boldsymbol{T}_+$ is not sourced by the bilayer geometry does of course not mean that it cannot be sourced at all—it can for instance be excited by integral membrane proteins whose cross-sectional area at the bilayer center is bigger or smaller than their area at the head group region.

4.3 Fluctuation Spectra

Measuring the wave vector dependent fluctuation spectrum of fluid membranes is a time-honored way to access their elastic properties. Monitoring membrane shape undulations has long been used to measure the bending modulus—both in experiment [BL75, BdGP76, SJW84a, SJW84b, FMM$^+$89, HRI04, LN04] and in simulations [GGL99, LE00, MM01, AV02, HLE03, Far03, MdVM04, BTB04, WF05, ISL05, CKD05, CD05, BPB05, WD10b, WD10a, WB10, SN11]. Exploring the predictions of more finely resolved models, especially those accounting for lipid tilt, have not only helped to clarify well-known deviations from the classical undulation spectrum [MNK07b, MNK07a, WPWB11, BBS$^+$11], but permitted measurement of the lipid tilt modulus [WBWB12, LVW$^+$14], even from experiments [JAN14, Nag17a] only looking at shape undulations.

We will now show how the additional terms in our revised HK theory modify the fluctuation spectra of shape, tilt, and lipid orientation. As a brief reminder, recall the basic procedure for calculating the fluctuation spectrum for the tilt free case, when the energy density is $\frac{1}{2}\kappa K^2 + \overline{\kappa} K_{\mathrm{G}}$. First, the Gauss-Bonnet theorem renders the Gaussian curvature contribution an irrelevant topological constant [Kre59, dC76], and so we can ignore it for the spectrum. And second, in the weak deformation limit we can describe the membrane in Monge gauge as a function $h(x, y)$ above a flat reference surface, and upon further linearization the curvature is simply its second derivative: $K \approx -\Delta h$ (where $\Delta = \partial_x^2 + \partial_y^2$ is the ordinary Laplacian in the base plane). This renders the Hamiltonian a quadratic functional that can be diagonalized via Fourier transformation. If the membrane spans a frame of size $L \times L$ in the xy-plane and satisfies periodic boundary conditions, then we can expand its shape as

$$h(\boldsymbol{r}) = \frac{1}{L} \sum_{\boldsymbol{q}} h_{\boldsymbol{q}}\, \mathrm{e}^{\mathrm{i}\boldsymbol{q}\cdot\boldsymbol{r}} \quad , \quad \boldsymbol{q} = \frac{2\pi}{L} \begin{pmatrix} n_x \\ n_y \end{pmatrix} \quad , \quad n_x, n_y \in \mathbb{Z} \,, \tag{4.28}$$

where $h_{\boldsymbol{q}} = h^*_{-\boldsymbol{q}}$ because $h(\boldsymbol{r}) \in \mathbb{R}$. In Fourier space the energy then has the form

$$E = \frac{1}{2}\kappa \sum_{\boldsymbol{q}} q^4 \left|h_{\boldsymbol{q}}\right|^2 \,, \tag{4.29}$$

and assuming that the Fourier modes are the independent quadratic degrees of freedom, the well-known classical fluctuation spectrum immediately follows from the equipartition theorem:

$$\left\langle \left| h_{\boldsymbol{q}} \right|^2 \right\rangle = \frac{k_\mathrm{B} T}{\kappa q^4} \,. \tag{4.30}$$

It has long been known that at high q-vectors the $1/q^4$ form transitions to a weaker decay, even before the continuum assumption may be expected to fail. The earliest suggested explanation for this behavior were so-called "lipid protrusion modes" [LG93], but recently May, Narang, and Kopelevich (MNK in the following) argued that the more likely origin is a contamination of the undulation spectrum by lipid tilt fluctuations [MNK07b, MNK07a]. Indeed, they showed that HK-theory predicts the modified spectrum

$$\left\langle \left| h_{\boldsymbol{q}} \right|^2 \right\rangle = \frac{k_\mathrm{B} T}{\kappa q^4} + \frac{k_\mathrm{B} T}{\kappa_\mathrm{t} q^2} \,, \tag{4.31}$$

which features a crossover to a $1/q^2$ decay at $q\ell \sim 1$. This insight has then been used to determine the tilt modulus in simulations [MNK07b, MNK07a, WPWB11] (by fitting to the power spectrum of a flat tensionless membrane), and in experiments [JAN14, Nag17a] (by analyzing the high-q region of the diffuse X-ray scattering spectrum of a stack of lipid bilayers).

It is straightforward to extend the MNK calculation to our revised version of the HK Hamiltonian. Notice, first, that the tilt-sum field $\boldsymbol{T}_+$ does not couple to the curvature, and so we can subsequently ignore it. The remaining tilt-difference field is usefully split into its longitudinal and transverse components, by defining $T^{\parallel}_{\boldsymbol{q}} = \hat{\boldsymbol{q}} \cdot \boldsymbol{T}_-$ and $T^{\perp}_{\boldsymbol{q}} = (\hat{\boldsymbol{q}} \times \boldsymbol{T}_-) \cdot \hat{\boldsymbol{z}}$, where $\hat{\boldsymbol{q}} = \boldsymbol{q}/q$ is the normalized wave vector [WPWB11]. One then finds that the transverse modes again split off from the undulations, giving a term $\frac{1}{2}[\kappa_\mathrm{t} + q^2 \kappa_\mathrm{tw}] |T^{\perp}_{\boldsymbol{q}}|^2$, which immediately leads to the fluctuation spectrum

$$\left\langle \left| T^{\perp}_{\boldsymbol{q}} \right|^2 \right\rangle = \frac{k_\mathrm{B} T}{\kappa_\mathrm{t} + \kappa_\mathrm{tw} q^2} \,. \tag{4.32}$$

In contrast, the longitudinal modes end up being quadratically coupled to the shape undulations. The Hamiltonian in the associated 2×2 subspace takes the form

$$E_{h,\parallel} = \frac{1}{2} \sum_{\boldsymbol{q}} \boldsymbol{f}^\dagger_{\boldsymbol{q}} \cdot \mathbf{A}_{\boldsymbol{q}} \cdot \boldsymbol{f}_{\boldsymbol{q}} \quad \text{with } \boldsymbol{f}_{\boldsymbol{q}} = \begin{pmatrix} h_{\boldsymbol{q}} \\ T^{\parallel}_{\boldsymbol{q}} \end{pmatrix} \,, \tag{4.33}$$

where the coupling matrix is given by

$$\mathbf{A}_{\boldsymbol{q}} = \begin{pmatrix} \kappa q^4 & -\mathrm{i}(1 + \frac{1}{2} r_\mathrm{d}) \kappa q^3 \\ \mathrm{i}(1 + \frac{1}{2} r_\mathrm{d}) \kappa q^3 & (1 + r_\mathrm{d}) \kappa q^2 + \kappa_\mathrm{t} \end{pmatrix} \,. \tag{4.34}$$

In the limit $r_\mathrm{d} \to 0$ and $r_\mathrm{tw} \to 0$, when our theory reduces to the original HK Hamiltonian, this matrix also reduces to the one found by MNK [MNK07b, MNK07a].

An immediate first and quite unexpected finding is that the matrix (4.34) is no longer necessarily positive definite. One may easily check that one of its eigenvalues becomes negative at sufficiently large q-vectors:

$$q > q_\mathrm{c} := \frac{2}{\ell|r_\mathrm{d}|} \quad \Longleftrightarrow \quad \det(\mathbf{A}_{\boldsymbol{q}}) < 0 \,. \tag{4.35}$$

This heralds the emergence of a soft mode at $q = q_\mathrm{c}$ and an instability beyond. For values $r_\mathrm{d} \approx 1$, this instability occurs at $q_\mathrm{c} = 2/\ell$, corresponding to a wavelength of $2\pi/q_\mathrm{c} = \pi\ell$. This is typically just a few nanometer, and so one might not expect this mode to have much of an impact.[1] However, it hugely affects the fluctuation spectrum, which must diverge at q_c, increasing its power at much smaller q and thus much larger scales. Indeed, applying the equipartition theorem to the subspace described by Eq (4.33) leads to

$$\left\langle \boldsymbol{f}_{\boldsymbol{q}} \cdot \boldsymbol{f}^\dagger_{\boldsymbol{q}'} \right\rangle = k_\mathrm{B}T\, \mathbf{A}^{-1}_{\boldsymbol{q}}\, \delta_{\boldsymbol{q},\boldsymbol{q}'} \,, \tag{4.36}$$

where the inverse matrix is given by

$$\mathbf{A}^{-1}_{\boldsymbol{q}} = \frac{1}{\Delta_q} \begin{pmatrix} \dfrac{1}{\kappa q^4} + \dfrac{1}{\kappa_{\mathrm{t,eff}} q^2} & \dfrac{\mathrm{i}(1+\frac{1}{2}r_\mathrm{d})}{\kappa_\mathrm{t} q} \\[2ex] \dfrac{-\mathrm{i}(1+\frac{1}{2}r_\mathrm{d})}{\kappa_\mathrm{t} q} & \dfrac{1}{\kappa_\mathrm{t}} \end{pmatrix} . \tag{4.37}$$

The factor out front describes the anticipated divergence associated with the soft mode,

$$\Delta_q = 1 - (q/q_\mathrm{c})^2 \,, \tag{4.38}$$

and we have also defined an effective tilt modulus

$$\kappa_{\mathrm{t,eff}} = \frac{\kappa_\mathrm{t}}{1+r_\mathrm{d}} = \kappa_\mathrm{t}\big(1 - r_\mathrm{d} + r_\mathrm{d}^2 + \mathcal{O}(r_\mathrm{d}^3)\big) \,. \tag{4.39}$$

Of course, the idea of a "diverging amplitude" does not sit well with the very framework within which this conclusion has been reached—linear Monge gauge. Higher order terms are needed to quantitatively understand the system when approaching the divergence, and certainly past the instability. Despite this, the conclusion that a soft mode occurs, and that this happens at the particular wave vector q_c, is quantitatively correct. This is because we can think of our calculation as a *linear stability analysis*, which proves that past q_c any mode, even an arbitrarily small one, will no longer experience a restoring force but rather an amplification—hence driving an instability.

[1] It nevertheless bears remembering that even though *typically* the characteristic length ℓ (and with it the wavelength of the unstable mode) is microscopic, there is no fundamental reason why it should *always* be microscopic—this all depends on the magnitude of the tilt modulus κ_t, and if κ_t vanishes, ℓ will become large.

Interestingly, the effective tilt modulus $\kappa_{\mathrm{t,eff}}$ entering the mode spectrum smoothly connects with the effective tilt decay length ℓ_{eff} introduced in the previous section, since

$$\ell = \sqrt{\frac{\kappa}{\kappa_{\mathrm{t}}}} \quad \longleftrightarrow \quad \ell_{\mathrm{eff}} \overset{(4.21)}{=} \sqrt{1 + r_{\mathrm{d}}}\ell \overset{(4.39)}{=} \sqrt{\frac{\kappa}{\kappa_{\mathrm{t,eff}}}} \,. \tag{4.40}$$

To parse out the fluctuations of shape and tilt field separately, we look at components of equations (4.36) and (4.37). From the first component of the inverse matrix we obtain the new undulation spectrum,

$$\left\langle \left| h_{\boldsymbol{q}} \right|^2 \right\rangle = \frac{1}{1 - (q/q_{\mathrm{c}})^2} \left[\frac{k_{\mathrm{B}}T}{\kappa q^4} + \frac{k_{\mathrm{B}}T}{\kappa_{\mathrm{t,eff}} q^2} \right] , \tag{4.41}$$

which is characterized by two major modifications. First, it exhibits the soft-mode divergence at $q = q_{\mathrm{c}}$, captured by one overall prefactor. And second, the remaining part looks essentially like the MNK result [MNK07b, MNK07a], except that the tilt modulus is replaced by the effective tilt modulus from Eq (4.39). Away from the divergence we might thus expect to still fit the spectrum with the MNK expression. Expanding Eq (4.41) for *small* wave vectors, we indeed find

$$\left\langle \left| h_{\boldsymbol{q}} \right|^2 \right\rangle = \frac{k_{\mathrm{B}}T}{\kappa q^4} + \frac{k_{\mathrm{B}}T}{\kappa^*_{\mathrm{t,eff}} q^2} + \frac{k_{\mathrm{B}}T}{\kappa^*_{\mathrm{t,eff}} q_{\mathrm{c}}^2} + \mathcal{O}(q^2) \,. \tag{4.42}$$

The bending term is hence unaffected by either tilt or divergence, but the tilt term changes. Somewhat annoyingly, the effective tilt modulus which this type of fitting would yield is *not* the one defined in Eq (4.39) but instead

$$\kappa^*_{\mathrm{t,eff}} = \frac{\kappa_{\mathrm{t}}}{(1 + \frac{1}{2} r_{\mathrm{d}})^2} = \kappa_{\mathrm{t}} \Big(1 - r_{\mathrm{d}} + \frac{3}{4} r_{\mathrm{d}}^2 + \mathcal{O}(r_{\mathrm{d}}^3) \Big) \,, \tag{4.43}$$

because expanding the divergence $1/\Delta_q$ creates a second effective q^{-2} tilt contribution from the bending term. Comparison with Eq (4.39) shows that the two effective moduli agree to linear order in r_{d}. The first (relative) difference is quadratic, $\frac{1}{4} r_{\mathrm{d}}^2$, which is likely quite small using the numbers from Table 4.5.

In the height fluctuation calculation we used the linear Monge gauge expression $K = -\Delta h$ for the curvature. However, Watson *et al.* [WBWB12] have pointed out that one can alternatively describe the effective curvature via the divergence of the lipid director: $\boldsymbol{\nabla} \cdot \boldsymbol{n} = \tilde{K}$. This is true up to cubic order in the fields (K_{ij} or $\boldsymbol{T}$), as we show in Appendix C, and it of course also holds on the linearized Monge level.

Extending this thinking to our revised HK Hamiltonian, we can express the critical subspace of undulations and longitudinal tilt modes instead in terms of *lipid director* and lipid tilt modes. Again following Watson *et al.* [WBWB12] and defining $n^{\parallel}_{\boldsymbol{q}} = \hat{\boldsymbol{q}} \cdot \boldsymbol{n}_q$ as the longitudinal

Lipids	κ (10^{-20}J)	κ_t (pN/nm)	ℓ (nm)	κ_tw (10^{-20}J)	$[\![\sigma_0]\!]_2$ (10^{-20}J)	K_A (pN/nm)	$d_\mathrm{P:P}$ (nm)	$d_\mathrm{C2:C2}$ (nm)
DPPC	15.8	48.8	1.80	2.04	-1.33	210.0	3.90	2.79
DMPC	12.2	40.2	1.74	2.18	-1.32	210.0	3.56	2.45
DOPC	11.8	64.0	1.36	0.99	-0.84	290.0	3.83	2.74
DNPC	22.0	47.4	2.15	2.23	-1.38	220.0	5.11	3.99
DOPE	11.8	84.7	1.18	1.44	0.24	250.0	4.08	3.00
POPC	13.2	55.2	1.55	1.45	-1.09	280.0	3.85	2.75
PDPC	9.6	65.0	1.22	0.95	-0.64	260.0	3.79	2.71
POPE	13.3	80.4	1.29	2.36	0.06	260.0	4.16	3.07
PDPE	9.9	77.2	1.13	1.48	0.42	200.0	4.02	2.96
SDPE	10.6	74.8	1.19	1.65	0.52	300.0	4.21	3.15
PSM	27.8	39.1	2.67	4.76	-4.10	310.0	4.08	3.03
POPG	11.3	61.5	1.36	1.05	1.43	180.0	3.48	2.69

Table 4.1: Mechanical properties of twelve different lipids measured by fully atomistic molecular dynamic simulations by VBP [VBP15].

component of the Fourier transformed lipid director field, we get

$$E_{n,\parallel} = \frac{1}{2}\sum_{\boldsymbol{q}} \boldsymbol{e}_{\boldsymbol{q}}^{\dagger} \cdot \mathbf{B}_{\boldsymbol{q}} \cdot \boldsymbol{e}_{\boldsymbol{q}} \quad \text{with } \boldsymbol{e}_{\boldsymbol{q}} = \begin{pmatrix} n_{\boldsymbol{q}}^{\parallel} \\ T_{\boldsymbol{q}}^{\parallel} \end{pmatrix} , \tag{4.44}$$

where the coupling matrix is now given by

$$\mathbf{B}_{\boldsymbol{q}} = \begin{pmatrix} \kappa q^2 & -\frac{1}{2}\mathrm{i}r_\mathrm{d}\kappa q^2 \\ \frac{1}{2}\mathrm{i}r_\mathrm{d}\kappa q^2 & \kappa_\mathrm{t} \end{pmatrix} . \tag{4.45}$$

The fluctuation spectrum again follows from

$$\left\langle \boldsymbol{e}_{\boldsymbol{q}} \cdot \boldsymbol{e}_{\boldsymbol{q}'}^{\dagger} \right\rangle = k_\mathrm{B}T\, \mathbf{B}_{\boldsymbol{q}}^{-1}\, \delta_{\boldsymbol{q},\boldsymbol{q}'} , \tag{4.46}$$

where the inverse matrix is found to be

$$\mathbf{B}_{\boldsymbol{q}}^{-1} = \frac{1}{\Delta_q} \begin{pmatrix} \dfrac{1}{\kappa q^2} & \dfrac{\mathrm{i}r_\mathrm{d}}{2\kappa_\mathrm{t}} \\ \dfrac{-\mathrm{i}r_\mathrm{d}}{2\kappa_\mathrm{t}} & \dfrac{1}{\kappa_\mathrm{t}} \end{pmatrix} . \tag{4.47}$$

Observe that this features the same divergence that we encountered before.

The director-tilt subspace contains the same longitudinal tilt axis as the undulation-tilt subspace, and hence it also gives the same result for the longitudinal tilt fluctuations. Much more

Lipids	[VBP15] $\kappa(10^{-20}\mathrm{J})$	Eq (4.4) κ^{est}	$f^{\mathrm{est}}=1$ κ^{est}	$-2[\![\sigma_0]\!]_2/\kappa^{\mathrm{est}}$	$\kappa_{\mathrm{tw}}/\kappa^{\mathrm{est}}$	% diff	$f^{\mathrm{est}}=1$ % diff
DPPC	15.80	12.69	11.38	0.21	0.16	19	27
DMPC	12.20	11.44	10.45	0.23	0.19	6	14
DOPC	11.80	13.54	11.56	0.12	0.07	-14	1
DNPC	22.00	19.53	16.94	0.14	0.11	11	22
DOPE	11.80	11.58	9.64	-0.04	0.12	1	18
POPC	13.20	14.13	12.29	0.15	0.10	-7	6
PDPC	9.60	11.73	10.02	0.11	0.08	-22	-4
POPE	13.30	13.73	11.61	-0.01	0.17	-3	12
PDPE	9.90	8.92	7.38	-0.09	0.17	9	25
SDPE	10.60	14.18	11.70	-0.07	0.12	-33	-10
PSM	27.80	26.30	23.76	0.31	0.18	5	14
POPG	11.30	9.30	8.59	0.31	0.11	17	24
$\langle\lvert\%\rvert^2\rangle^{1/2}$						15	17

Table 4.2: The bending modulus values for twelve different lipid types. The table shows the κ values from the all-atom MD simulations taken from Ref. [VBP15]. Values for the estimates from Eq (4.4), and contribution of the second moment of the stress profile and the twist modulus to the estimations of κ is also tabulated. In the last column, the relative difference between estimated and measured κ values is given. The last row gives the root mean square percentile difference.

interesting are the longitudinal director fluctuations:

$$\left\langle \left| n_{\boldsymbol{q}}^{\parallel} \right|^2 \right\rangle = \frac{1}{1-(q/q_{\mathrm{c}})^2} \, \frac{k_{\mathrm{B}}T}{\kappa q^2} \tag{4.48a}$$

$$= \frac{k_{\mathrm{B}}T}{\kappa q^2} + \frac{k_{\mathrm{B}}T}{\kappa q_{\mathrm{c}}^2} + \mathcal{O}(q^2) \, . \tag{4.48b}$$

This shows that the bending modulus can hence be extracted from lipid director fluctuations, which requires much smaller system sizes for equilibration [WBWB12]. Pleasingly, the divergence at $q = q_{\mathrm{c}}$ due to our additional term in HK theory does *not* interfere with the lowest order expression (even though it now bounds the spectrum from below). As long as the analysis stays sufficiently far below q_{c}, which is not a severe restriction, it remains unaffected.

4.4 Discussion

In the Section 4.1, we determined estimates for the bending modulus and the coupling modulus using the definitions of the elastic moduli derived in Chapter 3. Then, we calculated the effects of the novel coupling term and the lipid twist term to the Euler-Lagrange equations and the

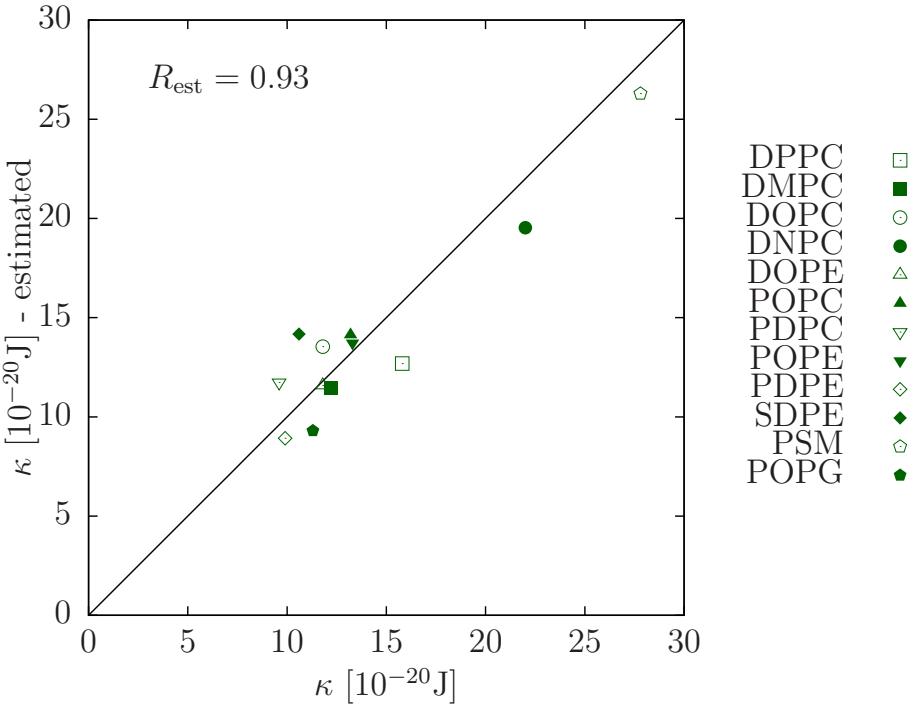

Figure 4.1: Correlation between κ values determined directly from undulation spectrum in [VBP15] and estimations κ^{est} given in Eq (4.4). The coefficient for effective thickness is $f^{\text{est}} = 1.1$ for this figure. The solid line gives the total correlation with slope 1 between κ and κ^{est}. Correlation coefficient is $R = 0.93$. Twelve different lipid types represented by shapes as given in the legend on the right.

fluctuation spectra. In the present section, we will have a closer look at these consequences and quantitatively show the effect of modifications of the theory in certain cases.

First, we check the validity of the estimation of the bending modulus that is given in Eq (4.4) and compare it with estimates based on two other models. Eq (4.4) expresses κ in terms of other elastic parameters which can be measured by computer simulations independent of the measurement of κ. Indeed, Venable, Brown and Pastor (VBP) [VBP15] have measured various mechanical properties of twelve different lipids in fully atomistic molecular dynamic simulations based on CHARMM36 force field. VBP measured κ for twelve different lipids from the undulation power spectrum as well as all the individual terms on the right hand side of Eq (4.4). For ease of reference, we tabulated some of the results of VBP in Table 4.1.

There are two different monolayer thickness measurements in VBP. The first one is the distance between phosphate groups of two leaflets $d_{\text{P:P}}$ and the second one is the thickness of the hydrophobic region $d_{\text{C2:C2}}$, *i. e.*, the separation across the bilayer between the average positions of carbon 2 of the lipid chains. As we discussed earlier, there is an ambiguity of the membrane thickness so we will use an effective thickness, defined as $d_{\text{m}}^{\text{eff}} := f^{\text{est}} d_{\text{m}}$, where $d_{\text{m}} = \frac{1}{2} d_{\text{p:p}}$ is half of the distance between the phosphate atoms of two individual monolayers as reported in VBP, and f^{est} is a coefficient that is the same for all twelve different lipids.

In table 4.2, we list κ values measured from fluctuation spectra by VBP, κ^{est} values determined using Eq (4.4) and their relative difference for the twelve different lipids used in [VBP15].

We determined the effective thickness coefficient by minimizing the mean square difference between measured κ and estimated κ^{est} from Eq (4.4) and found to be $f \approx 1.1$. Figure 4.1 illustrates the agreement between estimated values and measured values. The correlation coefficient between κ^{est} and the measured κ is found to be $R = 0.93$ for Eq (4.4) where $R = 1$ means perfect correlation.

The estimate of κ in Eq (4.4) can be compared with two other predictions, namely, the polymer brush model [ROM$^+$00] and the uncoupled two-dimensional fluid film model [GGL99]. The polymer brush model predicts a relationship between bending modulus and area expansion modulus [ROM$^+$00],

$$\kappa^{\mathrm{PBM}} = \frac{K_{\mathrm{A}} d_{\mathrm{h}}^2}{24}\,, \tag{4.49}$$

where d_{h} is the thickness of the hydrophilic region $d_{\mathrm{C2:C2}}$. VBP also gives the estimates for polymer brush model. Furthermore, we combine the PBM with our effective thickness approach by defining an effective thickness $d_{\mathrm{h}}^{\mathrm{eff}} = f^{\mathrm{PBM}} d_{\mathrm{h}}$. Minimization of the mean square difference between κ^{PBM} and κ gives us the coefficient $f^{\mathrm{PBM}} \approx 1.2$. The values of κ^{PBM} and its relative difference to κ is also listed in Table 4.3. The estimation of κ^{PBM} with κ is plotted in Figure 4.2 and the correlation coefficient between them is found to be much smaller, $R = 0.56$. Another relation between κ and K_{A} comes from modeling bilayers as two uncoupled two-dimensional fluid sheets [GGL99]:

$$\kappa^{\mathrm{GGL}} = \frac{K_{\mathrm{A}} d^2}{48}\,, \tag{4.50}$$

where d is the bilayer thickness. We calculate the values of κ^{GGL} and list them in Table 4.4. We also combine estimation of two uncoupled fluid sheet model with our effective thickness approach by defining the thickness as $d^{\mathrm{eff}} = f^{\mathrm{GGL}} d$. Minimization of the mean square difference between κ^{GGL} and κ gives us $f^{\mathrm{GGL}} \approx 1.3$. The comparison of κ^{GGL} and κ is shown in Table 4.4 and in Figure. 4.3. The correlation coefficient between κ and κ^{GGL} is $R = 0.53$. Note that, using effective distance does not change the correlation coefficients for Eq (4.49) and Eq (4.50) because f is an overall coefficient which does not affect R. If we use the same thickness values, we would expect to find the same correlation coefficients for both models, Eq (4.49) and Eq (4.50), because both equations have the same form. However, the correlation coefficients are slightly different because the ratios between hydrophobic thickness, d_{h}, and the bilayer thickness, d, are not same for different lipids. It is easily seen that the estimation given in Eq (4.4) agrees with the measurements of κ significantly better than those given by the polymer brush theory and the two-dimensional fluid sheet model.

The Gaussian curvature modulus is probably the most mysterious curvature elastic parameter of lipid membranes. Yet, knowing the value of $\overline{\kappa}$ is crucial to understand the energetics of fusion and fission events [BJB$^+$18]. Using the underlying microscopic theory, Helfrich showed that the monolayer modulus $\overline{\kappa}_{\mathrm{m}}$ is equal to the second moment of the stress profile, $[\![\sigma_0]\!]_2$ [Hel81]. The bilayer counterpart $\overline{\kappa}$ in terms of monolayer elastic parameters is given in Eq (3.46b) which

Lipids	[VBP15] $\kappa(10^{-20}\mathrm{J})$	[VBP15] κ^{PBM}	% diff	Eq (4.49) + f^{PBM} κ^{PBM}	% diff
DPPC	15.80	7.37	53	10.35	34
DMPC	12.20	5.75	52	7.98	34
DOPC	11.80	9.71	17	13.70	-16
DNPC	22.00	15.44	29	22.13	0
DOPE	11.80	9.87	16	14.15	-19
POPC	13.20	9.50	28	13.37	-1
PDPC	9.60	8.44	12	12.09	-25
POPE	13.30	10.78	18	15.42	-15
PDPE	9.90	7.58	23	11.02	-11
SDPE	10.60	12.89	-21	18.76	-76
PSM	27.80	12.24	55	17.90	35
POPG	11.30	5.67	49	8.20	27
$\langle\lvert\%\rvert^2\rangle^{1/2}$			35		32

Table 4.3: The bending modulus values for twelve different lipid types. The table shows the κ values from the all-atom MD simulations taken from Ref. [VBP15]. The third column lists the values of bending modulus that are calculated from Eq (4.49) and given in [VBP15], and the fifth column lists the values from PBM model using effective thickness. The relative differences between estimates and the measured values as well as the root mean square percentile differences are tabulated.

is determined solely by geometric identities and without relying on any knowledge of the underlying physics [Des15]. The combination $\kappa_{\mathrm{m}}K_{0,\mathrm{m}}$ enters Eq (3.46b), and it is given as the first moment of stress profile, Eq (3.40c). Thus, the lateral stress profile, its first and second moments, and the position of pivotal plane z_0 are sufficient to calculate $\overline{\kappa}$.

Even though the lateral stress profile cannot be measured by experiments, it is relatively easy and computationally inexpensive to measure from simulations. Recently, Wang and Deserno [WD15] proposed a method for determining z_0 from computer simulations. Combining the stress profile, z_0, and measurement of κ from one of the standard methods gives us the ratio of the two elastic moduli $\overline{\kappa}/\kappa$.

The ratio $\overline{\kappa}/\kappa$ is known to be in the range $-2 < \overline{\kappa}/\kappa < 0$ [Des15] for stable bilayers in the lamellar phase. Even though, a few studies give reasonable $\overline{\kappa}/\kappa$ values, most simulation results are either outside of the range $-1 < \overline{\kappa}/\kappa < 0$ or are very small [OHSE08, OME10, OE11, HBD12, HdJMD13, VBP15]. Hu *et al.* [HBD12, HdJMD13] proposed the so called *patch-closure* method to measure $\overline{\kappa}$ from simulations. These authors also used the stress profile formula and observed that the results of these two methods do not agree. Their results raise questions about the validity of the stress profile method.

Observe now that in the revised quadratic framework we propose, the twist modulus enters the definition of the Gaussian curvature modulus in Eq (4.9b). This correction is a possible

	[VBP15]	Eq (4.50)		Eq (4.50) + f^{GGL}	
Lipids	$\kappa(10^{-20}\mathrm{J})$	κ^{GGL}	% diff	κ^{GGL}	% diff
DPPC	15.80	6.66	57	11.04	30
DMPC	12.20	5.56	54	9.22	24
DOPC	11.80	8.89	24	14.73	-24
DNPC	22.00	11.95	45	19.81	9
DOPE	11.80	8.67	26	14.37	-21
POPC	13.20	8.66	34	14.36	-8
PDPC	9.60	7.78	18	12.91	-34
POPE	13.30	9.35	29	15.50	-16
PDPE	9.90	6.72	32	11.14	-12
SDPE	10.60	11.08	-4	18.37	-73
PSM	27.80	10.74	61	17.81	35
POPG	11.30	4.54	59	7.52	33
$\langle\lvert\%\rvert^2\rangle^{1/2}$			41		32

Table 4.4: The bending modulus values for twelve different lipid types. The table shows the κ values from the all-atom MD simulations taken from Ref. [VBP15]. The third column lists the values of bending modulus that are calculated from PBM, Eq (4.50), and the fifth column lists the same values using the effective thickness. The relative differences between estimates and the measured values as well as the root mean square percentile differences are tabulated.

solution to the discrepancies concerning the microscopic definition of the Gaussian curvature modulus. We can calculate the ratio $\overline{\kappa}/\kappa$ by the stress profile method and include the twist modulus correction using the results of VBP [VBP15]. For twelve different lipids, the bilayer moduli ratio $\overline{\kappa}/\kappa$ is found to be in the range $(-0.48, 0.61)$ before the twist modulus correction. When we use the twist modulus correction, the range of values improves to $(-0.82, 0.34)$. However, while the twist modulus correction is a step in the right direction towards solving the stress profile discrepancy, it can not eliminate all questions about the validity of the stress profile method, or more generally, the underlying microscopic framework.

Besides the changes in the definitions of elastic moduli in terms of the underlying mechanical parameters, we have two additional terms in the energy density Eq (3.39). We have shown how this terms affect the Euler-Lagrange equations of the system, as well as the fluctuations of membrane shape and lipid orientation. Perhaps the first thing to notice is that the effect of these new terms is not small. For instance, at the level of the Euler-Lagrange equation (4.12), the derivative $\boldsymbol{\nabla\nabla}\cdot\boldsymbol{T}$ gets multiplied by the new prefactor $1 + r_{\mathrm{d,m}} - r_{\mathrm{tw}}$. This reduces to the HK prefactor 1 when $r_{\mathrm{d,m}} = r_{\mathrm{tw}} = 0$, but it becomes 0 if $r_{\mathrm{d,m}} = -1$ and $r_{\mathrm{tw}} = 0$. In the latter case, the differential equation actually loses its derivatives, and tilt becomes locally enslaved to the geometry, as Eq (4.23) indicates. This leads to fundamentally different physics, and the entire spectrum of behavior between these two limits is possible within the new theory—depending on the value of the coupling and lipid tilt moduli. For this to work, the observable of interest and

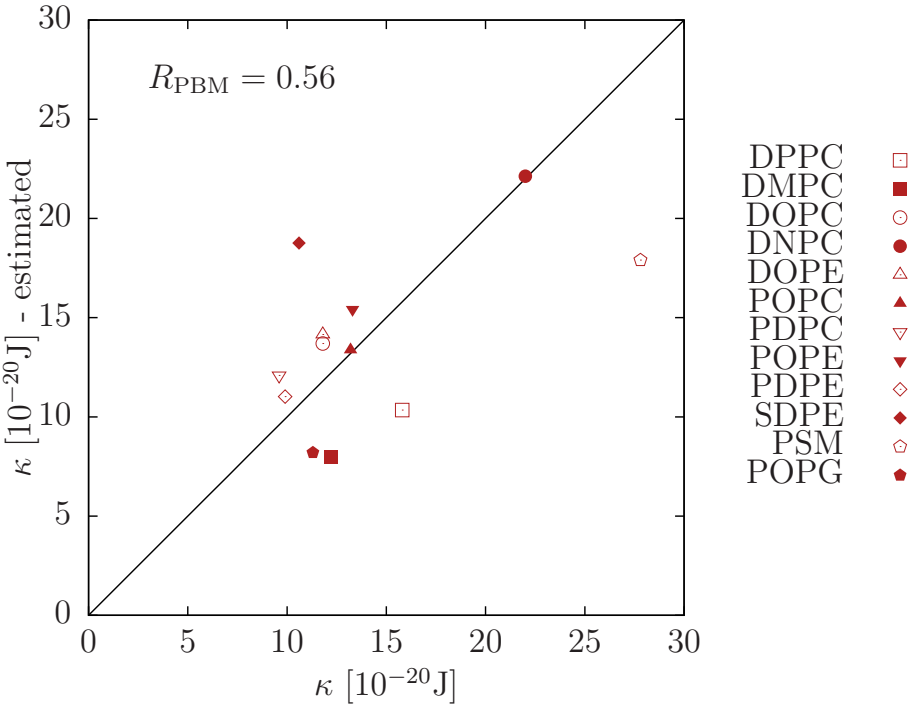

Figure 4.2: Correlation between κ values determined directly from undulation spectrum in [VBP15] and estimations κ^{PBM} given in Eq (4.49). The solid line gives the total correlation with slope 1 between κ and κ^{PBM}. Correlation coefficient is $R = 0.56$. Twelve different lipid types represented by shapes as given in the legend on the right.

r_{d} must enter the analytical expression to which one intends to fit in such a way that the two can be disentangled. Of course, this not always needs to be the case, and Eqs (4.48a) and (4.48b) provide an example: the power spectrum of the longitudinal orientation modes, $\langle |n^{\parallel}_{\boldsymbol{q}}|^2 \rangle$, contains κ and q_{c} as its two fitting parameters, but $q_{\mathrm{c}} = 2/\ell|r_{\mathrm{d}}|$ involves the two additional parameters κ_{t} and κ_{d} only in the combination $\kappa_{\mathrm{t}}/\kappa_{\mathrm{d}}^2$ that prevents them from being disentangled.

In contrast, the undulation spectrum $\langle |h_{\boldsymbol{q}}|^2 \rangle$ from Eq (4.41) contains the three parameters κ, κ_{t}, and r_{d} in such a way that they all can in principle be identified.[2] This is easy to see from the functional form, but let us illustrate that it also works in practice. To this end we will look at the very high quality undulation spectra published in [WPWB11] for two different types of coarse-grained models—a generic coarse-grained implicit solvent model due to Brannigan, Philips, and Brown (BPB in the following) [BPB05], and the coarse-grained MARTINI model (specifically for DPPC) by Marrink *et al.* [MRY$^+$07]. We refer the reader to these original publications for further information on these two models; for here it suffices to say that (in a suitable parameter range) they both result in fluid self-assembled lipid membranes with well-characterized physical behavior.

[2]The fitting of the undulation spectrum $\langle |h_{\boldsymbol{q}}|^2 \rangle$ actually gives us the values of κ, $\kappa_{\mathrm{t,eff}}$ and q_{c}. Then, we calculate κ_{t}, and r_{d} using these three values. However, values of κ_{t}, and r_{d} are degenerate. In other words, there are two sets of κ_{t} and r_{d} which correspond to the same $\kappa_{\mathrm{t,eff}}$ and q_{c} values. Because of the degeneracy, one needs to be careful to interpret these results. In our analysis, we use the set of κ_{t} and r_{d} values which has $r_{\mathrm{d}} < 0$ because in the earlier version of our theory [TD17] we had the monolayer Gaussian curvature modulus ($\overline{\kappa}_{\mathrm{m}} < 0$) in front of the novel coupling term, $r_{\mathrm{d}} = r_{\mathrm{m}} < 0$.

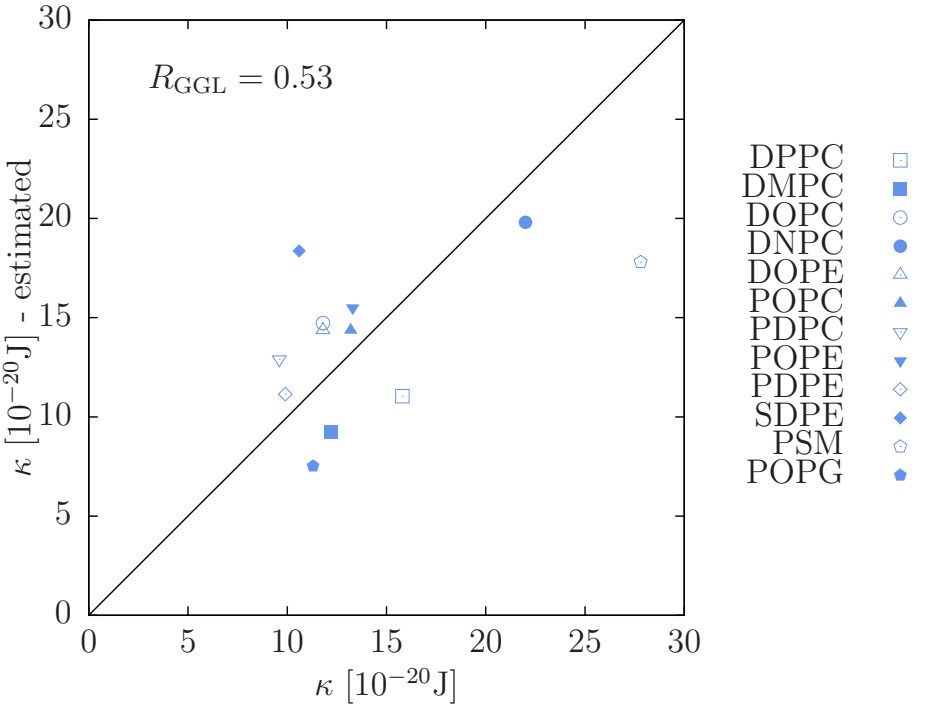

Figure 4.3: Correlation between κ values determined directly from undulation spectrum in [VBP15] and estimations κ^{GGL} given in Eq (4.50). The solid line gives the total correlation with slope 1 between κ and κ^{GGL}. Correlation coefficient is $R = 0.53$. Twelve different lipid types represented by shapes as given in the legend on the right.

Figures 4.4 and 4.5 show fits of Eq (4.41) to the shape undulation spectra of these models, which are multiplied by a factor q^4 in order to make their "fine structure" better visible. The red curves indeed capture the data points very well, yielding results for κ, κ_{t}, and r_{d} (see Table 4.5). In contrast, the power spectrum belonging to the original HK theory, Eq (4.31), can not describe the full datasets, since it fails to capture the uptick created by the divergence at q_{c}. Aware of this limitation, Watson *et al.* [WBWB12] in a follow-up publication fit Eq (4.31) only to the low-q regime; the green dashed curves in the figures illustrate the result when restricting to the first 7 q-vectors. Finally, instead of using our full result from Eq (4.41), one could take the three leading order terms in the expansion from Eq (4.42). This function has the same number of fitting parameters as the full expression and also permits disentangling κ, κ_{t}, and r_{d} (observe that q_{c} of course no longer signifies an actual divergence).

Table 4.5 lists the parameter values resulting from all three fits. Even though the different fits often give similar answers, sometimes the deviations are very large. For instance, the value of κ_{m} for the generic BPB model deviates by a factor of 2 between the HK fit and our theory, while the tilt modulus for the same model is almost the same in all three fits (even though it actually should not be, considering that $\kappa_{\mathrm{t}} \neq \kappa^*_{\mathrm{t,eff}}$). Conversely, the bending moduli for the MARTINI DPPC model are relatively close, while now the tilt moduli vary substantially. Especially the strong deviations for the bending moduli of the BPB model are perhaps unexpected, since all fits make the same prediction for the low-q regime. Notice also that the root-mean-square residuals

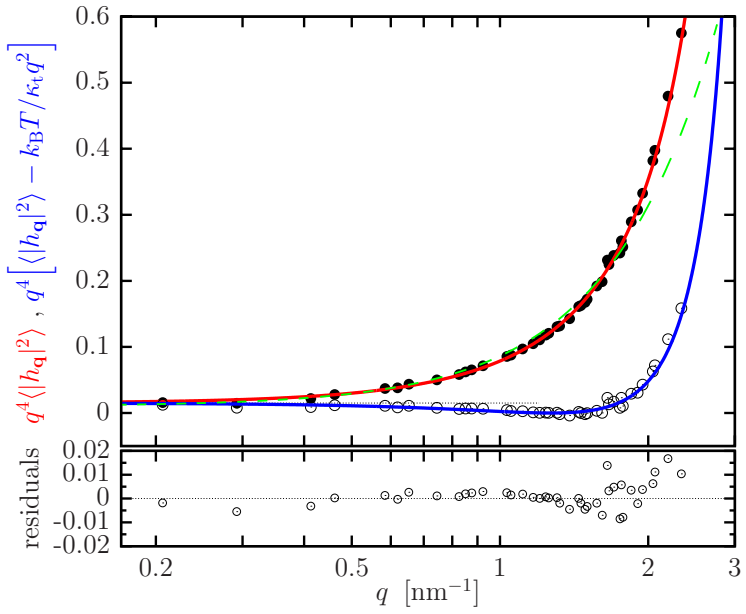

Figure 4.4: Power spectrum of membrane undulations for the coarse-grained BPB model [BPB05]. The filled circles are the spectrum published in [WPWB11], the red curve is a fit to Eq (4.41). The open circles and the blue curve have the term $k_{\mathrm{B}}Tq^2/\kappa_{\mathrm{t}}$ subtracted. The green dashed curve is a fit to Eq (4.31) using the first 7 wave vectors. The lower panel shows the residuals between the data and the fit to our model. Fitting coefficients are listed in Tab. 4.5.

for the expanded equation (4.42) are slightly larger than those for the full expression (4.41), even though both contain the same number of parameters.

To understand the quality of these fits better, we would have to dive into many numerical details—such as, what is the appropriate q-range to fit to, how do we decorrelate the errors in these nonlinear fits, do the residuals hint at systematics, *etc.* This, however, goes beyond the goal of our illustration.[3] For now, we simply wish to illustrate that our new fluctuation formula (4.41) provides a systematically derived power spectrum that in principle offers access to three relevant material parameters. The best way to assess its usefulness is to apply it to a wider set of data and scrutinize the predictions it makes.

As a final comment on the generic form of the spectrum, we wish to point out an interesting feature already noted by Watson *et al.* [WBWB12]. These authors suggested to subtract the tilt contamination from the undulation spectrum by considering the expression $q^4\langle|h_{\boldsymbol{q}}|^2\rangle - k_{\mathrm{B}}Tq^2/\kappa_{\mathrm{t}}$, which in standard HK theory reduces to the q-independent constant $k_{\mathrm{B}}T/\kappa$. Doing so, they however noticed that the resulting expression is not a constant, but initially drops below the low-q asymptotic value, which they identify with $k_{\mathrm{B}}T/\kappa$, and at larger q again picks up rather rapidly. Figures 4.4 and 4.5 illustrate this with the open circles as data points and the blue curves as the corresponding fits.

[3] We could—*very* roughly—use the scatter around the residuals as a proxy for the error bars. Subsequent fits then indicate a 10% error for κ_{d}, a 5%–10% error for r_{d}, and a 1% error for κ_{t}. This strikes us as too precise. Also, the quality of the HK-MNK fit depends strongly on the chosen q-range, since its functional form does not represent the full dataset.

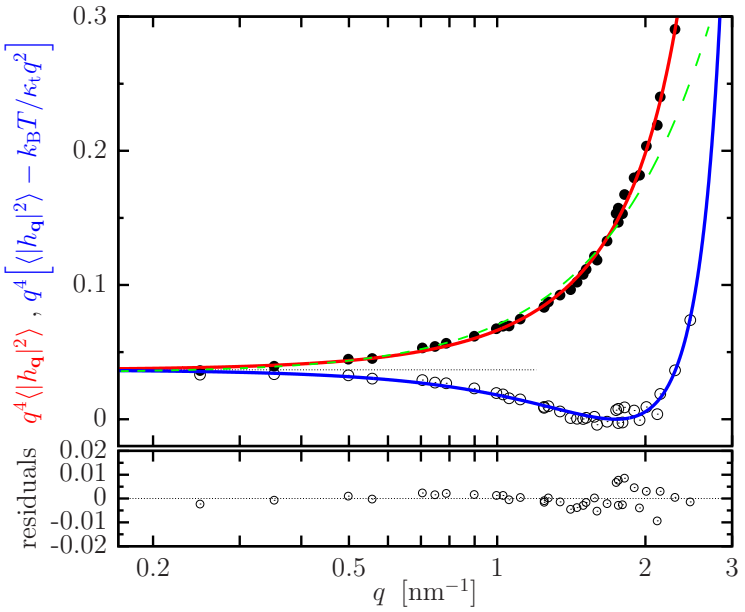

Figure 4.5: Same as Fig. 4.4, but for the coarse-grained MARTINI model of DPPC at 50°C [MRY+07], using again the spectrum from [WPWB11].

Both features can be readily understood within our revised fluctuation formula. First, the initial decline of the expression $q^4\langle|h_{\boldsymbol{q}}|^2\rangle - k_\mathrm{B}Tq^2/\kappa_\mathrm{t}$ with increasing q happens because *the second term subtracts too much*: combining Eqs (4.42) and (4.43), and recalling that we are choosing $r_\mathrm{d} \leq 0$, we find (up to $\mathcal{O}(q^2)$)

$$q^4\langle|h_{\boldsymbol{q}}|^2\rangle - \frac{k_\mathrm{B}Tq^2}{\kappa_\mathrm{t}} \approx \frac{k_\mathrm{B}T}{\kappa} + \frac{k_\mathrm{B}Tq^2}{\kappa_\mathrm{t}}\Big[\underbrace{\left(1+\tfrac{1}{2}r_\mathrm{d}\right)^2 - 1}_{\leq 0}\Big]\,, \tag{4.51}$$

a simple consequence of the fact that the lowest order tilt correction contains the effective modulus $\kappa^*_{\mathrm{t,eff}} < \kappa_\mathrm{t}$. And second, the strong increase at even larger q-values is the result of the divergence Δ_q^{-1} in Eq (4.41) at $q = q_\mathrm{c}$. The open symbols and the blue curves in Figs. 4.4 and 4.5 recast the data in this representation, showing that the functional form of a quadratic decline multiplied by a divergence captures the high-q-regime of both spectra very well.

Recall that the coupling modulus, κ_d, does not just enter the fluctuation spectra, but also the Euler-Lagrange equation for the tilt. One example where this matters can be found in a recent paper by Wang and Deserno [WD16], who determined the tilt modulus from simulating membrane buckles. The basic idea is that a buckled membrane features periodic curvature gradients, which in turn excite periodic tilt field undulations (see Fig. 3.3 for an illustration). Measuring those and comparing to theory gives access to the tilt modulus.[4] However, Wang and Deserno used the *original* HK theory for this comparison, and since our revision of HK theory affects the Euler-Lagrange equation for the tilt, this implies that the value deduced by them, let's call it

[4]Strictly speaking, the authors of Ref. [WD16] do not *directly* measure the tilt field, for this entails large uncertainties. But their analysis effectively exploits the connection between lipid tilt and membrane geometry as implied by Eq (4.11).

Eq	$\#q$	δ_{res}	model	lipid	T(K)	$\frac{\kappa_{\text{d}}}{[\text{pN nm}]}$	$\frac{\kappa_{\text{t}}}{[\text{pN/nm}]}$	r_{d}	ℓ(nm)	$\frac{q_{\text{c}}}{(\text{nm}^{-1})}$
(4.31)	7	1.8×10^{-3}	BPB	generic	300	199	54.6	—	2.7	—
		7.5×10^{-4}	MARTINI	DPPC	323	64.2	125.2	—	1.0	—
(4.42)	41	5.6×10^{-3}	BPB	generic	300	99	52.6	-0.49	1.9	(2.1)
	35	4.5×10^{-3}	MARTINI	DPPC	323	53.5	72.0	-0.95	1.2	(1.7)
(4.41)	41	4.5×10^{-3}	BPB	generic	300	135	54.4	-0.25	2.2	3.5
	35	3.7×10^{-3}	MARTINI	DPPC	323	60.7	92.6	-0.50	1.1	3.5

Table 4.5: Fitting results to the power spectra of membrane undulations belonging to the generic BPB [BPB05] and the MARTINI DPPC [MRY+07] coarse-grained models, based on trajectories and spectra presented in Ref. [WPWB11]. The three sets of numbers are determined by fitting to (i) the MNK fluctuation formula [MNK07b, MNK07a] belonging to the original HK theory [HK00], Eq (4.31); (ii) the third order expansion of our theory, Eq (4.42); and (iii) our full fluctuation formula (4.41). The relevant equation and the number of q-vectors included in the fit ("$\#q$") are listed in the first two columns. The goodness of fit can be judged by the root-mean-square of the residuals, δ_{rms}, calculated with the actual number of degrees of freedom (number of data points minus number of fitting parameters).

$\kappa_{\text{t}}^{\text{WD}}$, requires a correction. Repeating their analysis with the new equation (4.24), we find that an additional prefactor arises:

$$\kappa_{\text{t}} = \Big(1 + \frac{1}{2} r_{\text{d}}\Big) \kappa_{\text{t}}^{\text{WD}} \,. \tag{4.52}$$

This is again a case where no independent determination of r_{d} is possible, so one cannot extract κ_{t} and r_{d} simultaneously from the buckling data alone—at least not by the procedure described in Ref. [WD16]. If we take the value $r_{\text{d}} \approx -0.5$ from the fluctuation data discussed above as an estimate, we see that Eq (4.52) implies $\kappa_{\text{t}} \approx 0.75\, \kappa_{\text{t}}^{\text{WD}}$, showing that the bare tilt moduli might be about 25% smaller than the values given by Wang and Deserno. This downgrades the good agreement of their results with previous simulations [WBWB12, LVW+14, VBP15] and more recent experiments [JAN14, Nag17a]. Notice, however, that the comparison data were all determined from analyzing fluctuations. If this is done via the *undulation* spectrum, this will renormalize κ_{t} to lowest order by a factor of $1 + r_{\text{d}}$ (see Eq (4.39) or Eq (4.43)), which is actually a *stronger* correction than the one applying to the tilt-from-buckling analysis (namely, a 50% reduction in the above example). This in particular holds for the experimental data, which analyze the undulation modes of a stack of lipid membranes [JAN14, Nag17a]. If, on the other hand, one extracts the tilt modulus κ_{t} from either the *tilt* or the *director* spectrum, the subsequent analysis remains unaffected by our revision of HK theory.

4.5 Conclusion

The derivation of the complete curvature-tilt theory reveals the definitions of the two-dimensional elastic constants in terms of their three-dimensional counterparts. Due to the differences between our derivation and Hamm and Kozlov theory [HK00], these definitions of elastic constants got

modified from earlier forms. Using these new forms, we derived estimates for the bending modulus κ, the coupling modulus κ_{d} and the Gaussian curvature modulus $\overline{\kappa}$ in terms of other elastic parameters. We can use them as consistency checks when we can independently measure the elastic modulus and the corresponding mechanical parameters that are needed for the estimation. For the bending modulus case, we check the consistency of our estimate. We use the measurements from an extensive study of computer simulations of lipid membranes by Venable, Brown, and Pastor [VBP15] and find a very good correlation between κ values determined directly from the fluctuation power spectrum and our estimates. We also compared our estimates with two other models, namely the polymer brush model [ROM$^+$00] and the two uncoupled fluid sheet model [GGL99]. Our estimates correlate with the direct measurements of κ significantly better that these other two models. Besides the bending modulus, we can use estimations of coupling modulus and Gaussian curvature modulus to check the consistency of our theory. We showed that the coupling modulus can be extracted from the undulation spectrum, which is a widely used way to the measure bending modulus.

On the other hand, direct measurements of the Gaussian curvature modulus are limited, because the Gauss-Bonnet theorem prevents accessing the K_{G}-term in the Hamiltonian, unless one changes either the topology or the boundary [Kre59, dC76]. The former definition of the Gaussian curvature modulus, which is the second moment of the stress profile, is modified by the lipid twist modulus. Even though this correction doest not solve the discrepancy about the second moment condition completely, it changes the estimates of the Gaussian curvature modulus in the correct direction.

In Ref [TD17], it is showed that the coefficient of both Gaussian curvature and the novel coupling term is the second moment of the stress profile and the coefficient of the novel coupling term can be measured from the height fluctuation spectrum and hence the value of $\overline{\kappa}_{\mathrm{m}}$. However, coefficients of both terms are modified. The value κ_{d} extracted from the undulation spectrum is no longer equal to Gaussian curvature modulus.

Our new terms significantly affect both the Euler-Lagrange equation for the tilt and all fluctuation spectra. We have shown two examples in which very well converged power spectra of membrane undulations can be fit remarkably well by our revised fluctuation expression (4.41), and three important moduli can be extracted in one go: bending modulus, tilt modulus, and coupling modulus. Of course, having three fitting parameters available makes it easier to capture the spectrum, and so we curb our enthusiasm regarding the good-looking fits. Moreover, it remains to be explored how high in q-range it even makes sense to push this theory, considering that, after all, it is based on continuum elasticity. One way to potentially make headway in this endeavor would be to better understand the nature and origin of the divergence and the concomitant instability predicted at $q = q_{\mathrm{c}}$. If it has a counterpart in the simulated systems (or in experiment), this would significantly strengthen confidence in the high-q regime of our extended HK theory. The next step clearly is to apply Eq (4.41) to a wider set of measured spectra, in order to get more parameters about which one can then summarily reason.

In this chapter we have also provided derivations of the Euler-Lagrange equations for both a single leaflet, as well as a bilayer comprising two coupled and perfectly sliding monolayers. Tilt-sum and -difference fields arise, which decay in identical ways once excited, but only the difference field is actually sourced by the membrane geometry. The new monolayer term creates expected bilayer counterparts, and once more the elastic ratio r_{d} enters the EL equations. However, due to the generally weaker curvatures which intact bilayer geometries show, it will likely be harder to use shapes to measure the coupling modulus.

Chapter 5

Higher Order Coupling in Curvature-Tilt Elasticity

In Chapter 3, we derived the quadratic curvature-tilt theory in which we only kept terms up to quadratic order in curvature and tilt. Therefore, the only possible curvature-tilt coupling term is bilinear, $\mathcal{O}(KT)$. However, there are two interesting terms in energy density (3.39) that do indeed have higher order contributions: the effective Gaussian curvature $\tilde{K}_{\mathrm{G}}$ and the lipid twist term $(\boldsymbol{\nabla} \times \boldsymbol{T})^2$. Both our theory and Hamm and Kozlov theory have the $\tilde{K}_{\mathrm{G}}$ term [HK00]. We will explicitly show that the difference between $\tilde{K}_{\mathrm{G}}$ and K_{G} is a term quadratic in both tilt *and* curvature; it is *biquadratic* and as such leads to qualitatively new physical phenomena—most noticeably a curvature-dependent *effective local tilt modulus*, which needs not be positive.

In the derivation of the quadratic curvature-tilt theory, when we encountered a biquadratic term we discarded it—on account of it being higher order and thus small. And yet, such a term would be of the same order as the correction hidden in $\tilde{K}_{\mathrm{G}}$ (whose biquadratic nature is, admittedly, not immediately evident). We believe that consistency demands to either drop the tilde over K_{G} (leaving everything at the quadratic or bilinear level) or to systematically keep all biquadratic terms. The former approach is easy, but the latter one is more intriguing. All the more so since at the high curvatures where Hamm and Kozlov's theory bears interesting fruits, the biquadratic terms contribute very noticeably.

A systematic formulation of the theory for bilayers requires shifting the two individual monolayer expressions from their respective intra-monolayer reference surfaces towards the bilayer midplane, as we did for the quadratic theory. However, shifting the biquadratic term is a task that is surprisingly laborious.

5.1 Elastic Free Energy Density of a Monolayer

In Chapter 3, our point of departure for the bottom-up derivation of the quadratic theory was the three-dimensional energy density, which we derived in Chapter 2. In the present chapter, we again start from the same three-dimensional energy as we did in the quadratic theory. However,

we will calculate the strain terms in the energy density in terms of curvature and tilt field up to the *bi-quadratic* terms. In addition to the quadratic terms we determined in Chapter 3, we will also derive the higher order coupling terms up to $\mathcal{O}(K^2T^2)$. Recall the underlying energy density given in Eq (2.40),

$$e_{3\mathrm{d}} = \sigma_0(z)\epsilon(\zeta) + \tfrac{1}{2}\tilde{E}(u^\alpha_\alpha)^2 + 2\lambda_\mathrm{t} u_{\alpha z}u^{\alpha z} + \tfrac{1}{2}\lambda_\mathrm{s}\left[(u_\alpha{}^\alpha)^2 - 4\det u^\beta_\alpha\right] . \tag{2.40}$$

This energy density is three-dimensional; yet, our goal is a two-dimensional one—an *energy per unit area*, like the Helfrich Hamiltonian. This is achieved by integrating Eq (2.40) over the transverse direction, which requires re-expressing the area strain ϵ as well as the strain terms u^α_α, $\det u^\beta_\alpha$ and $u_{\alpha z}$ in terms of geometry and tilt.

In the next section we will determine the area strain in terms of curvature and tilt field. It turns out that the consistent derivation of the area strain up to bi-quadratic terms is not as straightforward as the derivations for the quadratic theory. Then, we will introduce the three-dimensional metric tensor, and determine the strain tensor components using this framework.

5.1.1 Area strain and additional pre-stress

In order to derive the area strain, we will use the same parametrization as in Chapter 3. However, there are subtle points we need to clarify which are irrelevant for the quadratic order yet significant for the derivation of the bi-quadratic theory. We know that both lipid tilt and geometric deformations can change the area per lipid throughout the monolayer and hence lead to in-plane strain. To make progress, it turns out to be convenient to classify this in-plane strain as arising from two different contributions: the first one is *zeroth order area strain*, which is independent of the transverse coordinate; and the second one is *higher order area strain*, which explicitly depends on the transverse coordinate. We ignored the zeroth order area strain, because, as we will show later, it does not contribute to the quadratic energy.

The zeroth order area strain can have two origins. The first one is simple membrane stretching; however, we will ignore this part in this thesis work by only considering membranes not subject to an additional lateral tension. The second origin for area strain is lipid tilt. To make this more precise, we need to think carefully about what we mean by tilt. Hamm and Kozlov assumed that tilting happens by *shearing* lipids sideways (*i. e.*, with a vorticity direction parallel to the membrane) [HK98, HK00]. This will leave the height of the membrane unchanged, and hence also the area per lipid. However, Kopelevich and Nagle have recently shown in simulations that the length of a lipid does not strongly depend on its orientation [KN15], which suggests that lipids do not shear but instead *rotate*, as illustrated in Fig. 5.1. This implies that the thickness of the monolayer decreases, and hence that the area per lipid increases [KZCC01, CM04] due to volume conservation.[1]

Besides the flat untilted state and the final curved and tilted state (illustrated in part (a) and (c) of Fig. 5.1), it is convenient to define an *intermediate* state of deformation, namely a flat

[1] Volume conservation means that the Poisson ratio has the value $1/2$ throughout the membrane.

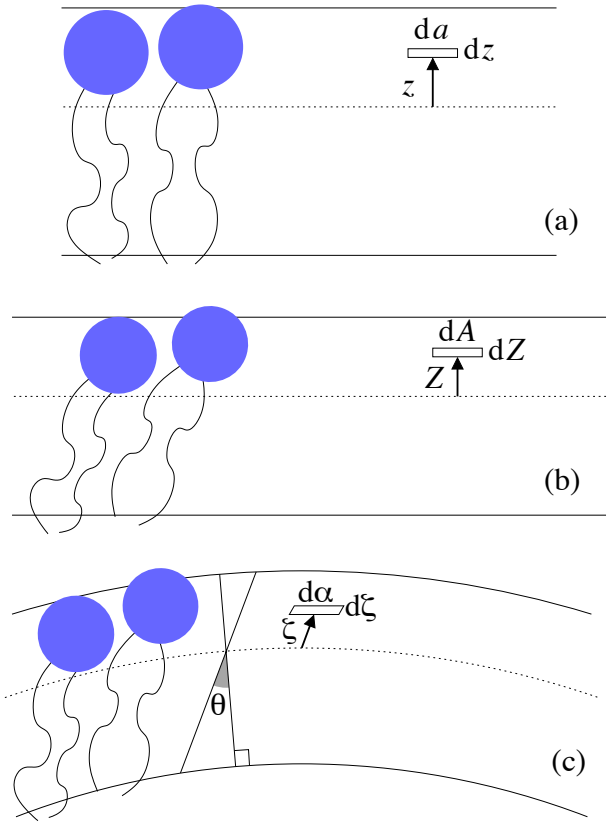

Figure 5.1: Illustration of the three states we use to describe the complete deformation of a monolayer leaflet: (a) is the flat untilted reference state; (b) is the flat state in which tilt has happened and hence the area per lipid has changed; and (c) is the final curved state. The dotted line in (c) is the pivotal plane, and the dotted lines in (b) and (a) are its pre-image. The small rectangle illustrates a volume element somewhere inside the leaflet, and its displacement away from its respective reference surface.

state which accounts only for the zeroth order area strain due to tilting—the *flat tilted* state (b) in Fig. 5.1. Since the energy is a function of state, the elastic energy of the final state does not depend on the order in which a set of deformations leads to that state. The definition of this intermediate state will then permit us to disentangle higher order effects that vary throughout the thickness of the membrane (and derive from its geometry) from tilt effects that apply homogeneously throughout the thickness of the leaflet.

Even in a curved monolayer there will be a surface, which by generalizing our notation from previous chapters we will again call the *pivotal plane*, on which the area per lipid remains unchanged compared to the *intermediate* state, and on which therefore the higher order in-plane strain vanishes. We will use this surface (as well as its pre-image in states (b) and (a)) as the reference surface for describing the monolayer leaflet. In order to quantify the higher order strains arising in the curved leaflet away from the pivotal plane, we will again use *lipid shifted surfaces* which is defined in Section 3.2.4. Recall that the distance between the pivotal plane and a lipid shifted surface, *as measured along the material frame of a lipid*, is constant. For instance, if the pivotal plane happens to pass through the 12^{th} carbon atom (as counted from the tail of a lipid), then the local displacement field that maps each such carbon atom to, say, the

corresponding 6^{th} carbon atom on the same lipid will define a lipid shifted surface (which in this case lies closer to the bilayer midplane). In particular, this mapping also transports the area element of the pivotal plane to the lipid shifted surface.

Let us pause here to introduce some important notation. To describe coordinates or differentials in the initial, intermediate, and final state, we will use lower case roman, upper case roman, and lower case Greek letters, respectively. In particular, local area element and transverse height differential in these three states will be denoted as

$$\begin{aligned} \text{initial:} \qquad & \{\mathrm{d}a; \mathrm{d}z\} \,, \\ \text{intermediate:} \qquad & \{\mathrm{d}A; \mathrm{d}Z\} \,, \\ \text{final:} \qquad & \{\mathrm{d}\alpha; \mathrm{d}\zeta\} \,, \end{aligned}$$

as also illustrated in Fig. 5.1. Notice that in the first two states the transverse coordinate z or Z is perpendicular on the area element, but this is *not* the case in the final state. Hence, the volume element is *not* given by $\mathrm{d}\alpha\,\mathrm{d}\zeta$ but instead by $\mathrm{d}\alpha\,\mathrm{d}\zeta\cos\theta$, where θ is the tilt angle.[2] This will become important below.

On the pivotal plane of configuration (c), the area element $\mathrm{d}\alpha$ is equal to the area element of the intermediate configuration, $\mathrm{d}\alpha(\zeta = 0) = \mathrm{d}A$, but away from the pivotal plane the area element generally differs due to curvature effects. Hence, we can define the local higher order area strain as

$$\epsilon_\zeta = \frac{\mathrm{d}\alpha - \mathrm{d}A}{\mathrm{d}A} \,. \tag{5.1}$$

Its value depends on the position within the leaflet, which we can parametrize by the two-dimensional position on the pivotal plane, and the local displacement ζ away from that surface along the local lipid orientation. Moreover, we can also define the zeroth order area strain, which occurs due to the transition from the flat untilted reference configuration to the intermediate configuration:

$$\epsilon_0 = \frac{\mathrm{d}A - \mathrm{d}a}{\mathrm{d}a} \,. \tag{5.2}$$

The *total* area strain is the relative change in the area element of the curved monolayer with respect to the flat untilted reference configuration. Using Eqns. (5.1) and (5.2), we can write it in terms of the zeroth order and higher order area strain:

$$\epsilon(\zeta) = \frac{\mathrm{d}\alpha - \mathrm{d}a}{\mathrm{d}a} = (1+\epsilon_0)(1+\epsilon_\zeta) - 1 \,. \tag{5.3}$$

Higher Order Area Strain

We derived the area strain up to quadratic order in both curvature and tilt field in Chapter 3. In this section, we will revisit and extend these calculations. The definition of the higher order area

[2] The extra factor $\cos\theta$ is what in a $3+1$ foliation treatment of general relativity is called the "Lapse function" [Whe64]. I thank Jemal Guven for alerting us to this subtlety, which initially had slipped our attention.

strain (5.1) is the same as the area strain that is used in the quadratic theory Eq (2.43): the change in the area element of a lipid shifted surface with respect to the pivotal plane.

Recall that we must express the strains entering Eq (2.40) as a function of geometry and tilt field. To do so, we first have to parametrize the three-dimensional bent sheet as a function of the surface geometry of its two-dimensional reference surface (the pivotal plane) and the local lipid tilt.

The parametrization for the pivotal plane and the lipid shifted surfaces has been given in Chapter 3. Recall that $\boldsymbol{X}$ is a point on the pivotal plane, which we displace by a distance ζ along the local material direction $\boldsymbol{n}$:

$$\boldsymbol{X}' = \boldsymbol{X} + \zeta\, \boldsymbol{n}\ . \tag{5.4}$$

For any given (smooth) vector field $\boldsymbol{n}$ and displacement ζ, this defines a new surface $\boldsymbol{X}'$, and if $\boldsymbol{n}$ coincides with the lipid orientation, we arrive at a mathematically precise definition of the *lipid shifted surfaces*. Notice that $\boldsymbol{X}'$ inherits its parametrization from that of the reference surface $\boldsymbol{X}$, but it has its own metric, curvature tensor, *etc.*, and this will permit us to compute the strains we seek. For instance, to calculate the area strain from Eq (5.1), we need to calculate the area elements $\mathrm{d}A$ and $\mathrm{d}\alpha$ on the reference surface and the shifted surface, respectively. The area element in terms of the determinant on the pivotal plane and on a lipid shifted surface is given in Eq (2.43) and Eq (2.44),

$$\epsilon_\zeta(\zeta) = \frac{1}{2}\varepsilon^{\alpha\beta}|\nabla_\alpha \boldsymbol{X}' \times \nabla_\beta \boldsymbol{X}'| - 1\ . \tag{5.5}$$

The derivation of $\epsilon_\zeta(\zeta)$ is identical to the one we previously showed in Section 3.2.4 and Appendix A. The difference in what we will show now is the order of the terms we keep during the calculations. Therefore, we do not repeat most of the basic steps and defer the reader to Section 3.2.4 for important points of the calculations and to Appendix A for the detailed derivation. The higher order area strain is given in Eq (A.18) in Appendix A:

$$\epsilon_\zeta(\zeta) = \epsilon_1\zeta + \epsilon_2\zeta^2 + \mathcal{O}(\zeta^3, |\boldsymbol{T}|^3)\ , \tag{5.6}$$

with the expansion coefficients from Eq (A.19a) and Eq (A.19b)

$$\epsilon_1 = \big(1 - \frac{1}{2}T^2\big)\tilde{K}\ , \tag{5.7a}$$

$$\epsilon_1 = (1 - T^2)\tilde{K}_{\mathrm{G}} - \frac{1}{2}\boldsymbol{T}\cdot\boldsymbol{\nabla}\tilde{K} + \frac{1}{2}T^\delta T^\gamma K_{\delta\beta}K^\beta_\gamma\ . \tag{5.7b}$$

5.1.2 The Zeroth Order Area Strain

The higher order area strain ϵ_ζ is calculated using the lipid shifted surfaces. The only term left in the total area strain $\epsilon(\zeta)$ to be determined is the zeroth order area strain, ϵ_0. To find it, we will use the result that the lipid length remains constant upon tilting [KN15], and we exploit an incompressibility relation (*i. e.*, we assume the Poisson ratio is equal to $1/2$).

When lipids rotate, the transverse differential $\mathrm{d}Z$ of the intermediate configuration must be the projection of the transverse coordinate of the flat reference coordinate, $\mathrm{d}Z = \mathrm{d}z\,\cos\theta$. Therefore, the transverse strain is given as

$$u^0_{zz} = \frac{\mathrm{d}Z - \mathrm{d}z}{\mathrm{d}z} = \cos\theta - 1 \overset{*}{=} \frac{1}{\sqrt{1+|\boldsymbol{T}|^2}} - 1 = -\frac{1}{2}T_l T^l + \mathcal{O}(|\boldsymbol{T}|^4)\,, \tag{5.8}$$

where at "$*$" we used $|\boldsymbol{T}| = \tan\theta$.

Next, we will exploit the thin plate assumption that the stress normal to the plate vanishes throughout the material, which relates the transverse and lateral strains [LL86]

$$-\left(u^0_{xx} + u^0_{yy}\right) = u^0_{zz} \overset{(5.8)}{=} -\frac{1}{2}T_l T^l\,. \tag{5.9}$$

The area strain can not depend on the transverse position through the leaflet, because we assumed the lipids to rotate rigidly. Finally, using the fact that at $\mathcal{O}(\zeta)$ the area strain equals the sum of the in-plane diagonal components of the strain tensor, we then arrive at the zeroth order area strain

$$\epsilon_0 = \frac{1}{2}T_l T^l\,. \tag{5.10}$$

Note that if we relax the incompressibility assumption and allow a Poisson ratio different than $1/2$, we would get a Poisson ratio dependence in Eq (5.10). The complete area strain is found by inserting Eq (5.6) and Eq (5.10) into Eq (5.3):

$$\epsilon(\zeta) = \frac{1}{2}T^2 + \zeta\tilde{K} + \zeta^2\big[(1-\frac{1}{2}T^2)\tilde{K}_{\mathrm{G}} - \frac{1}{2}\boldsymbol{T}\cdot\boldsymbol{\nabla}\tilde{K} + \frac{1}{2}K_{\beta\alpha}K^\alpha_\gamma T^\beta T^\gamma\big]\,. \tag{5.11}$$

5.1.3 Strain Tensor Components from Three-dimensional Metric

There are three terms left to be determined in the three-dimensional energy density 5.1: $(u^\alpha_\alpha)^2$, $u_{\alpha z}u^{\alpha z}$ and $(u^\alpha_\alpha)^2 - 4\det u_{\alpha\beta}$. In order to determine these terms up to bi-quadratic order, we need to find the components of the three-dimensional strain tensor, u_{ij}.

A commonly used measure of strain is given as the change in the metric of the material coordinates between deformed (present) state and the zero strain (reference) state [GZ92, ESK09]

$$u_{ij} = \frac{1}{2}(g'_{ij} - a_{ij})\,, \tag{5.12}$$

where g'_{ij} and a_{ij} are the metric tensor of the deformed state and *the zero strain state*, respectively. In the earlier chapters, we choose the reference configuration for the monolayer as the flat and untilted state in which the elastic energy is set to be zero. However, due to the fluid nature of the lipid membranes, lipids are allowed to diffuse passed each other freely upon deformations. In other words, in-plane movements of lipids do not cost elastic energy. This condition causes the

deformed state of the membrane to be *incompatible* [ESK09]. The formal definition of incompatibility is that the reference metric tensor is not necessarily immersible in three-dimensional Euclidean space. For a monolayer, incompatiblity means that there exists no global physically realizable zero-strain state without the rearrangement of the lipids.[3] With fixed lipid positions with respect to each other—without allowing in-plane diffusion—we cannot find a configuration in which the components of the strain tensor vanishes *at every point* of a membrane, even though we can find a configuration where all the components of a strain tensor vanishes *for a given point* on a membrane. Therefore, the reference metric, a_{ij} in Eq (5.12), does not represent a physically realizable configuration. We called this *configuration* the zero strain state in which the strain tensor vanishes everywhere, but it actually is not physically realizable.

The Zero Strain State

As we mentioned earlier, our choice of zero energy state for the lipid membranes is a flat and zero-tilt configuration. Therefore, the local distances between material points of a lipid membrane in the flat untilted configuration give rise to the zero strain tensor. In our case, the local distances could be interpreted as the average distance between neighboring atoms. For the reference metric (the zero strain metric) in the strain tensor, we need to find a metric that mimics the flat configuration. However, incompatibility tells us that we cannot find such a metric globally,[4] we can only find it locally [ESK09]. Fortunately, we know the relations between the material points of a deformed and the flat state of the pivotal plane: In the case of zero-tilt, the strain tensor vanishes on the pivotal plane (from Section 5.1.2, we know that the zeroth order area strain is proportional to the square of the tilt field). We also know the geometric relations between the pivotal plane and any other point on the membrane. Therefore, the metric on the pivotal plane is the key to find the zero strain state metric, a_{ij}, for every point on the membrane.

The two-dimensional metric on the pivotal plane is defined as $g_{\alpha\beta}$. We know that in the case of zero-tilt, strains vanish on the pivotal plane, so we define the in-plane components of the zero strain state metric as $a_{\alpha\beta} = g_{\alpha\beta}(T^{\gamma} = 0)$. The reason that we can write a metric on the pivotal plane in the case of zero-tilt is that we assume that lipids do not move upon tilting, so the zero-tilt case is compatible with the deformed configuration. For the case of zero tilt, we also know that the transverse coordinate is perpendicular to the pivotal plane, so the three-dimensional metric is block diagonal[5]

$$a_{ij} = \begin{pmatrix} & & 0 \\ & a_{\alpha\beta} & 0 \\ & & \\ 0 & 0 & 1 \end{pmatrix} . \tag{5.13}$$

[3] Another example of an incompatible deformation are the growth processes for which the zero-stress state cannot be achieved upon continuous deformations.

[4] In this context, global stands for the state in which the strains vanish everywhere on the membrane simultaneously.

[5] Note that when we write down a three-dimensional metric tensor in a block diagonal form, the first entry, $a_{\alpha\beta}$, represents a two-dimensional tensor.

Then, the determinant of the 3-dimensional metric is equal to the determinant of the in-plane part,

$$\det a_{ij} = \det a_{\alpha\beta}\,. \tag{5.14}$$

The Three-dimensional Metric of the Deformed State

We use the same parametrization that we used in Section 5.1.1

$$\boldsymbol{X}'(u^1,u^2,z) = \boldsymbol{X}(u^1,u^2) + \zeta(u^1,u^2,z)\,\boldsymbol{n}(u^1,u^2), \tag{5.15}$$

where the vector $\boldsymbol{X}'$ describes the coordinates of a *lipid shifted surface* and $\boldsymbol{X}$ describes the coordinates of the pivotal plane. Lipid shifted surfaces are a family of surfaces that are a fixed distance away from the pivotal plane, as measured along the material frame of a lipid, which is z in our notation. Recall that ζ is the distance between the lipid shifted surface and the pivotal plane in the deformed state in the direction of the lipid director $\boldsymbol{n}$. Recall that the lipid director $\boldsymbol{n}$ is normalized, $\boldsymbol{n}\cdot\boldsymbol{n} = 1$.

The tangent vectors for the lipid shifted surfaces are,

$$\boldsymbol{e}'_\alpha = \nabla_\alpha \boldsymbol{X}' = \nabla_\alpha \boldsymbol{X} + (\nabla_\alpha\zeta)\boldsymbol{n} + \zeta\nabla_\alpha\boldsymbol{n}\,, \tag{5.16}$$

$$\boldsymbol{e}'_z = \frac{\partial \boldsymbol{X}'}{\partial z} = \frac{\partial\zeta}{\partial z}\boldsymbol{n}\,, \tag{5.17}$$

where the usage of the covariant derivatives for the in-plane directions and the partial derivative for the transverse direction are by choice. Because $\boldsymbol{X}$ is a scalar with respect to the surface coordinate frame, its covariant and partial derivatives with respect to these surface coordinates agree. Then, by setting ζ or z to zero, the tangent vectors on the pivotal plane are found:

$$\boldsymbol{e}_\alpha = \nabla_\alpha \boldsymbol{X}\,, \tag{5.18}$$

$$\boldsymbol{e}_z = \boldsymbol{n}\,, \tag{5.19}$$

where $(\nabla_\alpha\zeta)$ vanishes on the pivotal plane and $\partial\zeta/\partial z(z=0) = 1$, because we assume that z and ζ agree at the linear order, $\zeta = z + \mathcal{O}(z^2)$. Then, $\nabla_\alpha\zeta = \mathcal{O}(\zeta^2)$.

The in-plane components of the three-dimensional metric are found to be

$$\begin{aligned} g'_{\alpha\beta} = \boldsymbol{e}'_\alpha\cdot\boldsymbol{e}'_\beta &= [\boldsymbol{e}_\alpha + (\nabla_\alpha\zeta)\boldsymbol{n} + \zeta\nabla_\alpha\boldsymbol{n}]\cdot[\boldsymbol{e}_\beta + (\nabla_\beta\zeta)\boldsymbol{n} + \zeta\nabla_\beta\boldsymbol{n}] \\ &= g_{\alpha\beta} + \zeta[\boldsymbol{e}_\alpha\cdot\nabla_\beta\boldsymbol{n} + \boldsymbol{e}_\beta\cdot\nabla_\alpha\boldsymbol{n}] \\ &\quad + \zeta^2(\nabla_\alpha\boldsymbol{n})\cdot(\nabla_\beta\boldsymbol{n}) + (\nabla_\beta\zeta)\boldsymbol{e}_\alpha\cdot\boldsymbol{n} + (\nabla_\alpha\zeta)\boldsymbol{e}_\beta\cdot\boldsymbol{n}\,. \end{aligned} \tag{5.20}$$

The mixed and the transverse components are

$$g'_{\alpha z} = \frac{\partial\zeta}{\partial z}[\boldsymbol{e}_\alpha\cdot\boldsymbol{n} + (\nabla_\alpha\zeta)]\,, \tag{5.21a}$$

$$g'_{zz} = \Big(\frac{\partial\zeta}{\partial z}\Big)^2\,, \tag{5.21b}$$

where we used the fact that $\boldsymbol{n}$ is normalized and hence orthogonal to $\nabla_\alpha \boldsymbol{n}$.

Recall the definition of the lipid director

$$\boldsymbol{n} = \beta(\boldsymbol{N} + \boldsymbol{T}) \,, \tag{5.22}$$

where $\boldsymbol{N}$ is the normal vector of the pivotal plane and $\boldsymbol{T}$ is the tilt vector. Since, by definition, the components of the tilt vector are in the direction of the tangent vectors of the pivotal plane, $\boldsymbol{T} = T^\alpha \boldsymbol{e}_\alpha$, the square of the normalization factor is

$$\beta^2 = \frac{1}{1 + T^\alpha T^\beta g_{\alpha\beta}} \,. \tag{5.23}$$

The covariant derivative of the director, $\nabla_\alpha \boldsymbol{n}$, is determined in Appendix A and given in Eq (A.5). The projection of the director onto the pivotal plane, $\boldsymbol{e}_\alpha \cdot \boldsymbol{n}$, is determined from Eq (5.22):

$$\boldsymbol{e}_\alpha \cdot \boldsymbol{n} = T_\alpha + \mathcal{O}(T^3) \,. \tag{5.24}$$

Then the components of the three-dimensional metric tensor, Eqs (5.20, 5.21a, and 5.21b), can be written as

$$\begin{aligned} g'_{\alpha\beta} &= g_{\alpha\beta} + \zeta\beta[\tilde{K}_\beta{}^\gamma g_{\gamma\alpha} + \tilde{K}_\alpha{}^\gamma g_{\gamma\beta}] \\ &\quad + \zeta^2\big[T^\gamma T^\delta K_{\alpha\gamma} K_{\beta\delta} + \beta^2 \tilde{K}_\alpha{}^\gamma \tilde{K}_\beta{}^\delta g_{\gamma\delta}\big] + (\nabla_\beta \zeta) T^\gamma g_{\alpha\gamma} + (\nabla_\alpha \zeta) T^\gamma g_{\beta\gamma} \,, \end{aligned} \tag{5.25a}$$

$$g'_{\alpha z} = \frac{\partial \zeta}{\partial z}[\beta T^\gamma g_{\alpha\gamma} + (\nabla_\alpha \zeta)] \,, \tag{5.25b}$$

$$g'_{zz} = \Big(\frac{\partial \zeta}{\partial z}\Big)^2 . \tag{5.25c}$$

As we mentioned earlier, $\nabla_\alpha \zeta = \mathcal{O}(\zeta^2)$, so the off-diagonal component has the following form on the pivotal plane

$$g_{\alpha z} = \beta T^\gamma g_{\alpha\gamma} \,. \tag{5.26}$$

5.1.4 Connection between z and ζ

We are now in the position to link the transverse coordinate z of the flat untilted state with the lipid-aligned coordinate ζ of the final curved state. The relation between the transverse coordinate of the deformed and undeformed configurations ζ and z is calculated from the incompressibility condition. Upon deformation, the local volume of the lipid membrane is conserved. Hence, the volume elements of the two configurations are equal,as are, therefore, the determinants of the corresponding metric tensors [GZ92]

$$\det g'_{ij} = \det g_{ij} = \det a_{ij} \,. \tag{5.27}$$

These are very useful equalities. For example, from the second equality, $\det g_{ij} = \det a_{ij}$, we can derive the zeroth order area strain, which is given in Eq (5.2),

$$\epsilon_0 = \frac{\mathrm{d}A}{\mathrm{d}a} - 1 = \frac{\sqrt{\det g_{\alpha\beta}}}{\sqrt{\det a_{\alpha\beta}}} - 1 \,. \tag{5.28}$$

In the second equality we used the fact that the ratio of two area elements of two surfaces can be written as the ratio of the square root of the metric determinant on these two surfaces. The determinant, $\det a_{ij}$, from Eq (5.14), is equal to the determinant of the in-plane part $\det a_{\alpha\beta}$. However, the same is not true for the pivotal plane, $\det g_{ij} \neq \det g_{\alpha\beta}$. The three-dimensional metric tensor on the pivotal plane is given as $g_{ij} = g'_{ij}(\zeta = 0)$

$$g_{ij} = \begin{pmatrix} g_{\alpha\beta} & \beta T^{\gamma} g_{\alpha\gamma} \\ \beta T^{\gamma} g_{\beta\gamma} & 1 \end{pmatrix} . \tag{5.29}$$

For the off-diagonal terms, $g_{\alpha z}$, we used Eq (5.26) and for g_{zz} we used the assumption of $\zeta = z + \mathcal{O}(z^2)$ so the following partial derivative becomes

$$\frac{\partial \zeta}{\partial z} = 1 + \mathcal{O}(z) \,. \tag{5.30}$$

Therefore, the transverse component of the metric tensor, given in Eq (5.21b), is calculated at $\zeta = 0$

$$g_{zz} = g'_{zz}(\zeta = 0) = 1 \,. \tag{5.31}$$

The detailed calculation of $\det g_{ij}$ is given in Appendix D, and the final result is given in Eq (D.11)

$$\det g_{ij} = \beta^2 \det g_{\alpha\beta} \,. \tag{5.32}$$

With the combination of Eq (5.27), Eq (5.28), Eq (5.32), and Eq (5.23), we arrive at

$$\epsilon_0 = \frac{1}{2} T^2 + \mathcal{O}(T^3) \,. \tag{5.33}$$

As we expected, Eq (5.33) agrees with the zeroth order area strain, Eq (5.10), that we derived in Section 5.1.2.

For the relation between ζ and z, we need to determine the determinant of the three-dimensional metric g'_{ij}. This calculation is straightforward but tedious, so we defer the reader to Appendix D for the details of the derivation. The final result is given up to a bi-quadratic order in Eq (D.18)

$$\zeta(z) = z - \frac{1}{2} z^2 (\tilde{K} - \frac{1}{2} \tilde{K} T^2 + 2 T^{\gamma} T^{\delta} \tilde{K}_{\gamma\delta}) + \mathcal{O}(z^3) \,. \tag{5.34}$$

From this expression, the covariant derivative of ζ follows immediately:

$$\nabla_\alpha \zeta(z) = -\frac{1}{2} z^2 \nabla_\alpha (\tilde{K} - \frac{1}{2} K T^2 + 2 T^\gamma T^\delta K_{\gamma\delta}) + \mathcal{O}(z^3)\,, \tag{5.35}$$

$$= -\frac{1}{2} z^2 \nabla_\alpha \tilde{K} + \mathcal{O}(z^3, T^2)\,. \tag{5.36}$$

This is same with the expression we found in Section 3.2.4.

5.1.5 The Strain Terms in the Energy Density

In this section we will use the three-dimensional metric to calculate the strain terms in the energy density (5.1). For example, the second term in Eq (5.1) is the trace of the in-plane part of the strain tensor. For taking its trace, one index must be raised. However, the choice of the metric that will be used to raise indices is not obvious. One can use the inverse of the reference metric or the current metric to raise indices of the strain tensor. Efrati *et al.* [ESK09] use the reference metric to raise, and we will follow their approach and use the inverse reference metric.[6]

Inverse of the reference metric: a^{ij}

The reference metric as given in Eq (5.13) is block diagonal so its inverse is also block diagonal

$$a^{ij} = \begin{pmatrix} a^{\alpha\beta} & 0 \\ 0 & 1 \end{pmatrix}\,, \tag{5.37}$$

which satisfies the relation $a^{ij} a_{kj} = \delta^i_k$. The block diagonal form of the metric allows us to write the similar relation for the in-plane part of the metric

$$a^{\alpha\beta} a_{\gamma\beta} = \delta^\alpha_\gamma\,. \tag{5.38}$$

The two-dimensional fluidity assumption says that there is no in-plane shear *on the pivotal plane*, which means that the pure shear part of the strain tensor vanishes there:

$$0 = u_\alpha^{\ \beta}(\zeta = 0) - \frac{1}{2} u_\gamma^{\ \gamma}(\zeta = 0)\delta^\beta_\alpha\,, \tag{5.39}$$

$$= \frac{1}{2}(a^{\beta\delta} g_{\alpha\delta} - \delta^\beta_\alpha) - \frac{1}{2}(\frac{1}{2} a^{\gamma\delta} g_{\gamma\delta} \delta^\beta_\alpha - \delta^\beta_\alpha)\,, \tag{5.40}$$

which gives us

$$a^{\beta\delta} g_{\alpha\delta} = \frac{1}{2} a^{\gamma\delta} g_{\gamma\delta} \delta^\beta_\alpha\,. \tag{5.41}$$

When we multiply both sides with $a_{\beta\mu}$, we see that $a_{\alpha\beta}$ and $g_{\alpha\beta}$ are proportional. The proportionality constant can be determined from the incompressibility condition Eq (5.32)

$$a_{\alpha\beta} = \beta g_{\alpha\beta}\,. \tag{5.42}$$

[6] Wood and Hanna [WH18], and Hanna [Han18] discuss different choice of basis, choice of invariant strain measures, and of approximating material energies in their recent publications.

This equation is very important, because the two-dimensional metric on the pivotal plane is used to find the trace and the determinant of the curvature tensor, as well as raise and lower the indices of both the curvature tensor and the components of the tilt field. However, the inverse of the two-dimensional part of a three-dimensional tensor and the two-dimensional part of the inverse of a three-dimensional tensor is not generally equal. In Appendix D, we defined the inverse of the two-dimensional part of the metric with capital letter G, $G^{\alpha\beta}g_{\gamma\beta} := \delta^{\alpha}_{\gamma}$ and $G'^{\alpha\beta}g'_{\gamma\beta} := \delta^{\alpha}_{\gamma}$. The curvature tensor lives on the pivotal plane, so the total curvature is written as

$$K = G^{\alpha\beta}K_{\alpha\beta} \, . \tag{5.43}$$

Then the two dimensional part of the inverse of the reference metric becomes

$$a^{\alpha\beta} = (1 + \frac{1}{2}T^2)G^{\alpha\beta} \, . \tag{5.44}$$

The Trace of the In-plane Strain Components: u^{α}_{α}

The second term in the energy density (5.1) is found by contracting the strain tensor by the inverse of the reference metric

$$u^{\alpha}_{\alpha} = a^{\alpha j}u_{\alpha j} \, , \tag{5.45}$$

where α is summed over the in-plane coordinates, but j is summed over the three-dimensions. Let us insert Eq (5.12) in Eq (5.45)

$$u^{\alpha}_{\alpha} = \frac{1}{2}a^{\alpha j}(g'_{\alpha j} - a_{\alpha j}) = \frac{1}{2}a^{\alpha j}g'_{\alpha j} - 1 \tag{5.46}$$

where in the second equality we use the fact that $a^{ij}a_{kj} = \delta^{i}_{k}$. We know from Eq (5.37) that the inverse reference metric is block diagonal and the components $a^{\alpha z}$ are zero, so

$$u^{\alpha}_{\alpha} = \frac{1}{2}a^{\alpha\beta}g'_{\alpha\beta} - 1 \overset{(5.44)}{=} \frac{1}{2}(1 + \frac{1}{2}T^2)G^{\alpha\beta}g'_{\alpha\beta} - 1 \, , \tag{5.47}$$

in the second equality we used Eq (5.44). Next, we insert Eq (5.25a) into Eq (5.47) and subsequently combine Eq (5.25a) and Eq (5.36) and insert in into Eq (5.47) to find the final result

$$u^{\alpha}_{\alpha} = \frac{1}{2}T^2 + \zeta\tilde{K} + \frac{1}{2}\zeta^2\big[T^{\gamma}T^{\mu}K_{\alpha\gamma}K^{\alpha}_{\mu} + (1 - \frac{1}{2}T^2)\tilde{K}_{\alpha\gamma}\tilde{K}^{\alpha\gamma} - T^{\alpha}(\nabla_{\alpha}\tilde{K})\big] \, . \tag{5.48}$$

Comparing this equation with the area strain in Eq (5.11), we see that they agree up to the first order in ζ: $\epsilon(\zeta) = u_{xx}(\zeta) + u_{yy}(\zeta) + \mathcal{O}(\zeta^2)$. Then, the square of the trace of the in-plane strain term becomes,

$$(u^{\alpha}_{\alpha})^2 = \zeta KT^2 + \zeta^2\big[\tilde{K}^2 + \frac{1}{2}T^2K_{\alpha\gamma}K^{\alpha\gamma}\big] \, . \tag{5.49}$$

The Lateral Shear Term: $(u^{\alpha}_{\alpha})^2 - 4\det u_{\alpha\beta}$

The in-plane shear term in Eq (5.1) is given as $(u^{\alpha}_{\alpha})^2 - 4\det u_{\alpha\beta}$. We can write this term as

$$(u^{\alpha}_{\alpha})^2 - 4\det u_{\alpha\beta} = 2u^{\beta}_{\alpha}u^{\alpha}_{\beta} - (u^{\alpha}_{\alpha})^2 \, , \tag{5.50}$$

where the last term is determined in Eq (5.49). We obtain the term $u_\alpha^\beta u_\beta^\alpha$ from Eq (5.12) by raising the indices with the reference metric

$$2u_\alpha^\beta u_\beta^\alpha = 2a^{\beta j}u_{\alpha j}a^{\alpha k}u_{\beta k}\,, \tag{5.51}$$

$$= \frac{1}{2}a^{\beta\gamma}a^{\alpha\delta}(g'_{\alpha\gamma}-a_{\alpha\gamma})(g'_{\beta\delta}-a_{\beta\delta})\,, \tag{5.52}$$

where in the second line we used that the reference metric is block diagonal with $a_{\alpha z}=0$. We insert Eq (5.25a) with Eq (5.36) into Eq (5.52). Then, the lateral shear term is written as

$$(u_\alpha^\alpha)^2 - 4\det u_{\alpha\beta} = \zeta^2\tilde{K}^2 - 4\zeta^2\tilde{K}_{\mathrm{G}} + \zeta^2(\boldsymbol{\nabla}\times\boldsymbol{T})^2 - \zeta^2 T^\gamma T^\delta K_{\alpha\gamma}K_\delta^\alpha\,, \tag{5.53}$$

where the derivation of the lipid twist term is given in Appendix E.

Quadratic Transverse Shear: $u_{\alpha z}u^{\alpha z}$

The transverse shear term in the three-dimensional energy density (5.1) is

$$u_{\alpha z}u^{\alpha z} = u_{\alpha z}\,a^{\alpha j}a^{zk}u_{jk}\,, \tag{5.54}$$

and we know that the inverse reference metric is block diagonal with $a^{\alpha z}=0$. Then, Eq (5.54) becomes

$$u_{\alpha z}u^{\alpha z} = u_{\alpha z}\,a^{\alpha\beta}a^{zz}u_{\beta z} \overset{(5.12)}{=} \frac{1}{2}a^{\alpha\beta}a^{zz}(g'_{\alpha z}-a_{\alpha z})(g'_{\beta z}-a_{\beta z})\,. \tag{5.55}$$

Again using the fact $a_{\alpha z}=0$, we find

$$u_{\alpha z}u^{\alpha z} = \frac{1}{2}a^{\alpha\beta}a^{zz}g'_{\alpha z}g'_{\beta z}\,. \tag{5.56}$$

The transverse part of the inverse of the reference metric is given in Eq (5.37), $a^{zz}=1$. The in-plane part $a^{\alpha\beta}$ is proportional to the inverse of the two-dimensional metric on the pivotal plane, Eq (5.44). The off-diagonal parts of the three-dimensional metric, $g'_{\alpha z}$, is given in Eq (5.21a), and it contains the terms $\nabla_\alpha\zeta$ and $\frac{\partial\zeta}{\partial z}$. The covariant derivative of ζ is found in Eq (5.36) by directly taking the derivative of ζ given in Eq (5.34). Because, in Eq (5.56), we have the multiplication $g'_{\alpha z}g'_{\beta z}$, we need to determine $(\frac{\partial\zeta}{\partial z})^2$. However, the derivation of this term is trickier and needs more caution: if we use the expression for ζ given in Eq (5.34) and take its derivative with respect to z, we find

$$\frac{\partial\zeta}{\partial z} = 1 - z(\tilde{K} - \frac{1}{2}KT^2 + 2K_{\alpha\beta}T^\alpha T^\beta) + \mathcal{O}(z^2)\,. \tag{5.57}$$

Unfortunately, this gives $\frac{\partial\zeta}{\partial z}$ only up to linear order in z, but we need to determine it up to a second order, because our final goal is to get $(\frac{\partial\zeta}{\partial z})^2$ up to second oder in z. In order to that, we again use the incompressibility condition Eq (5.27). Because $g'_{zz} = (\frac{\partial\zeta}{\partial z})^2$ as stated in Eq (5.21b) and the incompressibility assumption gives us an expression for g'_{zz} in terms of other the components of the metric tensors. The derivation of $(\frac{\partial\zeta}{\partial z})^2$ is given in in Appendix D. Keeping

the terms up to zeroth order in the tilt field from Eq (D.15) we get

$$\left(\frac{\partial\zeta}{\partial z}\right)^2 = 1 - 2\zeta K + \zeta^2(3K^2 - 2K_{\mathrm{G}}) + \mathcal{O}(T)\,. \tag{5.58}$$

Finally, we find the quadratic transverse shear term,

$$u_{\alpha z}u^{\alpha z} = \frac{1}{4}\big[1 - 2\zeta K + \zeta^2(3K^2 - 2K_{\mathrm{G}})\big]T^2 - \frac{1}{4}\zeta^2 T^\gamma \nabla_\gamma \tilde{K}\,. \tag{5.59}$$

5.1.6 Three Dimensional Energy Density

The monolayer energy is the integral of the energy density given in Eq (2.40)

$$\mathcal{H}_{\mathrm{m}} = \int \mathrm{d}V e_{3d} = \int \mathrm{d}\alpha\,\mathrm{d}\zeta\,\cos\theta e_{3\mathrm{d}}\,. \tag{5.60}$$

However, we cannot yet do the integral in these coordinates, because the pre-stress $\sigma_0(z)$ involves the transverse direction in the initial flat configuration. Also, the area element $\mathrm{d}\alpha$ depends on the transverse coordinate and should be rewritten in terms of the area element of the pivotal plane, $\mathrm{d}\alpha(\zeta = 0) = \mathrm{d}A$, which is independent of transverse position. The volume element does not change upon deformation due to the incompressibility, so we can use the coordinates of the flat untilted monolayer,

$$\mathrm{d}V = \mathrm{d}a\;\mathrm{d}z = \mathrm{d}A\,\mathrm{d}z\big[1 - \tfrac{1}{2}T_l T^l\big]\,. \tag{5.61}$$

In the second equality we used Eq (5.2) and Eq (5.10) to connect $\mathrm{d}A$ and $\mathrm{d}a$.

Putting everything together, we then arrive at the following overall elastic energy, which is correct up to order ζ^2, squared curvature, squared tilt, and biquadratic terms:

$$\begin{aligned}
\mathcal{H}_{\mathrm{m}} = \int \mathrm{d}A\,\mathrm{d}z\,\big[1 - \tfrac{1}{2}T^2\big] \times \\
\Big\{\sigma(z)\Big[\frac{1}{2}T^2 + \zeta\tilde{K} + \zeta^2\big[(1 - \frac{1}{2}T^2)\tilde{K}_{\mathrm{G}} - \frac{1}{2}\boldsymbol{T}\cdot\boldsymbol{\nabla}\tilde{K} + \frac{1}{2}K_{\beta\alpha}K^\alpha_\gamma T^\beta T^\gamma\big]\Big] \\
+ \tfrac{1}{2}\tilde{E}(z)\Big[\zeta K T^2 + \zeta^2\big[\tilde{K}^2 + \tfrac{1}{2}T^2 K_{\alpha\gamma}K^{\alpha\gamma}\big]\Big] \\
+ \tfrac{1}{2}\lambda_{\mathrm{t}}\big[\big(1 - 2\zeta K + \zeta^2(3K^2 - 2K_{\mathrm{G}})\big)T^2 - \zeta^2\boldsymbol{T}\cdot\boldsymbol{\nabla}\tilde{K}\big] \\
+ \tfrac{1}{2}\lambda_{\mathrm{s}}\big[\zeta^2\tilde{K}^2 - 4\zeta^2\tilde{K}_{\mathrm{G}} + \zeta^2(\boldsymbol{\nabla}\times\boldsymbol{T})^2 - \zeta^2 T^\gamma T^\delta K_{\alpha\gamma}K^\alpha_\delta\big]\Big\}\,.
\end{aligned} \tag{5.62}$$

As we did for the quadratic theory, we use integration by parts for the coupling term $\frac{1}{2}T^\beta\nabla_\beta\tilde{K}$ and hence it becomes $\frac{1}{2}\tilde{K}\nabla_\beta T^\beta - \frac{1}{2}\nabla_\beta\big(\tilde{K}T^\beta\big)$. The second term only contributes on the boundary.

The only remaining item to be careful about is to recall the functional dependence of ζ on z, which is determined from the incompressibility condition and given in Eq (5.34). Then we

collect terms of similar form and find

$$\begin{aligned}\mathcal{H}_{\mathrm{m}} = \int \mathrm{d}A\,\mathrm{d}z\Big\{&\sigma_0(z) z\tilde{K} + \frac{1}{2}\big[\tilde{E}(z) + \sigma_0(z) + \lambda_{\mathrm{s}}(z)\big] z^2\tilde{K}^2 + \big[\sigma_0(z) - 2\lambda_{\mathrm{s}}(z)\big] z^2\tilde{K}_{\mathrm{G}} \\ &+ \frac{1}{2}\big[\sigma_0(z) + \lambda_{\mathrm{t}}\big] z^2\tilde{K}\boldsymbol{\nabla}\cdot\boldsymbol{T} + \frac{1}{2}\lambda_{\mathrm{s}}(z) z^2(\boldsymbol{\nabla}\times\boldsymbol{T})^2 \\ &+ \frac{1}{2}T^\alpha T^\beta\Big(\big[\sigma_0(z) + \lambda_{\mathrm{t}}(z)\big] g_{\alpha\beta} + \big[\tilde{E}(z) - \sigma_0(z) - 2\lambda_{\mathrm{t}}\big] z K g_{\alpha\beta} \\ &\qquad + \big[-\frac{1}{2}\tilde{E}(z) + \sigma_0(z) + 4\lambda_{\mathrm{t}}(z) - \frac{1}{2}\lambda_{\mathrm{s}}(z)\big] z^2K^2 g_{\alpha\beta} \\ &\qquad + \big[-\tilde{E}(z) - 3\sigma_0(z) - 2\lambda_{\mathrm{t}}(z) - \lambda_{\mathrm{s}}(z)\big] z^2K_{\mathrm{G}}^2 g_{\alpha\beta} \\ &\qquad + \big[-\sigma_0(z) - \lambda_{\mathrm{s}}(z)\big] z^2 K K_{\alpha\beta}\Big)\Big\}\,, \end{aligned} \tag{5.63}$$

where we used $K_{\mathrm{G}} g_{\alpha\beta} = R_{\alpha\beta} = K K_{\alpha\beta} - K_{\gamma\alpha}K^{\gamma}_{\beta}$ (which is the once-contracted Gauss equation Eq (2.22a)), and $2K_{\mathrm{G}} = K^2 - K^{\beta}_{\alpha}K^{\alpha}_{\beta}$ (which is the twice-contracted Gauss equation Eq (2.22b)).

5.1.7 Free Energy of a Monolayer

Finally, we can calculate the *elastic surface energy density* as an integral of Eq (5.63) over the transverse direction z. Doing this integral, we arrive at the surface energy density

$$\begin{aligned} e_{2\mathrm{d}} = &\frac{1}{2}\kappa_{\mathrm{m}}(\tilde{K} - K_{0,\mathrm{m}})^2 + \frac{1}{2}\kappa_{\mathrm{d,m}}\tilde{K}\boldsymbol{\nabla}\cdot\boldsymbol{T} + \overline{\kappa}_{\mathrm{m}}\tilde{K}_{\mathrm{G}} \\ &+ \frac{1}{2}\kappa_{\mathrm{tw,m}}(\boldsymbol{\nabla}\times\boldsymbol{T})^2 + \frac{1}{2}\kappa_{\mathrm{t,m}}M'_{\alpha\beta}T^\alpha T^\beta\,. \end{aligned} \tag{5.64}$$

Four new elastic constants, $K_{0,\mathrm{b}}$, $\kappa_{\mathrm{b1,m}}$, $\kappa_{\mathrm{b2,m}}$, and $\kappa_{\mathrm{b3,m}}$ now arise, all of which are given as integrals over lower-level parameters:

$$-\kappa_{\mathrm{m}}K_{0,\mathrm{b}} = [\![\tilde{E}]\!]_1 - 2[\![\lambda_{\mathrm{t}}]\!]_1\,, \tag{5.65a}$$

$$\kappa_{\mathrm{b1,m}} = -\frac{1}{2}[\![\tilde{E}]\!]_2 + [\![\sigma_0]\!]_2 + 4[\![\lambda_{\mathrm{t}}]\!]_2 - \frac{1}{2}[\![\lambda_{\mathrm{s}}]\!]_2\,, \tag{5.65b}$$

$$\kappa'_{\mathrm{b2,m}} = -[\![\tilde{E}]\!]_2 - 3[\![\sigma_0]\!]_2 - 2[\![\lambda_{\mathrm{t}}]\!]_2 - [\![\lambda_{\mathrm{s}}]\!]_2\,, \tag{5.65c}$$

$$\kappa'_{\mathrm{b3,m}} = -[\![\sigma_0]\!]_2 - [\![\lambda_{\mathrm{s}}]\!]_2\,. \tag{5.65d}$$

Recall the double bracket notation, defined in Eq (3.15). The definitions of the other elstic constants are the same with the ones given in the quadratic theory, Eqs (3.40). The quadratic tilt term in Eq (5.64) now requires not just a scalar modulus but a full *tensor*, given by

$$M'_{\alpha\beta} = \Big[1 + \ell^2 K(K_{0,\mathrm{m}} - K_{0,\mathrm{b}}) + \ell^2_{\mathrm{b1}}K^2 + \ell'^2_{\mathrm{b2}}K_{\mathrm{G}}\Big] g_{\alpha\beta} + \ell'^2_{\mathrm{b3}} K K_{\alpha\beta}\,. \tag{5.66}$$

Here, ℓ is the characteristic tilt-versus-bending length, and the other lengths are defined via the new moduli; together, these four lengths are defined as

$$\ell^2 = \frac{\kappa_\mathrm{m}}{\kappa_\mathrm{t,m}} \quad , \quad \ell_\mathrm{b1}^2 = \frac{\kappa_\mathrm{b1,m}}{\kappa_\mathrm{t,m}} \quad , \quad \ell_\mathrm{b2}'^2 = \frac{\kappa_\mathrm{b2,m}}{\kappa_\mathrm{t,m}} \quad , \quad \ell_\mathrm{b3}'^2 = \frac{\kappa_\mathrm{b3,m}}{\kappa_\mathrm{t,m}} \,. \tag{5.67}$$

Observe that in the absence of tilt Eq (5.64) simplifies to the Helfrich Hamiltonian. Moreover, in the limit of small curvatures (meaning, curvature radii substantially larger than any of the microscopic lengths ℓ, ℓ_b1, ℓ_b2' and ℓ_b3') $M'_{\alpha\beta} \to g_{\alpha\beta}$, and our result reduces to the quadratic Hamiltonian (3.39) derived in Chapter 3.

5.1.8 Disentangling Tilt and Curvature in $\tilde{K}_\mathrm{G}$

While tilt and curvature decouple trivially in the effective curvature $\tilde{K} = K + \nabla_\alpha T^\alpha$, the same is not true for the effective Gaussian curvature $\tilde{K}_\mathrm{G}$. But we can, in fact, disentangle geometry from tilt in this case, too, finding that the difference between $\tilde{K}_\mathrm{G}$ and K_G is a biquadratic term and a largely irrelevant boundary contribution.

To do so, recall the definition of the effective Gaussian curvature as a determinant, Eqn.(3.10):

$$\begin{aligned}
\tilde{K}_\mathrm{G} = \det\big(\tilde{\mathbf{K}}\big) &\overset{d=2}{=} \frac{1}{2}\Big\{\big[\mathrm{Tr}(\tilde{\mathbf{K}})\big]^2 - \mathrm{Tr}\big(\tilde{\mathbf{K}}^2\big)\Big\} && \text{(5.68a)}\\
&= \frac{1}{2}\big(\tilde{K}^2 - \tilde{K}_\beta{}^\gamma \tilde{K}_\gamma{}^\beta\big) && \text{(5.68b)}\\
&\overset{(3.9)}{=} K_\mathrm{G} + K\boldsymbol{\nabla}\cdot\boldsymbol{T} + \frac{1}{2}(\boldsymbol{\nabla}\cdot\boldsymbol{T})^2 \\
&\quad - K_\beta^\gamma \nabla_\gamma T^\beta - \frac{1}{2}\nabla_\beta T^\gamma \nabla_\gamma T^\beta \,. && \text{(5.68c)}
\end{aligned}$$

Up to minus sign conventions, this agrees with the result of Hamm and Kozlov [HK00], who then move on to consign the two mixed terms in the second line of Eq (5.68c) to the boundary, following Fournier [Fou99]. This is impermissible, however, because Fournier's calculation used *partial* derivatives, not *covariant* ones, a difference that matters in curved geometries. To see why, we will further rewrite Eq (5.68c) by pulling out a *covariant* boundary term:

$$\begin{aligned}
\tilde{K}_\mathrm{G} = K_\mathrm{G} &+ \frac{1}{2}T^\beta\left(\nabla_\alpha\nabla_\beta - \nabla_\beta\nabla_\alpha\right)T^\alpha \\
&+ \left(\nabla_\alpha K_\gamma^\alpha - \nabla_\gamma K\right)T^\gamma + \nabla_\beta B^\beta \,.
\end{aligned} \tag{5.69}$$

The first term in the second line vanishes because of the contracted Codazzi-Mainardi equation (2.20). The last term is a total divergence, permitting us to almost always ignore it.

We hence see that the only remaining difference between $\tilde{K}_\mathrm{G}$ and K_G involves the commutator of covariant derivatives, and this is why resorting to partial derivatives won't do: for unlike ordinary partial derivatives, *covariant derivatives do not generally commute*. Instead [Spi79],

$$\left[\nabla_\alpha, \nabla_\beta\right] T_\gamma = R_{\alpha\beta\gamma\delta} T^\delta \,, \tag{5.70}$$

where $R_{\alpha\beta\gamma\delta}$ is the Riemann curvature tensor. With the help of its contraction $R_{\beta\delta} = g^{\alpha\gamma} R_{\alpha\beta\gamma\delta}$, the Ricci tensor, we can rewrite the commutator term in Eq (5.69) as

$$T^{\beta} \left[\nabla_{\alpha}, \nabla_{\beta}\right] T^{\alpha} = R_{\alpha\beta} T^{\alpha} T^{\beta} \,. \tag{5.71}$$

Furthermore, in two dimensions the Ricci curvature tensor is proportional to the metric, with the Gaussian curvature as its prefactor, $R_{\alpha\beta} = K_{\mathrm{G}}\, g_{\alpha\beta}$, which is a consequence of Gauss' Theorema Egregium. We can hence conclude that (up to a total divergence)

$$\tilde{K}_{\mathrm{G}} = K_{\mathrm{G}} + \frac{1}{2} K_{\mathrm{G}}\, T^2 \,, \tag{5.72}$$

showing that the difference between $\tilde{K}_{\mathrm{G}}$ and K_{G} is a pure biquadratic term, contrary to the disentanglement proposed by Hamm and Kozlov. It is this fact which motivates us to also keep all other biquadratic terms in the theory.

5.1.9 Biquadratic part of Lipid Twist Term

The lipid twist term is also has a biquadratic contribution. We determine the lipid twist term in Appendix E, and it can be written as the tilt derivative terms and a biquadratic terms in Eq (E.6). We rewrite lipid twist as

$$(\boldsymbol{\nabla} \times \boldsymbol{T})^2 = \nabla^{\alpha} T_{\beta} \nabla_{\alpha} T^{\beta} - \nabla_{\beta} T^{\alpha} \nabla^{\alpha} T_{\beta} + K K_{\alpha\beta} T^{\alpha} T^{\beta} - K_{\mathrm{G}} T^2 \,, \tag{5.73}$$

in the last term, we use the once-contracted Gauss equation (2.22a).

Therefore, after disentangling tilt and curvature in the effective Gaussian curvature and separate the biquadratic terms in the lipid twist, we arrive at one of our main results, the monolayer elastic energy density up to biquadratic order:

$$\begin{aligned} e_{2\mathrm{d}} = e_{2\mathrm{d}} = {} & \frac{1}{2}\kappa_{\mathrm{m}} (\tilde{K} - K_{0,\mathrm{m}})^2 + \frac{1}{2}\kappa_{\mathrm{d,m}} \tilde{K} \boldsymbol{\nabla} \cdot \boldsymbol{T} + \overline{\kappa}_{\mathrm{m}} K_{\mathrm{G}} \\ & + \frac{1}{2}\kappa_{\mathrm{tw,m}} (\nabla^{\alpha} T_{\beta} \nabla_{\alpha} T^{\beta} - \nabla_{\beta} T^{\alpha} \nabla^{\alpha} T_{\beta}) + \frac{1}{2}\kappa_{\mathrm{t,m}} M_{\alpha\beta} T^{\alpha} T^{\beta} \,, \end{aligned} \tag{5.74}$$

where the tensor $M_{\alpha\beta}$ is equal to the tensor $M'_{\alpha\beta}$ from Eq (5.66), plus the biquadratic term that comes from disentangling $\overline{\kappa}_{\mathrm{m}} \tilde{K}_{\mathrm{G}}$ and separating biquadratic terms in the lipid twist:

$$M_{\alpha\beta} = \Big[1 + \ell^2 K (K_{0,\mathrm{m}} - K_{0,\mathrm{b}}) + \ell^2_{\mathrm{b1}} K^2 + \ell^2_{\mathrm{b2}} K_{\mathrm{G}}\Big] g_{\alpha\beta} + \ell^2_{\mathrm{b3}} K K_{\alpha\beta} \,, \tag{5.75}$$

with the following definition of the elastic modulus,

$$\kappa_{\mathrm{b2,m}} = \kappa'_{\mathrm{b2,m}} + \overline{\kappa}_{\mathrm{m}} - \kappa_{\mathrm{tw,m}} = -[\![\tilde{E}]\!]_2 - 2[\![\sigma_0]\!]_2 - 2[\![\lambda_{\mathrm{t}}]\!]_2 - 4[\![\lambda_{\mathrm{s}}]\!]_2 \,, \tag{5.76}$$

$$\kappa_{\mathrm{b3,m}} = \kappa'_{\mathrm{b3,m}} + \kappa_{\mathrm{tw,m}} = -[\![\sigma_0]\!]_2 - 2[\![\lambda_{\mathrm{s}}]\!]_2 \,, \tag{5.77}$$

and the characteristic lengths,

$$\ell_{\mathrm{b2}}^2 = \frac{\kappa_{\mathrm{b2,m}}}{\kappa_{\mathrm{m}}}\,, \quad \text{and} \quad \ell_{\mathrm{b3}}^2 = \frac{\kappa_{\mathrm{b3,m}}}{\kappa_{\mathrm{m}}}\,. \tag{5.78}$$

5.1.10 A First Comparison With the Quadratic Theories

As mentioned before, Eq (5.74) reduces to the quadratic theory (3.39) if we replace $M'_{\alpha\beta} \to g_{\alpha\beta}$, which is permissible for small curvatures. This is *not* true if we make the same replacement in the disentangled equation (5.74), because the biquadratic term in $\tilde{K}_{\mathrm{G}}$ was moved into $M_{\alpha\beta}$ and would now be neglected.

The underlying elastic theory predicts not just the *form* of the curvature-tilt functional, but also the *values* of the higher-level elastic constants—see Eqns. (5.65). Of these, our expressions for κ_{m}, $\overline{\kappa}_{\mathrm{m}}$, $\kappa_{\mathrm{d,m}}$, $\kappa_{\mathrm{t,m}}$, and $K_{0,\mathrm{m}}$ agree with those derived in Chapter 3. In contrast, the terms $K_{0,\mathrm{b}}$, $\kappa_{\mathrm{b1,m}}$, $\kappa_{\mathrm{b2,m}}$, and $\kappa_{\mathrm{b3,m}}$ do not appear in quadratic treatments, since these parameters are exclusively related to biquadratics.

Our disentanglement shows that all biquadratic terms effectively act as position-dependent contributions to the tilt modulus. Notice that these are generally even *anisotropic* (meaning, not simply proportional to the metric) due to the explicit occurrence of the curvature *tensor* in $M_{\alpha\beta}$. The eigenvectors of $M_{\alpha\beta}$ coincide with those of $K_{\alpha\beta}$, and so the principal curvature directions of the surface also play a special role for *tilting*—unless the surface is part of a sphere (*i. e.*, $K_{\alpha\beta} \propto g_{\alpha\beta}$) or minimal (*i. e.*, $K = 0$). Notice that in the latter case the anisotropic contribution to tilt vanishes even though the surface itself is not isotropic.

Interestingly, there is even a term quadratic in the tilt and *linear* in the curvature—the one involving $\ell^2 K(K_{0,\mathrm{m}} - K_{0,\mathrm{b}})$ in the tilt matrix. It owes its existence to the two potential ways for breaking up-down symmetry of the monolayer: a monolayer spontaneous curvature $K_{0,\mathrm{m}}$ arises if the first moment of the pre-stress does not vanish around the pivotal plane; and the term $K_{0,\mathrm{b}}$ arises if the first moment of the three dimensional moduli $\tilde{E}$ and λ_{t} does not vanish around the pivotal plane. One might expect this linear term to dominate the remaining quadratic ones, but this is not necessarily the case. The reason is that the higher order terms become especially interesting in high-curvature regions (such as open edges, pores, or fusion stalks). Nevertheless, the combination $(K_{0,\mathrm{m}} - K_{0,\mathrm{b}})$ may be very large, as we will show in the next chapter, in which case the linear term matters even in highly curved geometries.

5.1.11 A first look at the higher order coupling terms

The elastic moduli of the higher order coupling terms can be expressed in terms of the moduli of quadratic theory. The only exception to this is the term $K_{0,\mathrm{b}}$, for which we can not find an exact relationship, but we will derive an approximation for it in the next chapter.

The three biquadratic moduli, κ_{b1}, κ_{b2}, and κ_{b3} are defined as second moments of the underlying elastic parameters, $\tilde{E}$, σ_0, λ_{s}, and λ_{t}. The same second moments are used in the definitions of the moduli of quadratic terms, κ_{m}, $\overline{\kappa}_{\mathrm{m}}$, $\kappa_{\mathrm{d,m}}$, and $\kappa_{\mathrm{tw,m}}$. Fortunately, these definitions are

independent functions of the second moments, and so we can invert them to find all four second moments in terms of elastic moduli

$$[\![\tilde{E}]\!]_2 = \kappa_{\mathrm{m}} + \overline{\kappa}_{\mathrm{m}} + \kappa_{\mathrm{tw,m}} \,, \tag{5.79a}$$

$$[\![\sigma_0]\!]_2 = \overline{\kappa}_{\mathrm{m}} + 2\kappa_{\mathrm{tw,m}} \,, \tag{5.79b}$$

$$[\![\lambda_{\mathrm{s}}]\!]_2 = \kappa_{\mathrm{d,m}} - \kappa_{\mathrm{m}} - 2\kappa_{\mathrm{tw,m}} \,, \tag{5.79c}$$

$$[\![\lambda_{\mathrm{t}}]\!]_2 = \kappa_{\mathrm{tw,m}} \,. \tag{5.79d}$$

If we insert these four equations into the definitions of the biquadratic moduli Eqs (5.65b, 5.76, and 5.77), we get the following relations

$$\kappa_{\mathrm{b1,m}} = -\frac{1}{2}\kappa_{\mathrm{m}} - \frac{7}{2}\overline{\kappa}_{\mathrm{m}} + 4\kappa_{\mathrm{d,m}} - 7\kappa_{\mathrm{tw,m}} \,, \tag{5.80a}$$

$$\kappa_{\mathrm{b2,m}} = -\kappa_{\mathrm{m}} - \overline{\kappa}_{\mathrm{m}} - 2\kappa_{\mathrm{d,m}} - 5\kappa_{\mathrm{tw,m}} \,, \tag{5.80b}$$

$$\kappa_{\mathrm{b3,m}} = -\kappa_{\mathrm{m}} - 2\kappa_{\mathrm{tw,m}} \,. \tag{5.80c}$$

Thanks to the strong microscopic constraints inherent in the bottom-up approach, the biquadratic theory has only *one* additional extra independent elastic parameter compared to the quadratic theory. That parameter is the *biquadratic curvature* $K_{0,\mathrm{b}}$. In the assumption of constant three-dimensional elastic moduli $\tilde{E}$ and λ_{t} we will find an approximation for $K_{0,\mathrm{b}}$.

5.2 Free Energy of a Bilayer

Up to now we have treated membrane elasticity on the monolayer level, and this is in fact the natural framework when also dealing with tilt. However, often we care about the whole bilayer, under conditions where curvatures are moderate, and then an effective bilayer theory would be welcome.

5.2.1 Combining two leaflets into one

Since a bilayer comprises two monolayers that can slide past each other, the bilayer elastic energy density is found by summing two monolayer contributions as we did in both Section 2.4.3 and Section 3.2.7. We need to write the geometric objects on the two pivotal planes (which we will denote by primes) as functions of the midplane objects (which will be unprimed). As we did in Section 3.2.7, we use a symmetrization, $\boldsymbol{T}_+$, and anti-symmetrization, $\boldsymbol{T}_-$ of the two tilt fields $\boldsymbol{T}_\uparrow$ and $\boldsymbol{T}_\downarrow$ in the two monolayers. The sum and the difference tilt fields are defined in Eq (3.43).

The calculations that transport curvatures and the tilt field from the pivotal plane to the bilayer midplane are unfortunately a bit protracted, especially in the biquadratic case. However, they are conceptually very similar to the calculations for the zero-tilt case given in Section 2.4.3. In here, we will generalize the parallel surface calculations done in Section 2.4.3, and instead of shifting the surfaces in the direction of the normal vector, we shift the surfaces in the direction

of the lipid director. Extending this calculation from parallel surfaces to lipid shifted surfaces for biquadratic terms is significantly more cumbersome. We will only give the basic steps in the argument and skip some tedious but straightforward algebra. First, for the two lipid shifted surfaces not the normals but the *directors* coincide, $\boldsymbol{n} = \boldsymbol{n}'$, implying the new derivative relation $\nabla_\alpha \boldsymbol{n} = \nabla'_\alpha \boldsymbol{n}'$. The directors are given in Eqn. (5.22), and their derivatives are given in Eq (A.5), where we see that—unlike in the case of $\nabla_j \boldsymbol{N}$—the result also depends on the normal vector. Therefore, the equality for the covariant derivative of director can be written as

$$\beta \tilde{K}_\alpha^{\ \beta} \boldsymbol{e}_\beta - T^\beta \tilde{K}_{\alpha\beta} \boldsymbol{N} = \beta' \tilde{K}'^{\ \beta}_\alpha \boldsymbol{e}'_\beta - T'^\beta \tilde{K}'_{\alpha\beta} \boldsymbol{N}' \,. \tag{5.81}$$

This relation gives us a set of equations in the tangential and normal directions: $\boldsymbol{N} \cdot [\nabla_j \boldsymbol{n} = \nabla'_j \boldsymbol{n}']$

$$- T^\beta \tilde{K}_{\alpha\beta} = \beta' \tilde{K}'^{\ \beta}_\alpha \ \boldsymbol{N} \cdot \boldsymbol{e}'_\beta - T'^\beta \tilde{K}'_{\alpha\beta} \ \boldsymbol{N} \cdot \boldsymbol{N}' \,, \tag{5.82}$$

and $\boldsymbol{e}^\gamma \cdot [\nabla_j \boldsymbol{n} = \nabla'_j \boldsymbol{n}']$

$$\beta \tilde{K}_\alpha^{\ \gamma} = \beta' \tilde{K}'^{\ \beta}_\alpha \ \boldsymbol{e}^\gamma \cdot \boldsymbol{e}'_\beta - T'^\beta \tilde{K}'_{\alpha\beta} \ \boldsymbol{e}^\gamma \cdot \boldsymbol{N}' \,. \tag{5.83}$$

This is vexing, for the normals now differ between the two surfaces, and so we first need to calculate them.

Using the definition of the lipid director from Eq (5.22), and the equality $\boldsymbol{n} = \boldsymbol{n}'$, we arrive at an equation for $\boldsymbol{N}'$:

$$\boldsymbol{N}' = \frac{\beta}{\beta'} [\boldsymbol{N} + T^\gamma \boldsymbol{e}_\gamma] - T'^{\,\gamma} \boldsymbol{e}'_\gamma \,, \tag{5.84}$$

where β is defined in Eq (5.23), and similarly, β' is defined as

$$\beta'^{\,2} := \frac{1}{1 + T'^{\,\alpha} T'^{\,\beta} g'_{\alpha\beta}} \,. \tag{5.85}$$

We already determined the tangent vector on a lipid shifted surface, $\boldsymbol{e}'_\alpha$, in Appendix A and in terms of the pivotal plane parameters in Eq (A.6). At this point, we are two steps away from finding a relation between primed and unprimed effective curvatures. First, we can insert Eq (A.6) and Eq (5.84) into Eq (5.82) and multiply it by T^δ. This allows us to find an expression for the term $(\beta/\beta') T'^\beta \tilde{K}'_{\alpha\beta} T^\delta$. In the second step, we insert the primed tangent vector from Eq (A.6) and the primed normal vector from Eq (5.84) into the tangential component Eq (5.83). We combine the result of the first step (the expression for the term $(\beta/\beta') T'^\beta \tilde{K}'_{\alpha\beta} T^\delta$) and the result of the second step. This yields the condition

$$P_\beta^{\ \gamma} = \left(\delta_\mu^\gamma + \zeta P_\mu^{\ \gamma}\right) P'^{\,\mu}_\beta =: B_\mu^\gamma P'^{\,\mu}_\beta \,, \tag{5.86a}$$

or $\mathbf{P} = \mathbf{B}\mathbf{P}'$, where the matrix $P_\beta^{\ \gamma}$ is defined as

$$P_\beta^{\ \gamma} = \tilde{K}_\beta^{\ \gamma} - \frac{1}{2} K_\beta^\gamma T^2 + K_{\beta\mu} T^\mu T^\gamma + \mathcal{O}(T^3) \,, \tag{5.86b}$$

and $P_j'^m$ equals the obvious primed analog. Eqn. (5.86a) is of precisely the same form as Eqn. (2.57), and so an analogous version of Eqns. (2.60a,2.60b) holds:

$$P' := \mathrm{Tr}(\mathbf{P}') = \frac{P + 2\zeta P_\mathrm{G}}{1 + \zeta P + \zeta^2 P_\mathrm{G}} , \tag{5.87a}$$

$$P'_\mathrm{G} := \det(\mathbf{P}') = \frac{P_\mathrm{G}}{1 + \zeta P + \zeta^2 P_\mathrm{G}} . \tag{5.87b}$$

We will soon pry the new curvatures from these equations. However, we also need the new tilt fields. Looking back at $\boldsymbol{n}' = \boldsymbol{n}$ and multiplying by $\boldsymbol{e}'_\alpha$, we find that the *covariant* components of the tilt field are found at relevant order,

$$T'_\alpha = T_\alpha - \frac{1}{2}\zeta^2 \beta \nabla_\alpha \epsilon_1 + \mathcal{O}(T^3) , \tag{5.88}$$

but the same does not hold for the *contravariant* components, because lifting the index will introduce lower order corrections via the primed inverse metric $G'^{\alpha\beta}$. We derived the latter in Appendix D and it is given in Eq (D.3). Since we multiply this by an expression that is already quadratic in tilt, we fortunately only need $G'^{\alpha\beta}$ up to zeroth order in T, from Eq (D.3)

$$G'^{\alpha\beta} = G^{\alpha\beta} - 2\zeta K^{\alpha\beta} + 3\zeta^2 K^\alpha_\gamma K^{\beta\gamma} + \mathcal{O}(\boldsymbol{T}) . \tag{5.89}$$

When we combine Eq (5.88) and Eq (5.89), we find

$$\boldsymbol{T}'^2 = T^2 - 2\zeta K_{\alpha\beta} T^\alpha T^\beta + 3\zeta^2 K_{\alpha\gamma} K^\gamma_\beta T^\alpha T^\beta - \zeta^2 T^\gamma \nabla_\gamma \tilde{K} . \tag{5.90}$$

There are two terms left for which we did not determine the correction, $K\boldsymbol{\nabla}\cdot\boldsymbol{T}$ and $(\boldsymbol{\nabla}\times\boldsymbol{T})^2$. However, neither of them gets a correction. The reason for the lipid twist term is straightforward: it has two derivatives (inverse square length) and two tilt fields ($\mathcal{O}(T^2)$), which is already in the highest order in our order counting for the biquadratic theory, and any correction will be higher order than biquadratic. That is not the case for the coupling term $K\boldsymbol{\nabla}\cdot\boldsymbol{T}$, which is quadratic in inverse length but linear in the tilt field. Thus, there could in principle be a correction term to $K\boldsymbol{\nabla}\cdot\boldsymbol{T}$ of order $\mathcal{O}(K\nabla T^2)$. However, we can eliminate this possibility: we cannot construct a scalar from $K_{\alpha\beta}$, $T^\alpha T^\beta$, and ∇_α, because the number of indices is odd, and so we cannot contract all of them the at the same time to obtain a scalar.

We now have everything ready to also extract the primed curvatures from Eqns. (5.87a,5.87b). First of all, the right hand sides of these equations are readily evaluated and expanded in powers of ζ, so P' and P'_G are known in terms of the *old* (unprimed) curvatures and tilt fields. To get P' in terms of the new curvatures and tilt field, we trace over the primed version of Eqn. (5.86b):

$$P' = \tilde{K}' - \frac{1}{2}K'\boldsymbol{T}'^2 + K'_{\alpha\beta} T'^\alpha T'^\beta . \tag{5.91}$$

To extract $\tilde{K}'$ from this, we need to remove the second and third term. We get the second one by multiplying this equation by $\boldsymbol{T}'^2$ and canceling to the relevant order, and the third one by

multiplying Eqn. (5.86a) with $T'^{\beta}T'_{\gamma}$ and again canceling higher orders. This leads to

$$\tilde{K}' = \tilde{K} - \zeta(\tilde{K}^2 - 2\tilde{K}_{\mathrm{G}}) + \frac{1}{2}\zeta(K^2 - 2K_{\mathrm{G}})\boldsymbol{T}^2 + \text{h.o.} \tag{5.92a}$$

To get the new effective Gaussian curvature, we take the determinant of Eqn. (5.86b). For two-dimensiuonal matrices we use the simple formula $\det(\mathbf{P}') = \frac{1}{2}[(\mathrm{Tr}(\mathbf{P}'))^2 - \mathrm{Tr}(\mathbf{P}'^2)]$. From there we get the conveniently simple result

$$\tilde{K}'_{\mathrm{G}} = \tilde{K}_{\mathrm{G}} + \text{h.o.} \tag{5.92b}$$

We can now express the curvatures and tilt fields on the pivotal plane as functions of their midplane analogs. From the monolayer sections we already know how to do this for area elements. Taking all this together, we can therefore write the *bilayer energy density* arising from the two individual leaflets as an area integral over the bilayer midplane, using curvatures on the midplane and tilt fields transported to the midplane, which we express as sum- and difference-fields via Eqn. (3.43):

$$\begin{aligned} e_{2\mathrm{d}}^{\mathrm{bi}} = {} & \frac{1}{2}\kappa\,(K + \boldsymbol{\nabla}\cdot\boldsymbol{T}_-)^2 + \frac{1}{2}\kappa_{\mathrm{d}}\tilde{K}\boldsymbol{\nabla}\cdot\boldsymbol{T}_- + \overline{\kappa}K_{\mathrm{G}} \\ & + \frac{1}{2}\kappa_{\mathrm{tw}}(\nabla_\alpha T_-^\beta \nabla_\alpha T_-^\beta - \nabla_\beta T_-^\alpha \nabla_\alpha T_-^\beta)^2 \\ & + \frac{1}{2}\kappa\,(\boldsymbol{\nabla}\cdot\boldsymbol{T}_+ - K_{0,\mathrm{m}})^2 - \frac{1}{2}\kappa K_{0,\mathrm{m}}^2 + \frac{1}{2}\kappa_{\mathrm{d}}(\boldsymbol{\nabla}\cdot\boldsymbol{T}_+)^2 \\ & + \frac{1}{2}\kappa_{\mathrm{tw}}(\nabla_\alpha T_+^\beta \nabla_\alpha T_+^\beta - \nabla_\beta T_+^\alpha \nabla_\alpha T_+^\beta)^2 \\ & + \frac{1}{2}\kappa_{\mathrm{t}} M_{\alpha\beta}^{(\mathrm{S})}\left(T_-^\alpha T_-^\beta + T_+^\alpha T_+^\beta\right) + \kappa_{\mathrm{t}} M_{\alpha\beta}^{(\mathrm{A})}\, T_-^\alpha T_+^\beta\,. \end{aligned} \tag{5.93}$$

This is again correct up to quadratic terms in curvature and tilt, as well as maximally biquadratic couplings. All elastic parameters are now bilayer parameters, and they are the same with the ones determined in quadratic theory. The definitions in terms of monolayer constants are given in Eqs 3.46. The symmetric tilt matrix $M_{\alpha\beta}^{(\mathrm{S})}$ and the antisymmetric tilt-coupling matrix $M_{\alpha\beta}^{(\mathrm{A})}$ are given by

$$\begin{aligned} M_{\alpha\beta}^{(\mathrm{S})} = {} & \big[1 + (\ell_{\mathrm{b1}}^2 - \frac{1}{2}z_0^2)K^2 + (\ell_{\mathrm{b2}}^2 + 2\ell^2(K_{0,\mathrm{m}} - K_{0,\mathrm{b}})z_0 - 2z_0^2)K_{\mathrm{G}}\big]g_{\alpha\beta} \\ & + (\ell_{\mathrm{b3}}^2 - 2\ell^2(K_{0,\mathrm{m}} - K_{0,\mathrm{b}})z_0 + 2z_0^2)KK_{\alpha\beta}\,, \end{aligned} \tag{5.94a}$$

$$M_{\alpha\beta}^{(\mathrm{A})} = \ell^2(K_{0,\mathrm{m}} - K_{0,\mathrm{b}})Kg_{\alpha\beta} + z_0(Kg_{\alpha\beta} - 2K_{\alpha\beta})\,. \tag{5.94b}$$

Note that again in the small curvature limit, the symmetric tilt matrix reduces to metric tensor, $M_{\alpha\beta}^{(\mathrm{S})} \to g_{\alpha\beta}$ and the antisymmetric tilt matrix vanishes, $M_{\alpha\beta}^{(\mathrm{A})} \to 0$, the energy density agrees with the quadratic theory.

5.3 Validity and Consistency of our Theory

The underlying "microscopic" theory of the present treatment is quadratic elasticity—comprising Eq (2.25) and the linear pre-stress from Eq (2.38). The emergent theory, which instead expresses the energy as a functional of the membrane's surface geometry and a possible tilt field, is traditionally also truncated at quadratic order in curvatures (Helfrich) and possibly tilt (Hamm and Kozlov). Here we lobby for higher order biquadratic terms in the latter, but is this consistent?

When contemplating this question, it is first helpful to recall that "quadratic order" in these two theories does not mean the same thing. Displacements in the original $3d$ elastic theory are necessarily small, since they refer to a three-dimensional bulk material. The situation for the curvature description is different, though, since bending of thin sheets can result in arbitrarily large displacements. These displacements are described more efficiently by the local curvatures, but it is not immediately obvious why this new parametrization also ought to terminate at quadratic order—this time in the curvatures. This distinction is especially noteworthy since the reparametrization of the shape in geometric surface invariants gives rise to many higher order nonlinearities *even if the underlying theory is exactly quadratic*. In other words, it is perfectly conceivable that the underlying constitutive theory is *exactly* of linear response type, but in order to capture its phenomenology using a geometric surface representation, we need to account for the *geometric* nonlinearities which such a change in description invariably entails. It is true that if we were to add additional terms to the underlying theory that go beyond linear response, they would resurface as beyond-quadratic terms on the curvature level, and hence there are contributions to the higher order terms we discuss that do *not* merely originate from the geometric transformations we perform. In that specific sense, we are not consistent. However, we feel that it is worthwhile to explore what predictions a true underlying linear theory would make after rewriting it as a surface functional, and in that case we are obliged to take the nonlinearities that arise purely for geometric reasons seriously.

There is a second sense in which consistency may be questioned. Since we expand the energy functional in terms of small curvatures and small tilts, our biquadratic terms are essentially fourth order in smallness. If we account for them, why not account for other fourth order small terms, such as K^4 or T^4? The reason here is pragmatic: the biquadratic terms create *qualitative* changes in the underlying theory because they introduce a *new mode of coupling* between curvature and tilt that is absent on the quadratic level. One may thus expect that they give rise to "new physics"—and we will soon see that they indeed do. In contrast, quartic terms in the curvature would (at least initially) only *quantitatively* change the physics, for instance by adding to the curvature resistance and hence changing equilibrium shapes, while only indirectly affecting the partnering field. While one would ultimately need such terms for truly quantitative predictions, it is easier to investigate the major effects of coupling in theories which do not yet contain nonlinearities on the non-coupled level. Moreover, it is of note that the geometric transformations we discuss indeed create terms quartic in curvature, but they do not create purely quartic terms in tilt.

However, this approach has its own limitations: in the next chapter we will encounter an instability that pushes our theory towards the limit of its validity—precisely because we ignored the quartic terms.

Chapter 6

Applications of Biquadratic Theory

In Chapter 5, we derived the biquadratic energy density for both monolayers and bilayers, in which we kept the higher order curvature-tilt coupling terms as an addition to quadratic theory. In the present Chapter, we will look at the immediate consequences of the higher order coupling terms.

There are four elastic parameters connected with the biquadratic terms, and three of them can be written exactly in terms of quadratic constants as we showed in Chapter 3. However, the fourth one, the biquadratic curvature, $K_{0,\mathrm{b}}$, cannot be expressed exactly in terms of other elastic constants. In the next section, we will derive an estimation for $K_{0,\mathrm{b}}$, and look at the numerical values of biquadratic constants in specific cases. Then, we will derive the Euler-Lagrange equations from the tilt variations, and look at the effects of the biquadratic terms to these equations.

As we mentioned in the previous chapter, we treat the higher order coupling as an effective tilt modulus. In Section 6.3, we will look at the effective tilt modulus closely and find the curvature values where it becomes negative. We also apply our theory to two simple cases, namely straight edge and triple line junction.

6.1 Biquadratic Elastic Parameters

All the biquadratic elastic parameters can be written in terms of quadratic moduli except the biquadratic curvature $K_{0,\mathrm{b}}$, which is defined in Eq (5.65a). If we assume $\tilde{E}$ and λ_{t} constant (*i. e.*, not dependent on the z-position within a leaflet), we determine an approximation for $K_{0,\mathrm{b}}$:

$$-\kappa_{\mathrm{m}} K_{0,\mathrm{b}} \approx [\tilde{E} - 2\lambda_{\mathrm{t}}] d_{\mathrm{m}}^2 \big(\frac{1}{2} - \frac{z_0}{d_{\mathrm{m}}}\big) \,. \tag{6.1}$$

The area stretching modulus is given as the zeroth moment of $\tilde{E}(z)$: $K_{\mathrm{A}} = 2[\![\tilde{E}]\!]_0$, given in [CAMK14]. The tilt modulus is defined in Eq (3.40d) as the zeroth moment of $\lambda_{\mathrm{t}}(z)$: $\kappa_{\mathrm{t,m}} =$

$[\![\lambda_\mathrm{t}]\!]_0$. Therefore, Eq (6.1) can be written in terms of tilt modulus and area stretching modulus

$$-\kappa_\mathrm{m} K_{0,\mathrm{b}} \approx \frac{1}{2}[K_\mathrm{A} - 4\kappa_{\mathrm{t,m}}] d_\mathrm{m} \big(\frac{1}{2} - \frac{z_0}{d_\mathrm{m}}\big) \,. \tag{6.2}$$

If the pivotal plane is in the middle of the leaflet $z_0 = d_\mathrm{m}/2$, then $K_{0,\mathrm{b}} = 0$. This is usually not the case, though: experiments indicate that the pivotal plane sits closer to the headgroup region, typically about two thirds up along the lipid [RFGP90, LKFR96, CR98]. Using this rule of thumb, we get

$$K_{0,\mathrm{b}} \approx \frac{1}{12} d_\mathrm{m} \left(\frac{2K_\mathrm{A}}{\kappa} - 4\ell^{-2} \right) \qquad (\text{if } z_0 = \tfrac{2}{3} d_\mathrm{m}) \,. \tag{6.3}$$

This approximation is sensitive to the value of the ratio z_0/d_m because the combination of elastic parameters inside the parenthesis is generally large. When we insert the values from Venable *et al.* [VBP15]—see Table 4.1, we find $(2K_\mathrm{A}/\kappa - 4\ell^{-2}) \sim 1 - 3\ \mathrm{nm}^{-2}$. Therefore, even a small relative distance between the pivotal plane and the middle of the monolayer leads to a large contribution to the value of $K_{0,\mathrm{b}}$. Despite the large values, $K_{0,\mathrm{b}}$ does not directly affect bilayer stability and morphology, because unlike $K_{0,\mathrm{m}}$ it does not enter the bending term. It *does* contribute to the effective tilt modulus, though, and can hence have a massive influence on the cost of lipid tilting (even to the point of making that cost *negative*). It is potentially disconcerting, therefore, that the magnitude of this term depends so crucially on observables that are challenging to get hold of: the extent to which the pivotal plane is "off-center".

To illustrate the significance of the higher order elastic constants, we will use the results from the study by Venable, Brown and Pastor [VBP15], which is listed in Table 4.1. Inserting the quadratic parameters into Eq (6.3), we arrive at $K_{0,\mathrm{b}}$ values in the range $(0.14, 0.42)\ \mathrm{nm}^{-1}$, or the range of corresponding curvature radii $(2.4, 6.7)\ \mathrm{nm}$. The estimated values are listed in Table 6.1. These are relatively strong, if we compare them with the known monolayer spontaneous curvatures.

On the other hand, we do not need to make an assumption to find the relationships between other biquadratic constants and regular quadratic ones. We already determined them in Eqs (5.80). We take again elastic constants from VBP Table 4.1 and find values for the three biquadratic constant and list them in Table 6.1. The values fot $\kappa_{\mathrm{b2,m}}$ and $\kappa_{\mathrm{b3,m}}$ are negative for all twelve different lipids, and $\kappa_{\mathrm{b1,m}}$ has both negative and positive values.

6.2 Tilt Variation

The Euler-Lagrange (EL) equations for the quadratic theory from the tilt variation is derived in Section 4.2. In this section, we repeat the calculations for the biquadratic theory. The aim of this section is to show how the higher order coupling changes the induced tilt field due to curvature. Most of the derivation follows the one given in Section 4.2, except the lipid twist term. As given in Eq (E.6), the quadratic lipid twist term not only contains the derivative of the tilt fields, but

Lipids	$K_{0,\mathrm{b}}$ (nm^{-1})	$\kappa_{\mathrm{b1,m}}$ $(10^{-20}\mathrm{J})$	r_{b1}	$\kappa_{\mathrm{b2,m}}$ $(10^{-20}\mathrm{J})$	r_{b2}	$\kappa_{\mathrm{b3,m}}$ $(10^{-20}\mathrm{J})$	r_{b3}
DPPC	0.12	-2.56	-0.32	-7.96	-1.01	-9.94	-1.26
DMPC	0.18	-2.30	-0.38	-6.05	-0.99	-8.28	-1.36
DOPC	0.23	-0.75	-0.13	-6.21	-1.05	-6.89	-1.17
DNPC	0.09	-2.78	-0.25	-11.77	-1.07	-13.23	-1.20
DOPE	0.11	1.08	0.18	-10.73	-1.82	-7.34	-1.24
POPC	0.21	-1.58	-0.24	-6.55	-0.99	-8.05	-1.22
PDPC	0.23	-0.12	-0.02	-5.65	-1.18	-5.75	-1.20
POPE	0.12	0.56	0.08	-12.32	-1.85	-9.01	-1.35
PDPE	0.08	1.21	0.24	-10.24	-2.07	-6.43	-1.30
SDPE	0.24	1.30	0.24	-11.21	-2.11	-6.95	-1.31
PSM	0.14	-7.23	-0.52	-9.43	-0.68	-18.66	-1.34
POPG	0.08	-1.46	-0.26	-4.02	-0.71	-6.70	-1.19

Table 6.1: Biquadratic constants and ratios determined from the mechanical properties of twelve different lipids measured by fully atomistic molecular dynamic simulations by VBP [VBP15].

it also contains higher order couplings. First, we derive the tilt variation of the lipid twist term, and then show the EL-equations for both monolayer and bilayer Hamiltonians.

6.2.1 Variation of the Lipid Twist Term

The quadratic lipid twist term also contains biquadratic terms, from Eq (E.6)

$$(\boldsymbol{\nabla}\times\boldsymbol{T})^2=\frac{1}{2}(\nabla^\alpha T_\beta-\nabla_\beta T^\alpha)(\nabla_\alpha T^\beta-\nabla^\beta T_\alpha)+T^\mu T^\nu K^\alpha_\mu K_{\nu\alpha}\,.$$

The tilt variation of this term up to a total derivative is determined after a straightforward calculation

$$\delta_{T^\alpha}(\boldsymbol{\nabla}\times\boldsymbol{T})^2=\big[-2\nabla^2T_\alpha+2\boldsymbol{\nabla}\boldsymbol{\nabla}\cdot\boldsymbol{T}+2KK_{\alpha\beta}-4K_{\mathrm{G}}T_\alpha\big]\delta T^\alpha\,, \tag{6.4}$$

where there are two sources for the K_{G} term. The first one is rewriting the biquadratic term in Eq (E.6) using the once contracted Gauss equation (2.22a). The second source of the $K_{\mathrm{G}}T^2$ term is the commutation of the covariant derivatives during the derivation. If we neglect the higher order terms, Eq (6.4) boils down to the contribution given in Section 4.2.

6.2.2 EL-equations

After deriving the tilt variation of the lipid twist term, the EL-equations are easily determined from the biquadratic monolayer Hamiltonian Eq (5.74)

$$\big[r_{\mathrm{tw}}\ell^2g_{\alpha\beta}\nabla^2+\ell^2_{\mathrm{eff}}\nabla_\alpha\nabla_\beta-\tilde{M}_{\alpha\beta}\big]\,T^\beta=-(1+\frac{1}{2}r_{\mathrm{d,m}})\ell^2\nabla_\alpha K\,, \tag{6.5}$$

where we defined $\tilde{M}_{\alpha\beta}$ as

$$\tilde{M}_{\alpha\beta} := M_{\alpha\beta} - r_{\mathrm{tw}}\ell^2 K_{\mathrm{G}} g_{\alpha\beta} \,. \tag{6.6}$$

The last two terms in this equation come from the variation of the lipid twist term and the tilt matrix, $M_{\alpha\beta}$, is given in Eq (5.75).

Eq (5.93) shows that the two tilt fields $\boldsymbol{T}_+$ and $\boldsymbol{T}_-$ enter quite differently into the bilayer Hamiltonian. While in the monolayer Hamiltonian (5.74) the tilt divergence $\boldsymbol{\nabla}\cdot\boldsymbol{T}$ adds to the total curvature, this role is played in the bilayer Hamiltonian (5.93) by the divergence of the tilt-difference field, $\boldsymbol{\nabla}\cdot\boldsymbol{T}_-$. In contrast, the tilt-sum divergence appears only together with the spatially constant *spontaneous* curvature $K_{0,\mathrm{m}}$.

An important consequence of this asymmetry between $\boldsymbol{T}_+$ and $\boldsymbol{T}_-$ is that they couple very differently to the underlying geometry. This is easiest seen by looking at their EL-equations, which are

$$\left[r_{\mathrm{tw}}\ell^2 g_{\alpha\beta}\nabla^2 + \ell_{\mathrm{eff}}^2\nabla_\alpha\nabla_\beta - \tilde{M}^{(\mathrm{S})}_{\alpha\beta}\right] T_-^\beta - M^{(\mathrm{A})}_{\alpha\beta}\, T_+^\beta = -(1+\frac{1}{2}r_{\mathrm{d,m}})\ell^2\nabla_\alpha K \,, \tag{6.7a}$$

$$\left[r_{\mathrm{tw}}\ell^2 g_{\alpha\beta}\nabla^2 + \ell_{\mathrm{eff}}^2\nabla_\alpha\nabla_\beta - \tilde{M}^{(\mathrm{S})}_{\alpha\beta}\right] T_+^\beta - M^{(\mathrm{A})}_{\alpha\beta}\, T_-^\beta = 0 \,, \tag{6.7b}$$

where ℓ_{eff} is defined in Eq (4.21) and $\tilde{M}^{(\mathrm{S})}_{\alpha\beta}$ is

$$\tilde{M}^{(\mathrm{S})}_{\alpha\beta} = M^{(\mathrm{S})}_{\alpha\beta} - 2r_{\mathrm{tw}}\ell^2 K G g_{\alpha\beta} + r_{\mathrm{tw}}\ell^2 K K_{\alpha\beta} \,. \tag{6.8}$$

Observe that the same second order differential operator acts on both tilt fields, and that these fields are coupled via the tensor $M^{(\mathrm{A})}_{\alpha\beta}$. This coupling vanishes for flat bilayers, and it is hence small for weakly curved bilayers (where a look at the definition of $M^{(\mathrm{A})}_{\alpha\beta}$ in Eq (5.94b) shows that "weakly curved" means curvature radii much larger than the microscopic lengths z_0 and $\ell^2(K_{0,\mathrm{m}} - K_{0,\mathrm{b}})$). A very crucial difference is that $\boldsymbol{T}_-$ is sourced by curvature gradients, while $\boldsymbol{T}_+$ *has no direct source*. Hence, $\boldsymbol{T}_+$ is only sourced *indirectly* through $\boldsymbol{T}_-$ to an extent proportional to curvature. This suggests that $\boldsymbol{T}_+$ is a subdominant field and might often be neglected.

To sharpen up this reasoning, note that $\tilde{M}^{(\mathrm{S})}_{\alpha\beta} \sim g_{\alpha\beta}$ to lowest order, with the next order corrections being quadratic in curvature. In contrast, the coupling matrix $M^{(\mathrm{A})}_{\alpha\beta}$ has two contributions, both *linear* in curvature. Of these, the second one tends to dominate, because typically ℓ and z_0 are comparable in magnitude (about a nanometer), and hence the first term contains the extra factor $\ell(K_{0,\mathrm{m}} - K_{0,\mathrm{b}})$, which can (but need not) be small. When we discuss the bilayer, we are interested in weak curvatures, say ones where the radius of curvature is an order of magnitude larger than the scale z_0, and so the second term in $M^{(\mathrm{A})}_{\alpha\beta}$ is of order 0.1 or smaller. (In fact, since it is traceless, it vanishes at umbilical points and is hence nonzero only to the extent that the local membrane geometry is anisotropic.) If we now imagine $M^{(\mathrm{A})}_{\alpha\beta}T^\beta_-$ as the source term for $\boldsymbol{T}_+$, we see immediately that $\boldsymbol{T}_+$ is suppressed by the same smallness factor of about 0.1 compared to $\boldsymbol{T}_-$.

Making use of this approximation and ignoring $\boldsymbol{T}_+$ altogether, and only taking the dominant term in $\tilde{M}^{(\mathrm{S})}_{\alpha\beta}$, the elastic bilayer energy simplifies to

$$e^{\mathrm{bi}}_{2\mathrm{d}} \approx \frac{1}{2}\kappa\,(K + \boldsymbol{\nabla}\cdot\boldsymbol{T}_-)^2 + \kappa_{\mathrm{d}}\,(K + \boldsymbol{\nabla}\cdot\boldsymbol{T}_-)\,\boldsymbol{\nabla}\cdot\boldsymbol{T}_- + \overline{\kappa}K_{\mathrm{G}} + \frac{1}{2}\kappa_{\mathrm{tw}}(\boldsymbol{\nabla}\times\boldsymbol{T}_-)^2 + \frac{1}{2}\kappa_{\mathrm{t}}\boldsymbol{T}_-^2\,, \tag{6.9}$$

which looks essentially like the (lowest order) monolayer theory, with $\boldsymbol{T}_-$ taking over the role as the bilayer-relevant tilt field.[1] For instance, the elastic energy functional of Watson *et al.* [WPWB11] contains all the terms in Eq (6.9), except the second coupling term, because in their energy density, they also have the accidental symmetry of Hamm and Kozlov, *i. e.*, curvature and divergence of tilt field always appear as addition to each other.

A word of warning in the end: while it is a fairly decent approximation to simply work with the average tilt field $\boldsymbol{T}_-$ and ignore the sum contribution $\boldsymbol{T}_+$, this only holds inasmuch tilt-curvature-coupling is concerned. We hasten to add, though, that tilt can get excited by means other than curvature. For instance, transmembrane proteins with suitable cross-sections can excite $\boldsymbol{T}_+$ just as well as $\boldsymbol{T}_-$, and since the homogeneous part in the differential equations for the tilt is identical, these tilt fields also decay on the same length scale.

6.3 Effective Tilt Modulus

All terms that multiply the quadratic tilt in the monolayer Hamiltonian (5.74) can be summarily viewed as an effective tilt modulus, $\kappa_{\mathrm{t,m}}M_{\alpha\beta}$. Since they depend on curvature, via the biquadratic terms, the effective tilt modulus becomes *position dependent*. Moreover, $M_{\alpha\beta}$ is not merely proportional to $g_{\alpha\beta}$, and so the cost of tilting depends on the *direction* along which one tilts. And finally, since the curvature terms can also decrease the effective tilt modulus, geometry can *soften* the tilt field. In fact, we are not even guaranteed that the effective modulus is always positive. How to interpret a negative tilt modulus will be discussed in Section 6.3.1; let us first contemplate when it will happen.

To get a rough idea of the physics we ought to expect, we may at first ignore the anisotropy and focus on the isotropic contribution of $M_{\alpha\beta}$, which is given by

$$M := \frac{1}{2}G^{\alpha\beta}M_{\alpha\beta} = 1 + \ell^2 K(K_{0,\mathrm{m}} - K_{0,\mathrm{b}}) + \big(\ell^2_{\mathrm{b1}} + \frac{1}{2}\ell^2_{\mathrm{b3}}\big)K^2 + \ell^2_{\mathrm{b2}}K_{\mathrm{G}}\,. \tag{6.10}$$

To make the notation more compact and easy to compare with possible curvatures, we shall define

$$\mathcal{K} = \ell K\,,\quad \mathcal{K}_{\mathrm{G}} = \ell^2 K_{\mathrm{G}}\,,\quad \overline{\mathcal{K}}_{0,\mathrm{m}} = \ell(K_{0,\mathrm{m}} - K_{0,\mathrm{b}})\,, \tag{6.11}$$

[1] Note that the biquadratic parts of the lipid twist term are also neglected in this limit.

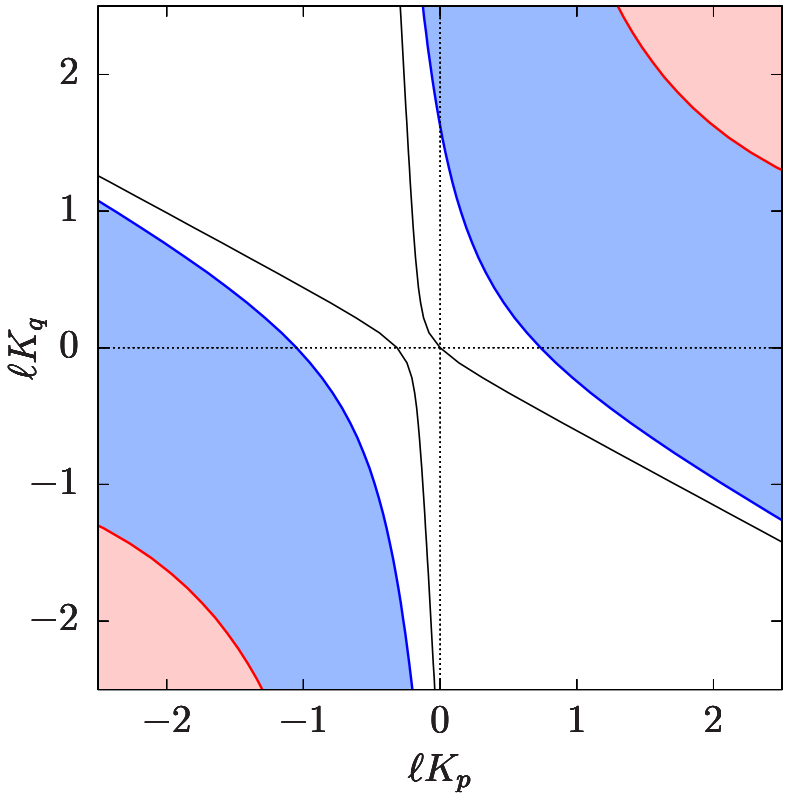

Figure 6.1: Example illustration indicating the magnitude of the eigenvalue $\kappa^p_{\mathrm{t,m}}$ of the tilt modulus tensor, as a function of the principal curvatures K_p and K_q. For our theory, the eigenvalue is larger than the bare tilt modulus within the two solid black lines where the Gaussian curvature is mostly negative. Outside, but still within the white region, it is smaller than the bare modulus but still positive, while outside in the shaded region it is negative. In contrast, for the Hamm and Kozlov theory the eigenvalue softens in the first and third quadrant, and stiffens in the third and fourth; it is negative only in the shaded red region of positive Gaussian curvature outside the two (red) hyperbolas. The parameters are for DOPC—see Table 4.1.

such that Eq (6.10) becomes

$$M = 1 + \mathcal{K}\overline{\mathcal{K}}_{0,\mathrm{m}} + (r_{\mathrm{b1}} + \tfrac{1}{2} r_{\mathrm{b3}})\mathcal{K}^2 + r_{\mathrm{b2}}\mathcal{K}_{\mathrm{G}} \,, \tag{6.12}$$

where we also used the following elastic ratios,

$$r_{\mathrm{b1}} = \frac{\kappa_{\mathrm{b1}}}{\kappa_{\mathrm{m}}} \,, \quad r_{\mathrm{b2}} = \frac{\kappa_{\mathrm{b2}}}{\kappa_{\mathrm{m}}} \quad \text{and} \quad r_{\mathrm{b3}} = \frac{\kappa_{\mathrm{b3}}}{\kappa_{\mathrm{m}}} \,. \tag{6.13}$$

To account for the direction dependence, notice that the anisotropic term in $M_{\alpha\beta}$ is proportional to $K_{\alpha\beta}$, and that means that the principal directions of the curvature tensor coincide with the eigenvectors of the tilt tensor. Let us label these two directions as p and q and call the

principal curvatures K_p and K_q. The corresponding eigenvalues of the tilt tensor are then

$$\frac{\kappa^p_{\mathrm{t,m}}}{\kappa_{\mathrm{t,m}}} = 1 + (\mathcal{K}_p + \mathcal{K}_q)\,\overline{\mathcal{K}}_{0,\mathrm{m}} + r_{\mathrm{b1}}\,(\mathcal{K}_p + \mathcal{K}_q)^2 + (r_{\mathrm{b2}} - r_{\mathrm{tw}})\mathcal{K}_p\mathcal{K}_q + (r_{\mathrm{b3}} - r_{\mathrm{tw}})\,(\mathcal{K}_p + \mathcal{K}_q)\,\mathcal{K}_p\,, \tag{6.14a}$$

$$= 1 + \mathcal{K}\overline{\mathcal{K}}_{0,\mathrm{m}} + r_{\mathrm{b1}}\mathcal{K}^2 + (r_{\mathrm{b2}} - r_{\mathrm{tw}})\mathcal{K}_{\mathrm{G}} + (r_{\mathrm{b3}} + r_{\mathrm{tw}})\mathcal{K}\mathcal{K}_p\,. \tag{6.14b}$$

and the eigenvalue $\kappa^q_{\mathrm{t,m}}$ follows simply by swapping p with q. This only affects the last term in Eq (6.14b), which is hence where the anisotropy comes from. If $K_p = \pm K_q$, the effective tilt modulus is therefore isotropic—which happens at umbilical points (for the $+$ sign) and at zero curvature points (for the $-$ sign). Globally, the anisotropy hence vanishes on either spheres or minimal surfaces.

To illustrate Eq (6.14b), we show in Figure 6.1 the region in curvature space for which the effective tilt modulus becomes negative. We use the DOPC values from Table 4.1 and corresponding biquadratic ones from Table 6.1. For sufficiently small curvatures (*i. e.*, in the center of the graph) and in the region where the Gaussian curvature becomes negative, the effective tilt modulus is positive, but as we move towards positive Gaussian curvature regions—in the first and third quadrant directions—we enter the realm of negative effective moduli. Notice that the boundary is not symmetric with respect to the 45° diagonal, which is the hallmark of anisotropy. For comparison, Figure 6.1 also shows the region of negative effective moduli predicted by the Hamm and Kozlov theory. In their case, the biquadratic arises exclusively from disentangling $\tilde{K}_{\mathrm{G}}$ (see Section 5.1.8), leading to a term $\frac{1}{2}\overline{\kappa}_{\mathrm{m}}K_{\mathrm{G}}\boldsymbol{T}^2$, which immediately gives the hyperbola $r_{\mathrm{m}}\mathcal{K}_p\mathcal{K}_q = -1$ as the locus where the eigenvalue vanishes. However, the corresponding region of $\kappa^p_{\mathrm{t,m}} < 0$ is *much* smaller than for the theory including all biquadratic terms. In particular, the effective modulus in the Hamm and Kozlov theory cannot become negative for $K_{\mathrm{G}} < 0$ (*i. e.*, in the second and fourth quadrant), including therefore on minimal surfaces. In our case, for certain values of the elastic constant, we can have negative effective tilt modulus.

The characteristic scale for the sign-reversal of the effective tilt modulus is $K \sim \ell^{-1}$, up to small corrections. These are fairly high curvatures, which do not arise in most ordinary membrane deformations, but we can expect them to occur in extreme cases such as edges, pores, or fusion stalks. Moreover, very high curvatures also arise in bicontinuous lipid phases, such as lipid cubic phases [BCC96]—phases, in which the membrane assumes the shape of triply periodic minimal surfaces, such as the gyroid [Sch70]. For a minimal surface, Eq (5.75) becomes

$$M_{\mathrm{min}} = 1 + \ell^2_{\mathrm{b2}}K_{\mathrm{G}}\,. \tag{6.15}$$

It is seen that for twelve different lipids, we estimated that the third biquadratic modulus is negative and hence $\ell^2_{\mathrm{b2}} < 0$ and for minimal surface $K_{\mathrm{G}} < 0$. Therefore, curvature corrections makes the effective tilt modulus more stiff.

6.3.1 What does a Negative Effective Tilt Modulus Mean?

If there were no tilt gradient term in the Hamiltonian, we would conclude that a negative effective tilt modulus would permit the tilt energy to become arbitrarily negative, and we would therefore demand the existence of a quartic tilt term with a positive prefactor to ensure that the energy is bounded below. However, in the presence of a gradient term, things are slightly different—in a delightfully subtle way.

Ignoring for simplicity the tilt sum field and the lipid twist term, $r_{\mathrm{tw}} \to 0$, and going to lowest order in $M^{(\mathrm{S})}_{\alpha\beta}$, the EL-equation (6.7a) for the dominant field $\boldsymbol{T}_-$ simplifies to

$$\boldsymbol{\nabla}\boldsymbol{\nabla}\cdot\boldsymbol{T}_- \mp |\ell|^{-2}\boldsymbol{T}_- = -\boldsymbol{\nabla}K\,, \tag{6.16}$$

where the "$-$" holds for a positive tilt modulus, and the "$+$" for a negative one. Hence, for a positive tilt modulus we expect *exponentially decaying solutions* with a characteristic scale ℓ, sourced by curvature gradients. If the tilt modulus becomes negative, we instead expect *oscillating solutions* with a wavelength of $2\pi|\ell|$. These seem perfectly fine, so why worry about the non-boundedness of the functional?

The answer is because the Euler-Lagrange solutions for the "$+$" case *are not necessarily minimizers of the energy functional*—unlike those for the "$-$" case, which always are. That something like this can happen is a very well understood (but much less appreciated) *global* aspect of functional variation, treated very generally in Morse theory [Mor34]. Our special "$+$" case corresponds (in one dimension) exactly to the Lagrangian of a harmonic oscillator, for which the lack of action-minimization beyond a half-period is one of the simplest demonstrable cases of this phenomenon. In the present situation, it manifests in the fact that a (spatially) oscillating solution only minimizes the energy functional as long as it extends over less than a half-period of the oscillation, meaning if the traversed distance Δx satisfies $\Delta x < \pi\ell$. In contrast, if the traversed distance is larger, then a variation $\delta T_1(s)$ exists that reduces the energy below that of the stationary solution—by arbitrarily much, and so the notion of energy minimization ceases to be meaningful. In fact, any additional half period adds a new independent variation which can drive the energy to minus infinity. A discussion of this topic can be found in a pedagogical paper by Gray and Taylor [GT07].

We are hence back at the realization that our energy functional can cease to be bounded below if the curvatures are sufficiently high, and that bounding it by a quartic term would be desirable. Indeed, our original *microscopic* functional was clearly bounded below, since Eq (2.25) is a positive definite quadratic expression and the pre-stress correction (2.38) does not change that because it is only linear. The trouble therefore stems from the fact that we have terminated the expansion of the curvature-tilt functional at the biquadratic level and have ignored stabilizing quartic terms. Including them adds considerably to the already substantial cumber, and it is well beyond the scope of the present chapter. And yet, there are still two conclusions we can draw—purely based on the knowledge that such higher order terms must exist. First, when the

effective tilt modulus vanishes, the lipid correlation length ℓ diverges (analogously to the divergence of the correlation length in a Landau theory at its critical point). This would for instance give rise to long-range (power law) tilt-mediated interactions. It also shows that even *before* that point, the softening of the tilt modulus can have important consequences by substantially lengthening ℓ. And second, once we are past the sign-flip, higher order terms will bound the energy functional below, but *its minimum will no longer be at zero tilt*: the lipid's orientational symmetry gets spontaneously broken and the monolayer acquires a nonzero average tilt. This, of course, is very different from the mechanism that gives rise to spontaneous tilt in gel phases, which arises even for flat membranes. For example, in a recent study, Nagle [Nag17b] suggested that a dramatic softening of the tilt modulus for DMPC lipids as temperature decrease may lead to a phase change and a spontaneous tilt field observed in ripple phase. Given that very substantial curvatures are needed to trigger the sign flip, one might wonder whether this also confines this spontaneous tilt to very small regions—such as the length πz_0 around a curved edge. The answer is: not necessarily, because the strong curvature *around* the edge can also render the tilt modulus *along* the edge negative, and this would lead to a spontaneous tilt all the way along the macroscopic dimension of an open edge. If this effect is real, it ought to be observable, for instance, in molecular dynamics simulations.

6.4 Worked-out Example: Tilt Fields Near Highly Curved Membrane Defect Lines

As a final application of our extended tilt-bend theory, we show as an example a simple calculation of the energy of two different types of linear defects in membranes, open edges and triple line junctions. We will see how their line tensions depend on the spontaneous lipid curvature $K_{0,\mathrm{m}}$ and the effect of tilting, and how this may change a crossover between the type of defect a membrane chooses to have—if it can pick.

As we realized in Section 6.3, very high curvatures can lead to a negative effective tilt modulus, and Section 6.3.1 then warned us that functional minimization might no longer be meaningful. As we shall see, this situation indeed arises for the membrane edge, but by the narrowest of margins our Euler-Lagrange solution remains a minimizer.

6.4.1 Straight Edge

At the edge of a lipid bilayer a highly curved semi-cylindrical monolayer connects the lipids from the upper and lower leaflet, thereby reducing the exposure of hydrophobic tails to water, at the expense of curvature and possibly tilt [Lit75, MS96, TLMM03, JBK04]. The resulting excess free energy per unit length, Γ_1, is called *edge tension* (the subscript "1" reminds us that the defect is connected to a single bilayer membrane). A simple estimate for it, $\Gamma_1^{(0)}$, would be the bending energy of a semi-cylindrical monolayer of rigidity κ_{m}, using a radius of curvature

ζ_0, which gives

$$\Gamma_1^{(0)} = \frac{1}{2}\pi\kappa_\mathrm{m}\big(\zeta_0^{-1} - 2K_{0,\mathrm{m}}\big) \,. \tag{6.17}$$

Approximating the length ζ_0 by the pivotal plane distance z_0 gives $\Gamma_1^{(0)} \approx 85.7\,\mathrm{pN}$ (using DOPC values, see Table 4.1). The spontaneous curvature contribution is significant ($13\,\mathrm{pN}$, a 15% increase), since $K_{0,\mathrm{m}}$ is relatively small for DOPC. However, we see that a smaller (negative) or a larger (positive) spontaneous curvature lowers the edge tension—which is reasonable, given the geometry of the edge. In any case, this simple numerical estimate neglects the shifts of the pivotal plane due to deformations, and Eq (6.17) of course neglects both lipid tilt and any possibility of tilt modulus softening.

May has theoretically calculated Γ_1 using a simple model for lipid elasticity, including stretching and bending, which predicts values around $30{-}40\,\mathrm{pN}$ [May00a], somewhat smaller than the simple estimate from above. Line tensions of this magnitude have indeed been obtained in various experimental studies—around $10\,\mathrm{pN}$ [CKM$^+$85, ZN93, EHLR03, KSG$^+$03].

Molotkovsky and Akimov have used Hamm and Kozlov theory to work out the edge tension, considering several possibilities for the shape of the edge, including the existence of a hydrophobic void inside the edge. They find values around $20\,\mathrm{pN}$ vs. $10\,\mathrm{pN}$ in the absence vs. presence of a void, which seems to support the idea that such a void maybe exists. In later refined work, Akimov *et al.* predict the even smaller edge tension of $6.8\,\mathrm{pN}$ [AMV$^+$14]. However, since tilt modulus softening is not yet part of these calculations, it is worthwhile to see what its implications are. We will therefore in the following use our monolayer tilt-bend functional to calculate the elastic energy associated with a very simple guess for the edge morphology: a semi-cylindrical region and the tilt field excited by it.

The cross section of the straight edge is illustrated in Figure 6.2: it has translational symmetry along the edge, and around the edge consists of a straight region (upper leaflet), connected to a curved region (edge), connected again to a straight region (lower leaflet). Away from the edge, we hence assume the curvature tensor to be zero, while on the edge we write it as

$$K_j^k = \begin{pmatrix} 1/\zeta_0 & 0 \\ 0 & 0 \end{pmatrix} \quad \text{for } -s_1 < s < s_1 = \frac{\pi\zeta_0}{2} \,, \tag{6.18}$$

where s measures arc length around the edge at the height of the pivotal plane, which in the curved region is ζ_0, and $\pm s_1$ denotes the two points where the curved region connects with the straight ones. To calculate ζ_0 (instead of merely approximating it by z_0), recall the connection between ζ and z from Eq (5.34). Taking $z = -z_0$, and $-\zeta_0$ as the corresponding $-\zeta$, we get

$$\zeta_0 = z_0 + \tfrac{1}{2}z_0^2\big(\tilde{K} - \tfrac{1}{2}KT^2 + 2K_{\alpha\beta}T^\alpha T^\beta\big) \,. \tag{6.19}$$

Let us make the following approximation,

$$\tilde{K} - \frac{1}{2}KT^2 + 2K_{\alpha\beta}T^\alpha T^\beta \approx K = \zeta_0^{-1} \,, \tag{6.20}$$

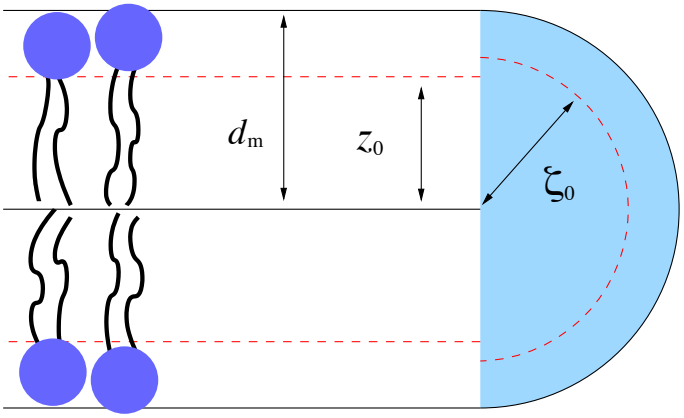

Figure 6.2: Cross-sectional sketch of straight edge, where z_0 is the distance between pivotal plane and mid-plane, ζ_0 is its stretched counterpart in the curved region, and d_m is the thickness of the (flat) monolayer. The pivotal plane is shown by red dashed lines.

in order to avoid higher order nonlinearities in the tilt equation. Combining Eq (6.19) with Eq (6.20), we get

$$\zeta_0 = \frac{1+\sqrt{3}}{2} z_0 \approx 1.37\, z_0 \,. \tag{6.21}$$

The fact that $\zeta_0 > z_0$ makes sense, since compressing the tails will stretch them out.

Due to translation and reflection symmetry, we take the tilt field *along* the edge to be zero and only consider tilting *around* the edge (meaning, tilting within the plane of Figure 6.2). We assume that the associated component $T(s)$ of the tilt field vanishes far away from the edge, but we will soon see that it penetrates the straight region adjacent to the edge. The Euler-Lagrange equation for the tilt Eq (6.5), corresponding to the monolayer energy density (5.74), is easily seen to be

$$\frac{\mathrm{d}^2 T}{\mathrm{d}s^2} - \lambda^{-2} T = -\frac{1 - r_{\mathrm{d,m}}/2}{1 + r_{\mathrm{d,m}}} \frac{\mathrm{d}K}{\mathrm{d}s} \,, \tag{6.22}$$

where λ generalizes the bare tilt length ℓ by including the biquadratic terms in the effective tilt modulus. In the two flat regions we of course simply have $\lambda_0 = \sqrt{1 + r_{\mathrm{d,m}}}\,\ell$, but in the highly curved region we must use the effective tilt modulus in s direction from Eq (6.6), which shows that

$$\frac{\kappa^{\mathrm{s}}_{\mathrm{t,m}}}{\kappa_\mathrm{m}} =: \lambda^{-2} = \frac{1}{1 + r_{\mathrm{d,m}}} \big(\ell^{-2} + (K_{0,\mathrm{m}} - K_{0,\mathrm{b}}) K + (r_{\mathrm{b1}} + r_{\mathrm{b3}}) K^2 \big) \,. \tag{6.23}$$

Together with DOPC parameters from Table 4.1 and from Table 6.1 and $K = 1/\zeta_0$, we then find

$$\left(\frac{\zeta_0}{\lambda}\right)^2 = \left(\frac{1}{1 + r_{\mathrm{d,m}}}\right) \left[\left(\frac{\zeta_0}{\ell}\right)^2 + \zeta_0 (K_{0,\mathrm{m}} - K_{0,\mathrm{m}}) + (r_{\mathrm{b1}} + r_{\mathrm{b3}} + r_{\mathrm{tw}}) \right] \approx -0.17 \,. \tag{6.24}$$

Since this expression is negative, the effective tilt modulus is negative, and we shall have to take the *magnitude* of the right hand side (to get a real length λ) and then flip the sign in front of the term $\lambda^{-2} T$ in the tilt equation (6.22) from minus to plus. However, now we are in the case where it is not guaranteed that the solution of this equation minimizes the functional. The

half-wavelength condition mentioned in Section 6.3.1 then amounts to $1 > \zeta_0/\lambda \approx 0.4$. This is actually one of the reasons why we chose DOPC because functional minimization does not work for every lipid. For example, Eq (6.24) for DMPC leads to $\zeta_0/\lambda \approx 1.2$ and the half-wavelength condition is not satisfied. However, there is no obvious reason why the minimization property actually holds for DOPC. A larger spontaneous curvature will make it easier to satisfy this condition, while a smaller one will make it harder.

The full solution is now constructed as follows: in the flat region we get exponential solutions with decay length $\lambda_0 := \sqrt{1 + r_{\mathrm{d,m}}}\,\ell$, and in the curved region an oscillatory solution with wavelength $2\pi\lambda$. Together with obvious symmetry requirements, we can write this as

$$T(s) = T_{1,\max} \times \begin{cases} \mathrm{e}^{(s_1+s)/\lambda_0} & , \quad s < -s_1 \\ -\frac{\sin(s/\lambda)}{\sin(s_1/\lambda)} & , \; -s_1 < s < s_1 \\ -\mathrm{e}^{(s_1-s)/\lambda_0} & , \quad s_1 < s \end{cases} , \tag{6.25}$$

where we already enforced the condition that the tilt field be continuous. To find its maximum amplitude $T_{1,\max}$, which it takes at the junction points $\pm s_1$, we need a second boundary condition. It specifies that the derivative of the field must satisfy jump conditions at $s = \pm s_1$, which follow from integrating Eq (6.22) over an infinitesimal region of width ε across the jump, giving

$$\big[T'\big]_{\pm s_1-\varepsilon}^{\pm s_1+\varepsilon} = -\big[K\big]_{\pm s_1-\varepsilon}^{\pm s_1+\varepsilon} = \pm\frac{1 - r_{\mathrm{d,m}}/2}{1 + r_{\mathrm{d,m}}}\zeta_0^{-1} \, . \tag{6.26}$$

Enforcing them yields the maximum tilt

$$T_{1,\max} = \frac{1 + r_{\mathrm{d,m}}/2}{1 + r_{\mathrm{d,m}}} \left[\frac{\zeta_0}{\lambda_0} + \frac{\zeta_0}{\lambda}\cot\frac{s_1}{\lambda}\right]^{-1} \, . \tag{6.27}$$

The resulting solution is illustrated in Figure 6.3. Knowing it, we obtain the edge tension by integrating the energy density corresponding to $T(s)$ and subtracting the energy of an equivalent flat leaflet, a calculation that gives the pleasingly concise analytical result

$$\Gamma_1 = \Gamma_1^{(0)} - \frac{\kappa_{\mathrm{m}}}{\zeta_0}\big(1 + \frac{1}{2}r_{\mathrm{d,m}}\big)T_{1,\max} \, , \tag{6.28}$$

where $\Gamma_1^{(0)}$ is the tilt-free result from Eq (6.17), now using the proper stretched radius of curvature from Eq (6.21).

At this point it is easy to see how we can also get the edge tension that follows from the theory of Hamm and Kozlov, if we make the same simple ansatz for the edge shape [HK98, HK00]. Since their only biquadratic term involves the Gaussian curvature, and hence vanishes at a cylindrically curved edge, their tilt modulus does not get softened, and so $\lambda = \lambda_0$. Also, HK theory does not have the coupling term multiplied by $\kappa_{\mathrm{d,m}}$, so $r_{\mathrm{d,m}} = 0$. Then, the characteristic length λ_0 further simplifies: $\lambda_0 = \ell$. This also implies that no sign change happens in Eq (6.22), which ends up merely changing the flavor of the trigonometric function in Eq (6.27) from "cot"

to "coth":

$$T_{1,\max}^{\mathrm{HK}} = \left[\frac{\zeta_0}{\ell} + \frac{\zeta_0}{\ell}\coth\frac{s_1}{\ell}\right]^{-1} = \frac{\ell}{2\zeta_0}\left(1 - \mathrm{e}^{-2s_1/\ell}\right) . \tag{6.29}$$

The form of Eq (6.28) remains unaffected (with $r_{\mathrm{d,m=0}}$). Curiously, this implies that in the limit $\ell \gg \pi\zeta_0$ the Hamm and Kozlov correction cancels the first term in the parenthesis of Eq (6.17). In the opposite limit, that parenthesis gets reduced by an additional $-\ell/\pi\zeta_0$.

Let us see what all this implies in terms of actual numbers. Using again the DOPC values from Table 4.1 and Table 6.1, we find

$$\Gamma_1^{(0)} = 66.3\,\mathrm{pN} \qquad \text{(only bending)} , \tag{6.30a}$$

$$\Gamma_1^{\mathrm{HK}} = 53.4\,\mathrm{pN} \qquad \text{(Hamm and Kozlov)} , \tag{6.30b}$$

$$\Gamma_1 = 48.1\,\mathrm{pN} \qquad \text{(this section)} , \tag{6.30c}$$

showing that (i) the use of the correct curvature length ζ_0 reduces the simple ($\zeta_0 = z_0$) tilt-free estimate from above by almost 25%, (ii) the subsequent tilt correction reduces the edge tension much further, (iii) more so for our theory in which the tilt modulus is softened. Even though the softening of the tilt modulus reduces the line tension for DOPC, it does not lower it enough to match experimental values, $\Gamma_1 \sim 20 - 25\,\mathrm{pN}$ [GGR$^+$93, KSG$^+$03]. If we use a different lipid, we can get line tension values comparable to the experimental measurements. For example, the reduction in the line tension due to softening of the effective tilt modulus is greater in DMPC lipids. However, this is not a valid result because it does not satisfy the half-wavelength condition and the EL-equations is not an energy minimizer for DMPC lipids.

As a final comment, we want to verify that treating the tilt *along* the edge as zero is more than convenience. For the high edge curvature $K\ell = \ell/\zeta_0 \approx 0.8$ the tilt modulus *along* the edge remain positive—as a quick look at Figure 6.1 confirms. However, this does not mean that a negative effective tilt modulus *along* the edge is not possible. When we have a $\kappa_{\mathrm{t,m,eff}}^t < 0$, we would hence expect a tilt component $T_{||}$ along the edge, but recall that we are in the regime where the Euler-Lagrange solutions are only proper minimizers over half an oscillation wavelength. Since the edge is generally longer than that, we have no means of calculating $T_{||}$, which we expect to exhibit a spontaneous nonzero value, the magnitude of which can only be predicted if we know the quartic tilt contribution to the monolayer Hamiltonian. Absent that, insisting on $T_{||} = 0$ is better than suffering the incorrect prediction $T_{||} = \infty$.

6.4.2 Triple Line Junction

A different type of one-dimensional membrane defect is a triple line junction: a line where three bilayers meet, in such a way that each pair of bilayers shares one leaflet with the third bilayer, as illustrated in Figure 6.4. The resulting excess free energy per unit length along the junction, Γ_3, also acts like a line tension (the subscript "3" indicating that three bilayer membranes connect to the linear defect). The value of this triple-line tension can be (and has been) determined in simulations by similar means as open edge tensions [Nog12, GDA16].

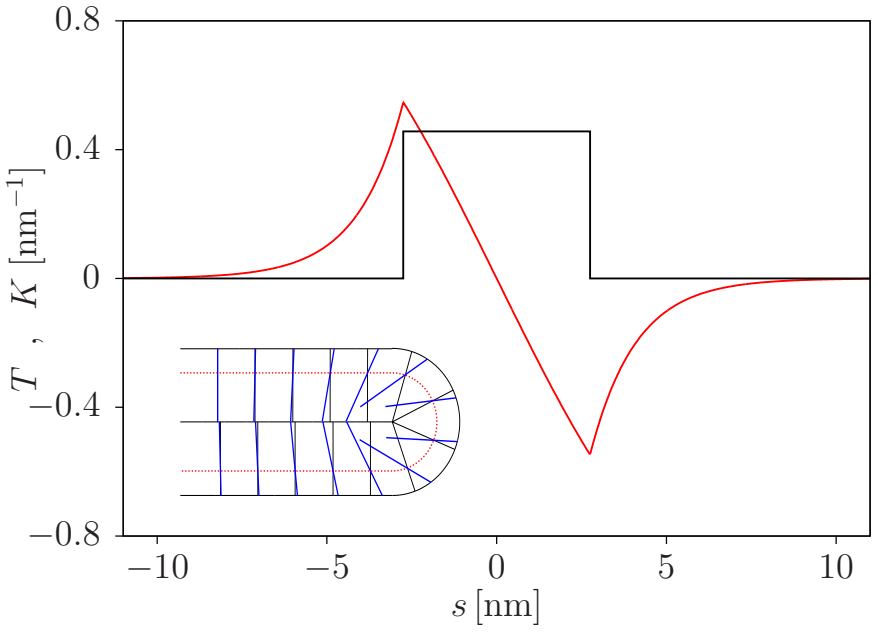

Figure 6.3: Tilt field as a function of arc length on the pivotal plane (red curve); the piecewise constant curvature $K(s)$ near the edge is also given (black line). The inset sketches a cross-section of the straight edge, in which the lipid direction is shown in blue and the leaflet normal as black. The membrane parameters are from Table 4.1 and Table 6.1.

The elastic calculation from the previous section can be revised quite straightforwardly to the case of a triple line junction (see also [MA02]). The major differences are the following: (i) we have three curved leaflet patches instead of just one, but each only turns an angle of $\pi/3$; (ii) the curvature is negative; (iii) the radius of curvature is not the distance of the pivotal plane to the end of the lipid tails, but instead to the top of the lipid head. For the uncurved leaflet this distance is $y_0 = d_\mathrm{m} - z_0$, for the curved one, reworking the argument that led to Eq (6.21) yields $\eta_0 := \frac{1+\sqrt{3}}{2} y_0$. For the same parameters we used before for DOPC (and $d_\mathrm{m} = 1.91\,\mathrm{nm}$), this leads to $\eta_0 = 0.87\,\mathrm{nm}$.

A prediction based on curvature elasticity alone gives

$$\Gamma_3^{(0)} = \frac{1}{2}\pi\kappa_\mathrm{m}(\eta_0^{-1} + 2K_{0,\mathrm{m}}) \,, \tag{6.31}$$

so the line tension increases if the spontaneous curvature becomes more positive, since this is opposite to a leaflet's curvature in the triple line geometry. Executing the equivalent calculation for the triple line gives the tilt-corrected result

$$\Gamma_3 = \Gamma_3^{(0)} - 3\,\frac{\kappa_\mathrm{m}}{\eta_0}\left(1 + \frac{1}{2} r_{\mathrm{d,m}}\right) T_{3,\max} \,, \tag{6.32}$$

where the maximum tilt field in the triple line case is given by

$$T_{3,\max} = \left[\frac{\eta_0}{\lambda_0} + \frac{\eta_0}{\lambda}\cot\frac{s_3}{\lambda}\right]^{-1} \quad \text{with } s_3 = \frac{1}{6}\pi\eta_0 \,, \tag{6.33}$$

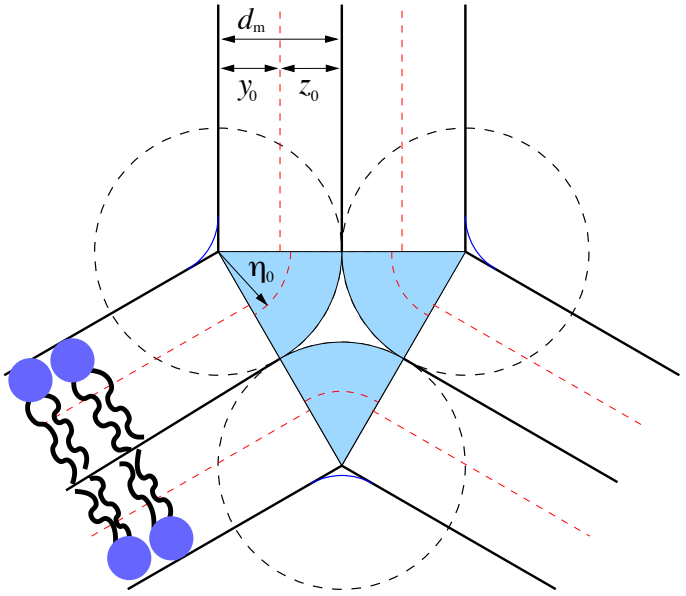

Figure 6.4: Cross-sectional sketch of a triple line junction, where z_0 is the distance between the pivotal plane and the mid-plane, d_m is the thickness of the (flat) monolayer, $y_0 = d_\mathrm{m} - z_0$, and η_0 is its stretched counterpart in the curved region. The pivotal plane is shown by red dashed lines.

and where λ is calculated from Eq (6.23) with $K = -1/\eta_0$; its right hand side will again come out negative, so we need to take its magnitude and flip the sign of the λ-term in Eq (6.22). As in the case of the free edge, the prediction for Hamm and Kozlov's theory results by replacing $\lambda \to \ell$ and $\cot \to \coth$ in Eq (6.33), while Eq (6.32) remains unaffected.

Inserting the DOPC values from Table 4.1 and Table 6.1, we find

$$\Gamma_3^{(0)} = 92.9\,\mathrm{pN} \qquad \text{(only bending)}\,, \tag{6.34a}$$

$$\Gamma_3^{\mathrm{HK}} = 15.6\,\mathrm{pN} \qquad \text{(Hamm and Kozlov)}\,, \tag{6.34b}$$

$$\Gamma_3 = -89.5\,\mathrm{pN} \qquad \text{(this thesis)}\,. \tag{6.34c}$$

Notice that $\Gamma_3^{(0)} \approx 2\,\Gamma_1^{(0)}$, which holds because the radius of curvature at the junction is almost two times smaller than that at the edge. This, however, also implies that more tilt is induced via Eq (6.22). Combined with the additional prefactor of 3 in the tilt correction term in Eq (6.32) this leads to a stronger reduction of the curvature-only value and brings the triple line tension down to *negative* values. The negative value for a triple line junction means that the membrane prefers to be in a triple line junction than a flat configuration, therefore it goes into an inverse hexagonal phase ($\mathrm{H_{II}}$). However, we know that DOPC stays in bilayer configuration.

Figure 6.4 shows that our "ansatz" for the triple-line geometry posits a hole in the center of the junction. This is of course unphysical, but will it affect our calculation of Γ_3? The cross-sectional area of the empty region is $(\sqrt{3} - \pi/2)d_\mathrm{m}^2 \approx 0.161\,d_\mathrm{m}^2$. Creating it in a real bilayer requires doing work against its internal pressure, which is anisotropic. The normal pressure at the center of the bilayer is equal to the ambient pressure ($P_\perp = 1\,\mathrm{bar}$ under standard conditions),

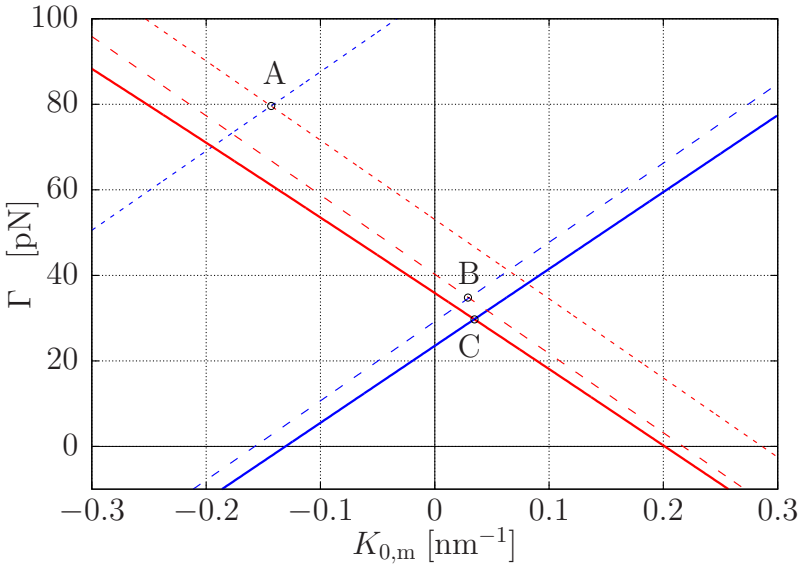

Figure 6.5: Edge tension Γ_1 (red curves with negative slope) and triple line tension Γ_3 (blue curves with positive slope) as a function of spontaneous lipid curvature $K_{0,\mathrm{m}}$ (all other parameters are taken from Table 4.1 and Table 6.1). The dotted lines are the predictions based on bending alone ($\Gamma_1^{(0)}$ and $\Gamma_3^{(0)}$), the dashed lines are derived from the theory of Hamm and Kozlov [HK98, HK00], and the solid curves are our results from Section 6.4.1 and 6.4.2. The intersection points A, B, and C mark the spontaneous curvatures of the three theories at which the stability switches from a triple junction (left of intersection) to an open edge (right of intersection).

while the lateral pressure $P_{||} = \mathcal{O}(10^2)\,\mathrm{bar}$ [SBSG90, Saf94, BS95, Mar96, Can97, Can99]. Assuming that the hole is created by pushing against the soft and not against the hard direction, the change in surface tension amounts to

$$\Delta\Gamma_3 \approx -P_\perp(\sqrt{3}-\pi/2)d_\mathrm{m}^2 \approx -0.08P_{||}d_\mathrm{m}^2 \approx -0.05\,\mathrm{pN}\,, \tag{6.35}$$

which is negligible.

6.4.3 Straight Edge vs. Triple Line Junction

If we pull one of the three bilayer sheets merging at a triple line junction away from that junction, we obtain a single continuous membrane and a detached membrane with an open edge. Hence, we can change between a state in which the triple line tension is the dominant contribution to the free energy and a state where this role is played by the edge tension. Whether a triple line junction splits off one of its membranes, or whether an open membrane strives to conjoin with an existing membrane, therefore depends on which of these two defect line energies is lower.

Gardner *et al.* have recently studied this situation using a highly coarse grained model and a simple theory (without tilt corrections) [GDA16]. They find that the answer depends on the spontaneous curvature of a monolayer leaflet, with a higher spontaneous curvature favoring edges and a lower one favoring junctions, but they change the spontaneous curvature by mixing two lipid species with different spontaneous curvatures, and so they also need to account for the entropy

of mixing. If we instead consider a single lipid species and vary its spontaneous curvature $K_{0,\mathrm{m}}$, we can use the types of elastic theories discussed in this paper to study this transition.

Figure 6.5 shows edge tensions and triple line tensions as a function of lipid spontaneous curvature (with all other parameters taken from Table 4.1 and Table 6.1). It compares the results for a pure bending theory (*i. e.*, what we called $\Gamma_1^{(0)}$ and $\Gamma_3^{(0)}$), the prediction following from the treatment of Hamm and Kozlov (Γ_1^{HK} and Γ_3^{HK}), and our own results (Γ_1 and Γ_3). In all cases we find that edge tensions decrease with increasing $K_{0,\mathrm{m}}$, while the opposite is true for triple line tensions. The bending-only results are larger than either one of the tilt-corrected predictions, because "opening up" the tilt degree of freedom can significantly lower the elastic cost of creating either of the two line defects. As we have already explained, tilt-induced lowering of the defect energies is more pronounced for the triple junction than for the edge, and this shifts the prediction of the transition curvature between triple line and edge significantly towards more positive spontaneous curvatures compared to the naïve curvature-only calculation (thereby helping to stabilize junctions). Furthermore, our own results for either defect energy are lower (by about $10\,\mathrm{pN}$) than those derived from the energy density of Hamm and Kozlov, because their only biquadratic term is proportional to the Gaussian curvature, which vanishes at both edge and junction, and so no softening of the modulus happens. In contrast, both a linear and a biquadratic term contributes to tilt modulus softening in our case—see Eq (6.23)—which further lowers the energy. In fact, the effective modulus becomes negative, which requires extra care in interpreting the results.

Our theory predicts $\Gamma_1 = \Gamma_3$ at $K_{0,\mathrm{m}} = 0.026\,\mathrm{nm}^{-1}$. This seems to suggest that if a lipid has a similar spontaneous curvature, that membrane has essentially no preference between an edge and a junction, but it is important to realize how strongly these numbers depend on the spontaneous curvature: taking $K_{0,\mathrm{m}} = 0.025\,\mathrm{nm}^{-1}$, the accumulated difference in defect energy along a merely $12\,\mathrm{nm}$ long strip favors the junction over a edge by $1\,k_{\mathrm{B}}T$, and at $K_{0,\mathrm{m}} = 0.012\,\mathrm{nm}^{-1}$ this energy is reached already along a single nanometer.

If the values of $K_{0,\mathrm{m}}$ deviate even more from this balance point, either the edge tension or the triple line tension can become negative. The former happens at $K_{0,\mathrm{m}} \approx 0.141\,\mathrm{nm}^{-1}$, and it would indicate that beyond this point edges would want to grow indefinitely, suggesting that the lamellar phase decays into cylindrical micelles. Conversely, for spontaneous curvatures below $K_{0,\mathrm{m}} \approx -0.074\,\mathrm{nm}^{-1}$ the triple line tension becomes negative, which we may interpret as the system wanting to create more triple line defects and hence transitioning into an inverse hexagonal ($\mathrm{H_{II}}$) phase, which essentially consists of nothing but triple line junctions. However, these predictions are neither quantitatively reliable nor formally correct, because it is neither obvious how one would merely shift the spontaneous curvature without affecting any of the other membrane parameters, nor is it clear what would correspond to the (positive!) tilt energy in the adjacent flat membranes, which are not present in either cylindrical micelles or inverse hexagonal phases.

6.5 Conclusion

Biquadratic terms manifest as local geometry dependent corrections to the energy of tilting, giving rise to an effective tilt modulus *tensor* that shares its eigenvectors with the curvature tensor. The cost of tilting is hence not just position but also direction dependent, except on spheres and minimal surfaces. The magnitude of the correction depends on how the local curvature radii compare to certain (generally microscopic) lengths, such as the distance z_0 of the pivotal plane from the bilayer midplane, the tilt decay length ℓ, or a novel tilt-associated spontaneous curvature $K_{0,\mathrm{b}}$—which can be written in terms of the underlying microscopic elastic model.

The effective tilt modulus can decrease and *softening* of the modulus is unbounded, such that at sufficiently high curvature it can even become negative. We have discussed the interpretation of this possibility and argued that it foreshadows curvature-induced spontaneous tilt, even though this cannot be made quantitative without introducing quartic tilt terms. We have shown that negative effective tilt moduli actually occur for highly curved configurations, such as the monolayer geometries at open membrane edges or triple line junctions. These two geometries have also served as illustrative examples, allowing us to calculate the excess elastic energy (line tension) of these linear defects for our theory, as well as for the alternative theories of Hamm and Kozlov (no tilt modulus softening) and Helfrich (no tilt at all). Corrections due to tilt and tilt modulus softening have turned out to be significant, even though our results for the edge tension are not in good agreement with the experimental results, they agree better than the other two theories. However, we cannot say the same for the triple line junction.

Appendix A

Details of the Derivation of Area Strain

The definition of the area strain is given in Eq (2.43), and using Eq (2.44), it boils down to the following cross product,

$$\epsilon(\zeta) = \frac{1}{2}\varepsilon^{\alpha\beta}|\boldsymbol{e}'_\alpha \times \boldsymbol{e}'_\beta| - 1 \,, \tag{A.1}$$

where the *prime* represents the lipid shifted surfaces, and $\boldsymbol{e}'_\alpha$ up to quadratic order in fields is given in Eq (3.23),

$$\boldsymbol{e}'_\alpha = \boldsymbol{e}_\alpha - \frac{1}{2}\zeta^2(\nabla_\alpha\epsilon_1)\boldsymbol{n} + \zeta\nabla_\alpha\boldsymbol{n} \,, \tag{A.2}$$

where ϵ_1 is the first term in the expansion of area strain in terms of ζ. The covariant derivative of the director is derived in Appendix C but we need to determine it up to bi-quadratic order, $\mathcal{O}(K^2, T^2)$. Let us therefore calculate $\nabla_\alpha \boldsymbol{N}$ exactly. The derivative of $\boldsymbol{n}$ is

$$\begin{aligned}\nabla_\alpha\boldsymbol{n} &= \nabla_\alpha\Big[\frac{\boldsymbol{N}+\boldsymbol{T}}{\sqrt{1+T^2}}\Big] \\ &= \frac{1}{\sqrt{1+T^2}}[\nabla_\alpha\boldsymbol{N} + \nabla_\alpha\boldsymbol{T}] - \frac{-T_\beta\nabla_\alpha T^\beta}{(1+T^2)^{3/2}}[\boldsymbol{N}+\boldsymbol{T}] \,.\end{aligned} \tag{A.3}$$

We use the Weingarten equation Eq (2.15) to express the derivative of the normal vector, and the derivative of the tilt vector is determined in Eq (C.3b). Then, Eq (A.3) becomes

$$\nabla_\alpha\boldsymbol{n} = \frac{1}{\sqrt{1+T^2}}[K_\alpha^\beta\boldsymbol{e}_\beta + (\nabla_\alpha T^\beta)\boldsymbol{e}_\beta - T^\beta K_{\alpha\beta}\boldsymbol{N}] - \frac{-T_\beta\nabla_\alpha T^\beta}{(1+T^2)^{3/2}}[\boldsymbol{N}+\boldsymbol{T}] \,, \tag{A.4}$$

where the first two terms in the bracket are is equal to the effective total curvature. Eq (A.4) gives the exact relation for $\nabla_\alpha\boldsymbol{n}$, but we only need it up to bi-quadratic order, so we can expand the terms in the denominators and find

$$\nabla_\alpha\boldsymbol{n} = (1 - \frac{1}{2}T^2)\tilde{K}_\alpha^\beta\boldsymbol{e}_\beta - T^\beta\tilde{K}_{\alpha\beta}\boldsymbol{N} \,. \tag{A.5}$$

The area strain A.2 is written using Eq (A.5) and the expansion of the lipid director Eq (C.1),

$$\boldsymbol{e}'_\alpha = E_\alpha^\gamma\boldsymbol{e}_\gamma + F_\alpha\boldsymbol{N} \,. \tag{A.6}$$

To clean up the subsequent calculation, we introduced the two tensors $E_\alpha^{\ \gamma}$ and F_α, which are functions of ζ, curvature, and tilt field:

$$E_\alpha^{\ \gamma} = \delta_\alpha^\gamma + \zeta\big(1 - \frac{1}{2}T^2\big)\tilde{K}_\alpha^{\ \gamma} - \frac{1}{2}\zeta^2 T^\gamma \nabla_\alpha \epsilon_1 \,, \tag{A.7a}$$

$$F_\alpha = -\zeta T^\gamma \tilde{K}_{\alpha\gamma} - \frac{1}{2}\zeta^2\big(1 - \frac{1}{2}T^2\big)\nabla_\alpha \epsilon_1 \,. \tag{A.7b}$$

Then, the area strain is calculated from Eq (A.1),

$$\begin{aligned}\epsilon(\zeta) &= \frac{1}{2}\varepsilon^{\alpha\beta}\big|\big(E_\alpha^{\ \gamma}\boldsymbol{e}_\gamma - F_\alpha \boldsymbol{N}\big) \times \big(E_\beta^{\ \delta}\boldsymbol{e}_\delta - F_\beta \boldsymbol{N}\big)\big| - 1 \,, \\ &= \frac{1}{2}\varepsilon^{\alpha\beta}\big|E_\alpha^{\ \gamma}E_\beta^{\ \delta}\boldsymbol{e}_\gamma \times \boldsymbol{e}_\delta + E_\alpha^{\ \gamma}F_\beta \boldsymbol{e}_\gamma \times \boldsymbol{N} + F_\alpha E_\beta^{\ \delta}\boldsymbol{N} \times \boldsymbol{e}_\delta\big| - 1 \,.\end{aligned} \tag{A.8}$$

The following identities now become useful:

$$\boldsymbol{N} \times \boldsymbol{e}_\alpha = \varepsilon_{\alpha\beta}\boldsymbol{e}^\beta \,, \tag{A.9a}$$

$$\boldsymbol{e}_\alpha \times \boldsymbol{e}_\beta = \varepsilon_{\alpha\beta}\boldsymbol{N} \,, \tag{A.9b}$$

$$\varepsilon^{\alpha\beta}\varepsilon_{\gamma\beta} = \delta_\gamma^\alpha \,, \tag{A.9c}$$

$$\varepsilon^{\alpha\beta}\varepsilon_{\alpha\beta} = 2 \,. \tag{A.9d}$$

Using them, Eq (A.8) can be simplified to the following form,

$$\epsilon(\zeta) = \frac{1}{2}\big|\varepsilon^{\alpha\beta}\varepsilon_{\gamma\delta}E_\alpha^{\ \gamma}E_\beta^{\ \delta}\boldsymbol{N} - \varepsilon^{\alpha\beta}\varepsilon_{\gamma\mu}E_\alpha^{\ \gamma}F_\beta \boldsymbol{e}^\mu + \varepsilon^{\alpha\beta}\varepsilon_{\delta\mu}F_\alpha E_\beta^{\ \delta}\boldsymbol{e}^\mu\big| - 1 \,, \tag{A.10}$$

where the first term in the absolute value is the determinant of the tensor $E_\alpha^{\ \beta}$ and the second and third terms can be by relabeling the dummy indices, $\alpha \leftrightarrow \beta$ and $\gamma \leftrightarrow \delta$. Therefore, the area strain has the form,

$$\epsilon(\zeta) = \big|\det E_\alpha^{\ \beta}\boldsymbol{N} - \varepsilon^{\alpha\beta}\varepsilon_{\gamma\mu}E_\alpha^{\ \gamma}F_\beta \boldsymbol{e}^\mu\big| - 1 \,. \tag{A.11}$$

We now insert $E_\alpha^{\ \beta}$ and F_α, which are defined in Eq (A.7a) and Eq (A.7b), and only keep terms up to bi-quadratic order in fields,

$$\begin{aligned}\epsilon(\zeta) = \Big|&\big\{1 + \zeta(1 - \frac{1}{2}T^2)\tilde{K} + \zeta^2(1 - T^2)\tilde{K}_{\mathrm{G}} - \frac{1}{2}\zeta^2 \boldsymbol{T}\cdot\boldsymbol{\nabla}\epsilon_1\big\}\boldsymbol{N} \\ &+ \zeta\big\{T^\delta \tilde{K}_{\delta\mu} + \zeta T^\nu(K_{\mu\nu}K - K_{\beta\nu}K_\mu^{\ \nu}) + \frac{1}{2}\zeta\nabla_\mu\epsilon_1\big\}\boldsymbol{e}^\mu\Big| - 1 \,.\end{aligned} \tag{A.12}$$

Let us write this expression in the following notation,

$$\epsilon(\zeta) = \Big|R\boldsymbol{N} + L_\mu \boldsymbol{e}^\mu\Big| - 1 \,, \tag{A.13}$$

where R is the normal component and L_μ is in the tangential component of the terms inside the absolute value. The absolute value of an expression is found by multiplying it by itself, and

taking its square root. Then, Eq (A.13),

$$\epsilon(\zeta) = \Big| R^2 + L_\mu L^\mu \Big| - 1 \,, \tag{A.14}$$

where the cross term between $\boldsymbol{N}$ and $\boldsymbol{e}^\mu$ vanishes because these vectors are perpendicular. We are left with the square of the terms in normal and tangential directions. However, the smallest term in the tangential direction is of order ζ: $L_\mu = \big[\zeta T^\delta \tilde{K}_{\delta\mu} + \mathcal{O}(\zeta^2)\big]\boldsymbol{e}^\mu$. Therefore, the square of this term is $L_\mu L^\mu = \zeta^2 T^\delta T^\gamma K_{\delta\beta} K^\beta_\gamma + \mathcal{O}(\zeta^3)$. Then, the area strain becomes

$$\epsilon(\zeta) = \Big[1 + 2\zeta\big(1 - \frac{1}{2}T^2\big)\tilde{K} + \zeta^2\big[(1-T^2)(\tilde{K}^2 + 2\tilde{K}_{\rm G}) - \boldsymbol{T}\cdot\boldsymbol{\nabla}\epsilon_1 + T^\delta T^\gamma K_{\delta\beta}K^\beta_\gamma\big]\Big]^{1/2} - 1 \,, \tag{A.15}$$

and expand the square root in powers of ζ, up to bi-quadratic order

$$\epsilon(\zeta) = \zeta\big(1 - \frac{1}{2}T^2\big)\tilde{K} + \zeta^2(1-T^2)\tilde{K}_{\rm G} - \frac{1}{2}\zeta^2 \boldsymbol{T}\cdot\boldsymbol{\nabla}\epsilon_1 + \frac{1}{2}\zeta^2 T^\delta T^\gamma K_{\delta\beta}K^\beta_\gamma + \mathcal{O}(\zeta^3) \,. \tag{A.16}$$

The first term in this expression gives us ϵ_1 and hence the third term becomes,

$$-\frac{1}{2}\zeta^2 \boldsymbol{T}\cdot\boldsymbol{\nabla}\epsilon_1 = -\frac{1}{2}\zeta^2 \boldsymbol{T}\cdot\boldsymbol{\nabla}\tilde{K} + \mathcal{O}(T^3) \,. \tag{A.17}$$

Using this result, we can write the area strain up to bi-quadratic order in terms of curvature and tilt field as

$$\epsilon(\zeta) = \zeta\epsilon_1 + \zeta^2\epsilon_2 + \mathcal{O}(\zeta^3, T^3) \,, \tag{A.18}$$

where the expansion coefficients are

$$\epsilon_1 = \big(1 - \frac{1}{2}T^2\big)\tilde{K} \,, \tag{A.19a}$$

$$\epsilon_1 = (1-T^2)\tilde{K}_{\rm G} - \frac{1}{2}\boldsymbol{T}\cdot\boldsymbol{\nabla}\tilde{K} + \frac{1}{2}T^\delta T^\gamma K_{\delta\beta}K^\beta_\gamma \,. \tag{A.19b}$$

In Chapter 3, we need the area strain up to quadratic order in both curvature and tilt. Then, we easily find

$$\epsilon(\zeta) = \zeta\tilde{K} + \zeta^2\big[\tilde{K}_{\rm G} - \frac{1}{2}\boldsymbol{T}\cdot\boldsymbol{\nabla}\tilde{K}\big] + \mathcal{O}(\zeta^3) + \mathcal{O}(T^3) \,. \tag{A.20}$$

Appendix B

Monolayer to Bilayer: Shifting the Reference Surface: Quadratic Case

B.1 Correction to Curvature

In this Appendix we derive an expression that relates the effective total curvatures of two lipid shifted surfaces. One thing we know about such surfaces is that *by definition* their directors coincide, $\boldsymbol{n} = \boldsymbol{n}'$. In a first step, let us take the covariant divergence of this equality by scalar multiplying with the operator $\boldsymbol{\nabla} = \boldsymbol{e}^i \nabla_i$. And in a more subtle second step, we will exploit that (i) the covariant derivative is equal to the simpler partial derivative when it acts on an index-free object (even if it is a 3-vector!), and that (ii) the partial derivative is independent of the reference surface.[1] We hence get

$$\nabla_i(\text{scalar}) = \partial_i(\text{scalar}) \equiv \partial'_i(\text{scalar}) = \nabla'_i(\text{scalar}) \; . \tag{B.1}$$

In Appendix C we show that $\tilde{K} = \boldsymbol{\nabla} \cdot \boldsymbol{n}$, and together with the previous result this then implies

$$\tilde{K} = \boldsymbol{\nabla} \cdot \boldsymbol{n} = \boldsymbol{\nabla} \cdot \boldsymbol{n}' = \boldsymbol{e}^i \cdot \nabla_i \boldsymbol{n}' \overset{\text{(B.1)}}{=} \boldsymbol{e}^i \cdot \nabla'_i \boldsymbol{n}' \; . \tag{B.2}$$

Moreover, Appendix C also gives an expression for the covariant derivative of the director,

$$\nabla_i \boldsymbol{n} \overset{\text{(C.4)}}{=} \boldsymbol{e}_j \tilde{K}_i{}^j - \boldsymbol{N} \tilde{K}_{ij} T^j \; , \tag{B.3}$$

and hence Eq (B.2) becomes

$$\tilde{K} = \boldsymbol{e}^i \cdot \boldsymbol{e}'_j \tilde{K}'^j_i - \boldsymbol{e}^i \cdot \boldsymbol{N}' \tilde{K}'_{ij} T'^j \; , \tag{B.4}$$

where we used $\boldsymbol{e}^i \cdot \boldsymbol{N} = 0$ and $\boldsymbol{e}^i \cdot \boldsymbol{e}_j = \delta^i_j$.

[1] The partial derivatives are really just derivatives with respect to the two coordinates, and we use the same coordinates on the two surfaces. The covariant derivatives, on the other hand, are decorated with Christoffel symbols, which depend on the metric and hence the geometry of the surface they refer to. Since lipid shifted surfaces differ in their geometry, so do their associated covariant derivatives.

The second term on the right hand side of Eq (B.4) is not necessarily zero, because $\boldsymbol{e}^i \cdot \boldsymbol{N}'$ generally does not vanish—for two reasons: first, because of tilt (which yields a correction $\propto T^i$); and second, because ζ might be position dependent (which yields a correction $\propto \tilde{K}$). Either way, $\boldsymbol{e}^i \cdot \boldsymbol{N}'$ is at least linear in one of the fields. Since in Eq (B.4) it multiplies the quadratic term $\tilde{K}'_{ij} T'^j$, this would overall result in a cubic term, which we may safely neglect, considering the accuracy we aim for. Equation (B.4) then becomes

$$\tilde{K} = \tilde{K}'_i{}^j \, \boldsymbol{e}^i \cdot \boldsymbol{e}'_j \; + \; \text{cubic order} \, . \tag{B.5}$$

To calculate the leading order, we need to work out how much $\boldsymbol{e}^i \cdot \boldsymbol{e}'_j$ deviates from δ^i_j, but since this term multiplies the effective curvature tensor, it will be enough to get the answer to first order in curvature. Using the definition of the lipid shifted surface from Eq (3.17b), we find

$$\begin{aligned} \boldsymbol{e}'_j &= \nabla'_j \boldsymbol{X}' \overset{\text{(B.1)}}{=} \nabla_j \boldsymbol{X}' \overset{\text{(3.17b)}}{=} \nabla_j \big(\boldsymbol{X} + \zeta \boldsymbol{n} \big) && \text{(B.6a)} \\ &= \boldsymbol{e}_j + \zeta \nabla_j \boldsymbol{n} + \boldsymbol{n} \nabla_j \zeta && \text{(B.6b)} \\ &= \boldsymbol{e}_j \overset{\text{(B.3)}}{+} \zeta \Big[\boldsymbol{e}_k \tilde{K}_j{}^k - \boldsymbol{N} \tilde{K}_{jk} T^k \Big] \overset{\text{(3.26)}}{-} \frac{1}{2} \boldsymbol{n} \zeta^2 \nabla_j \tilde{K} \, , && \text{(B.6c)} \end{aligned}$$

and since $\boldsymbol{e}^i \cdot \boldsymbol{n} = T^i + \mathcal{O}(T^3)$, we get

$$\boldsymbol{e}^i \cdot \boldsymbol{e}'_j = \delta^i_j + \zeta \tilde{K}_j{}^i \; - \frac{1}{2} \zeta^2 T^i \nabla_j \tilde{K} \, , \tag{B.7}$$

where the last term is quadratic. Reinserting into Eq (B.5), the relationship between the effective curvatures of two lipid shifted surface, correct up to quadratic order, becomes

$$\tilde{K} = \tilde{K}' + \zeta \tilde{K}'_i{}^j \tilde{K}_j{}^i \; + \; \text{cubic order} \, . \tag{B.8}$$

Notice that we can actually drop the prime on the effective curvature tensors in the quadratic term: the difference between $\tilde{K}'_i{}^j$ and $\tilde{K}_i{}^j$ is at least quadratic in the curvature and would thus only contribute to the cubic correction. Finally, using the identity $\tilde{K}_i{}^j \tilde{K}_j{}^i = \tilde{K}^2 - 2\tilde{K}_{\mathrm{G}}$,[2] and solving for $\tilde{K}'$, we arrive at

$$\tilde{K}' = \tilde{K} - \zeta \big(\tilde{K}^2 - 2\tilde{K}_{\mathrm{G}} \big) \; + \; \text{cubic order} \, . \tag{B.9}$$

More calculations will be put on appanedix if it needed.

[2] This is merely the identity $\mathrm{Tr}(\mathbb{K}^2) = \mathrm{Tr}(\mathbb{K})^2 - 2\det(\mathbb{K})$, which holds for any second rank tensor in two dimensions and follows from the Cayley-Hamilton theorem.

Appendix C

Relation between director and curvature

The fluctuation analysis in Sec. 4.3 used a relation between the lipid director $\boldsymbol{n}$ and the effective curvature of the membrane. Here we derive this relation using a covariant formalism, which also clarifies the accuracy to which this relation holds.

Recall that the normalized lipid director can be written as

$$\boldsymbol{n} \overset{(3.7)}{=} \frac{\boldsymbol{N}+\boldsymbol{T}}{\sqrt{1+\boldsymbol{T}^2}} = \boldsymbol{N}\Big(1-\frac{1}{2}\boldsymbol{T}^2\Big)+\boldsymbol{T}+\mathcal{O}(T^3)\,. \tag{C.1}$$

Taking its covariant derivative gives

$$\nabla_i\boldsymbol{n} = \Big(1-\frac{1}{2}\boldsymbol{T}^2\Big)\nabla_i\boldsymbol{N}+\big(\mathbb{1}-\boldsymbol{N}\otimes\boldsymbol{T}\big)\nabla_i\boldsymbol{T}+\mathcal{O}(T^3)\,. \tag{C.2}$$

The Weingarten equation permits expressing the derivative of the normal vector as $\nabla_j\boldsymbol{N} = K_j^k\boldsymbol{e}_k$, while the derivative of the tilt vector $\boldsymbol{T}$ can be rewritten as

$$\begin{aligned}\nabla_i\boldsymbol{T} &= \nabla_i(T^k\boldsymbol{e}_k) = \boldsymbol{e}_k\nabla_iT^k+T^k\nabla_i\boldsymbol{e}_k && \text{(C.3a)}\\ &= \boldsymbol{e}_k\nabla_iT^k-T^kK_{ik}\boldsymbol{N}\,, && \text{(C.3b)}\end{aligned}$$

where we used the Gauss equation $\nabla_i\boldsymbol{e}_k = -K_{ik}\boldsymbol{N}$ in the second step. Inserting these two results into Eq (C.2), and keeping everything up to quadratic order, we get

$$\begin{aligned}\nabla_i\boldsymbol{n} &= \boldsymbol{e}_k\Big[K_i^k+\nabla_iT^k\big(\mathbb{1}-\boldsymbol{N}\otimes\boldsymbol{T}\big)\Big]-\boldsymbol{N}T^kK_{ik} && \text{(C.4a)}\\ &= \boldsymbol{e}_k\underbrace{(K_i^k+\nabla_iT^k)}_{\text{linear}}-\boldsymbol{N}\underbrace{(K_{ik}+\nabla_iT_k)T^k}_{\text{quadratic}} && \text{(C.4b)}\\ &\overset{(3.9)}{=} \tilde{K}_{ik}(\boldsymbol{e}^k-\boldsymbol{N}T^k)\,. && \text{(C.4c)}\end{aligned}$$

It is easy to check that the $\boldsymbol{e}^k-\boldsymbol{N}T^k$ is normal to $\boldsymbol{n}\propto\boldsymbol{N}+T^i\boldsymbol{e}_i$. This must of course be true, since $|\boldsymbol{n}|=1$ implies $\nabla_i\boldsymbol{n}\perp\boldsymbol{n}$.

After projecting Eq (C.4c) into the local tangent plane, we are left with the linear contribution

$$\boldsymbol{e}^j \cdot \nabla_i \boldsymbol{n} = \tilde{K}_i{}^j \ . \tag{C.5}$$

In particular, contracting i with j and defining the coordinate-free covariant derivative $\boldsymbol{\nabla} = \boldsymbol{e}^i \nabla_i$, we get

$$\boldsymbol{\nabla} \cdot \boldsymbol{n} = K + \boldsymbol{\nabla} \cdot \boldsymbol{T} = \tilde{K} \ . \tag{C.6}$$

In other words, *the covariant divergence of the director field is the effective curvature*, up to additional *cubic* terms.

As a side note: contracting the Weingarten equation immediately shows that $K = \boldsymbol{\nabla} \cdot \boldsymbol{N}$, and so Eq (C.6) essentially states that

$$\boldsymbol{\nabla} \cdot \big(\boldsymbol{n} = \boldsymbol{N} + \boldsymbol{T}\big) \ , \tag{C.7}$$

and the expression in parentheses is simply Eq (C.1) without the $\mathcal{O}(T^2)$ correction due to the normalization. We have basically shown that upon taking the covariant divergence, the correction terms again only enter two orders higher.

Appendix D

Three-dimensional Metric

In this Appendix, we work out the derivations connected to the three dimensional metric tensors. The difference between the three dimensional metric of present and reference states gives us the strain. Therefore, by determining them, we determine the strain tensor components. Moreover, the determinant of the metric is proportional to the volume element and hence for incompressible materials the metric determinant must stay constant. In the first section we define two objects that will be useful later. Then, we determine the relationship between ζ and z using the incompressibility condition.

D.1 Useful Definitions

It turns out to be convenient to define the inverse of the in-plane part of the metric,

$$\begin{pmatrix} G'^{11} & G'^{12} \\ G'^{21} & G'^{22} \end{pmatrix} := \frac{1}{\det g'_{\alpha\beta}} \begin{pmatrix} g'_{22} & -g'_{21} \\ -g'_{12} & g'_{11} \end{pmatrix} . \tag{D.1}$$

This component-wise relation can be derived from the following definition,

$$G'^{\beta\gamma} g'_{\alpha\gamma} = \delta^{\beta}_{\alpha} . \tag{D.2}$$

Note that the inverse of the in-plane part of the metric is not necessarily equal to the in-plane part of the inverse metric: $G'^{\alpha\beta} \neq g'^{\alpha\beta}$. The in-plane part of the metric is given in Eq (5.25a) and we know that $\nabla_\alpha \zeta$ is of the order $\mathcal{O}(\zeta^2)$. Then, from Eq (D.2) and Eq (5.25a), the inverse metric is found

$$\begin{aligned} G'^{\alpha\beta} = G^{\alpha\beta} &- \zeta[\tilde{K}^{\alpha\beta} + \tilde{K}^{\beta\alpha} - K^{\alpha\beta} T^2] \\ &+ \zeta^2 \big[(\tilde{K}^{\alpha\gamma} + \tilde{K}^{\gamma\alpha})(\tilde{K}_{\gamma}^{\ \beta} + \tilde{K}^{\beta}_{\ \gamma}) - \tilde{K}^{\alpha}_{\ \gamma} \tilde{K}^{\beta\gamma} \\ &\quad - 3 K^{\alpha}_{\gamma} K^{\beta\gamma} T^2 - T^{\gamma} T^{\delta} \tilde{K}^{\alpha}_{\gamma} \tilde{K}^{\beta}_{\delta} \big] \\ &- T^{\alpha} \nabla^{\beta} \zeta - T^{\beta} \nabla^{\alpha} \zeta + \mathcal{O}(\zeta^2, T^2) . \end{aligned} \tag{D.3}$$

We also define the following useful notation to simplify some of the calculations

$$\overline{g}'_{\alpha z} := [\beta T^{\gamma} g_{\alpha\gamma} + (\nabla_{\alpha}\zeta)] \,, \tag{D.4}$$

so the mixed part of the metric tensor from Eq (5.25b) can be written as

$$g'_{\alpha z} = \frac{\partial \zeta}{\partial z}\, \overline{g}'_{\alpha z} \,. \tag{D.5}$$

Finally, by inserting Eq (5.25c), we have

$$g'_{\alpha z} g'_{\beta z} = g_{zz} \overline{g}'_{\alpha z} \overline{g}'_{\beta z} \,. \tag{D.6}$$

D.2 Local Incompressibility

The local incompressibility assumption states that the volume anywhere on the membrane stays locally constant. This means that the determinant of the three-dimensional metric, which is given in Eq (5.27), is constant. Therefore, using this assumption we calculate: (i) the relationship between metric of the zero strain state and the pivotal plane, and (ii) the relationship between the transverse coordinates after and before the deformations, $\zeta(z)$.

The determinant of the metric on the pivotal plane

Let us write down the determinant of the metric on the pivotal plane,

$$\begin{aligned} \det g_{ij} &= \frac{1}{6} \epsilon^{ikm} \epsilon^{jln} g_{ij} g_{kl} g_{mn} \\ &= g_{zz} g_{11} g_{22} - g_{zz} g_{12} g_{21} - g_{11} g_{2z} g_{2z} + g_{21} g_{1z} g_{2z} + g_{12} g_{1z} g_{2z} - g_{22} g_{1z} g_{1z} \,, \end{aligned} \tag{D.7}$$

where the first two terms can be written as g_{zz} times the determinat of the in-plane components of metric, $\det g_{\alpha\beta}$. For the rest, the inverse of the in-plane part of the metric tensor, $G^{\alpha\beta} = G'^{\alpha\beta}(\zeta = 0)$, is used. Then, Eq (D.7) becomes,

$$\begin{aligned} \det g_{ij} &= g_{zz} \det g_{\alpha\beta} - \det g_{\alpha\beta} \big[\frac{g_{11}}{\det g_{\alpha\beta}} g_{2z} g_{2z} + \frac{-g_{21}}{\det g_{\alpha\beta}} g_{1z} g_{2z} \\ &\qquad + \frac{-g_{12}}{\det g_{\alpha\beta}} g_{1z} g_{2z} + \frac{g_{22}}{\det g_{\alpha\beta}} g_{1z} g_{1z} \big] \\ &= g_{zz} \det g_{\alpha\beta} - \det g_{\alpha\beta} G^{\alpha\beta} g_{\alpha z} g_{\beta z} \,, \qquad \text{(D.8)} \\ &= \det g_{\alpha\beta} \big[g_{zz} - G^{\alpha\beta} g_{\alpha z} g_{\beta z} \big] \,. \qquad \text{(D.9)} \end{aligned}$$

Then, we insert $g_{zz} = 1$ and $g_{\alpha z} = \beta T^{\gamma} g_{\alpha\gamma}$ from Eq (5.29),

$$\begin{aligned} \det g_{ij} &= \det g_{\alpha\beta} \big[1 - \beta^2 T^{\gamma} T^{\delta} g_{\alpha\gamma} g_{\beta\delta} G^{\alpha\beta} \big] \,, \qquad \text{(D.10)} \\ &= \beta^2 \det g_{\alpha\beta} \,. \qquad \text{(D.11)} \end{aligned}$$

where in the second line we used the identity (5.27) and the definition of β from Eq (5.23).

The determinant of the three-dimensional metric

The determinant of the three dimensional metric $\det g'_{ij}$ is calculated similarly to $\det g_{ij}$ and from Eq (D.8), we write

$$\begin{aligned}\det g'_{ij} &= \det g'_{\alpha\beta}\left[g'_{zz} - g'_{\alpha z}g'_{\beta z}G'^{\alpha\beta}\right], \\ &= g'_{zz}\det g'_{\alpha\beta}\left[1 - \overline{g}'_{\alpha z}\overline{g}'_{\beta z}G'^{\alpha\beta}\right],\end{aligned} \tag{D.12}$$

where in the second line we use the identity (D.6). The incompressibility assumption, Eq (5.27), is applied between the pivotal plane and away from the pivotal plane, and combining Eq (D.11) and Eq (D.12) will give us an expression for the transverse part of the metric tensor

$$g'_{zz} = \frac{\det g_{\alpha\beta}}{\det g'_{\alpha\beta}}\frac{\beta^2}{1 - \overline{g}'_{\alpha z}\overline{g}'_{\beta z}G'^{\alpha\beta}}. \tag{D.13}$$

The left hand side gives the relationship between the transverse coordinates z and ζ. The right hand side is written as two terms, the first one is the area strain ϵ_ζ which is the relative area change between the pivotal plane and the lipid shifted surface,

$$\epsilon_\zeta = \frac{\mathrm{d}\alpha - \mathrm{d}A}{\mathrm{d}A} = \frac{\mathrm{d}\alpha}{\mathrm{d}A} - 1 = \frac{\sqrt{\det g'_{\alpha\beta}}}{\sqrt{\det g_{\alpha\beta}}} - 1, \tag{D.14}$$

where the area strain between the pivotal plane and a lipid shifted surface is given in Appendix A. The rest of the terms in Eq (D.13) are already determined, with the exception of $\nabla_\alpha\zeta$ in the components of the metric tensor. Fortunately, we know that $\nabla_\alpha\zeta$ is of second order in ζ. We combine g'_{zz} from Eq (5.25c), ϵ_ζ from Eq (A.18), β^2 from Eq (5.23), $G'^{\alpha\beta}$ from Eq (D.3), and $\overline{g}'_{\alpha z}$ from Eq (D.5), and expand every term on the right hand side of Eq (D.13) up to quadratic order in ζ and T^2,

$$\begin{aligned}\left(\frac{\partial\zeta}{\partial z}\right)^2 &= 1 - 2\zeta\left[\tilde{K}^2 - \frac{1}{2}K^2 + K_{\alpha\beta}T^\alpha T^\beta\right] \\ &\quad + \zeta^2\left[(3\tilde{K}^2 - 2\tilde{K}_{\mathrm{G}})(1 - T^2) + 2K^\gamma_\alpha K_{\beta\gamma}T^\alpha T^\beta + 4KK_{\alpha\beta}T^\alpha T^\beta\right].\end{aligned} \tag{D.15}$$

Note that, during the derivation of Eq (D.15) we use $G^{\alpha\beta}$ and $g_{\alpha\beta}$ to raise and lower indices of the curvature tensor, component of tilt field and covariant derivatives because all these objects live on the pivotal plane.

The connection between ζ and z

In order to determine the relation between the two transverse coordinates, we first write ζ as an expansion in z,

$$\zeta(z) = z + f_2 z^2 + \mathcal{O}(z^3). \tag{D.16}$$

Up to the first order ζ and z are equal. Then g'_{zz} becomes,

$$g'_{zz} = 1 + 2f_2 z + \mathcal{O}(z^2), \tag{D.17}$$

Then, from Eq (D.15) we can solve for f_2, and ζ becomes

$$\zeta(z) = z - \frac{1}{2}z^2\big(\tilde{K}^2 - \frac{1}{2}K^2 + K_{\alpha\beta}T^\alpha T^\beta\big) + \mathcal{O}(z^3)\,. \tag{D.18}$$

Appendix E

Notes on The Lipid Twist Term

In this Appendix, we will show that the lipid twist term comes from the anti-symmetric contraction of the curvature tensor by itself: $\tilde{K}_{\alpha}^{\ \beta}\tilde{K}_{\beta}^{\alpha}$ where the first index of the first term is contracted with the first index of the second term. First, we need to define the tilt twist as $\boldsymbol{\nabla}\times\boldsymbol{T}$ and it is expressed in terms of covariant derivatives and tangent vectors as,

$$\begin{aligned}\boldsymbol{\nabla}\times\boldsymbol{T} &= \boldsymbol{e}^{\alpha}\nabla_{\alpha}\times T^{\beta}\boldsymbol{e}_{\beta}\,, &\text{(E.1)}\\ &= G^{\alpha\beta}\boldsymbol{e}_{\gamma}\times(\boldsymbol{e}_{\delta}\nabla_{\alpha}T^{\delta}+T^{k}\nabla_{j}\boldsymbol{e}_{k})\,, &\text{(E.2)}\\ &= \epsilon_{\gamma\delta}(\nabla^{\gamma}T^{\delta})\boldsymbol{N}+\epsilon_{\gamma\mu}\boldsymbol{e}^{\mu}T^{\delta}K_{\delta}^{\gamma}\,, &\text{(E.3)}\end{aligned}$$

where in the third line we used the following relations:

$$\boldsymbol{e}_{\beta}\times\boldsymbol{e}_{\alpha}=\epsilon_{\alpha\beta}\boldsymbol{N}\quad\text{and}\quad\boldsymbol{e}_{\beta}\times\boldsymbol{N}=-\epsilon_{\beta\gamma}\boldsymbol{e}^{\gamma}\,, \tag{E.4}$$

where $\epsilon_{\alpha\beta}$ is the Levi-Civita tensor, $\epsilon_{11}=\epsilon_{22}=0$ and $\epsilon_{12}=-\epsilon_{21}=1/\sqrt{g}$. Then, the quadratic tilt twist term is written using the identity $\epsilon_{\alpha\beta}\epsilon_{\gamma\delta}=g_{\alpha\gamma}g_{\beta\delta}-g_{\alpha\delta}g_{\beta\gamma}$ as:

$$\begin{aligned}(\boldsymbol{\nabla}\times\boldsymbol{T})^{2} &= \epsilon_{\alpha\beta}\epsilon_{\gamma\delta}(\nabla^{\alpha}T^{\beta})(\nabla^{\gamma}T^{\delta})+\epsilon_{\alpha\beta}\epsilon_{\gamma\delta}G^{\beta\delta}T^{\mu}T^{\nu}K_{\mu}^{\alpha}K_{\nu}^{\gamma}\,,\\ &= \nabla^{\alpha}T_{\beta}\nabla_{\alpha}T^{\beta}-\nabla^{\alpha}T_{\beta}\nabla^{\beta}T_{\alpha}+T^{\mu}T^{\nu}K_{\mu}^{\alpha}K_{\nu\alpha}\,, &\text{(E.5)}\end{aligned}$$

where the first two terms can be rearranged as

$$(\boldsymbol{\nabla}\times\boldsymbol{T})^{2}=\frac{1}{2}(\nabla^{\alpha}T_{\beta}-\nabla_{\beta}T^{\alpha})(\nabla_{\alpha}T^{\beta}-\nabla^{\beta}T_{\alpha})+T^{\mu}T^{\nu}K_{\mu}^{\alpha}K_{\nu\alpha}\,. \tag{E.6}$$

Let us determine the anti-symmetric contraction of the curvature tensor with itself:

$$\tilde{K}_{\alpha}^{\ \beta}\tilde{K}_{\beta}^{\alpha}=\frac{1}{2}(\tilde{K}_{\alpha\beta}-\tilde{K}_{\beta\alpha})(\tilde{K}^{\alpha\beta}-\tilde{K}^{\beta\alpha})+\tilde{K}_{\alpha\beta}\tilde{K}^{\beta\alpha}\,, \tag{E.7}$$

where the first term is the antisymmetric part of the effective curvature,

$$\tilde{K}_{\beta}^{\ \alpha}-\tilde{K}_{\beta}^{\alpha}=K_{\beta}^{\alpha}+\nabla_{\beta}T^{\alpha}-K_{\beta}^{\alpha}-\nabla^{\alpha}T_{\beta}=\nabla_{\beta}T^{\alpha}-\nabla^{\alpha}T_{\beta}\,. \tag{E.8}$$

The curvature part vanishes in the antisymmetric part of the effective curvature term. By using Eq (E.6) and the identity $\tilde{K}_{\alpha}^{\ \beta}\tilde{K}_{\beta}^{\ \alpha} = \tilde{K}^2 - 2\tilde{K}_{\mathrm{G}}$, Eq (E.7) becomes,

$$\tilde{K}_{\alpha}^{\ \beta}\tilde{K}_{\ \beta}^{\alpha} = (\boldsymbol{\nabla}\times\boldsymbol{T})^2 + \tilde{K}^2 - 2\tilde{K}_{\mathrm{G}} - T^{\gamma}T^{\delta}K_{\alpha\gamma}K_{\delta}^{\alpha}\,. \tag{E.9}$$

Bibliography

[AFK+08] Sergey A Akimov, Vladimir AJ Frolov, Peter I Kuzmin, Joshua Zimmerberg, Yuri A Chizmadzhev, and Fredric S Cohen. Domain formation in membranes caused by lipid wetting of protein. *Phys. Rev. E*, 77(5):051901, 2008.

[AKZ+04] Sergey A Akimov, Peter I Kuzmin, Joshua Zimmerberg, Fredric S Cohen, and Yuri A Chizmadzhev. An elastic theory for line tension at a boundary separating two lipid monolayer regions of different thickness. *J. Electroanal. Chem.*, 564:13–18, 2004.

[AKZC07] Sergey A Akimov, Peter I Kuzmin, Joshua Zimmerberg, and Fredric S Cohen. Lateral tension increases the line tension between two domains in a lipid bilayer membrane. *Phys. Rev. E*, 75(1):011919, 2007.

[AMV+14] S. A. Akimov, A. A. Mukovozov, G. F. Voronina, Y. A. Chizmadzhev, and O. V. Batishchev. Line tension and structure of through pore edge in lipid bilayer. *Biochem. (Moscow) Suppl. Ser. A: Mem. Cell Biol.*, 8(4):297–303, 2014.

[AV02] Gary Ayton and G. A. Voth. Bridging microscopic and mesoscopic simulations of lipid bilayers. *Biophys. J.*, 83(6):3357–3370, 2002.

[BBS+11] Erik G. Brandt, Anthony R. Braun, Jonathan N. Sachs, John F. Nagle, and Olle Edholm. Interpretation of fluctuation spectra in lipid bilayer simulations. *Biophys. J.*, 100(9):2104–2111, 2011.

[BCC96] Jason Briggs, Hesson Chung, and Martin Caffrey. The temperature-composition phase diagram and mesophase structure characterization of the monoolein/water system. *Journal de Physique II*, 6(5):723–751, 1996.

[BCF12] Anne-Florence Bitbol, Doru Constantin, and Jean-Baptiste Fournier. Bilayer elasticity at the nanoscale: the need for new terms. *PloS one*, 7(11):e48306, 2012.

[BdGP76] F. Brochard, P.-G. de Gennes, and P. Pfeuty. Surface-tension and deformations of membrane structures—relation to 2-dimensional phase-transitions. *J. de Physique*, 37(10):1099–1104, 1976.

[BJB+18] Patricia Bassereau, Rui Jin, Tobias Baumgart, Markus Deserno, Rumiana Dimova, Vadim A Frolov, Pavel V Bashkirov, Helmut Grubmüller, Reinhard Jahn, H Jelger Risselada, et al. The 2018 biomembrane curvature and remodeling roadmap. *Journal of Physics D: Applied Physics*, 51(34):343001, 2018.

[BL75] F Brochard and J.F. Lennon. Frequency spectrum of the flicker phenomenon in erythrocytes. *J. de Physique*, 36(11):1035–1047, 1975.

[BPB05] G. Brannigan, P. F. Philips, and F. L. H. Brown. Flexible lipid bilayers in implicit solvent. *Phys. Rev. E*, 72(1):011915, 2005.

[BRBM04] Eveline Baesu, RE Rudd, J Belak, and M McElfresh. Continuum modeling of cell membranes. *Int. J. Nonlinear Mech.*, 39(3):369–377, 2004.

[BS95] A Ben-Shaul. *Molecular Theory of Chain Packing, Elasticity and Lipid-Protein Interaction in Lipid Bilayers*, volume 1, chapter 7, pages 359–402. Elsevier, Amsterdam, 1995.

[BTB04] Grace Brannigan, A. C. Tamboli, and Frank L. H. Brown. The role of molecular shape in bilayer elasticity and phase behavior. *J. Chem. Phys.*, 121(7):3259–3271, AUG 15 2004.

[CAMK14] Felix Campelo, Clement Arnarez, Siewert J. Marrink, and Michael M. Kozlov. Helfrich model of membrane bending: From gibbs theory of liquid interfaces to membranes as thick anisotropic elastic layers. *Adv. Colloid Interface Sci.*, 208:25–33, 2014.

[Can70] Peter B Canham. The minimum energy of bending as a possible explanation of the biconcave shape of the human red blood cell. *J. Theoret. Biol.*, 26(1):61–81, 1970.

[Can97] Robert S Cantor. Lateral pressures in cell membranes: a mechanism for modulation of protein function. *J. Phys. Chem. B*, 101(10):1723–1725, 1997.

[Can99] Robert S Cantor. Lipid composition and the lateral pressure profile in bilayers. *Biophys. J.*, 76(5):2625–2639, 1999.

[CD05] Ira R. Cooke and Markus Deserno. Solvent-free model for self-assembling fluid bilayer membranes: Stabilization of the fluid phase based on broad attractive tail potentials. *J. Chem. Phys.*, 123:224710, 2005.

[CKD05] Ira R. Cooke, Kurt Kremer, and Markus Deserno. Tunable generic model for fluid bilayer membranes. *Phys. Rev. E*, 72:011506, Jul 2005.

[CKM+85] L. V. Chernomordik, M. M. Kozlov, G. B. Melikyan, I. G. Abidor, V. S. Markin, and Yu. A. Chizmadzhev. The shape of lipid molecules and monolayer membrane fusion. *Biochim. Biophys. Acta*, 812(3):643–655, February 1985.

[CM04] F. S. Cohen and G. B. Melikyan. The energetics of membrane fusion from binding, through hemifusion, pore formation, and pore enlargement. *J. Mem. Biol.*, 199(1):1–14, 2004.

[CR98] Z. Chen and R. P. Rand. Comparative Study of the Effects of Several n-Alkanes on Phospholipid Hexagonal Phases. *Biophys. J.*, 74(2):944–952, 1998.

[dC76] Manfredo do Carmo. *Differential Geometry of Curves and Surfaces*. Prentice Hall, Englewood Cliffs, NJ, 1976.

[Des15] Markus Deserno. Fluid lipid membranes: From differential geometry to curvature stresses. *Chem. Phys. Lipids.*, 185:11–45, 2015.

[Des18] Luca Deseri. Elasticity and hereditariness. In David J. Steigmann, editor, *The Role of Mechanics in the Study of Lipid Bilayers*, pages 63–104. Springer, Cham, Switzerland, 2018.

[DPZ08] Luca Deseri, Mario D Piccioni, and Giuseppe Zurlo. Derivation of a new free energy for biological membranes. *Continuum Mech. Therm.*, 20(5):255–273, 2008.

[DPZD16] Luca Deseri, P Pollaci, M Zingales, and K Dayal. Fractional hereditariness of lipid membranes: Instabilities and linearized evolution. *J. Mech. Behav. Biomed. Mater.*, 58:11–27, 2016.

[DZ13] Luca Deseri and Giuseppe Zurlo. The stretching elasticity of biomembranes determines their line tension and bending rigidity. *Biomech. Model. Mechanobiol.*, 12(6):1233–1242, 2013.

[EHLR03] Evan Evans, Volkmar Heinrich, Florian Ludwig, and Wieslawa Rawicz. Dynamic tension spectroscopy and strength of biomembranes. *Biophys. J.*, 85(4):2342–2350, 2003.

[ESK09] Efi Efrati, Eran Sharon, and Raz Kupferman. Elastic theory of unconstrained non-euclidean plates. *Journal of the Mechanics and Physics of Solids*, 57(4):762–775, 2009.

[Far03] O. Farago. "water-free" computer model for fluid bilayer membranes. *J. Chem. Phys.*, 119(1):596–605, 2003.

[FBS93] Deborah R Fattal and Avinoam Ben-Shaul. A molecular model for lipid-protein interaction in membranes: the role of hydrophobic mismatch. *Biophys. J.*, 65(5):1795, 1993.

[FMM$^+$89] J. F. Faucon, M. D. Mitov, P. Méléard, I. Bivas, and P. Bothorel. Bending elasticity and thermal fluctuations of lipid-membranes—theoretical and experimental requirements. *J. de Physique*, 50(17):2389–2414, 1989.

[Fou99] J.-B. Fournier. Microscopic membrane elasticity and interactions among membrane inclusions: interplay between the shape, dilation, tilt and tilt-difference modes. *Eur. Phys. J. B*, 11(2):261–272, 1999.

[Fra11] Theodore Frankel. *The geometry of physics: an introduction*. Cambridge university press, 2011.

[GDA16] Jasmine M Gardner, Markus Deserno, and Cameron F Abrams. Effect of intrinsic curvature and edge tension on the stability of binary mixed-membrane three-junctions. *J. Chem. Phys.*, 145(7):074901, 2016.

[GGL99] Rüdiger Goetz, Gerhard Gompper, and Reinhard Lipowsky. Mobility and elasticity of self-assembled membranes. *Phys. Rev. Lett.*, 82(1):221, 1999.

[GGR+93] I Genco, A Gliozzi, A Relini, M Robello, and E Scalas. Electroporation in symmetric and asymmetric membranes. *Biochimica et Biophysica Acta (BBA)-Biomembranes*, 1149(1):10–18, 1993.

[GL97] A Goebel and Klaus Lunkenheimer. Interfacial tension of the water/n-alkane interface. *Langmuir*, 13(2):369–372, 1997.

[GT07] C. G. Gray and Edwin. F Taylor. When action is not least. *Am. J. Phys.*, 75(5):434–458, 2007.

[GZ92] Albert Edward Green and Wolfgang Zerna. *Theoretical elasticity*. Courier Corporation, 1992.

[Han18] JA Hanna. Some observations on variational elasticity and its application to plates and membranes. *arXiv preprint arXiv:1807.06426*, 2018.

[HBD12] Mingyang Hu, John J Briguglio, and Markus Deserno. Determining the Gaussian curvature modulus of lipid membranes in simulations. *Biophys. J.*, 102(6):1403–1410, 2012.

[HdJMD13] Mingyang Hu, Djurre H de Jong, Siewert J Marrink, and Markus Deserno. Gaussian curvature elasticity determined from global shape transformations and local stress distributions: a comparative study using the MARTINI model. *Faraday Discuss.*, 161:365–382, 2013.

[Hel73] Wolfgang Helfrich. Elastic properties of lipid bilayers: theory and possible experiments. *Z. Naturforsch. C*, 28(11):693–703, 1973.

[Hel81] Wolfgang Helfrich. Amphiphilic mesophases made of defects. In R. Balian, M. Kléman, and J. P. Poirier, editors, *Physics of Defects*, pages 715–755. North-Holland, Amsterdam, 1981.

[HK98] M. Hamm and M. M. Kozlov. Tilt model of inverted amphiphilic mesophases. *Eur. Phys. J. B*, 6(4):519–528, 1998.

[HK00] M. Hamm and M. M. Kozlov. Elastic energy of tilt and bending of fluid membranes. *Eur. Phys. J. E*, 3(4):323–335, 2000.

[HLE03] Christofer Hofsäß, Erik Lindahl, and Olle Edholm. Molecular dynamics simulations of phospholipid bilayers with cholesterol. *Biophys. J.*, 84(4):2192–2206, 2003.

[HRI04] J. Henriksen, A. C. Rowat, and J. H. Ipsen. Vesicle fluctuation analysis of the effects of sterols on membrane bending rigidity. *Eur. Biophys. J.*, 33(8):732–741, 2004.

[ISL05] Alberto Imparato, Julian C Shillcock, and Reinhard Lipowsky. Shape fluctuations and elastic properties of two-component bilayer membranes. *Europhys. Lett.*, 69(4):650, 2005.

[JAN14] Michael S Jablin, Kiyotaka Akabori, and J. F. Nagle. Experimental support for tilt-dependent theory of biomembrane mechanics. *Phys. Rev. Lett.*, 113(24):248102, 2014.

[JBK04] Frank Y Jiang, Yann Bouret, and James T Kindt. Molecular dynamics simulations of the lipid bilayer edge. *Biophys. J.*, 87(1):182–192, 2004.

[Jen77a] James T Jenkins. The equations of mechanical equilibrium of a model membrane. *SIAM J. Appl. Math.*, 32(4):755–764, 1977.

[Jen77b] James T. Jenkins. Static equilibrium configurations of a model red blood cell. *J. Math. Biol.*, 4(2):149–169, 1977.

[JHPP07] Hongyuan Jiang, Greg Huber, Robert A Pelcovits, and Thomas R Powers. Vesicle shape, molecular tilt, and the suppression of necks. *Phys. Rev. E*, 76(3):031908, 2007.

[KAC+05] Peter I Kuzmin, Sergey A Akimov, Yuri A Chizmadzhev, Joshua Zimmerberg, and Fredric S Cohen. Line tension and interaction energies of membrane rafts calculated from lipid splay and tilt. *Biophys. J.*, 88(2):1120–1133, 2005.

[KCK02] Yonathan Kozlovsky, Leonid V Chernomordik, and Michael M Kozlov. Lipid intermediates in membrane fusion: formation, structure, and decay of hemifusion diaphragm. *Biophys. J.*, 83(5):2634–2651, 2002.

[KESK04] Yonathan Kozlovsky, Avishay Efrat, David A Siegel, and Michael M Kozlov. Stalk phase formation: effects of dehydration and saddle splay modulus. *Biophys. J.*, 87(4):2508–2521, 2004.

[KGDM16] Boris Kheyfets, Timur Galimzyanov, Anna Drozdova, and Sergei Mukhin. Analytical calculation of the lipid bilayer bending modulus. *Phys. Rev. E*, 94(4):042415, 2016.

[KK02] Yonathan Kozlovsky and Michael M Kozlov. Stalk model of membrane fusion: solution of energy crisis. *Biophys. J.*, 82(2):882–895, 2002.

[KN15] Dmitry I Kopelevich and John F Nagle. Correlation between length and tilt of lipid tails. *J. Chem. Phys.*, 143(15):154702, 2015.

[Koz92] M. M. Kozlov. Energy of nonhomogeneous bending of surfactant monolayer. persistence length. *Langmuir*, 8(6):1541–1547, 1992.

[Kre59] E. Kreyszig. *Differential Geometry*. Differential Geometry. Dover Publications, 1959.

[KSG+03] E. Karatekin, O. Sandre, H. Guitouni, N. Borghi, P. H. Puech, and F. Brochard-Wyart. Cascades of transient pores in giant vesicles: Line tension and transport. *Biophys. J.*, 84(3):1734–1749, 2003.

[KZCC01] Peter I Kuzmin, Joshua Zimmerberg, Yuri A Chizmadzhev, and Fredric S Cohen. A quantitative model for membrane fusion based on low-energy intermediates. *Proc. Nat. Acad. Sci. (USA)*, 98(13):7235–7240, 2001.

[LE00] Erik Lindahl and Olle Edholm. Mesoscopic undulations and thickness fluctuations in lipid bilayers from molecular dynamics simulations. *Biophys. J.*, 79(1):426–433, 2000.

[LG93] R Lipowsky and S Grotehans. Hydration vs. protrusion forces between lipid bilayers. *Europhys. Lett.*, 23(8):599, 1993.

[LH62] V Luzzati and F Husson. The structure of the liquid-crystalline phases of lipid-water systems. *The Journal of cell biology*, 12(2):207–219, 1962.

[Lit75] J. D. Litster. Stability of lipid bilayers and red blood cell membranes. *Phys. Lett. A*, 53(3):193–194, 1975.

[LKFR96] S Leikin, M M Kozlov, N L Fuller, and R P Rand. Measured effects of diacylglycerol on structural and elastic properties of phospholipid membranes. *Biophys. J.*, 71(5):2623–2632, 1996.

[LL86] Lev D Landau and E. M. Lifshitz. *Theory of Elasticity, vol. 7*. Elsevier, New York, 3 edition, 1986.

[LM93] T. C. Lubensky and F. C. MacKintosh. Theory of "ripple" phases of lipid bilayers. *Phys. Rev. Lett.*, 71(10):1565, 1993.

[LN04] Y. F. Liu and John F. Nagle. Diffuse scattering provides material parameters and electron density profiles of biomembranes. *Phys. Rev. E*, 69:040901, 2004.

[LR89] David Lovelock and Hanno Rund. *Tensors, differential forms, and variational principles*. Courier Corporation, 1989.

[LS95] Reinhard Lipowsky and Erich Sackmann. *Structure and dynamics of membranes: I. from cells to vesicles*, volume 1. Elsevier, Amsterdam, 1995.

[LVW+14] Zachary A Levine, Richard M Venable, Max C Watson, Michael G Lerner, Joan-Emma Shea, Richard W Pastor, and Frank L. H. Brown. Determination of biomembrane bending moduli in fully atomistic simulations. *J. Am. Chem. Soc.*, 136(39):13582–13585, 2014.

[MA02] Vladislav S Markin and Joseph P Albanesi. Membrane fusion: stalk model revisited. *Biophys. J.*, 82(2):693–712, 2002.

[Mar96] Derek Marsh. Lateral pressure in membranes. *Biochim. Biophys. Acta*, 1286(3):183–223, 1996.

[May00a] Sylvio May. A molecular model for the line tension of lipid membranes. *Eur. Phys. J. E*, 3(1):37–44, 2000.

[May00b] Sylvio May. Protein-induced bilayer deformations: the lipid tilt degree of freedom. *Eur. Biophys. J.*, 29(1):17–28, 2000.

[May02] Sylvio May. Structure and energy of fusion stalks: the role of membrane edges. *Biophys. J.*, 83(6):2969–2980, 2002.

[MBS99] Sylvio May and Avinoam Ben-Shaul. Molecular theory of lipid-protein interaction and the L_α-H_{II} transition. *Biophys. J.*, 76(2):751–767, 1999.

[MDG05] Martin Michael Müller, Markus Deserno, and Jemal Guven. Interface-mediated interactions between particles: a geometrical approach. *Phys. Rev. E*, 72(6):061407, 2005.

[MdVM04] S. J. Marrink, A. H. de Vries, and A. E. Mark. Coarse grained model for semi-quantitative lipid simulations. *J. Phys. Chem. B*, 108(2):750–760, 2004.

[MKBSK04] S May, Y Kozlovsky, A Ben-Shaul, and M. M. Kozlov. Tilt modulus of a lipid monolayer. *Eur. Phys. J. E*, 14(3):299–308, 2004.

[ML91] F. C. MacKintosh and T. C. Lubensky. Orientational order, topology, and vesicle shapes. *Phys. Rev. Lett.*, 67(9):1169, 1991.

[MM01] S. J. Marrink and A. E. Mark. Effect of undulations on surface tension in simulated bilayers. *J. Phys. Chem. B*, 105(26):6122–6127, 2001.

[MNK07a] E. R. May, A. Narang, and D. I. Kopelevich. Molecular modeling of key elastic properties for inhomogeneous lipid bilayers. *Mol. Sim.*, 33(9-10):787–797, 2007.

[MNK07b] Eric R May, Atul Narang, and Dmitry I Kopelevich. Role of molecular tilt in thermal fluctuations of lipid membranes. *Phys. Rev. E*, 76(2):021913, 2007.

[Mor34] Marston Morse. *The calculus of variations in the large*, volume 18. American Mathematical Soc., Providence, RI, 1934.

[MRY+07] Siewert J Marrink, H Jelger Risselada, Serge Yefimov, D Peter Tieleman, and Alex H De Vries. The MARTINI force field: coarse grained model for biomolecular simulations. *J. Phys. Chem. B*, 111(27):7812–7824, 2007.

[MS96] M Müller and M Schick. Structure and nucleation of pores in polymeric bilayers: a monte carlo simulation. *J. Chem. Phys.*, 105(18):8282–8292, 1996.

[MSF13] Mohsen Maleki, Brian Seguin, and Eliot Fried. Kinematics, material symmetry, and energy densities for lipid bilayers with spontaneous curvature. *Biomech. Model. Mechanobiol.*, 12(5):997–1017, 2013.

[Nag17a] John F Nagle. Experimentally determined tilt and bending moduli of single-component lipid bilayers. *Chem. Phys. Lipids*, 205:18–24, 2017.

[Nag17b] John F Nagle. X-ray scattering reveals molecular tilt is an order parameter for the main phase transition in a model biomembrane. *Physical Review E*, 96(3):030401, 2017.

[Nog12] Hiroshi Noguchi. Line tension of branching junctions of bilayer membranes. *Soft Matter*, 8(11):3146–3153, 2012.

[NP92] Philip Nelson and Thomas Powers. Rigid chiral membranes. *Phys. Rev. Lett.*, 69(23):3409, 1992.

[NP93] Philip Nelson and Thomas Powers. Renormalization of chiral couplings in tilted bilayer membranes. *J. Phys. II (France)*, 3(10):1535–1569, 1993.

[NTN00] John F Nagle and Stephanie Tristram-Nagle. Structure of lipid bilayers. *Biochimica et Biophysica Acta (BBA)-Reviews on Biomembranes*, 1469(3):159–195, 2000.

[OE11] Mario Orsi and Jonathan W Essex. The elba force field for coarse-grain modeling of lipid membranes. *PLoS One*, 6(12):e28637, 2011.

[OHSE08] Mario Orsi, David Y Haubertin, Wendy E Sanderson, and Jonathan W Essex. A quantitative coarse-grain model for lipid bilayers. *The J. of Phys Chem B*, 112(3):802–815, 2008.

[OME10] Mario Orsi, Julien Michel, and Jonathan W Essex. Coarse-grain modelling of dmpc and dopc lipid bilayers. *J of Phys: Cond Mat*, 22(15):155106, 2010.

[PB84] A. G. Petrov and I. Bivas. Elastic and flexoelectic aspects of out-of-plane fluctuations in biological and model membranes. *Prog. Surf. Sci.*, 16(4):389–511, 1984.

[PN95] Thomas Powers and Philip Nelson. Fluctuating membranes with tilt order. *J. Phys. II (France)*, 5(11):1671–1678, 1995.

[RBA+14] Padmini Rangamani, Ayelet Benjamini, Ashutosh Agrawal, Berend Smit, David J Steigmann, and George Oster. Small scale membrane mechanics. *Biomech. modeling mechanobiol.*, 13(4):697–711, 2014.

[Red06] J. N. Reddy. *Theory and Analysis of Elastic Plates and Shells*. CRC Press, London, 2006.

[RFGP90] R. P. Rand, N. L. Fuller, S. M. Gruner, and V. A. Parsegian. Membrane curvature, lipid segregation, and structural transitions for phospholipids under dual-solvent stress. *Biochem.*, 29(1):76–87, 1990.

[ROM+00] W Rawicz, KC Olbrich, T McIntosh, D Needham, and E Evans. Effect of chain length and unsaturation on elasticity of lipid bilayers. *Biophysical journal*, 79(1):328–339, 2000.

[Saf94] Sam Safran. *Statistical Thermodynamics Of Surfaces, Interfaces, And Membranes*. Perseus, Cambridge, MA, 1994.

[SBSG90] I Szleifer, A Ben-Shaul, and W. M. Gelbart. Chain packing statistics and thermodynamics of amphiphile monolayers. *J. Phys. Chem.*, 94(12):5081–5089, 1990.

[Sch70] Alan H. Schoen. Infinite periodic minimal surfaces with our self-intersections. Technical Report TN D-5541, NASA, Electronics Research Center, Cambridge, MA, May 1970. http://ntrs.nasa.gov/archive/nasa/casi.ntrs.nasa.gov/19700020472_1970020472.pdf.

[Sch80] Bernard F Schutz. *Geometrical methods of mathematical physics*. Cambridge university press, 1980.

[SJW84a] M. B. Schneider, J. T. Jenkins, and W. W. Webb. Thermal fluctuations of large cylindrical phospholipid-vesicles. *Biophys. J.*, 45(5):891–899, 1984.

[SJW84b] M. B. Schneider, J. T. Jenkins, and W. W. Webb. Thermal fluctuations of large quasi-spherical bimolecular phospholipid-vesicles. *Biophys. J.*, 45(9):1457–1472, 1984.

[SMS96] J. V. Selinger, F. C. MacKintosh, and J. M. Schnur. Theory of cylindrical tubules and helical ribbons of chiral lipid membranes. *Phys. Rev. E*, 53(4):3804, 1996.

[SN11] Hayato Shiba and Hiroshi Noguchi. Estimation of the bending rigidity and spontaneous curvature of fluid membranes in simulations. *Phys. Rev. E*, 84:031926, 2011.

[Spi79] Michael Spivak. *Differential Geometry, vol. 2*. Publish or Perish, 1979.

[SS93] Jonathan V Selinger and Joel M Schnur. Theory of chiral lipid tubules. *Phys. Rev. Lett.*, 71(24):4091, 1993.

[SSN96] Udo Seifert, Julian Shillcock, and Philip Nelson. Role of bilayer tilt difference in equilibrium membrane shapes. *Phys. Rev. Lett.*, 77(26):5237, 1996.

[Ste99] DJ Steigmann. Fluid films with curvature elasticity. *Arch. Ration. Mech. An.*, 150(2):127–152, 1999.

[Ste13] David J Steigmann. A model for lipid membranes with tilt and distension based on three-dimensional liquid crystal theory. *Int. J. Nonlinear Mech.*, 56:61–70, 2013.

[Ste18] David J Steigmann. Mechanics and physics of lipid bilayers. In David J. Steigmann, editor, *The Role of Mechanics in the Study of Lipid Bilayers*, pages 1–61. Springer, Cham, Switzerland, 2018.

[TD17] M Mert Terzi and Markus Deserno. Novel tilt-curvature coupling in lipid membranes. *The Journal of chemical physics*, 147(8):084702, 2017.

[TD18] M Mert Terzi and Markus Deserno. Lipid membranes: From self-assembly to elasticity. In David J. Steigmann, editor, *The Role of Mechanics in the Study of Lipid Bilayers*, pages 105–166. Springer, Cham, Switzerland, 2018.

[TKS98] Richard H Templer, Bee J Khoo, and John M Seddon. Gaussian curvature modulus of an amphiphilic monolayer. *Langmuir*, 14(26):7427–7434, 1998.

[TLMM03] D Peter Tieleman, Hari Leontiadou, Alan E Mark, and Siewert-Jan Marrink. Simulation of pore formation in lipid bilayers by mechanical stress and electric fields. *J. Am. Chem. Soc.*, 125(21):6382–6383, 2003.

[VBP15] Richard M Venable, Frank L. H. Brown, and Richard W Pastor. Mechanical properties of lipid bilayers from molecular dynamics simulation. *Chem. Phys. Lipids*, 192:60–74, 2015.

[WB10] Max C. Watson and Frank L.H. Brown. Interpreting membrane scattering experiments at the mesoscale: The contribution of dissipation within the bilayer. *Biophys. J.*, 98(6):L9–L11, 2010.

[WBWB12] Max C Watson, Erik G Brandt, Paul M Welch, and Frank L. H. Brown. Determining biomembrane bending rigidities from simulations of modest size. *Phys. Rev. Lett.*, 109(2):028102, 2012.

[WD10a] Z.-J. Wang and M. Deserno. Systematic implicit solvent coarse-graining of bilayer membranes: lipid and phase transferability of the force field. *New J. Phys.*, 12:095004, 2010.

[WD10b] Z.-J. Wang and M. Deserno. A systematically coarse-grained solvent-free model for quantitative phospholipid bilayer simulation. *J. Phys. Chem. B*, 114(34):11207–11220, 2010.

[WD15] Xin Wang and Markus Deserno. Determining the pivotal plane of fluid lipid membranes in simulations. *J. Chem. Phys.*, 143(16):164109, 2015.

[WD16] Xin Wang and Markus Deserno. Determining the lipid tilt modulus by simulating membrane buckles. *J. Phys. Chem. B*, 120:6061–6073, 2016.

[WF05] Z.-J. Wang and D. Frenkel. Modeling flexible amphiphilic bilayers: A solvent-free off-lattice monte carlo study. *J. Chem. Phys.*, 122(23):234711, 2005.

[WH18] HG Wood and JH Hanna. Contrasting bending energies from bulk elastic theories. *arXiv preprint arXiv:1808.01310*, 2018.

[Whe64] John A Wheeler. Geometrodynamics and the issue of the final state. In C. DeWitt and B. S. DeWitt, editors, *Relativity, Groups and Topology*, page 316. Gordon and Breach, New York, 1964.

[Wil12] Thomas J. Willmore. *An Introduction to Differential Geometry*. Dover, New York, 2012.

[WMAWB13] Max C Watson, Alex Morriss-Andrews, Paul M Welch, and Frank L. H. Brown. Thermal fluctuations in shape, thickness, and molecular orientation in lipid bilayers. ii. finite surface tensions. *J. Chem. Phys.*, 139(8):084706, 2013.

[WPWB11] Max C Watson, Evgeni S Penev, Paul M Welch, and Frank L. H. Brown. Thermal fluctuations in shape, thickness, and molecular orientation in lipid bilayers. *J. Chem. Phys.*, 135(24):244701, 2011.

[ZN93] D. V. Zhelev and David Needham. Tension-stabilized pores in giant vesicles—determination of pore-size and pore line tension. *Biochim. Biophys. Acta*, 1147(1):89–104, 1993.

Glossary

$G'^{\alpha\beta}$ inverse of the two-dimensional part of the three-dimensional metric. 83

K the total curvature. 5

$K_{0,\mathrm{m}}$ monolayer spontaneous curvature. 16

$K_{0,\mathrm{b}}$ biquadratic curvature. 77

$K_{\alpha\beta}$ the curvature tensor. 5

K_{A} area extension modulus. 41

K_{G} the Gaussian curvature. 5

$M_{\alpha\beta}^{(\mathrm{A})}$ antisymmetric bilayer tilt matrix. 84

$M_{\alpha\beta}^{(\mathrm{S})}$ symmetric bilayer tilt matrix. 84

$M_{\alpha\beta}$ monolayer tilt matrix. 79

$R_{\alpha\beta\gamma\delta}$ Reimann curvature tensor. 6

$\Gamma_{\beta\gamma}^{\alpha}$ the Cristoffel symbol. 6

Γ_1 straight edge tension. 95

Γ_3 tension of a triple line junction. 99

β normalization factor for tilt director. 71

ℓ characteristic tilt length. 42

ℓ_{b1} characteristic length for the first biquadratic modulus. 78

ℓ_{b2} characteristic length for the second biquadratic modulus. 80

ℓ_{b3} characteristic length for the third biquadratic modulus. 80

ℓ_{eff} effective tilt decay length. 44

$\epsilon(\zeta)$ area strain. 13

ϵ_0 zeroth order area strain. 66

$\epsilon_\zeta(\zeta)$ higher order area strain. 66

κ bilayer total curvature modulus. 8

κ^{est} bending modulus estimation. 41

$\kappa_{\mathrm{b1,m}}$ first biquadratic modulus. 77

$\kappa_{\mathrm{b2,m}}$ second biquadratic modulus. 77, 79

$\kappa_{\mathrm{b3,m}}$ third biquadratic modulus. 77

$\kappa_{\mathrm{d,m}}$ monolayer coupling modulus. 34

κ_{d} bilayer coupling modulus. 37

κ_{m} monolayer total curvature modulus. 16

$\kappa_{\mathrm{t,m}}$ monolayer tilt modulus. 26

$\kappa_{\mathrm{tw,m}}$ monolayer twist modulus. 34

κ_{tw} bilayer twist modulus. 37

κ_{t} bilayer tilt modulus. 37

λ_{s} three-dimensional lateral shear modulus profile. 11

λ_{t} three-dimensional transverse shear modulus profile. 11

λ_{ijkl} elastic modulus tensor. 9

$\mathcal{H}$ Bilayer Hamiltonian. 8

$\mathcal{K}$ dimensionless total curvature. 91

$\mathcal{K}_{\mathrm{G}}$ dimensionless Gaussian curvature. 91

∇_α covariant derivative. 6

$\overline{\kappa}$ bilayer Gaussian curvature modulus. 8

$\overline{\kappa}_{\mathrm{m}}$ monolayer Gaussian curvature modulus. 16

$\overline{\mathcal{K}}_{0,\mathrm{m}}$ dimensionless spontaneous curvature. 91

$\sigma_0(z)$ lateral stress profile. 11

θ tilt angle. 23

$\tilde{E}$ three-dimensional elastic modulus profile. 11

$\tilde{K}$ effective total tensor. 23

$\tilde{K}_{\alpha\beta}$ effective curvature tensor. 23

$\tilde{K}_{\mathrm{G}}$ effective Gaussian tensor. 24

$\tilde{\nabla}^2$ renormalized Laplacian. 44

ε^{ij} the Levi-Civita tensor density. 5

ζ transverse coordinate in deformed configuration. 11

$\{u^1, u^2\}$ a local coordinate system on the surface. 4

$\{\boldsymbol{e}_1, \boldsymbol{e}_2\}$ a set of tangent vectors to a surface . 4

a^{ij} inverse of the three-dimensional metric of the zero strain state. 73

a_{ij} three-dimensional metric of the zero strain state. 68

$e_{\mathbf{2d}}$ two-dimensional energy density. 18

$e_{\mathbf{3d}}$ three-dimensional energy density. 9

g the determinant of the metric. 4

g'_{ij} three-dimensional metric of deformed state. 68

$g^{\alpha\beta}$ the inverse metric tensor on a surface. 4

$g_{\alpha\beta}$ the metric tensor on a surface. 4

$h(x, y)$ height function. 45

q_{c} critical wave vector. 47

r_{b1} first biquadratic elastic ratio. 92

r_{b1} second biquadratic elastic ratio. 92

r_{b3} third biquadratic elastic ratio. 92

$r_{\mathrm{d,m}}$ coupling modulus elastic ratio. 43

r_{m} monolayer elastic ratio. 43

r_{tw} twist elastic ratio. 43

u_{ij} strain tensor. 9, 68

z transverse coordinate in the flat configuration. 11

z_0 distance between the pivotal plane and mid-plane. 17

$\boldsymbol{N}$ the normal vector. 4

$\boldsymbol{T}$ tilt field. 21

$\boldsymbol{X}(u^1, u^2)$ embedding function for a surface. 4

$\boldsymbol{n}$ lipid director. 23

$\mathrm{d}A$ area element. 15